

SOLVENT-FREE BETA-CAROTENE NANOPARTICLES FOR FOOD
FORTIFICATION

By

PHONG TIEN HUYNH

A dissertation submitted to the

Graduate School – New Brunswick

Rutgers, The State University of New Jersey

in partial fulfillment of the requirements

for the degree of

Doctor of Philosophy

Graduate program in Food Science

written under the direction of

Professor PAUL TAKHISTOV

and approved by

New Brunswick, New Jersey

October 2012

ABSTRACT OF THE DISSERTATION
SOLVENT-FREE BETA-CAROTENE NANOPARTICLES FOR FOOD
FORTIFICATION

By PHONG TIEN HUYNH

Dissertation director:

Professor PAUL TAKHISTOV

Most nutraceutical compounds are poorly-water soluble. Their low solubility decreases the adsorption rate in living organisms leading to their low bioavailability. Utilization of nanoparticles is a promising way to improve the solubility of hydrophobic compounds. Nanoparticles increase the total surface area of the poorly-water soluble nutraceuticals making them more bioavailable.

Some traditional methods for decreasing particle size include pearl or jet milling, where particles are broken down through grinding or collisions under high pressure. These mechanical processes not only require high energy input but also raise a concern of milling media residues. The high pressure homogenizer approach applies implosion forces and collision of particles to generate nanosuspensions. This method requires microsuspensions as starting material and consumes high energy.

Among several emulsion-based techniques for preparing nanoparticles, solvent diffusion practice is a novel approach in which a poorly-water soluble compound is transferred into nanoemulsion droplets of a partially water-soluble organic solvent. The compound then crystallizes because the solvent diffuses out of the emulsion droplets. The key point of proposed emulsion-diffusion technology is that the phase transition occurs within an isolated nanoemulsion droplet.

The main purpose of this study is to develop a “green” and scalable method for preparing nanosuspensions of highly hydrophobic compounds. We use FDA GRAS ingredients to create nanoparticles of poorly-water soluble nutraceuticals. β -carotene is selected as a model hydrophobic nutraceutical. Triacetin, a partially- water soluble triacetate compound, is used as the dispersed phase of nanoemulsions. The influence of surfactant, water concentration, and homogenization time on particle size and stability is investigated. The impact of surfactant on diffusion flux of triacetin is studied. Kolmogorov theory is applied to reveal the breakup mechanism of emulsion droplets under shear and predict their size. A mathematical model is built to discover the size of emulsion droplet during the formation of nanosuspensions. It is hoped that the this work will greatly advance the manufacture of nanoparticles of poorly-water soluble nutraceuticals

ACKNOWLEDGEMENTS

I would like to thank my advisor Professor Takhistov, for his guidance, unending support, and for exposing me to a broad range of studies including nutraceuticals, simulations and colloidal science. I would also like to thank members of professor Takhistov's group including: Marlena Brown, Abhishek Sahay, Maha Ashehab for their collaborations knowledge, and support throughout the years. In addition, I would like to thank Dr Changhoon Chai for advice and helps at beginning. I would like to thank Professor Khusid, Professor Yam, and Professor Karwe for their great suggestions and discussions. I would like acknowledge US government and Vietnamese government for their program to give me a chance to study in the United States of America. I would like to thank Vietnam Foundation Education for sponsor my visa. I am deeply grateful to my international student adviser Mrs. Mukherjee for hers advice; Professor Waterman and Mrs. Bachmann for their helps.

DEDICATION

I dedicate this dissertation to my family who endlessly love and support me to make this work possible.

TABLE OF CONTENT

ABSTRACT OF THE DISSERTATION	ii
ACKNOWLEDGEMENTS.....	iv
DEDICATION.....	v
TABLE OF CONTENT	vi
LIST OF TABLES	ix
LIST OF FIGURES	x
INTRODUCTION	1
1. Functional food.....	1
2. Food fortification.....	7
3. Nanotechnology and nanoparticles in food.....	11
3.1. Liposomes.....	14
3.2. Nano-Cochleates.....	17
3.3. Hydrogels.....	18
3.4. Micellar systems.....	20
3.5. Dendrimers	22
3.6. Polymeric Nanoparticles.....	23
3.7. Nanoemulsions	27
3.8. Double emulsions	29
3.9. Lipid Nanoparticles	30
3.9.1. Solid lipid nanoparticle	30
3.9.2. Nanostructure lipid carriers.....	31
3.9.3. Lipid drug conjugate	32
3.10. Co-acervate nanoparticles.....	32
3.11. Nanocrystalline particles	33
3.12. Cubosomes.....	34
3.13. Polyelectrolyte	35
4. Nutraceuticals.....	35
5. Smaller size better solubility of nutraceuticals.....	39
NANOPARTICLE MANUFACTURING.....	48

1. Milling.....	48
2. High pressure homogenization.....	53
3. Solvent – based method.....	56
4. Emulsion as template method.....	58
5. Objective	61
MATERIALS AND METHODS.....	63
1. Materials.....	63
1.2. Beta-carotene	64
1.3. Triacetin.....	70
1.4. Surfactant.....	71
1.4.1. Tween 20	77
1.4.2. Tween 80	77
1.4.3. Lecithin.....	77
2. Method.....	81
2.1. Spectrofotometer for defining the solubility of beta-carotene in triacetin	81
2.2. Optical goniometer for surface tension	82
2.3. Suspension preparation.....	84
2.4. Dynamic light scattering technique for particle size and zeta potential	84
2.5. Differential scanning calorimetry.....	88
2.6. X-ray diffraction for characterizing crystallinity.....	91
2.7. Diffusing wave spectroscopy for nano-rheology of gels.....	94
PHYSICAL CHEMISTRY OF TRIACETIN – BETA CAROTENE SYSTEM.....	100
1. The formation of emulsion droplet in triacetin –water system	100
1.1. Definition of emulsion.....	100
1.2. Formation of emulsion droplets.....	101
2. Droplet breakup mechanism.....	103
2.1. Droplet breakup mechanism in laminar flow	105
2.2. Droplet breakup mechanism in turbulence flow.....	107
2.3. Impact of surfactant on emulsion droplet size.....	111
2.4. Impact of other factors to emulsion droplet size	114
3. The adsorption of surfactant on triacetin interface.....	115

4. Solubility of beta-carotene in triacetin	117
NANOSUSPENSION PREPARATION	150
1. Mathematic model for the diffusion of triacetin from an emulsion droplet	150
2. The crystallization of beta-carotene in emulsion droplet	156
3. The diffusion of triacetin from a droplet	164
4. Impact of surfactant on the particle size	168
5. Impact of operation parameters on the particle size and stability of nanosuspension	171
6. Shelf life of beta-carotene nanoparticles	174
CHARACTERIZATION OF BETA-CAROTENE NANO PARTICLES	179
EDIBLE FILM LOADED BETA-CAROTENE NANOPARTICLES: MODEL OF FOOD FORTIFICATION	154
1. Hydroxypropyl methylcellulose	154
2. Physical chemistry of aqueous hydroxypropyl methyl cellulose solution	156
3. Film formation	158
3.1. Film formation model	158
3.2. Factors impact the film formation	162
4. Nano-rheology of hydroxypropyl methyl cellulose gels	170
5. Moisture adsorption of the films	175
CONCLUSIONS	178
FUTURE WORKS	182
REFERENCES	183

LIST OF TABLES

Table 1: Physicochemical and biopharmaceutical drug properties and food effect [20].....	6
Table 2:Percentage of surface molecules for different particle sizes [68].....	12
Table 3: Sensitivity of some vitamins to the food matrix and environment factors	37
Table 4: Comparative challenges for delivery nutraceuticals: in-food and in-vivo.....	49
Table 5: The 10 foods having the highest beta-carotene content per serving.....	65
Table 6: Biochemical functions of beta-carotene in humans.....	67
Table 7: The HLB value of some chemical groups	75
Table 8: The application of emulsifiers based on their HLB value	76
Table 9: Dimensions of the lamellar[405]	79
Table 10 : Seven crystal systems	92
Table 11: High shear mixer properties and maximum particle size for triacetin – lecithin system	110
Table 12: The surface tension of triacetin – surfactant – water system and the maximum emulsion droplet size estimated by Kolmogorov theory	112
Table 13: Adsorption parameters of surfactant -triacetin system	116
Table 14: Molar factor of Triacetin	155
Table 15: Distance among surfactant molecules adsorbed on triacetin surface	168
Table 16: The sorption isotherm model confidence fit of the films	176

LIST OF FIGURES

Figure 1: Scale of the structural elements in food matrices.....	4
Figure 2: Factors influencing the stability of vitamins in foods [59].....	11
Figure 3: Loading mechanisms for nanoparticulate delivery systems.....	13
Figure 4: Schematic representations of modifications to the conventional liposome.	14
Figure 5: Schematic of methods for formation of two types of ionic hydrogels.	18
Figure 6: Schematics of micelle formation.....	21
Figure 7: Intestinal absorption pattern.....	40
Figure 8: The collision of particles during pearl milling.....	50
Figure 9: Jet milling chamber.....	51
Figure 10: Particles break under high shear in high pressure homogenizer.....	54
Figure 11: Morphology of particle prepared by spraying method [296].....	56
Figure 12 : Schematic procedure of preparation solid lipid nanoparticles [318].....	59
Figure 13 : The structure of chemicals used in the research.....	63
Figure 14: Force acting on the molecules at interface and in the bulk.....	72
Figure 15: The distribution of surfactant molecules with different HLB values in oil – water mixture.....	76
Figure 16: Lamellar structures of lecithin at interface.....	78
Figure 17: Schematic of a spectrophotometer.....	81
Figure 18 : Geometry of a pendant droplet.....	82
Figure 19: The fluctuation of scattering light from particles in a liquid medium.....	86
Figure 20 : Schematic diagram of heat flux differential scanning calorimetry cells.....	89
Figure 21: A typical DSC thermogram of a material.....	90
Figure 22: Unit cell.....	92
Figure 23: X-ray diffraction on a crystal (left) and the schematic of an X-ray diffraction (right).....	94
Figure 24: Schematic of DWS technique.....	99
Figure 25: A typical Oil/Water emulsion system.....	101
Figure 26: Physicochemical process of emulsification [416].....	103
Figure 27: The droplet breakup mechanism.....	104
Figure 28: The streamlines of laminar flow field for $1 \geq \alpha \geq 0$	106
Figure 29: Emulsion droplet size versus surface tension.....	110
Figure 30 : Surface tension of lecithin and Tween 20 solutions.....	116
Figure 31: Solubility of β -carotene in Triacetin Curve.....	117
Figure 32: The diffusion of triacetin from an emulsion droplet.....	150
Figure 33: The evolution of droplet radius over time.....	155
Figure 34: The diffusion flux of triacetin from a pendant droplet.....	156
Figure 35: Nucleation energy.....	161

Figure 36 : The mass fraction of solid beta-carotene versus emulsion droplet size during the diffusion of triacetin.....	163
Figure 37: Triacetin diffused from a pendant droplet.....	164
Figure 38 : The flux of triacetin in different surfactant solutions.....	165
Figure 39: Impact of surfactant on the particle size.....	170
Figure 40: impact of homogenization time on particle size.....	171
Figure 41: Particle size and zeta potential as function of water content and time.....	173
Figure 42 : The impact of Oswald ripening on particle size distribution	174
Figure 43: The evolution of particle size distribution during short storage time.....	177
Figure 44: The shelf life of beta-carotene nanoparticles during long time storage	177
Figure 45 : XRD spectra of pure beta – carotene and beta – carotene nanoparticles	179
Figure 46: DSC thermograms of pure beta-carotene, lecithin, and beta-carotene nanoparticle.....	180
Figure 47: Particle size distribution of beta-carotene nanoparticles before lyophilization and after lyophilization	182
Figure 48: SEM image of the beta-carotene nanoparticles.....	182
Figure 49: Structure of HPMC.....	154
Figure 50: The polymer - surfactant interaction in aqueous media	156
Figure 51: surface tension of lecithin - HPMC aqueous solution.....	158
Figure 52: Model of water removal from the polymer solution during film formation	158
Figure 53: The distribution of polymer concentration in the film at different evaporation rate.....	160
Figure 54: The evaporation flux of the films	163
Figure 55 : Surface of the HPMC films under microscope	164
Figure 56: Phase diagram of lecithin -water system.....	164
Figure 57: Diagrammatic reconstruction of the bimolecular lecithin leaflet in relation to the amount of water present.....	166
Figure 58: The mobility of particle during film formation	167
Figure 59: Surfactant - polymer - particle interaction tailors the film structure.....	169
Figure 60: The dynamic diffusion coefficient of the particles during film formation....	170
Figure 61: The polymer - particle interaction	174
Figure 62 : Dynamic storage and lost modulus of the film.....	174
Figure 63: Moisture isotherm of the films	175

INTRODUCTION

1. Functional food

Application of functional foods for health enhancement is of great public interest [1-4]. Currently, people are choosing more and more healthy foods in their daily lives. The rapidly expanding market for food functionalization and fortification is expected to reach \$177 billion by 2013 [5].

Understanding of powerful functionality of macro and micro nutrients has established a new group of food ingredients (nutraceuticals) positioned between nutrition and medicine [6]. People who consume the daily requirement of fruits and vegetables have being shown to have lower risk of cancer and certain other chronic diseases based on epidemiological studies [7]. These benefits have been attributed to certain components termed as nutraceuticals.

An evolution has taken place with functional foods containing nutrients since food is being linked to cure for diseases [8]. However, there is a strong need for a food grade delivery system that provides substantial health benefits aka prevention/ treatment of chronic diseases [1, 2]. Such products are looked upon as solutions to today's major public health problems.

New emerging technologies need to be developed that offer a solution for delivering these nutraceuticals by improving their stability and bioavailability. Due to complexity of

the food matrix, there is a major research question: What are the challenges we may encounter in delivering these nutraceuticals for their health benefits.

The choice of food system used for fortification by nutraceuticals plays a very critical role. Most foods are dispersed systems and are physically heterogeneous, multi-component and multi-phasic. Structure and properties of food systems depends on composition, process steps applied and storage conditions *etc.* Eventually, the food structure determines a range of quality aspects of food systems. In general, a food system can be represented by a matrix composed of protein, carbohydrates, fat, nutrients, colors, flavors, food additives *etc.* Water is also an important component of the food matrix.

Manufactured food represents a broad spectrum of structured matrices. For example beer foam is a solution containing gas bubbles, milk is a solution containing fat droplets and protein aggregates, a salad dressing may be just an emulsion. But other manufactured foods are structurally complicated in that they contain several different structural elements of widely varying size and state, for e.g. materials obtained by extrusion like margarine, dough, and bread have a very complex structure. Thus while considering the option of delivering nutraceutical using nanoparticle one needs to understand how structured food matrix interacts with nanoparticles.

The choice of food to fortify nutraceutical is also affected by its processing condition and composition of food. In fruits juices and drinks low pH could cause loss of vitamin A, folic acid and calcium. Whereas the different heat treatment could cause loss of heat labile vitamins thiamine, folic acid and ascorbic acid. For example a significant reduction in vitamin B1 (thiamin), B2 (riboflavin), B3 (niacin), B6, B127 and folate has been

reported under the influence of different milk processing regimes[9, 10]. Similar losses on heat processing has been reported for ascorbic acid in orange juice [11]. In yogurt the low pH could pose great challenge in stabilizing nutraceutical[12]. In high protein food, calcium and magnesium could destabilize proteins [13]. Ascorbic acid could involve itself in browning reaction [14, 15]. Lycopene emulsion was found to be more stable in orange juice and skimmed milk as compared to water [16]. Orange juice contains many antioxidant components like vitamin C, phenolic compounds preventing lycopene oxidation. In case of skimmed milk protein chelate metal ions preventing degradation of lycopene. Degradation in water was attributed to dissolved oxygen.

The various structural elements contributing to food are plant cells, cell walls, and meat fibers, small particulate materials in powders, starch granules, protein assemblies, food polymer network, crystals, oil-droplets, gas bubbles and colloidal particles [17]. The different scales of food process and elements in microstructure are as shown in Figure 1. Food functionality is highly dependent on its microstructure and with nanotech even smaller particles are part of food structure [18]. Today many micro and nano structure are generated based on colloidal science [19]. Air bubbles are important structural elements in solid foams, such as bread, whipped cream, cappuccino etc [17].

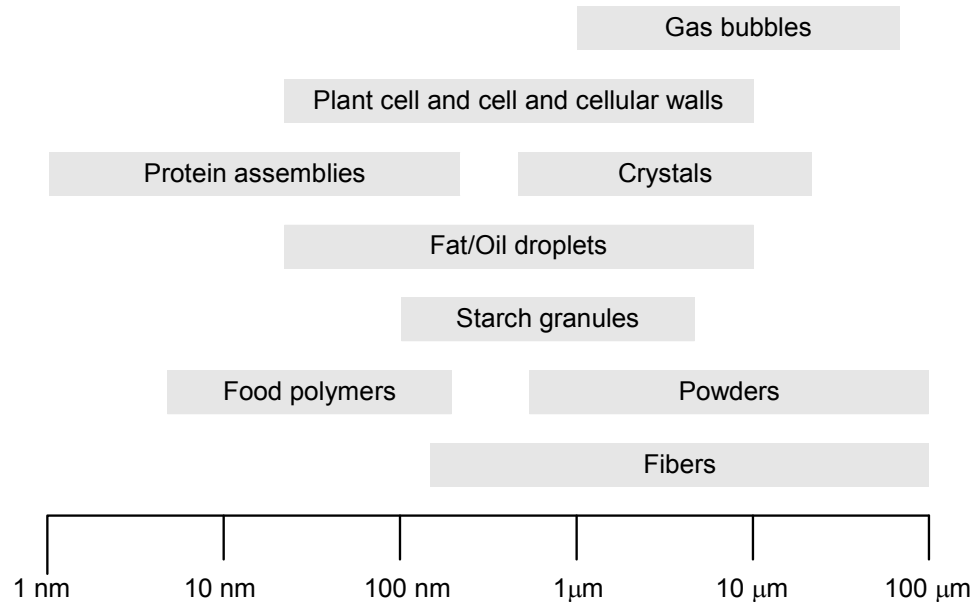


Figure 1: Scale of the structural elements in food matrices

Food is generally a complicated heterogeneous multi-phase system. A typical food is a multi-component system containing water; protein; lipid; polysaccharide; nutrition; flavor etc. For example, milk contains globules of protein and fat droplets distributed in water. Interaction among those components varies with the processing steps and storage condition. This contributes to food structure; properties; and complexity. In meat production, frozen beef and ground beef have the same components as fresh beef. However, their textures are very distinguishable because their processing steps and storage conditions are different. The characteristics and quality of a food are affected by several structure elements such as plant cells and cell walls, fibril of meats, starch granules, food polymer network, oil droplets, colloidal particles, gas bubbles and flavors [17].

Addition of nutraceutical faces several challenges because physical and chemical properties of food impact the nutrition. For example, addition of calcium and magnesium cation in high protein food may cause protein destabilization. Lycopene emulsion is reported to be oxidized in water leading to decomposition but is stable in orange juice because vitamin C and phenolic compounds in orange juice prevent the oxidation of lycopene [16]. High fat in food can improve bioavailability of poorly soluble nutraceutical via improved solubilization as well as transport to lymphatic system whereas a low fat diet will decrease the bioavailability. On the other hand, high protein content in food may impede absorption of certain amino acid based nutraceutical by competing for absorption. Calcium and heavy metals in certain food, such as milk and yogurt may bind to nutraceutical and form insoluble complex. Polycyclic aromatic hydrocarbons in smoked food, presence of enzyme inducers in certain spices and cruciferous vegetables may affect the bioavailability of certain nutraceutical. High fat in food can improve bioavailability of poorly soluble nutraceutical via improved solubilization as well as transport to lymphatic system whereas a low fat diet will decrease the bioavailability. On the other hand, high protein content in food may impede absorption of certain amino acid based nutraceutical by competing for absorption. Calcium and heavy metals in certain food, such as milk and yogurt may bind to nutraceutical and form insoluble complex. Polycyclic aromatic hydrocarbons in smoked food, presence of enzyme inducers in certain spices and cruciferous vegetables may affect the bioavailability of certain nutraceutical. There is huge data available on effect of food on drug performance in vivo. Interaction depends on physicochemical and biopharmaceutical drug properties and food induced physiological changes. Food can cause increase or decrease in absorption of drugs or nutraceuticals. An excellent compilation on this topic is available from Gokhale [20]. Food has positive effect on drugs with high pK_a by stabilizing them in stomach. Even with a low pK_a nutraceutical may precipitate due to food composition. Poorly solubilized drugs could

have increased stabilization in presence of food. Acid labile drugs have potential to undergo degradation in presence of food. As nutraceuticals are affected by food matrix, how nutraceuticals interact with food components becomes one of the issues that need to be clarified.

Table 1: Physicochemical and biopharmaceutical drug properties and food effect [20]

Property	Influence of food	Potential effect of food matrix
Weak acids, high pK_a	Increased solubilization in stomach due to delayed emptying,	Positive
Weak bases low pK_a	Drug precipitation due to altered pH	Negative
Acid labile compounds	Drug degradation in stomach due to delayed emptying	Negative
Poorly soluble compounds	Improved solubilization, drug bile acid micelles are soluble	Positive
Complexation with metal ions	Unabsorbed drug-metal complexes (e.g. calcium in milk)	Negative
Compounds binding to soluble fibers	Increased absorption	Positive
Substrates for enzyme inhibition	Enzyme inhibition	Positive
Substrates for enzyme or inducers	Enzyme induction	Negative

2. Food fortification

The simplest types of functional foods are those products that are fortified with additional nutrients no matter what the nutrients are originally contained in foods or not. The purpose of food fortification is preventing or correcting nutrient deficiency in population or group of community. There are three main types of food fortification. They are mass fortification, target fortification, and market-driven fortification [21]. If the mass fortification mentions the addition of one or more nutrients to foods which are commonly consumed by general public such as iodized table salt, the target fortification focuses on a group of people in community such as children or women in order to increase the intake of a particular group. These two kinds of fortification are regulated by law. The market-driven fortification can be considered as a special target fortification in which companies take business focusing on a specific amount of one or more nutrients.

The most widespread nutrient deficiencies in the world are iodine, vitamin A, and Iron. Iodine deficiency relates closely to the goiter disease and is prevalent in Europe [22]. According to generally accepted criteria, when the median urinary iodine concentration in a community is below 100 μ g/l, or when more than 5% of children aged 6–12 years of the community have goiter, this community faces iodine deficiency in populations. The implementation of iodine in salt decreases goiter globally[23]. Iron deficiency is high prevalent in developing countries. Anaemia is considered as an indicator of iron deficiency although 6 to 10% of all anaemia are not related to iron deficiency[23]. The community with high risk of anaemia is children and women, especially pregnant women. The ferric (Fe^{3+}) and its reduced form (Fe^{2+}) are the only natural forms found in food. Although the daily intake of iron is quite high, the major factor that causes the iron

deficiency is its low adsorption due to the presence of inhibitor such as phytic acid in foods [24, 25]. The iron compounds fortified in foods fall into three main categories including water soluble iron, poorly – water soluble but soluble in dilute acid, and poorly soluble in both water and dilute acid [26, 27]. The food matrices which serve as iron carriers are very broad, from grain based products such as cereals, wheat flour to milk powder and fish sauce. Food fortification is a low cost, long – term solution for iron deficiency [28]. It has been well documented that the vitamin A deficiency is associated with the abnormal visual adaptation to darkness, dry skin, dry hair, broken fingernails, and decreased resistance to infections [29]. There have been several studies which pointed out that the vitamin A deficiency causes maternal mortality and poor outcomes in pregnancy and lactation [30-32]. Some animal studies show evidences that the shortage of vitamin A induces changes in rats' bone marrow, is associated with anemia, and modifies lipid metabolism [33, 34]. Food fortification provides at least 15% of the recommended vitamin A daily intake in Central America countries [32].

Folate is known as vitamin B9 a vitamin that plays critical role in the synthesis of nucleotides which interfere in the cell division and tissue development. Folate deficiency relates to high risk of neural tube defects in infants and increases risk of cardiovascular diseases, cancer, and cerebral function in adults. Combination of very low folate intake and vitamin B12 deficiency can cause megaloblastic anaemia. Folate deficiency occurs prevalently in community with high intake of refined cereals [35-37]. Several surveys in different countries show that folate deficiency occurs rarely in population with high intake of green vegetable and fruits [38, 39]. The food fortification with folate compounds is mandatory in American countries such as Canada, US, Chile [40-42]. Food

fortification succeeds in increasing the daily intake of folate in these populations. In addition, food fortification is also a candidate for deliver other micronutrients such as trace elements like zinc[43, 44], selenium [45] and vitamin A[46, 47], C[48], D[49] and several type of vitamin B [50-52].

In order to prevent malnutrition on a national scale, micronutrients should be added in staple foods which dominate the meal plan. It is the cheapest, most efficient, and most effective way to supply large populations with essential micronutrients. Food matrix for micronutrients fortification is plentiful, for example, grain products with added folic acid, beverages enriched with vitamins, sugar fortified with vitamin or ferrous compound. Taking the advantages of dominant consumption products with high compliance, food fortification is considered a great alternative approach to prevent micronutrient malnutrition [53]. Furthermore, food fortification can have several forms to respond to the micronutrient deficiency. It can be mass fortified in order to serve the general population or targeted for focusing on small groups in community for example children or women. Market-driven fortification is quite flexible. Although food companies volunteer in adding a specific amount of one or group of micronutrients, this type of fortification is under the limitation which is regulated by government. The success of market – driven fortification in Ireland is evaluated by Hannon et al. [54]. This type of fortification contributes to the demand of micronutrients and thus reduces the risk of micronutrient undernourishment. Furthermore, market – driven fortification can cover the blank where mass fortification of staple food cannot achieve the demand due to limitation of technique, cost constrain, or safety [53]. It is suggested that food fortification with multiple micronutrients would be a better way to deliver micronutrients [55]. Besides the

advantages of food fortification in solving micronutrient malnutrition, there are quite well known limitations. For example, food fortification cannot correct the micronutrient malnutrition when the deficiency in the community is severe or when the deficiency occurs in an isolated community where there is a limit or no accessibility to fortified foods. In these cases dietary supplement pills are the better solution. Anyway, the advanced technology allows fortifying staple foods such as flour, salt and oil and condiments such as soy sauce can be transferred to developing countries. Fortified food is a cost effective solution to micronutrient deficiency in a global effort to improve overall nutritional status.

The addition of micronutrients to food may cause sensory changes leading to non consumer acceptance. For example, addition of iron to tea or cocoa –based products creates unacceptable change in color and taste [56, 57]. Another disadvantage of iron fortification is that iron participates in the degradation of vitamins leading to the lost of nutritional value due to complex formation. Furthermore, iron catalyzes the lipid oxidation in food causing rancidity[58].

Vitamins are sensitive compounds. During the food processing, delivering, and storage, vitamins are exposed to different environments leading to the change in physical and chemical properties of the vitamins. Factors that impact the stability of vitamins in food have been listed by Killeit [59]. Therefore, the stability of vitamins in foods is a key factor for maintaining nutrition in food products. Understanding the behavior of these nutrients under the change of environmental condition helps the producer in adopting technology for minimizing the vitamin loss in the shelf life of food products. It also provides information for labeling, justifying the nutrition retention as well as customer's

selection. Because each vitamin behaves differently, there is no common routine for vitamin fortification. The addition of vitamin in food has been reviewed by Counsell [60].

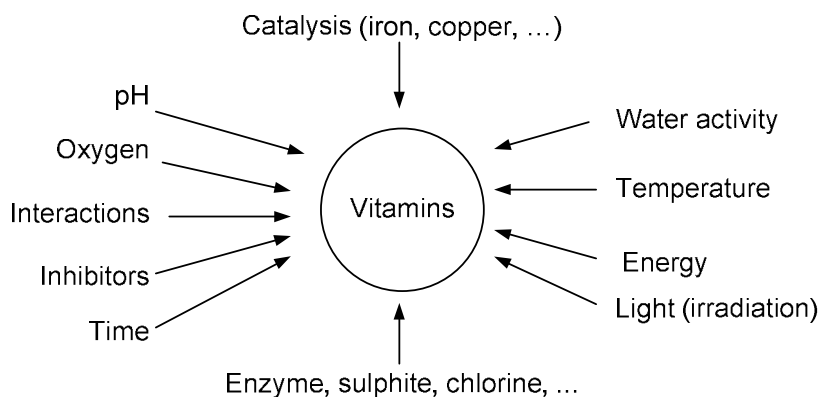


Figure 2: Factors influencing the stability of vitamins in foods [59]

There has been a concern of folate over intake via fortified food in the United States [61, 62]. Barbaresi et al. reported that there is possible relationship between overdose of folate and autism [63]. However, Beard and co-workers have not found solid proof for this association [62]. Since folate is water soluble, it can be removed out of human body via urination, thus the risk of folate overdose is very low [64]. The only concern relating to high folate intake is that it interferes with the adsorption of vitamin B12 leading to the vitamin B12 deficiency [65].

3. Nanotechnology and nanoparticles in food

Nutraceuticals are naturally occurring/derived bioactive compounds which display health benefits. Most nutraceuticals from food matrix are easily subjected to lose quality because of their sensitivity to environment, processing condition, reaction with other components, etc. Moreover, most of them are water insoluble, which leads to low

dissolution in the gastrointestinal tract and poor absorption and limited bioavailability[66]. As a result from these problems, particle size reduction to nanoparticles and nanotechnology have investigated and emerged multidisciplinary area. Nanoparticles have just resulted in significant improvement for both prolonged and good release characteristics and protect the encapsulated agent from degradation.

Nanoparticles in food are defined as colloidal particles in the range of 1nm to 1000nm, including solid nanoparticles, nanocapsules, polymeric nanoparticles, etc [67] . As the particle size decreases, the number of molecules present on a particle surface increasingly improves the dissolution rate for the nanoparticles [68]. For a spherical particle of diameter, d , with the molecular diameter, σ , the percentage of molecules on the surface monolayer is given as:

$$\% \text{ surface molecules} = 100 \left(\left(\frac{\sigma}{d} \right)^3 - 3 \left(\frac{\sigma}{d} \right)^2 + 3 \frac{\sigma}{d} \right).$$

These effects are calculated in Table 2 for a spherical molecule of 1nm diameter. The dissolution rate of nanoparticles is much better than microparticles because of higher percentage of molecules present on the surface.

Table 2:Percentage of surface molecules for different particle sizes [68]

Particle diameter (nm)	Surface molecules (%)
1	100.00
10	27.10
100	2.97
300	1.00
500	0.60
1,000	0.30
10,000	0.03

A wide variety of nanoparticles are currently under investigation for carriers as a therapeutic molecule such as liposome's, cochelates, co-acervates, hydro-gels, dendrimers, polymeric micelles, carbon nanoparticle, drug nanoparticle, nanoemulsions, and other nanoparticle (e.g. magnetic nanoparticle) with each of these offering various advantages and disadvantages [69]. Each nanoparticle based delivery vehicle differs in structure with the other [70]. Nanoparticles differ based on makeup, morphology and size.

Nutraceuticals can be attached on surface, encapsulated/entrapped, adsorbed/suspended or dissolved in the nanoparticle delivery system as compiled in Figure 3. Nanoparticles not only offer prolong and good release characteristic but also protect the encapsulated agent from degradation. Depending on particle charge, surface properties, and relative hydrophobicity, nanoparticles can be designed to adsorb preferentially on specific organs or tissues. Figure 3 presents the loading mechanisms for nanoparticulate delivery systems (from left to right: a- dissolution, dispersion, absorption; b – physical/chemical adsorption, chemical bonding, layer-by-layer deposition; c –coacervation, encapsulation; and d – entrapment)

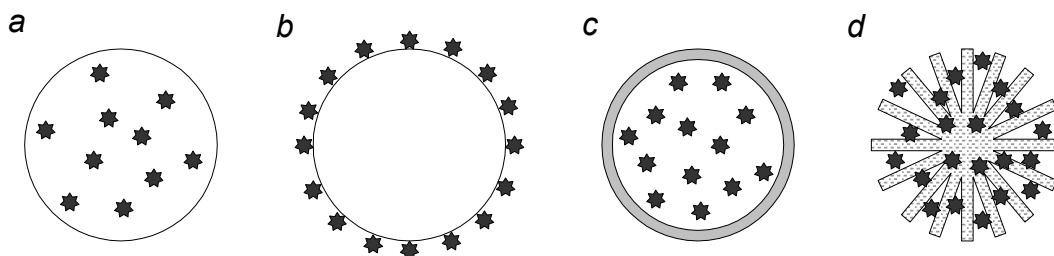


Figure 3: Loading mechanisms for nanoparticulate delivery systems

3.1.Liposomes

Liposomes are phospholipids vesicles [71-73]. The colloidal suspension consists of thermodynamically stable lipid bilayer membranes separated by a water component. These nano sized biodegradable lipid vesicles have aqueous space surrounded by a lipid bilayer. These hollow micro spheres are formed by self-assembly of phospholipids in water above their transition temperature [74-76]. Liposomes can be used for targeted delivery at 50°C (transition temperature of phospholipids) where it's content is released immediately.

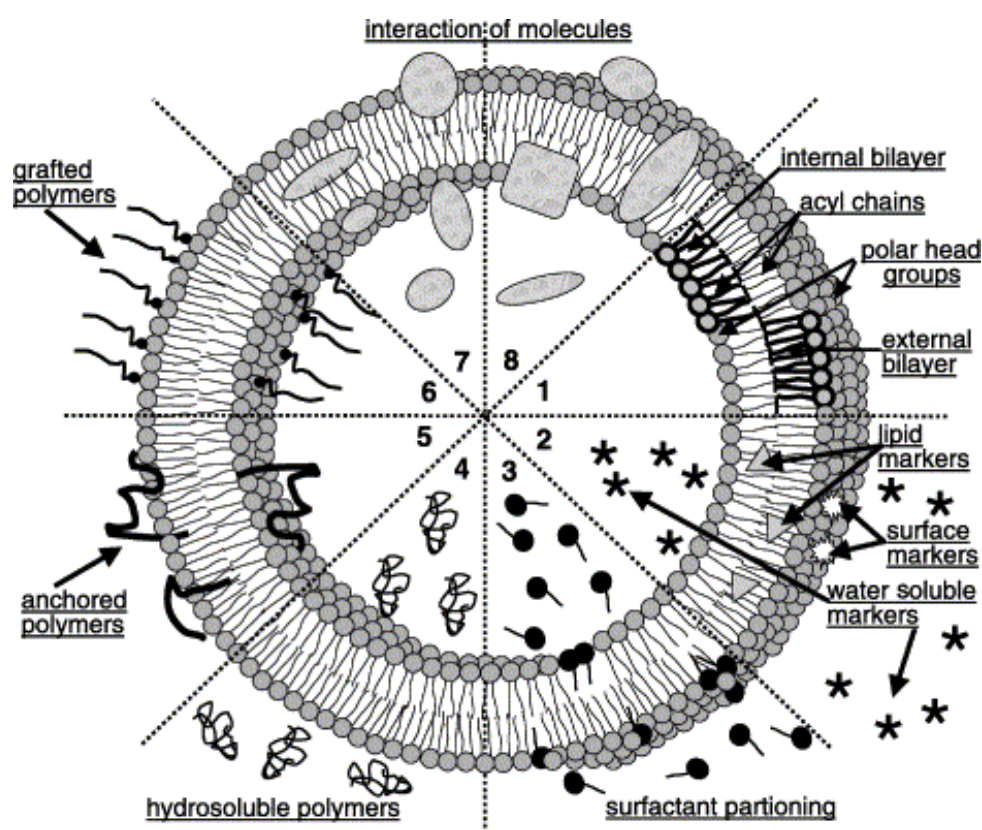


Figure 4: Schematic representations of modifications to the conventional liposome.

The biocompatibility of liposomes couple with thier amphiphilic character and smaller sizes makes them promising delivery systems. Liposomes are classified by their size and number of bilayers as either small unilamellar vesicles (SUV) (10–100 nm) or large unilamellar vesicles (LUV) (100–3000 nm). If multiple bilayers are present separated from one another by aqueous spaces, then they are referred to as multilamellar vesicles (MLV) [71, 77-80]. These phospholipids bilayer membranes can entrap both hydrophilic and hydrophobic drugs, where the lipophilic drug can be incorporated into lipid bilayer and hydrophilic drugs are solubilized in inner aqueous core. The performance of these vesicles are determined by size, surface charge, surface hydrophobicity, and membrane fluidity [81] and have been shown to be effective in reducing systemic toxicity and preventing early degradation of the encapsulated drug [82, 83].

The liposome surface could have positive or negative charges. Negatively charged lipids such as phosphatidic acids and phosphatidylglycerol usually provide surface charge to liposomes, whereas positively charged lipids such as stearylamin are used to charge lipid bilayer. In attempts to increase the specificity of interaction of liposomal ingredients to the site of its action, targeting moieties (ligands) are coupled to the liposome surface. These include antibody molecules or fragments resulting in immunoliposomes. Immunoliposomes are small molecular weight, naturally occurring or synthetic ligands like peptides, carbohydrates, glycoprotein's, or receptor ligands like folate [84]. Sterically stabilized liposomes with antibody attached on the surface have been shown to reduce tumor in mice [85, 86] . Lectin binding to carbohydrates on certain cells has been used for the synthesis of lectin-liposome conjugate by covalent binding [87]. The different

modifications of conventional liposome's are as shown in Figure 4 which shows the cationic, stealth and ligand targeted liposomes [78].

Currently liposomes are one of the delivery system applied to foods. Liposome encapsulated enzyme concentrate has been used in the curd during cheese fermentation [88]. For example, liposomes entrapped antioxidants containing ascorbic acid and α -tocopherol have provided synergistic bifunctional effect. α -tocopherol located at the emulsion interface where oxidation occurs is more effective than simply dissolved in the oil phase because it reduces the peroxy radicals before the radicals are able to initiate oxidation and ascorbic acid entrapped in the aqueous regions of the liposome could regenerate α -tocopherol. Therefore, liposomes with entrapped ascorbic acid would minimize the degradation of the ascorbic acid by other food components and ensure maximum α -tocopherol regeneration [89]. Bromelain loaded liposomes have being used as meat tenderizer to improve stability of enzymes [90]. Free nisin adheres to fat and protein leading to lower accessibility to bacterial cells, liposome has been shown to help protect nisin [91]. Incorporation of vitamin C in the inner core of liposome [92] has shown prevention decomposition against copper, ascorbate oxidase and lysine. Another example is the milk fat globule membrane (MFGM). It is a natural emulsifying agent preventing flocculation and coalescence of fat globule in milk. MFGM derived phospholipids can be used to make liposomes using micro fluidization technique. MFGM can form liposome capable of delivering bioactive compounds[93].

3.2.Nano-Cochleates

Cochleates are stable lipid based vaccine carriers and delivering formulation. Cochleates are composed of phosphatidylserine (PS), cholesterol and calcium. Cochleates have different properties and are structurally distinct from liposomes. Liposomes contain aqueous space within the compartments bounded by the lipid bilayers. Cochleates are maintained into rolled up form by calcium ions and are large, continuous, solid, lipid bilayer sheet with no internal aqueous space [94]. The two positive charges on the calcium ion interacts with negative charge on the phospholipids on the two opposing bilayers [95].

Oral administration of cochleates vaccines haave been shown to induce strong long lasting circulating and mucosal antibody response and long-term immunological response. Protein, peptides and DNA can be formulated into cochleates based vaccines [96]. Cochleates can be formulated with viral surface glycoprotein useful as vaccine delivery system. Cochleates have being shown to induce antigen specific immune response in vivo. DNA cochleates are more potent than naked DNA. Bio Delivery Sciences International has developed nano cochleates made from soy and calcium that can carry and deliver nutrients such as vitamins, lycopenes and omega fatty acids directly to cells. The company claims nano cochleates deliver omega-3- fatty acids to caked, muffins etc without affecting the color and the taste of food [97-99].

3.3. Hydrogels

Hydrogels are 3D hydrophilic polymeric networks. The network is formed by cross-linking polymer chains with covalent bonds, hydrogen bonding, Van der Waals interactions or physical entanglement [100]. Hydrogels are composed of insoluble homopolymer or copolymers and are capable of swelling in water [101]. Hydro gels have been extensively used in the development of the smart drug delivery system. This network of hydrophilic polymer can swell in water and hold a large amount of water while maintaining the structure [102]. Hydro gels can protect drugs from hostile environments e.g. the presence of enzymes and low pH in the stomach. They provide desirable protection to drugs and especially proteins from the potentially harsh environment in the vicinity of the release site [103-107].

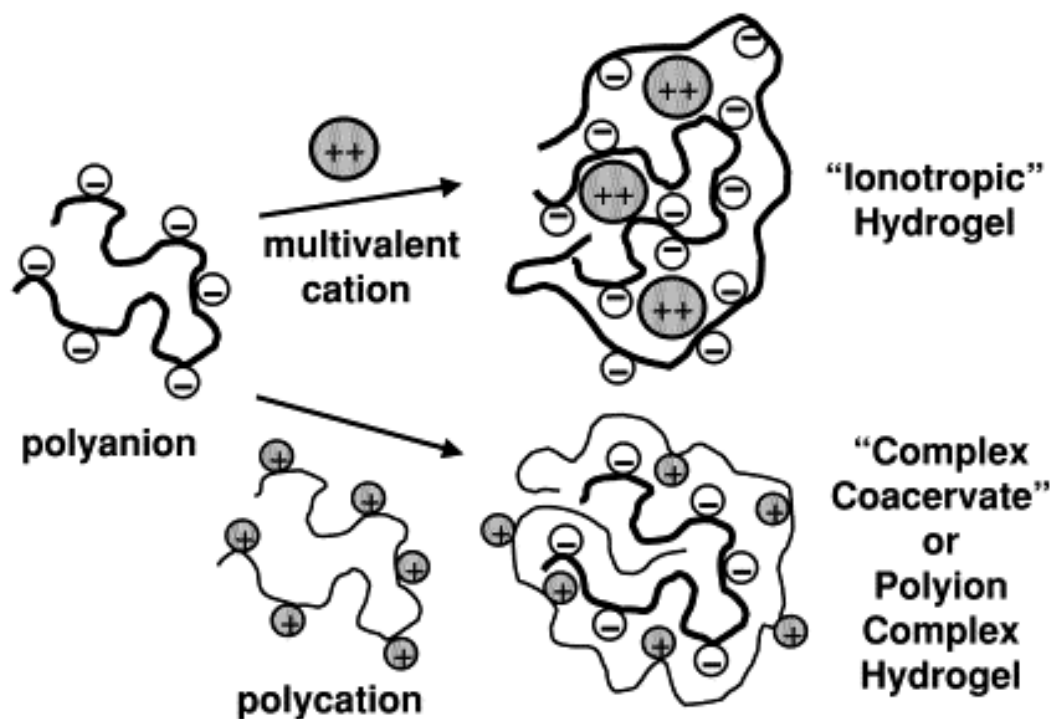


Figure 5: Schematic of methods for formation of two types of ionic hydrogels.

Hydro gels containing such 'sensor' properties can undergo reversible volume phase transitions or gel–sol phase transitions upon only minute changes in the environmental condition and are called 'Intelligent' or 'smart' hydro gels [100, 108]. The various physical (temperature, electric fields, solvent composition, light, pressure, sound and magnetic fields) and chemical stimuli (pH, ions and specific molecular recognition) can be utilized to induce various responses of the smart hydro gel systems. Hydrogels can be classified based on [104], nature of side group as neutral or ionic; method of preparation as homopolymer or copolymer; physical structure as amorphous, semi crystalline and hydrogen bonded etc and based on environmental sensitivity towards temperature, pH, ionic strength etc.

In recent years various hydro gels for drug delivery have being developed like Novels hydro gels ,environmentally responsive hydro gels connected to biosensor [102], bioadhesive hydro gels [109] , glucose sensitive hydro gels [110], pH and thermosensitive hydrogels [111, 112]. The method of formation of ionic hydrogel is shown in Figure 5 which is a schematic of methods for formation of two types of ionic hydrogels including an 'ionotropic' hydrogel of calcium alginate, and a polyionic hydrogel is a complex of alginic acid and polylysine [113]. Hydrogels contain component that are not GRAS and hence not suitable for food applications. Food proteins could be used to develop environment sensitive hydrogels[114]. Cold set β -lactoglobulin emulsion gels protect α -tocopherol under GIT conditions and that release is related to matrix degradation [115].

3.4. Micellar systems

Polymeric micelles (<100nm size) can be used as potential carriers for poorly soluble drugs in their inner core [116]. Polymeric micelles are copolymers having diblock, multiblock structure with a hydrophilic shell and hydrophobic polymer core. Figure 6 gives the schematic representation of micelle formation from amphiphilic unimers and drug incorporation by covalent binding or non covalent binding to the hydrophobic moiety [117, 118]. Micelles are formed in solution as aggregates in which the component molecules (e.g. amphiphilic AB type or ABA type block copolymers, where A is hydrophobic, B is hydrophilic component) are arranged in a spheroidal structure with hydrophobic cores shielded from water. Micelles are dynamic aggregates of amphiphilic like surfactant molecules that form spontaneously when the surfactant concentration exceeds the critical micelle concentration. However, formation of micelles is a reversible process and as the surfactant concentration falls below critical micelle concentration by dilution or other effects micelles spontaneously break up. The hydrophilic shell makes the micelle water-soluble while the hydrophobic core contributes to the microenvironment needed for the stability. First the hydrophobic core of micelles aid in the solubilization of the hydrophobic molecules in aqueous solutions because the hydrophobic molecules associate with the core microenvironment preferentially. Secondly, the incorporated compounds are prevented from diffusing out due to the steric effects [119]. There are three classes of block copolymers depending on type of functionalization [120]

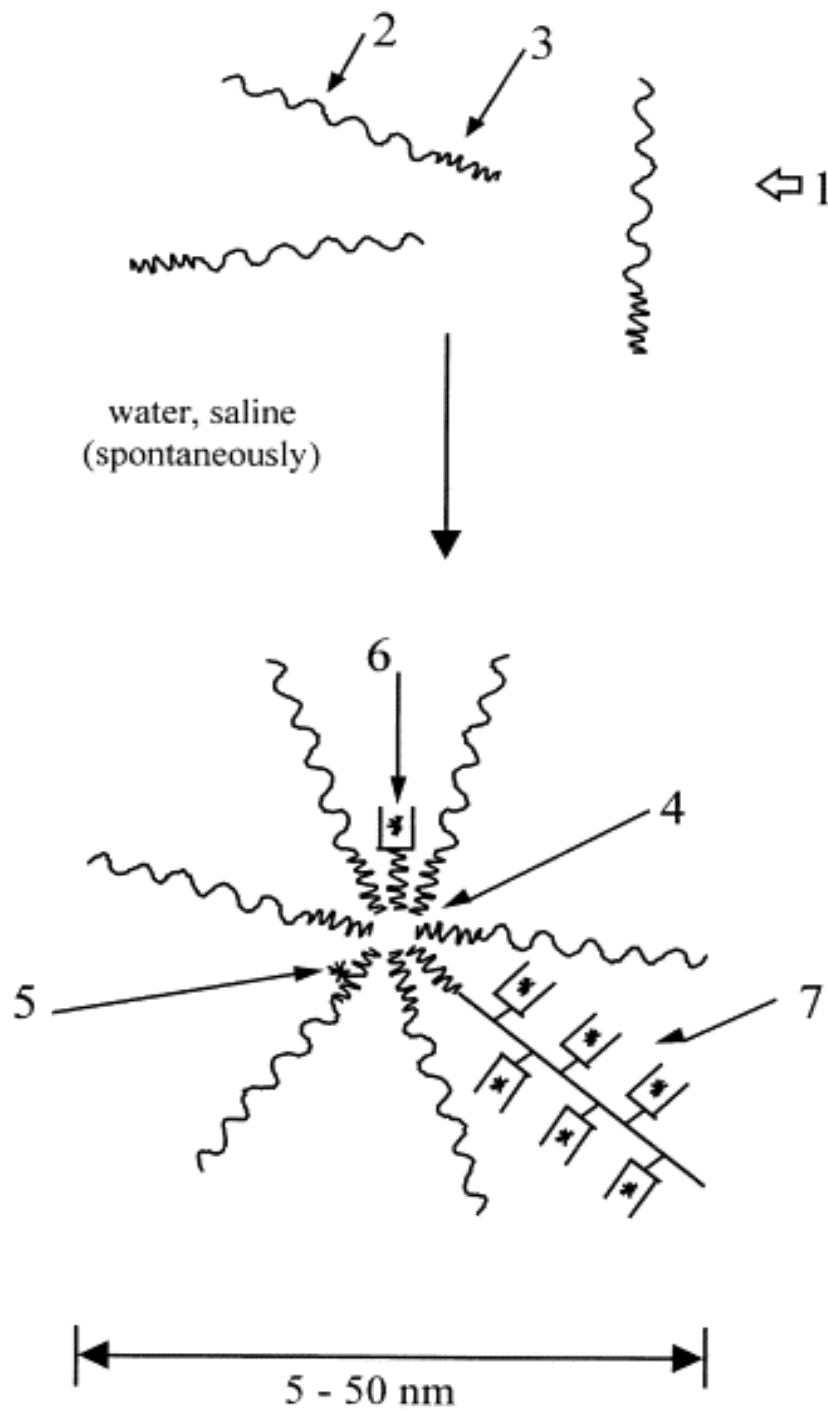


Figure 6: Schematics of micelle formation

3.5.Dendrimers

Dendrimers were discovered in early 1980's. Dendrimers are highly branched macromolecules which are organized in layers called generation and represent repeating monomer units of these macromolecules [121]. Dendrimers are branched structures consisting of three structural components: a multifunctional center core, branched unit and surface group [122]. Cavities in the core structure and folding of the branches create cages and channels. The surface groups are amenable to modification and the presence of many chain ends is responsible for high solubility and miscibility and high reactivity. Dendrimer solubility is strongly influenced by the nature of surface group. Dendrimers are highly soluble in a large number of organic solvents [123]. A number of poly (D, L, lactide) - b-polyethylene glycol (PLA-PEG) have been synthesized in this way by attachment of a methacryloyl group to the PLA chain end [124].

Dendrimers offer a great potential controlled delivery device for active compounds. Dendrimers have been shown to have potential as delivery system that can protect the drug within the macromolecular interior from its environment. This offers increased stability of the active component, tissue targeting and nanoscopic container molecules due to prolong residence time in blood circulation [122]. Drug molecules can be loaded by two methods one in the interior of the dendrimers or second attached to surface groups. Dendrimers have some unique properties related to their internal cavities. Dendrimers are stable structure for encapsulation due to the modifiable end group that allows improved water solubility and easy attachment of drug molecules. Presence of reactive functionality on the peripheral shell of dendrimers has also led to the synthesis of

dendrimer-conjugates with high control over loading of the active compounds and with reduced alteration of the physical and chemical properties of the dendrimers

When drug is embedded in the polymer matrix the release can be obtained by physical or chemical modifications such as swelling of the polymer and diffusion or chemical erosion. When the drug is covalently bound to the polymer, the drug diffuses more slowly than the free drug and can be absorbed in specific interfaces [125, 126]. Dendrimers can be used to increase entrapment of drug in liposome. Purohit et al, recently studied the [127] interaction of amphoteric cationic dendrimer with charged and neutral liposome. Amine terminated PAMAM dendrimer showed increased encapsulation of a model acidic drug in liposome. This is because dendrimers are entrapped by charge interaction that creates pH and solubility gradient across the bilayer that leads to an influx of acidic molecule into the liposome [128]. Dendrosomes, the phospholipids and dendrimer composites also offer good entrapment of the active ingredient [127, 129].

3.6. Polymeric Nanoparticles

Polymeric nanoparticle can be synthesized either from a monomer or from a preformed polymer [130]. Depending on the method of preparation nanoparticle, nanospheres or nanocapsules can be obtained with different properties and release characteristics for the encapsulated agent [131]. Polymeric nanoparticle is a collective name to nanosphere and nanocapsule [132]. Nanocapsules are vesicular systems in which the drug is confined to a cavity surrounded by unique polymer membrane. Nanospheres have a matrix type structure where active compound can be adsorbed at their surface, entrapped or dissolved in matrix [133]. Nanocapsules reservoir system in which an oily core is surrounded by a

thin polymer wall, have a polymeric shell and an inner core where active compounds are dissolved in the core or adsorbed at surface.

Polymeric nanoparticles consist of biodegradable polymer. Most biodegradable polymers consist of synthetic polyesters like polycyanoacrylate, poly (lactic acid) (PLA), polyglycolic acid (PGA), poly (-caprolactone) (PCL), poly (alkylcyanoacrylate) (PACA) [134]. Apart from these, there are several natural polymers that are used for the synthesis of nanoparticle. Chitosan, gelatin, sodium alginate and other hydrophilic/biodegradable polymers come into this category [135].

Polymeric particles used as delivery system have provided protection to peptides from extensive degradation in gastro intestinal tract [131]. Lipophilic drugs can be easily incorporated in oily core of nanocapsule or solubilized in nanosphere whereas hydrophilic compounds can be adsorbed on the surface [136]. Polymeric nanoparticles are taken up by intestinal tract [137]. Encapsulation of oligonucleotides (ODN) using nanocapsules help avoid the use of positively charged compounds to ensure ODN associations, thus avoiding the protein interaction and toxicity associated with this type of molecule [138].

Antisense oligonucleotides can be protected from cellular uptake by conjugating them with polymeric nanoparticles [139-141]. In order to completely shield oligonucleotides from nuclease attack, a new system based on polyisohexyl cyanoacrylate (PIHCA) nanocapsules with aqueous core was prepared by interfacial polymerization of isobutylcyanoacrylate in a w/o emulsion [138]. For lymphatic targeting, nanocapsules

coated with hydrophobic polymers tend to be easily captured by the lymphatic cells in the body [142].

However, the usefulness of conventional nanoparticle is limited due to its hydrophobic nature that leads to its uptake by the macrophages and thus not reaching the targeted site. A high curvature resulting in small size (<100nm) and/or a hydrophilic surface are required to reduce such opsonization reactions [143]. Small sized nanospheres have been prepared from polyvinyl pyrrolidone (50-60nm) and chitosan (100nm) [111, 144].

Surface modification with polymeric and biological materials have offered great solutions for specific applications or targeting to desired locations in the body. Developments of so-called 'Stealth' particles that are invisible to the macrophages have shown many promises. They use hydrophilic polymers that repel plasma proteins, such as polyethylene glycol (PEG), poloxamines, poloxamers and polysaccharides, to coat conventional nanoparticle surface, which can be introduced at the surface either by adsorption of surfactants or by use of block or branched copolymers [143, 145]. Use of surfactants like Polysorbate 80 on PIBCA nanospheres, polysorbate 80, poloxamer 407 and poloxamine 908 on PMMA nanospheres has been the first strategy in directing the nanoparticle. However, the covalent linkage of copolymers is the preferred method as it reduces the chance of desorption upon dilution. This approach has been employed with poly (lactic acid) (PLA), polycaprolactone (PCL), and poly (cyanoacrylate) that are chemically coupled to PEG. All of these methods are reviewed by [146, 147].

Lectins are proteins able to provide specific binding to biological surfaces bearing sugar residues located at the surface of the epithelial cells, thus rendering the polymer with

attached lectin, a bioadhesive nature [148]. An example for this is the binding of the lectins to the nanoparticle of poly(methyl vinyl ether-co-maleic anhydride) (PVM/MA) [149] and core(polyester)-shell(polysaccharides) [150].

Drug delivery for cancer therapy is one of the most important applications of nanoparticles. To achieve tumor specific targeting, antibodies that can recognize the specific antigens on the tumor cells can be attached to the nanoparticle surface [151]. The attachment can be brought about by nonspecific adsorption, specific adsorption, or by covalent linkage [152]. Non-specific adsorption is achieved by incubating the nanospheres with monoclonal antibodies (Mabs). Specific adsorption is obtained by first coupling the nanoparticle to a ligand, which can specifically bind to the antibodies. The Mabs are incubated with the precoated nanoparticle and bind to the spacer molecule via noncovalent linkage. Covalently bound Mabs offer the advantage of maintaining the integrity unlike other methods.

The several advantages associated with polymeric nanoparticle include a) small size can penetrate through smaller capillaries and are taken up by cells, b) use of biodegradable materials allows sustained drug release within the target site over a period of days or even weeks, c) in comparison to solid lipid nanoparticle or nanosuspensions polymeric nanoparticle consists of biodegradable polymer, d) increased stability of any volatile pharmaceutical agents, and are easily and cheaply fabricated in large quantities by a multitude of methods, e) a polymeric nanoparticle can be engineered specifically allowing them to deliver a higher concentration of pharmaceutical agents to a desired location, the possible chemical modification of these polymers offers great advantage and

f) polymeric nanoparticles are more stable *in vivo* and during storage as compared to liposome. The certain disadvantages include the fact that polymer conjugated drugs carrying capacity and high drug loading, influences water solubility of the product and biodistribution of the conjugate [153] and the possibility of polymer related toxicity, organic solvent residue, scaling up of production process and polymer hydrolysis during storage.

3.7.Nanoemulsions

Nanoemulsions are true emulsion with dispersed phase droplet and a continuous phase 50-100nm in diameter. The lipophilic cores separated from aqueous phase by a monomolecular layer of a surfactant material makes it suitable for nanoencapsulation of oil-based bioactive. Nanoemulsions are submicron droplet with narrow size distribution. Emulsions surface are stabilized by the adsorption of some surfactants or phospholipid. Generally, an emulsion consists of two immiscible liquids (usually oil and water), with one of the liquids dispersed as small spherical droplets in the other. Typically, the diameters of the droplets usually lie somewhere between 0.1 and 100 μm . Emulsions can be conveniently classified according to the distribution of the oil and aqueous phases. A system that consists of oil droplets dispersed in an aqueous phase is called an *oil-in-water* (O/W) emulsion, whereas a system that consists of water droplets dispersed in an oil phase is called *water-in-oil* (W/O) emulsion.

The substance that makes up the droplets in an emulsion is referred to as the dispersed phase, whereas the substance that makes up the surrounding liquid is called the continuous phase. In addition to the conventional O/W or W/O emulsions described

above, it is also possible to prepare various types of multiple emulsions, e.g., oil-in-water-in-oil (O/W/O) or water-in-oil-in-water (W/O/W) emulsions [154].

Emulsions are thermodynamically unfavorable systems that tend to break down over time due to a variety of physicochemical mechanisms, including gravitational separation, flocculation, coalescence and Ostwald ripening [155-157]. Stabilization of nanoemulsion can be achieved through electrostatic stabilization, steric stabilization or static by solid particle at interface or by increasing viscosity of emulsion.

It is possible to form emulsions that are kinetically stable for a reasonable period of time by including substances known as stabilizers, e.g., emulsifiers or texture modifiers [158]. Emulsifiers are surface-active molecules that adsorb to the surface and prevent the droplets from aggregating whereas texture modifiers thicken or gel the continuous phase improving stability by retarding or preventing droplet movement. The shelf life of emulsion based products is greatly governed by selection of the appropriate stabilizer(s).

Emulsions offer a great option for drug delivery [159, 160]. Their selective uptake into lymphatic regions is in the order oil-water > water-oil > aqueous solution [142]. Different emulsions have been compiled [160] and are listed below. The various emulsion systems are oil-in-water emulsion carrier for oil soluble drugs, lipid emulsion, water in oil emulsion for water soluble drug, self emulsifying drug delivery system, lipid nano emulsion, solid emulsions, multiple emulsions water-in-oil-in-water emulsions and modified emulsions. Emulsions currently play a significant role in food industries and the o/w, w/o, o/w/o or w/o/w emulsion types have been integrated in the food industry for

centuries. For this reason, nanoemulsions could prove to be a promising delivery system for nutraceuticals.

The several advantages of nanoemulsions include a) small size reduces gravity force and Brownian motion, which may prevent creaming or sedimentation, b) steric stabilization prevents any flocculation or coalescence of droplets and c) unlike micro emulsions which require high concentration of surfactant, nanoemulsions can be prepared with less surfactant concentration. The small size and high kinetic stability make nano emulsions suitable for delivery of active compounds in beverages

3.8. Double emulsions

Double emulsions are complex liquid dispersion system known as emulsions of emulsions in which droplet of one liquid are further dispersed in another liquid. The internal droplet can serve as an entrapping reservoir for active ingredients that can be released by a controlled transport mechanism. However sizes of droplets and thermodynamic instability are major drawbacks [161, 162]. Compartmentalized structure of a double emulsion globule is suitable for drug delivery. Using double emulsion encapsulation helps increase water solubility. The structure of a double-emulsion globule makes it a suitable possibility for applications in drug delivery, especially in case where the drug is soluble in the oil of the emulsion.

Drugs with poor solubility in aqueous media can be solubilized in the interfacial layer of emulsions. Use of double emulsions for this purpose was suggested as early as the 1960s. A double emulsion can be of two general types, water-in-oil-in-water (W/O/W) or oil-in-

water-in-oil (O/W/O). Specifically, W1/O/W2 emulsion consists of a continuous aqueous phase (W2) in which oil globules (O) are dispersed. For medical applications, a water-soluble therapeutic component can be solubilized within the inner W1 phase of the emulsion globule.

There are several advantages to this type of delivery. For instance, a therapeutic substance solubilized within the internal phase shows extended release, which can lessen toxic effects. Variations in the type and concentrations of surfactants can allow control of the stability of and release from a double-emulsion globule, making these molecules a key component in designing a double-emulsion system for any practical application [161, 163].

3.9. Lipid Nanoparticles

3.9.1. Solid lipid nanoparticle

Solid lipid nanoparticles (SLN) are comprised of a high melting point triglycerides core with a phospholipids coating and can incorporate both hydrophilic and lipophilic drugs [164-168]. Solid lipid nanoparticles were developed as an alternative carrier system to emulsions, liposomes and polymeric nanoparticle as a colloidal carrier system for controlled drug delivery. SLNs are nanoparticles with a matrix being composed of a solid lipid, i.e. the lipid is solid at room temperature and also at body temperature [169, 170]. In the solid lipid the drug mobility is considerably reduced as compared to liquid oil offering controlled drug release. The process used is melt emulsification wherein, the lipid is melted and the drug dissolved in it. In order to avoid aggregation and to stabilize the dispersions, surfactants with GRAS status are used. Solid lipid nanoparticles are

known to adhere to the gut wall and release the drug where it should be absorbed. Moreover, they have absorption promoting properties for the drug, not only for lipophilic drugs but all drugs in general. Stable drug loaded SLN with sufficient loading capacity could be formulated for controlled delivery [171]. In vivo, the fate of Solid lipid nanoparticle depends on administration route and interaction with biological surrounding. Cationic solid lipid nanoparticle is being studied for gene transfer [172, 173].

Apart from several advantages of controlled release and drug targeting, increased drug stability, high drug payload and incorporation of lipophilic and hydrophilic drug feasibility, SLNs have no toxicity of the carrier and they also avoid organic solvent and do not present a problem with respect to large scale production and sterilization. Some of the disadvantages include a) high pressure induced drug degradation, b) lipid crystallization, c) drug incorporation implied localization of the drug in the solid lipid matrix, d) coexistence of different lipid modification and different colloidal species, e) low drug loading capacity, f) storage stability issues and g) possibility of increase in particle size and drug explosion.

3.9.2. Nanostructure lipid carriers

Nanostructure lipid carriers (NLC) were introduced to overcome the potential difficulties with SLNs [174-176]. These are characterized such that a certain nanostructure is given to the particle matrix by similar process as for SLN, but in this case, the lipid matrix is prepared from a solid lipid and liquid oil [177, 178]. The compound to be encapsulated need to be sufficiently lipophilic to be used in SLN or NLC applications whereas in case

of hydrophilic they need to be made lipophilic by conjugating them with a lipid moiety [159].

3.9.3. Lipid drug conjugate

The limitations of SLN can be overcome by lipid drug conjugate (LDC). The approach for the synthesis of LDC is to incorporate soluble molecules into insoluble matrices resulting in the delay of dissolution and increase in stability. This also leads to increased permeation of lipophilic drug molecules through the gut wall. These conjugates are prepared by salt formation (e.g. amino group containing molecule with fatty acid) or alternatively by covalent linkage (e.g. ether, ester). The conjugates are melted, dispersed in hot surfactant solution, and are homogenized at high pressure [175]. The LDC have shown to have potential application in brain targeting of hydrophilic drugs [179].

3.10. Co-acervate nanoparticles

Co-acervation offers unique controlled release possibilities based on mechanical stress, temperature or sustained release. They are synthesized by phase separation process when interaction between the two biopolymers are favored in a rich solvent phase with very small amount of biopolymers and a rich biopolymer phase forming the so-called co-acervates [180-183]. The nature of interactions is electrostatic. The charge is the most significant factor affecting co-acervation and the maximum co-acervation is formed at a pH value where they carry equal and opposite charges. A very large number of hydrocolloid systems have been evaluated for co-acervation [184]. Co-acervation is typically used to encapsulate flavor oils [185] but can also be used to encapsulate fish oils

[186] nutrients, vitamins, preservatives and enzymes [187]. These co-acervates can be used to encapsulate nutraceutical for controlled release [188]. Encapsulation of nutraceutical using co-acervates enhances chemical and thermal stability.

Co-acervates from gelatin-pectin have been shown to have fat mimetic and flavor encapsulation ability [189]. Appeals of frozen baked foods have been shown to improve upon heating, through the encapsulation of flavor oil in complex co-acervates microcapsule using gelatin and gum Arabic [190]. Microcapsule of vitamin A palmitate prepared by gelatin-acacia complex co-acervates converts an oily vitamin to solid powders, prevents degradation from environment and enhances stability [188]. However, co-acervation has some disadvantages. It is expensive, complex, and cross linking of shell material involves glutaraldehyde/enzymatic cross linkers [191].

3.11. Nanocrystalline particles

Production of nanocrystals and nanosuspensions is called nanoisation [192]. Nanosuspensions solve several solubility related problems of poorly soluble drugs [193]. It consists of purely poor water soluble drugs, suspended in an appropriate dispersion media. The approach towards the synthesis of nanocrystals is based on the traditional knowledge that the dissolution of any substance is positively related to its surface area. Thus the concept of nanoionization with resultant nanocrystals of 200-400nm diameter has been thought to give increased saturation solubility.

Milling the substance and then stabilizing smaller particle with coating, forms nanocrystals in the size range for oral delivery and intravenous injection [192, 194, 195].

The drug is homogenized by high pressure homogenization [193], wet milling [196] or alternative technique like nanocrystallisation from saturated solution state or spray drying [197]. The development of nanocrystals in non-aqueous media or the media with reduced water content is called Nanopure Technology [178, 198]. The advantage of the process is that any drug or compound can be diminished to the nanoscale and temperature sensitive drugs can be processed by applying temperature control jackets or homogenizing at 0°C or below. Nanocrystals can also be injected intravenously as an aqueous nanosuspension. Stabilization of the nanosuspension is achieved by electrostatic stabilization (charged surfactants), or by steric stabilization (nonionic surfactants or polymers). The compounds that form crystals are best suited for nanosuspension technology and can be used for increasing bioavailability. Poorly soluble compounds show increased dissolution rate and absorption in GIT when formulated as nanosuspensions [199]. Oral administration of drugs in the nanocrystal form helps improve bioavailability, dose proportionality, reduce fed/fasted and inter subject variability, and enhance absorption rate [194].

3.12. Cubosomes

Bicontinuous cubic phases consists of two separate continuous but nonintersecting hydrophilic regions divided by a lipid layer that is contorted into a periodic minimal surface with zero average curvature [200]. Continuous and periodic structure results in a very high viscosity of bulk cubic phases. Compared to liposome they have much higher bilayer area to particle volume ratios. Cubosome structure can be changed by modifying the environmental conditions such as pH, ionic strength, or temperature thus achieving controlled release of carried compounds.

Cubosome may be used in controlled release of solubilized bioactive in food matrix as a result of their nanoporous structure (50-100nm) [114], ability to solubilize hydrophobic, hydrophilic and amphiphilic molecules and their biodegradability and digestibility by simple enzyme action [201]. The cubic phase is strongly bioadhesive, so maybe find application in flavor release via its mucosal deposition and delivery of effective compounds.

3.13. Polyelectrolyte

Surface coating of colloid particles with consecutive adsorption of oppositely charged polyelectrolyte forms films in nm range. Polyelectrolyte multilayer contains many charged groups available for binding metal ions. Multifunctional organic and composite film is made by adsorption or layer-by-layer deposition technique. Polyelectrolyte capsules are produced using layer by layer absorption of polyelectrolyte onto oppositely charged particles or layer of polyelectrolyte. By this method, micro particles with novel biofunctionality can be produced [202].

4. Nutraceuticals

The attempt to understand of vitamins, minerals and compounds like carotenoids, flavonoids, etc. on a molecular level supported by results from epidemiological studies can be linked to Hippocrates' statement of over 2500 years ago "Let food be thy medicine and medicine be thy food". The benefits of those compounds at the molecular level have been attributed to certain components termed as nutraceutical. These nutraceuticals create a channel where nutrition participates as medicine in preventing

disorder or diseases[203]. For example, there has been reported that people who regularly consume fruits and vegetable have being shown to have lower risk of cancer and certain other chronic diseases[8].

There have been several literature reports mentioning the health benefit of many food ingredients. Caffeine in coffee has been scientifically associated with reduced risk of type 2 diabetes, cancer and other diseases such as liver, cardiovascular; and parkinson[204]. Omega-3 fatty acid in fish oil not only is required for normal brain and nervous tissue development in fetus and young children[205-207] but also helps preventing atherosclerosis for adults as well as brings benefit in inflammation condition[208]. Vitamin is not only a critical factor in organs function but also brings much health benefit. For instance, vitamin C helps to reduce free radicals in brain[209]; vitamin E, β -carotene, and vitamin C serve as antioxidant agent to reduce oxidative stress and prevent cardiovascular diseases, cancer, and age associated macular degeneration[210]. Other antioxidant compounds widely found in foods such as carotenoids is found to be useful in prevention of cancer and cerebrovascular diseases[210]; quercetin is reported to play an important role in inhibiting lipid peroxidation and have a potential of preventing cardiovascular disease [211, 212].

Nutraceuticals are very sensitive. Vitamin loses vary in different foods considerably during both processing and storage of the final product. Stability of vitamins is affected by a number of factors outlined in Table 3 such as temperature, moisture, oxygen, light, pH, vitamin-vitamin interactions etc. [213] The most unstable vitamins are C, A, D, B and B₁₂. The breakdown of vitamins can be accelerated by vitamin-vitamin interaction [214].

Table 3: Sensitivity of some vitamins to the food matrix and environment factors

Stress factor	Light	Oxidizing agent	Reducing agent	Heat	Humidity	Acid	Alkali
Vitamin A	+++	+++	+	++	+	++	+
Vitamin D	+++	+++	+	++	+	++	++
Vitamin E	++	++	+	++	+	+	++
Vitamin K	+++	++	+	+	+	+	+++
Vitamin C	+	+++	+	++	++	++	+++
Thiamin	++	+	+	+++	++	+	+++
Riboflavin	+++	+	++	+	+	+	+++
Niacin	+	+	++	+	+	+	+
Vitamin B6	++	+	+	+	+	++	++
Vitamin B12	++	+	+++	+	++	+++	+++
Pantothenic acid	+	+	+	++	++	+++	+++
Folic acid	++	+++	+++	+	+	++	++
Biotin	+	+	+	+	+	++	++

(+ hardly sensitive; ++ sensitive; +++ -highly sensitive) [213].

Minerals are more resistant to processing but some are also lost during cooking. However they do undergo changes when exposed to. Minerals are affected by heat, air or light and may react with other food components such as proteins and carbohydrates [213].

Carotenoid (*e.g.* lycopene) can be easily isomerized by heat, acid or light. It can be easily oxidized because of the large number of conjugated double bonds [16, 215-217]. Such reactions can cause color loss of carotenoids in food and are the major degradation mechanism concern. Anthocyanins stability in food is greatly affected by pH and heat [218]. Catechins are unstable to pH and heat [219]. They are stable in black tea and unstable in green tea. Catechin isomerizes with browning at $\text{pH} > 6$. In the case of omega-3 fatty acid due to high degree of unsaturation it is very susceptible to oxidation and oxidized products are very harmful [220-223]. Incorporating these nutraceuticals into existing food formulations presents many challenges for example. on fortification of beverages with vitamin E, the disperse vitamin E droplets rise to top to form a whitish ring, increases the turbidity and changes its appearance [224] which is undesirable.

The health benefit strongly depends on the bioavailability of nutraceuticals. Bioavailability of a substance is defined as the absorption rate of that compound in a living system. Naturally, the bioavailability of a nutraceutical highly depends on its solubility. Poorly-water soluble nutraceuticals naturally have low bioavailability. For example, the solubility of curcumin a compound reported as prominent antioxidant and anti-inflammatory[225, 226] in water is very low. That decreases the rate of adsorption of curcumin in living organs. Thus, to gain the health benefit from poorly-water soluble nutraceuticals one often consumes a large amount of natural foods containing those compounds. For instance, tea catechins have been reported as a cancer prevention agents [227, 228]; however, one has to drink a huge volume of tea to have that benefit because of its low solubility in water

5. Smaller size better solubility of nutraceuticals

Solubility is the ability of maximum amount of solute to dissolve in a solvent. The intermolecular forces between solvent and solute determine the solubility. Solubility is affected by temperature and pressure as they alter this balance. Solubility is also affected by complex-forming ions and common-ion effect. Solute dissolves best in a solvent that has similar polarity to itself. Rate of dissolution is an important factor to be considered for controlled drug delivery, it depends on crystalline properties (crystalline and amorphous) and presence of polymorphism. Partition coefficient is a measure of differential solubility of a compound in a hydrophobic solvent and hydrophilic solvent. This difference in solubility poses a great challenge in incorporating them in food, and greatly affects their bioavailability in vivo to achieve therapeutic benefits.

Bioavailability refers to the degree and rate at which a substance is adsorbed in a living system or is made available at the site of physiological activity. Bioavailability of molecule is 100% when administered intravenously, but decrease when administered via other routes (for e.g. orally) due to incomplete absorption and first pass metabolism. Absolute bioavailability measure the availability of active drug in systemic circulation after non-intravenous administration, relative bioavailability measures the bioavailability of a molecule when compared with another formulation of the same molecule or bioavailability when administered via different route. Biopharmaceutics classification system guides through predicting intestinal drug absorption pattern based on solubility

and intestinal permeability (see Figure 7) and can be used as a guide for the nutraceuticals.

Bioavailability differs greatly among the nutraceuticals. For example curcumin a potent antioxidant and anti-inflammatory [226, 229] is practically insoluble in water making it less bioavailable. The bioavailability of quercetin is 17% and is strongly affected by the attached sugar moiety [230]. Bioavailability differs greatly from one polyphenol to another. The bioavailability of tea polyphenols such as Epigallocatechin gallate (EGCG) is not high. The peak plasma concentration of EGCG (free and conjugated form) is approximately 1 μM [231, 232].

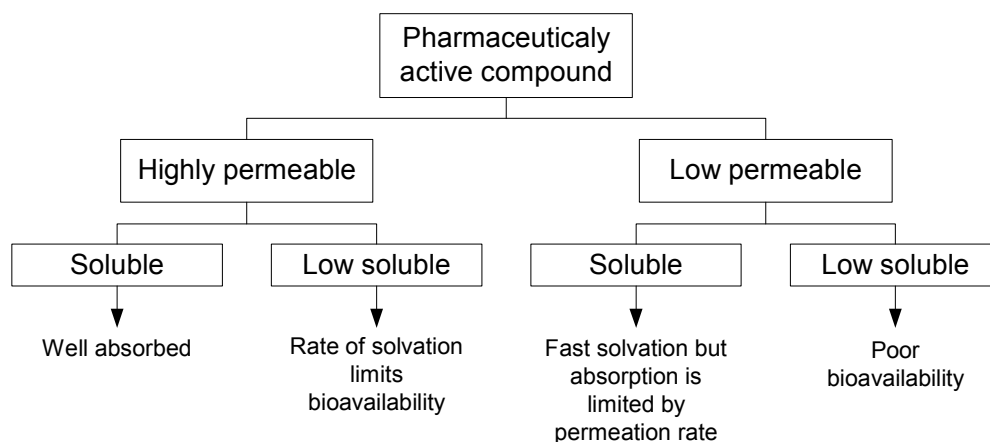


Figure 7: Intestinal absorption pattern

The bioavailability of carotenoids is also very poor [233]. Delivering lycopene which is apolar in nature is not easy. Lycopene are more bioavailable in oil than water [234]. In food carotenoids are bound to proteins further reducing their bioavailability [235-237].

Iron has very low bioavailability and adding high amounts has undesirable organoleptic effect. There are several factors in food matrix including aw, pH, osmolarity/ionic content, and presence of fats, lipid, proteins that can affect bioavailability of nutraceuticals.

There are many factors that affect bioavailability *in vivo* due to specific interaction with human tissues, like poor absorption from gastrointestinal tract (GIT), degradation or metabolism of drug prior to absorption, hepatic first pass effect, drug taken with or without food affect absorption, disease state etc. Omega 3's and 6's fatty acid could be made available *in vivo* only after they are hydrolyzed from dietary fats by pancreatic enzymes [238]. Flavonoids exist as glycosides and have low bioavailability as they are rapidly metabolized and have limited absorption [239-241]. Similar is the case for resveratrol which has low bioavailability due to rapid metabolism and elimination [242].

Another concern with nutraceutical is they cannot be readily adsorbed due to different molecular and physical forms like polarities, molecular weight, physical state, hydrophobicity, hydrophilicity etc. [243] that significantly affects their bioavailability. Overcoming cellular and tissue barriers like crossing blood brain barrier, GIT barrier etc is also a challenge for many nutraceuticals. This property causes problems in delivering these compounds in food systems as well as affects their bioavailability or absorption in biological systems, hence demanding for a delivery vehicle.

As mentioned earlier, the poor water-solubility of nutraceuticals decreases their bioavailability and their effectiveness. There are several methods to increase the bioavailability of poorly-water soluble nutraceuticals. One promising method is the use of

nanoparticles. Nanoparticles possess a very high surface to volume ratio and hence high dissolution rate. Nanoparticles have several advantages due to enhanced solubility, stability and long circulation time [133, 244-248].

Basically, the thermodynamics of a single crystal with surface area A of a compound in equilibrium with its solution phase at constant temperature and pressure is

$$\mu = \mu_0 + \sigma_{S-L} \frac{dA}{dn} \quad (1)$$

In equation (1) μ and μ_0 are the bulk chemical potential at considered temperature and at reference temperature respectively; σ_{S-L} is the interfacial surface tension; and n is the number of mole. Equation (1) can be rewritten as

$$\mu = \mu_0 + \frac{M}{\rho} \sigma_{S-L} \frac{dA}{dV}, \quad (2)$$

where M is the molecular weight of the compound; ρ is the density of the solid phase; and V is the volume of the crystal. Supposing the characteristic length of the crystal is l , the surface area A of the crystal is proportional to l^2 while its volume is proportional to l^3 . Substituting $\frac{dA}{dV} = \frac{2\varphi}{3l}$ where φ is the geometric factor into equation (2), we obtain

$$\mu = \mu_0 + \frac{2\varphi M}{3\rho l} \sigma_{S-L} \quad (3)$$

The chemical potential of solution phase is

$$\mu' = \mu'_0 + RT \ln a, \quad (4)$$

where a is the mean activity of the solute in the solution. At the saturated condition when the solid phase is large, the mean activity of the solute is a_∞ equation (4) becomes

$$\mu_0 = \mu'_0 + RT \ln a_\infty, \quad (5)$$

Combining equation (3), (4), and (5) we come to Kelvin equation for the solubility of a spherical particle size l

$$\ln \frac{S}{S_{\infty}} = \left(\frac{2M}{\rho v RT} \right) \frac{\sigma_{S-L}}{r}, \quad (6)$$

where the mean activity is replaced by the solubility; characteristic length is the radius of the particle; and v is the number of moles of ion formed by electrolyzing one mole solute. Equation (6) means that when all factors are constant the solubility of a compound increases with the decrease of the particle size. The enhanced solubility due to size reduction can be attributed to greater surface [249-251], which causes saturation solubility to increase for particle sizes of less than 1 μm according to Kelvin's equation [252]. Although there are some authors who have challenged that Kelvin's equation is applicable only for liquid – vapor systems[253], the validation of Kelvin or Gibbs – Thomson equations are proven by thermodynamic analysis [254] and several experimental works [252, 255-262]. Downsizing of a drug particle, particularly to the submicron level, boosts bioavailability due to simultaneous enhancement of the saturation solubility C_S and the reduction of diffusion layer surrounding the particles leading to the improvement of dissolution rate dC/dt [263, 264]. According to the Prandtl boundary layer equation, for a flow in contact with a flat surface, the thickness of the hydrodynamic boundary layer can be conveyed as

$$h = k \sqrt{\frac{d}{u}}, \quad (7)$$

where h is the diffusion boundary layer thickness; k is a constant; d is the characteristic length of the surface; and u is the relative velocity of the fluid against the surface. By

investigating the dissolution of solid particle in agitation, Bisrat et al. [264] have pointed out that the decreases in the size of particles associates with the decline of both characteristic length and the relative velocity. Although these two parameters frustrate, the net effect is a thinner hydrodynamic layer surrounding the particles leading to the increase in the surface specific dissolution rate [265]. Furthermore, equation (6) also implies the impact of the polymorph on the solubility of a material because each of the packaged crystal lattice gives its own density. Kipp [255] has calculated the solubility of a compound as function of particle size in different solutions. The results show that the solubility of a compound increases exponentially when particle size is smaller than 300 nm. However, when the particle size approaches 300 nm the solubility reaches its plateau.

Nanoparticles show higher intracellular uptake, 100nm particles showed higher uptake as compared to 1 μ m particles in Caco-2 cell [266]. As reported by Delie (1998), uptake of nanoparticle in the GIT tract is dependent on size, nature of polymer, zeta potential, coating with lectins or adhesion factors, or even presence of nutrients [137]. The size of nanoparticle is an important factor for uptake into the epithelial of GIT and sizes smaller than 500nm are required. Nanoparticle surface properties and hydrophilic/hydrophobic balance also affects the uptake of nutraceuticals. The submicron size of nanoparticle have helped in improving therapeutic and pharmacokinetic performance of drugs thus enabling effective drug delivery by various routes [196]. The nano size of these systems allows crossing biological barrier, ameliorates tissue tolerance and improves cellular uptake and transport [142, 267-271].

Surface property of the nanoparticle could be modified as desired to achieve controlled and targeted release of drug/nutraceutical. Nanoparticles have offered a great solution to many problems associated with drug delivery. The same could be extended to delivery of nutraceutical. Thus there is a direct clear correlation between particle size and *in vivo* exposures. It is found that nanoparticle colloidal dispersion formulation provides the highest exposure, suggesting dissolution-limited absorption. Due to small particle size and increased surface area, nanoparticles could overcome the narrow absorption window. These studies can be extended to the bioavailability and absorption characteristics of the health promoting constituents in foods. The increase in absorption can be achieved by formation of nanoparticle without affecting the mechanism of biological systems. The performance in biological systems can be further improved by controlled release and surface modification of these nanoparticles.

In vivo and *In vitro* studies have demonstrated that the nanoparticle is a promising carrier system for drug targeting. Nanoparticles have shown the ability to deliver to a wide range of varying areas in the body for sustained period of time[147]. Nanoparticle has been used to deliver hydrophilic drugs, proteins, vaccines, biological macromolecules, etc. to cells and tissues [147, 266]. The uptake of nanoparticle in endothelial cells is shown to be time and concentration dependent [272]. Delei (1998) has provided an excellent review compiling different studies on uptake of nano and micro particles by gastrointestinal tract [137]. These systems can be used to provide targeted (cellular/tissue) delivery of drugs, peptides, genes. They help solubilize drugs for intravascular delivery and improve stability of therapeutic agent especially proteins, peptides and nucleic acids against enzymatic degradation [273-275]. Overcoming the blood brain barrier is a challenge for

many drugs. Nanoparticles have been shown to be a promising alternative for delivering therapeutic molecules across the blood brain barrier [268, 270]. Nanoparticle can be formulated for targeted delivery to lymphatic system, brain, arterial valve, lungs, liver, and spleen or made for long term circulation [147].

Nanoparticle enters circulation; they are coated by plasma protein (opsonization) [276]. Opsonization renders particles recognizable by body's major defense system; whereas the Reticuloendothelial System (RES) specialized cells are phagocytic [277]. Macrophages (Kupffer) cells of liver and spleen play a critical role in removal of opsonized particles. Thus application of nanoparticle requires surface modification that would ensure particles were non-toxic, biocompatible and stable to RES.

Particles with hydrophobic surfaces are removed from circulation readily by phagocytic cells of the RES, but particles with hydrophilic surface (e.g hydrogels) are shown to clear slowly [278]. Initial disadvantages of nanoparticle such as rapid uptake by the reticuloendothelial system, due to phagocytosis by macrophages in the liver and spleen [279] had been overcome by sterically stabilizing the nanoparticle. PEGylation [280] is used for covalent modification of biological macromolecules and surfaces, shielding of antigenic and immunogenic epitopes, shielding receptor mediated uptake by RES, and preventing recognition and degradation by proteolytic enzymes. PEGylation increases size of polypeptide thus reducing renal filtration and altering biodistribution

Surface characteristics could be modified for targeted delivery [281]. The most common coatings are dextran, PEG, PEO, proloxamers and polyoxamines [282]. The role of dense

brushes of polymers is to inhibit opsonization and hence longer circulation time [146]. A further strategy in avoiding the RES is by reducing the particle size [133, 269].

Nanoparticles adhere to surface of intestinal mucosa through bioadhesion process increasing bioavailability [152]. The bioadhesion could occur through specific (ligands) or nonspecific (surface properties) interactions. Bioadhesive potential of a drug delivery system is affected by the affinity of the material to biological support, intensity of phenomena, relative duration of adhesive bonds, and elimination rate of adhered particle [149]. Modification of surface properties of PVM/MA nanoparticles with BSA and lectin has shown to affect the adhesive property of the nanoparticles. Nanoparticles could be targeted to specific cells and locations in body with help of appropriate ligands. The carrier can be activated by change in environmental pH, chemical stimuli, magnetic field, heat etc. Nanoparticles have offered several solutions towards specific and targeted delivery of several anticancer drugs like paclitaxel, doxorubicin, 5-fluorouracil, camptosor and topotecan solving different issues associated with each drug [283]. These issues include decreased solubility in aqueous solution, number of side effects, faster clearance and high hydrophobicity respectively.

Nanoparticles are very effective in controlled delivery of drugs. This characteristic property can be correlated to the food systems. Production of nanoparticle has proved to be an effective tool in dealing with solubility problems in case of drug delivery. The oral delivery of drug particles in the form of nanoparticle has following advantages: improved bioavailability, improved dose proportionality, and enhancing absorption rate. For the

optimal drug action, the most efficient way is to deliver the drug to the desired site of action in the body and decrease or avoid the side-effects at non-target site.

Various drug delivery systems such as liposome's [71], solid lipid nanoparticles [284], micelles [285], polymer micro/nanoparticle [286] have shown much promise in controlled release and targeted drug delivery. Among them, biocompatible and biodegradable polymer nanoparticles were the more preferable candidate for DDS [135]. The food particles act similar to drug particles. Thus conversion of coarse particles of nutraceutical compounds to nanoparticle or nanosuspensions can be effective in handling the solubility and bioavailability problems in delivery of nutraceutical [287].

Similar to drug delivery there are different goals to be achieved in food nutraceutical delivery. Nutraceuticals need to be made further bioavailable and protected from the environment (heat, moisture, and oxidation) and delivered to the appropriate site for them to perform the required function. These following factors as compiled in Table 4 provide some design insight for delivery vehicles.

Table 4: Comparative challenges for delivery nutraceuticals: in-food and in-vivo

In food:	<i>In vivo</i>
<p>High concentration of actives required to provide specific health benefits</p> <p>Disagreeable taste and aroma associated with most nutrients</p> <p>Chemical instability and undesirable interaction with other ingredients in the food system.</p> <p>The risk of reduce bioavailability due to active inability to reach its target site to provide desirable functionality</p> <p>Poor solubility.</p>	<p>To protect the nutraceutical</p> <p>To control the duration of action of the nutraceutical</p> <p>Maintain nutraceutical levels in the human body</p> <p>Target the nutraceutical to particular part or cells in the body</p> <p>Overcome certain cellular and tissue barriers etc</p>

NANOPARTICLE MANUFACTURING

1. Milling

The traditional methods for decreasing particle size is milling including pearl or jet milling, where particles are broken down through grinding or collisions under high pressure. In pearl milling, the particles are filled into a milling container with milling media. The grinding chamber contains several pearls made of glass, zircon oxide or special polymers such as hard polystyrene derivatives. The mixture is agitated by a stirrer. The particles are ground to nano size in the gap between the pearls while the pearls are moving. The moment of collision in which particles are trapped between two colliding pearls is shown in Figure 8. The collision of particles during milling contains three stages. It starts with the compaction of particles in zone I on the left of the pearls and follows by the sliding of particles in the gap between the pearls (zone II) where particles are compressed, deformed then cracked. In the third stage of the grinding, particles are released from the, gap fracture and produce secondary particles with smaller size. The crack propagation of particles during milling process is well described by Griffith theory in which the fundamental principle of size reduction in pearl milling lies in the energy transferred to the particles under compression by the pearls in milling media. According to Griffith theory, when a particle cracks it loses energy due to new surface formation, $U_s = 4\gamma l$. However, the particle also gains energy released from the strain energy when the crack develops, $U_m = \frac{\pi l^2 \sigma_A^2}{E}$. The total energy of the particle is

$$U = 4l\gamma - \frac{\pi l^2 \sigma_A^2}{E}, \quad (8)$$

where γ is the specific surface energy which is the energy per unit area required to break the bond of the milled material; σ_A is the stress applied on the surface A of the particle; E is Young's modulus of the particle; and l is half of the crack length. The crack grows when instability occurs. That mean $dU/dl = 0$. Thus, the critical stress applied on the particle surface is

$$\sigma_{crit} = \sqrt{\frac{2\gamma E}{\pi l}}. \quad (9)$$

According to Varin et al.[288] and Kim et al. [289] the fracture resistance increases as the size of particles decreases. That brings a limit size to the fineness of the particles as milling process continues. Because the cohesion among particles increases with the decrease of particle size, small particles tend to agglomerate on the surface of the larger ones or adhere on the pearl surface. That reduces friction among particles as well as friction between the pearl and the particles. Furthermore, the large cohesive force causes agglomeration that prevents the particles from fracture. In addition, the viscosity of milling media increases with the decrease of the particle size. Those factors contribute to the performance of pearl milling [290]. To improve the output of pear milling, polymer is added into the milling media. The polymer prevents particle agglomeration by providing steric stabilization. Besides, low molecular polymer molecule may penetrate into the crack that increases osmotic pressure leading to the development of fracture. Pearl milling consumes energy. Most of power supplied to the machine is utilized on moving the pearls because they occupy 80% volume of grinding chamber. Another disadvantage of pearl milling is the potential erosion of material from the milling pearls leading to

product contamination [291]. Furthermore, milling yields large particle size distribution. Milling media still remains in the nanosuspension. Those bring disadvantages to formulation.

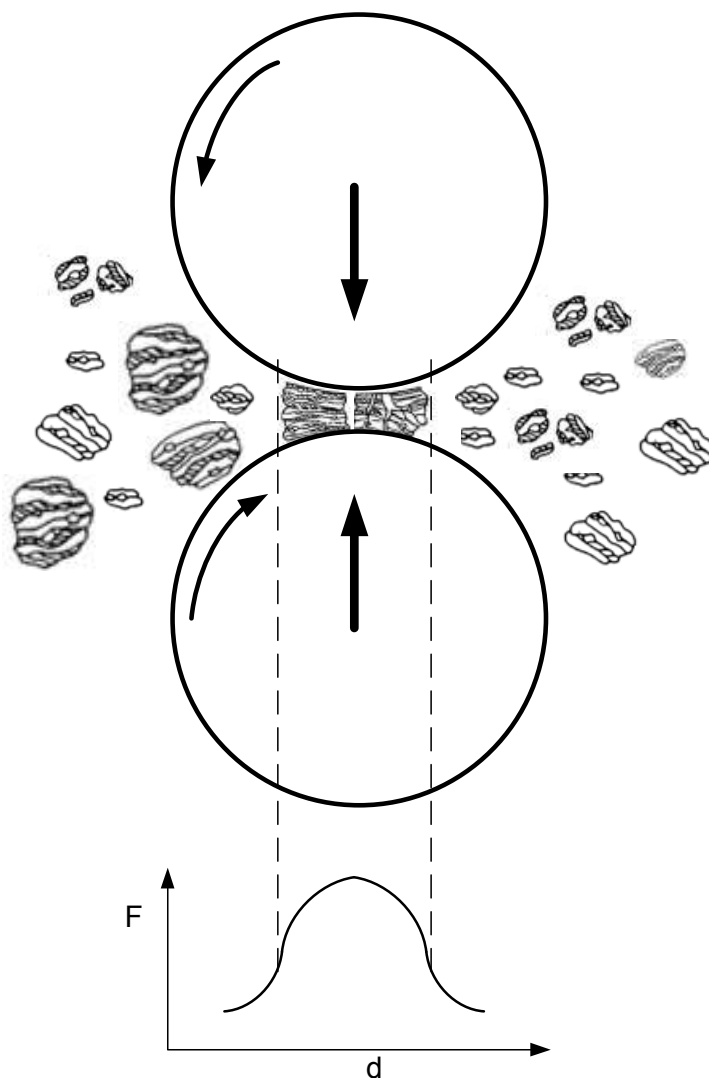


Figure 8: The collision of particles during pearl milling

In jet milling particles break under collision. The breakable energy in jet milling is similar to that in pearl milling i.e. equation (9). The gas stream sweeps the powder particles into grinding chamber due to negative pressure caused by venturi effect. The

feeding is continuously introduced to the milling chamber where the particles collide with each other or with the grinding chamber wall. When collisions take place, elastic deformations are produced leading to the generation of tension at the surface of the particles. If the stress on the surface of particles exceeds a critical value crack extension occurs. The fine particles are collected by gas stream after passing cyclone separator. Figure 9 shows a typical jet milling chamber with nozzle angle θ which is the tangent to grinding chamber. In Figure 9, the dash - dotted represents the outlet stream and the curve arrow stands for the circular stream for particle separation. If the particles are treated with blasts before size reduction the milling result will enhance due to the formation of microcracks [292].

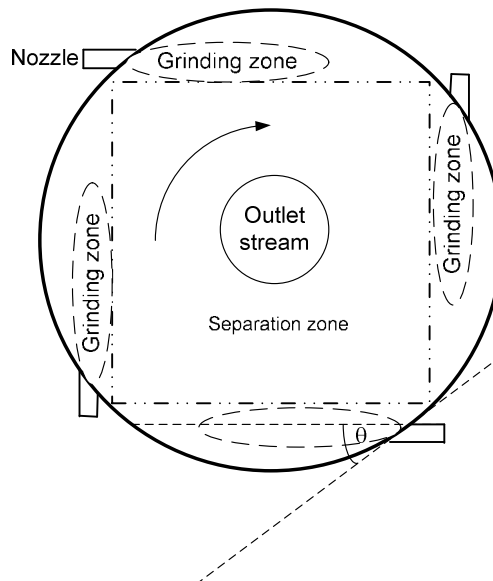


Figure 9: Jet milling chamber

The number of nozzles is an important feature for jet mill design. Keeping constant the total section of the nozzles, and the grinding gas rate, Skelton et al. [293] investigated

three alternative configurations, with 3, 6 and 12 nozzles at different feeding rate. The authors have suggested that the device of 12 nozzles give the best grinding ratio. The impact of number nozzle on grinding ratio can be explained by the fact that the greater the number of grinding nozzles is the more regular the pitch-circle is. Moreover, large number of grinding nozzles generates thinner jet leading to a minor perturbation of the spiral flow in the chamber. The authors have also recognized that the grinding ratio is improved at higher feeding rate. Because the jets form a circle separating the grinding and classification zones, it appears clearly that the nozzle angle decides the size of both areas and the grinding ratio of the product. Furthermore, the penetration of the nozzle jets in the gas stream is determined by this angle. Thus, it can be considered that the kinetic energy transmitted to the particles is determined by the relative velocity of gas flowing at the intersection. Therefore, the intensity of the collisions depends on the nozzle angle. According to Skelton et al. [293] this angle is between 52 and 60°.

As mentioned earlier, high feeding rate gives better grinding ratio. However, too high feeding rate can cause choke due to the instability of the solid- flow in the grinding chamber. Choking causes discontinuous discharge of the mill, and, consequently, larger particle size distributions. Another major parameter in jet milling is grinding pressure, which defines the gas mass flow rate input. Assuming that the nozzles are isentropic, according to the 'Barré de Saint Venan' equation, the relationship between initial grinding pressure P and the pressure at the nozzle throat P_t are

$$\frac{P}{P_t} = \left(1 + \frac{C-1}{2} M^2 \right)^{\frac{C}{C-1}}, \quad (10)$$

where M is Mach number at the orifice; and C is the heat capacity of the gas. The critical pressure corresponding to the minimum of pressure necessary to get a sonic flow at the nozzle exit is

$$P_c = P_t \left(\frac{C+1}{2} \right)^{\frac{C}{C-1}} . \quad (11)$$

Therefore, the mass flow rate of the gas at the throat of the nozzles with radius r at pressure $P > P_c$ is

$$\dot{m} = \pi r^2 P \sqrt{\frac{MC}{RT} \left(\frac{2}{C+1} \right)^{\frac{C+1}{C-1}}} . \quad (12)$$

The power supplied as gas kinetic energy for sonic nozzles can be expressed as $E = 0.5\dot{m}v^2$ where v is the gas velocity at the nozzle throat. Typically, neither jet milling yields particles without residue erosion nor milling media. However, like pearl milling, jet milling also requires expensive equipment and a substantial energy input.

2. High pressure homogenization

High pressure homogenization is widely used to manufacture nanosuspensions and nanoemulsions. There are two types of homogenizers including microfluidisation and piston – gap homogenizers. In microfluidisation, a jet stream of suspension is accelerated and passes with a high velocity through a homogenization chamber which has ‘Z’ shape [294]. The flow direction of the suspension changes a few times in the grinding chamber leading to particle collision and shear forces. In piston – gap homogenizer, the suspensions are suddenly pumped across the gap of the homogenizer under high pressure.

The diameter of the piston cylinder is 3cm while that of the gap is 25 μm as shown in Figure 10.

According to Bernoulli's equation, the velocity of the suspension increases leading to the simultaneous decrease in static pressure below the boiling point of water at operation temperature in the gap. As a result, water starts boiling, leading to the formation of gas bubbles. When the suspensions leave the gap, the bubbles implode to form cracks in the particles and the pressure achieves atmospheric pressure. Besides the implosion forces which are sufficiently high to break down the microparticles into nanoparticles, the collision of the particles at high speed also contributes to the achievement of particle size reduction. To achieve nano size, a sufficient high energy input is required to break down the particles into the nanometer range.

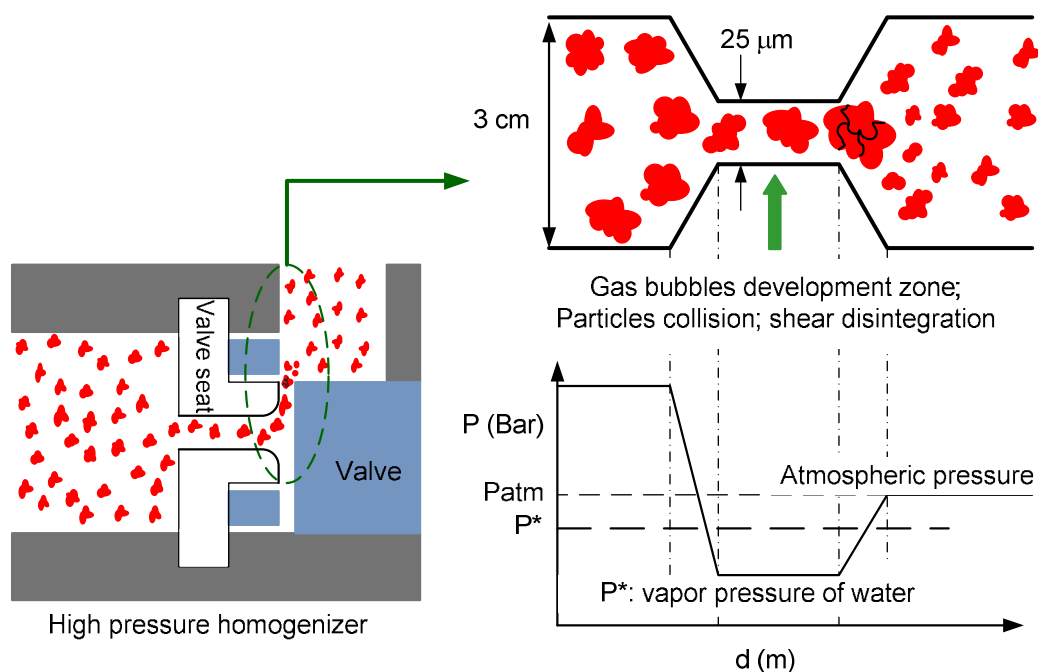


Figure 10: Particles break under high shear in high pressure homogenizer

According to Klinksiek and Koglin [295] the average droplet size, d , of nanoemulsion manufactured by jet dispergator is a function of the differential pressure drop, ΔP ; the interfacial surface tension, σ ; the viscosity of the continuous phase, μ_c , and that of dispersed phase, μ_d ; the density of the particles, ρ_d ; and the diameter of the gap, d_g .

This relationship has been provided as

$$d = \frac{C d_g^{0.165} \sigma^{0.365} \mu_d^{0.495}}{\Delta P^{0.6} \mu_c^{0.025} \rho_d^{0.235}}, \quad (13)$$

where C is a constant depending on the system. Interfacial surface tension plays a role in particle breakup. Therefore, viscosity enhancers are sometimes added into the microsuspensions to improve the efficiency of size reduction.

The size of the nanoparticles depends mainly on the number of homogenization cycles, operation temperature, and power density which relates to the pressure drop in the homogenizer gap. During a milling process, the particles break advantageously at their imperfections. When the particles become finer, the number of flaws decreases. It means the remaining particles approach perfect. Thus, the force required to break the crystals increases with decreasing particle size. That defines the finest size the particles can reach. When the particles approach to the size limit, the force (power density) in the homogenizer chamber is equal to the interaction forces in the particles, and the size reduction will not further improve, regardless of the number of homogenization cycles applied. That means the maximum size reduction at the given power density is reached. Therefore, in general, to obtain smaller sizes it requires more energy (higher differential pressure), e.g. from 500 to 1000 or 1500 bar [294]. Thus high pressure homogenizer is a

high energy consumer. Another disadvantage of high pressure homogenizer is that it requires microsuspensions as an input to manufacture nanosuspensions.

3. Solvent – based method

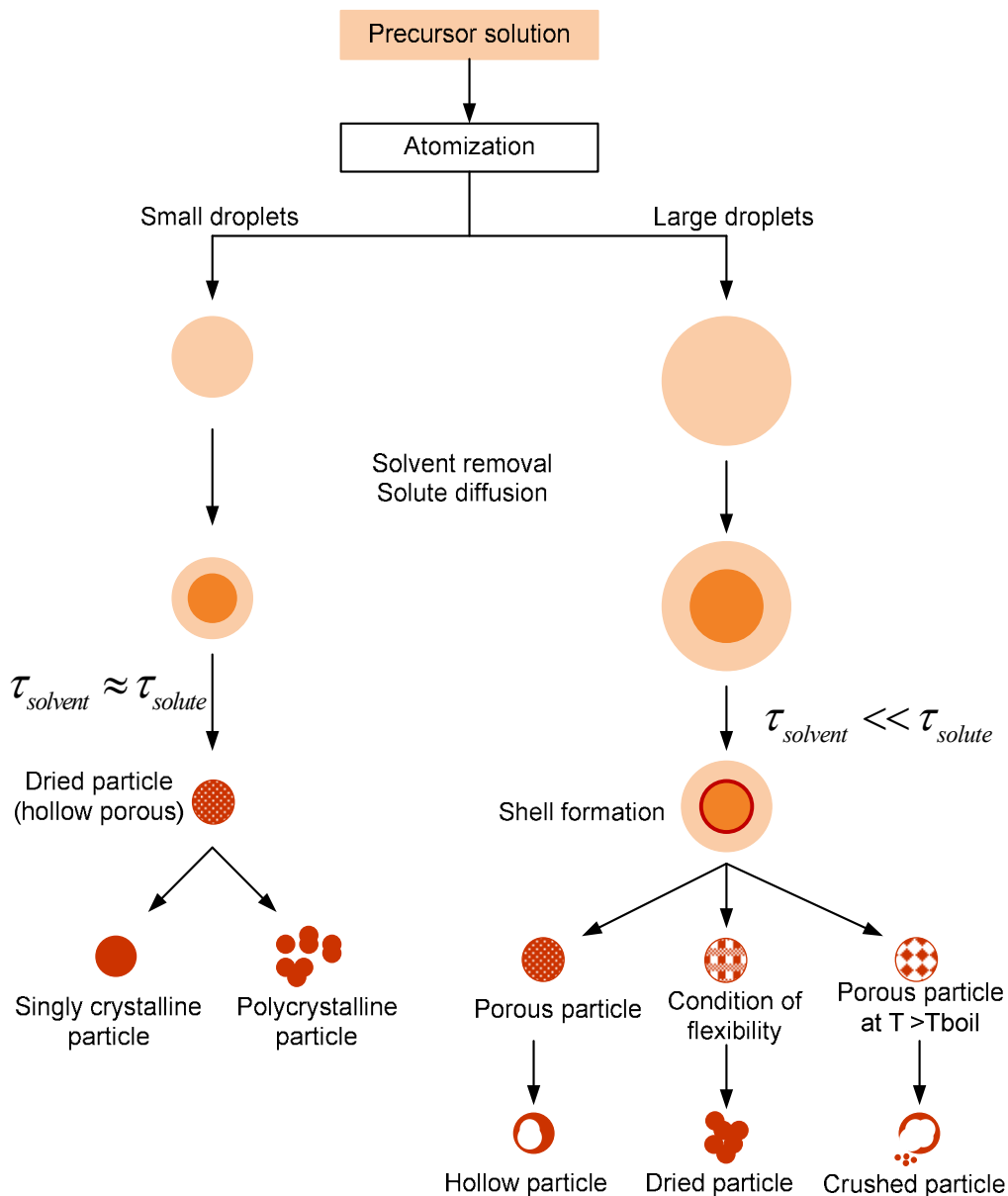


Figure 11: Morphology of particle prepared by spraying method [296]

To prepare nanoparticles from the solvent – based method, poorly-water soluble compound is dissolved in a suitable solvent. Then, the solution is atomized into tiny droplets to remove the solvent. For example, a poorly-water soluble compound is dissolved in organic/water cosolvent system. The solution is then sprayed into supercritical CO₂ [297, 298] to extract the solvents. Particles are formed due to the extraction of solvents out of the spraying droplet and the precipitation of solute at super saturated condition due to solvent removal. Therefore, high mass transfer is required to prevent the particles from agglomeration and reduce the drying time [298-301]. To obtain high mass transfer, the solvents must be soluble in liquid CO₂, such as tetrahydrofuran/water [297], dimethyl sulfoxide, dichloromethane, or ethanol[299]. Instead of spraying drugs solution into supercritical CO₂, the solutions of drugs in organic solvents are atomized into boiling halocarbon cryogen [302], halocarbon refrigerant [303] or liquid nitrogen [304] to lyophilize. Hebert and Healy [305] as well as Gombotz et al [306] have atomized the organic feedstock in to gaseous nitrogen before applying liquid nitrogen to evaporate the solvent. Another approach of the solvent – based method is the combination of rapid expansion from liquefied – gas solution into aqueous surfactant solution to obtain nanosuspensions of poorly-water soluble drugs [307, 308]. This process stimulates rapid nucleation of the solute due to the quick expansion of supercritical fluid at atmospheric pressure.

The removal of the solvent causes the precipitation of solute within the droplets leading to the formation of nanoparticles. The size of the particles and their morphology are functions of spraying precursor solution concentration, size of initial droplet at the spraying nozzle, and the rate of solvent removal. A variety of atomization methods has

been used in spray pyrolysis studies, such as air – assist or a two-fluids nozzle, ultrasonic, vibrating orifice and spinning disk [309]. The morphology of the particles depends on the rate of solvent removal and the diffusion rate of solute inside the droplet as summarized in Figure 11. Solvent – based methods are not attractive because residual solvent presents a safety and regulatory problem. Furthermore, it requires specialized equipment for the manufacturing of nanoparticles.

4. Emulsion as template method

Emulsion as template method has been used for manufacturing polymeric nanospheres for decades. The polymerization reaction occurs within isolated nanoemulsion droplets of monomer [310-312]. It has been applied in the manufacture of solid lipid nanoparticles (SLN) as early as 1990's [313]. SLN are particles made from solid lipids which are solid at room temperature and also at body temperature and stabilized by surfactant [314-317]. A poorly-water soluble active pharmaceutical ingredients (API) is loaded in molten lipid then mixed with hot aqueous surfactant solution to obtain coarse emulsions. The emulsions are then passed through a high pressure homogenizer at high temperature for nanoemulsions. SLN particles are obtained by solidifying the nanoemulsions. In cold homogenization process, the lipid loaded API is rapid solidified in liquid nitrogen or dry ice. After that, it is milled to obtain micron size particles before dispersion in aqueous surfactant solution. The obtained microsuspensions are homogenized at room temperature for SLNs. The procedures of SLNs preparation are summarized in Figure 12.

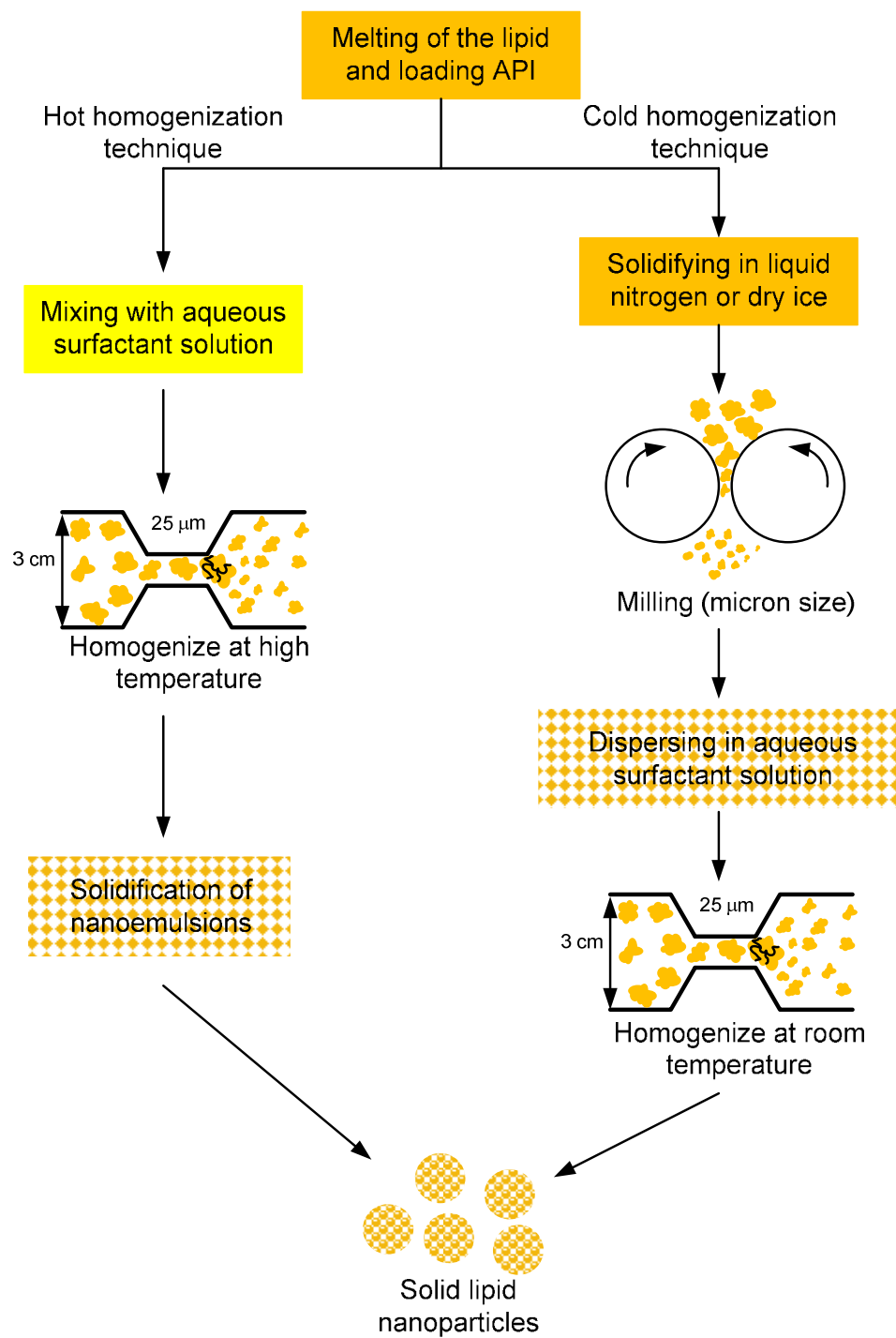


Figure 12 : Schematic procedure of preparation solid lipid nanoparticles [318]

Recently, emulsion as template method has been applied to prepare nanoparticles of poorly-water soluble APIs. Briefly, poorly-water soluble API is dissolved in either volatile organic solvent or partially water-miscible solvent. Such solvents can be used as the dispersed phase of the emulsion. There are two ways of fabricating drug nanosuspensions depending on type of organic solvents used. In the first method, a solution of a volatile organic solvent or mixture of solvents loaded with an API is dispersed in the aqueous phase containing suitable surfactants to form nanoemulsions. After that, pressure is reduced to evaporate the solvent to obtain API nanoparticles due to the instantaneously precipitation of the drug. Because the precipitation of the API is isolated in each emulsion droplet, it is possible to control the particle size of the nanosuspension by controlling the size of the emulsion. The drug loading capacity of the nanoemulsions is regulated by its solubility in the organic solvent used. Originally, methylene chloride and chloroform were used to dissolve APIs for the dispersed phase of nanoemulsions[319]. However, those compounds are environmental hazardous and unsafe for humans. They have raised concerns about residual solvents in the nanosuspension. Therefore, this process has become limited in routine manufacturing processes. Later, relatively safer solvents such as ethyl acetate and ethyl formate have been still considered [320-322]. The second method makes use of partially water-miscible solvents which are much safer than those mentioned above such as butyl lactate, benzyl alcohol and triacetin as the dispersed phase [248, 323]. The nanoemulsions are prepared by the conventional method. Then they are diluted to obtain API nanosuspensions. The dilution of the nanoemulsions with water causes complete diffusion of the solvent from emulsion droplets into aqueous phase, leading to immediate

formation of a nanosuspension. The API nanoparticles formed can be separated from the aqueous phase and surfactants by means of ultra filtration in order to make it suitable for administration. However, if all the ingredients that are used for the production of the nanosuspension are present in a concentration acceptable for the desired route of administration, then simple centrifugation or ultracentrifugation is sufficient to separate the nanosuspension.

Emulsion as template method has several advantages. It does not require special equipment for manufacturing particles with designed purposes. The process is simple and easy to optimize properly. However, this method can be applied only for compounds soluble in organic solvents or in lipid. Therefore, it raises a concern of hazardous solvent in the nanoparticles when organic solvents are in the process. Furthermore, high amount of surfactant is needed to stabilize the nanoparticles.

5. Objective

In this chapter, the current background, theory, and application for the manufacture of nanoparticles has been detailed. It is important to note that although many techniques including milling, homogenization, solvent-based method, and emulsion as template process have been refined over the past few years, the emulsion as template approach using water miscible compounds fulfills the criteria as a method that is simple, robust, and capable of manufacturing nanoparticles of poorly-water soluble compounds. However, there are several unclear factors, for example what is the breakup mechanism of emulsion droplets while high stress is applied; how does the surfactant impact the formation of nanoparticles when the nanoemulsions are diluted? Furthermore, there is an opening question of using GRAS compounds to manufacture nanoparticles of

nutraceuticals. Therefore, we hypothesis that some FDA GRAS chemicals can be used to directly manufacture nanoparticles of nutraceuticals without chemical modification by the utilization of emulsion as template technique. Based on the hypothesis, several goals intended to be addressed:

1. To discover the breakup mechanism of emulsion droplet to control particle size distribution.
2. To define the optimum operation parameters for preparing nanoparticles using rotor-stator homogenizer.
3. To develop a “green” and scalable method for preparing nanoparticles of poorly-water soluble nutraceuticals.

MATERIALS AND METHODS

1. Materials

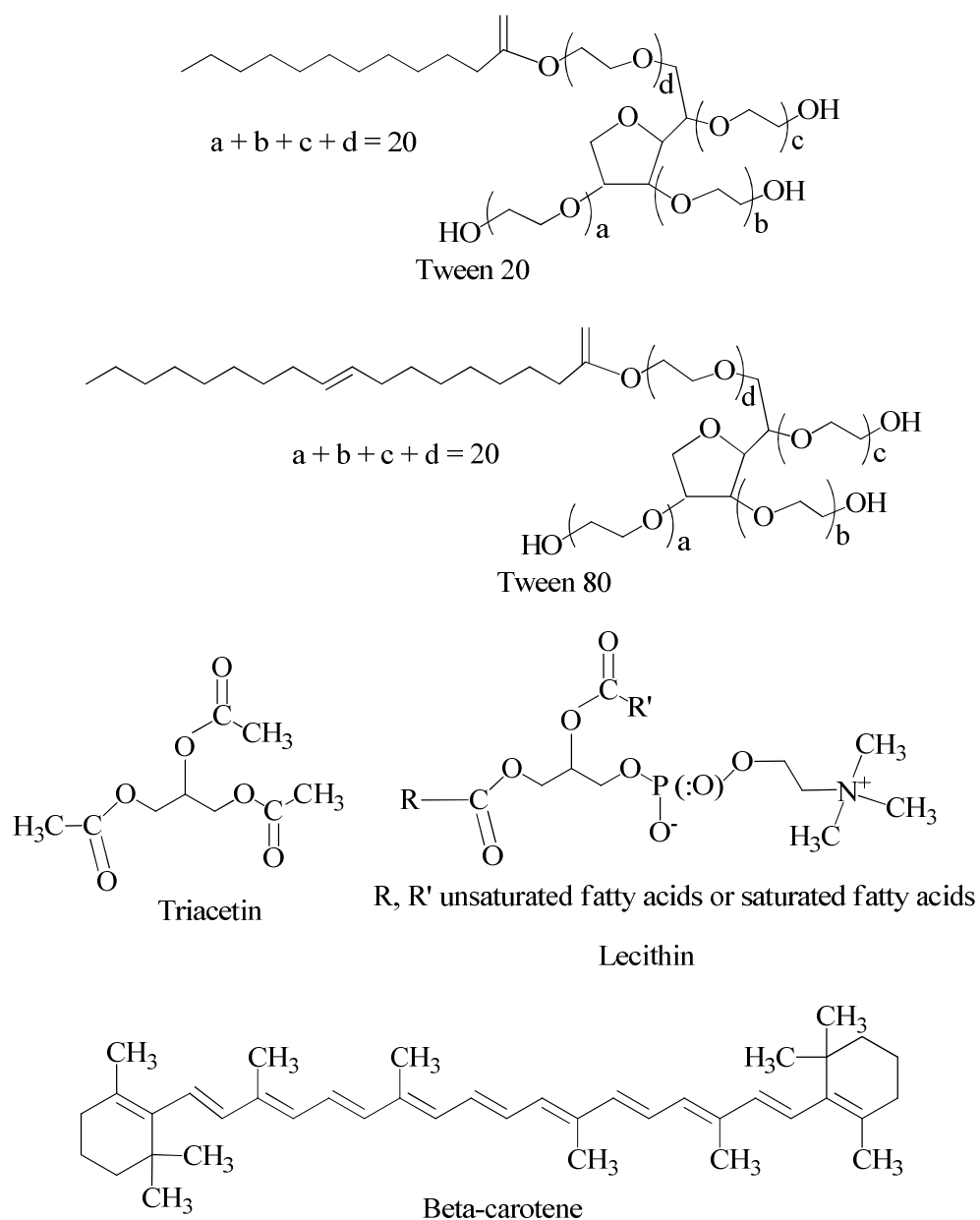


Figure 13 : The structure of chemicals used in the research

The materials used are all GRAS by the FDA. The nutraceuticals model is β -carotene purchased from Sigma Aldrich. Triacetin purchased from Spectrum Chemical MFJ. Corp. is selected as oil for dispersed phase because its solubility in water is approximately 7% (w/w). The three surfactants investigated are all non-ionic. Tween-20 was purchased from EMJ. Tween-80 was purchased from Spectrum Chemical MFJ. Corp. These surfactants have relatively high hydrophile-lipophile balance (HLB) values (16.7 and 15.0, respectively), so they prefer water phase. Soy lecithin refined was purchased from MP Biomedical LLC. Its HLB is quite low (4-5).

1.2. Beta-carotene

Beta – carotene (MW = 536.87 g/mol) is a strongly-colored red-orange pigment which is abundant in plants and fruits. The compound is chemically classified as a hydrocarbon and specifically as a terpenoid (isoprenoid), in order to emphasize that it is synthesized from isoprene units. β -carotene is biosynthesized from geranylgeranyl pyrophosphate [324]. It has beta-rings at both ends of the molecule as shown in Figure 13. Beta – carotene contributes to the orange color of many different fruits and vegetables. The composition of carotenoids on food and their dietary intake have been well studied and published [325-327], and the data has been used as guidelines for healthy diet. According to USDA the following foods listed in Table 5 contain highest beta-carotene content per serving [328].

Table 5: The 10 foods having the highest beta-carotene content per serving

Item	m of food (g)	m β -carotene (mg)	β -carotene portion (ppm)
Carrot juice, canned	236	22	93.22034
Pumpkin, canned, without salt	245	17	69.38776
Sweet potato, cooked, baked in skin, without salt	146	16.8	115.0685
Sweet potato, cooked, boiled, without skin	156	14.7	94.23077
Spinach, frozen, chopped or leaf, cooked, boiled, drained, without salt	190	13.8	72.63158
Carrots, cooked, boiled, drained, without salt	156	13	83.33333
Spinach, canned, drained solids	214	12.6	58.8785
Sweet potato, canned, vacuum pack	255	12.2	47.84314
Carrots, frozen, cooked, boiled, drained, without salt	146	12	82.19178
Collards, frozen, chopped, cooked, boiled, drained, without salt	170	11.6	68.23529

Among 100 carotenoid compounds found in richly colored fruits and vegetables, beta-carotene and four other carotenoids are classified as pro-vitamin A carotenoids. In theory, beta-carotene can be metabolically cleaved into two molecules of vitamin A, an essential vitamin necessary for normal development, growth, and eyesight [329, 330]. It is an antioxidant with a high capacity of capturing reactive oxygen species and free radicals to inhibit oxidative stress [331, 332]. β -carotene plays a role in the prevention of cancer

Table 6: Biochemical functions of beta-carotene in humans

<ul style="list-style-type: none"> • <i>Vitamin A formation</i> As a major source of vitamin A for humans, Beta-carotene is converted to vitamin A by the enzyme β – carotene 15, 15' – monooxygenase [352-354]. • <i>Lipoxygenase</i> [355] β-Carotene restrains the oxidation of linoleic acid by soybean lipoxygenase as well as the formation of the hydroperoxide product. Lipoxygenases are involved in arachadonic acid metabolism and progesterone production which is required for pregnancy [356, 357]. • <i>3-Hydroxy-3-methylglutaryl coenzyme A (HMG CoA) reductase (EC 1.1.1.34)</i> [358] Beta-carotene inhibits HMG-CoA reductase which participates in atherosclerosis and cardiovascular disease [359]. • <i>Connexin43</i> [349, 360-362] Beta-carotene excites connexin43 gene to increase gap junction formation; thereby increasing cell to cell communication. Connexin43 gene plays crucial role in hear malformations and defects of laterality [363] as well as thyroid disease [364]. • <i>Antioxidant/prooxidant</i> [339, 347, 355, 365-368] Beta-carotene captures free radicals, thereby reduces oxidative stress on human. It is reported that beta-carotene is a special type of biological redox reagent that reduces oxidation products best at low partial pressures of oxygen. It acts as a single oxygen
--

quencher.

- ***Immunological response*** [350, 369-371]

It is proven that carotenoids, especial beta-carotene, affect the activity of immune cells. Both T – and B – lymphocyte proliferative are enhanced with the presence of carotenoids.

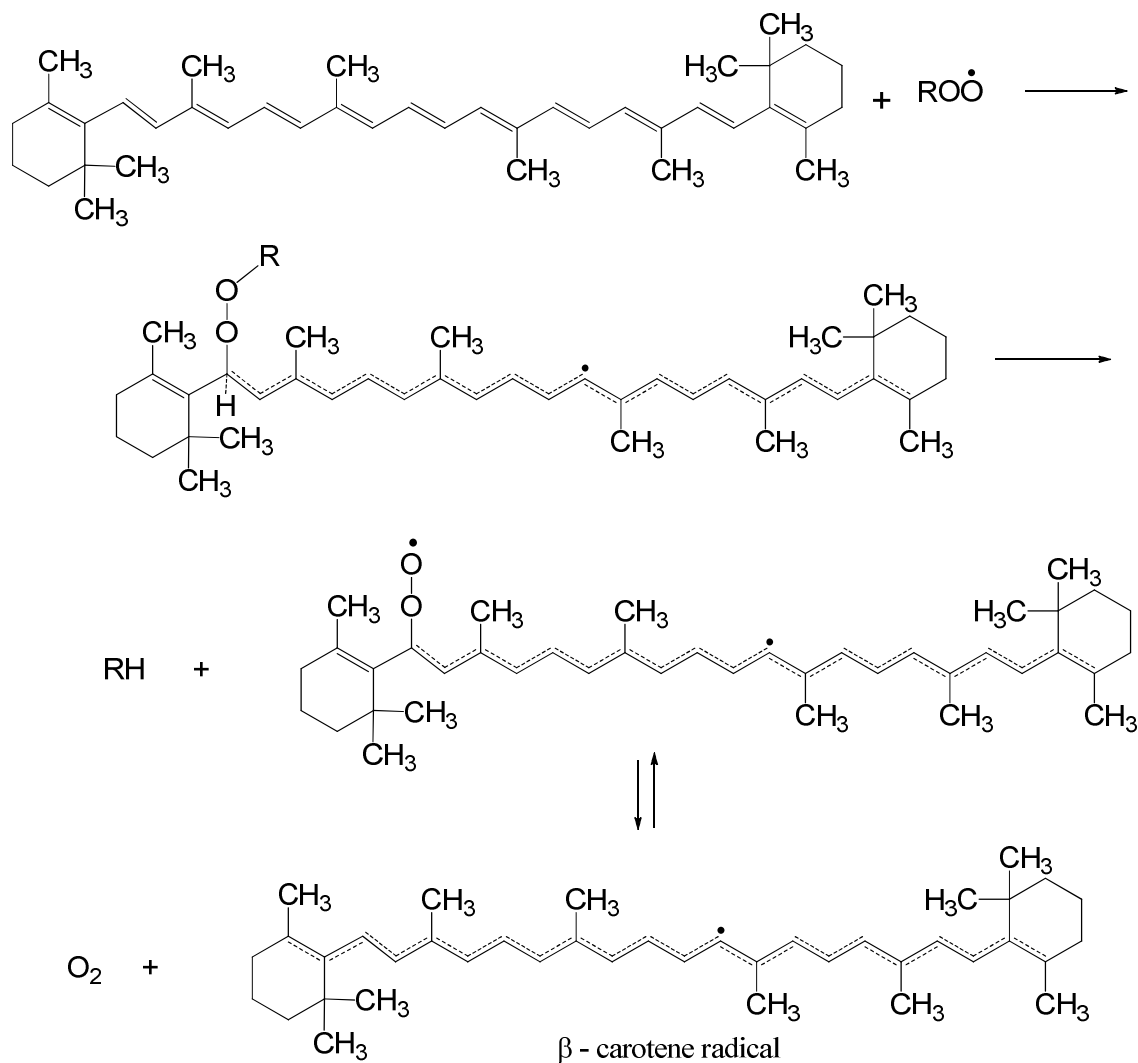
- ***Hormone regulation and fertility*** [372-375]

The impact of beta-carotene on fertility is still controversial. There are numerous reports of beta-carotene supplementation causing fertility improvements in herbivores, but a substantial number of studies have also found no effect. A few reports that carotenoids influence menstrual cycle and thyroid hormones in humans.

The excess of vitamin A is stored in liver. The recommended daily allowance (RDA) of vitamin A is 300 to 600 µg for children and 900 to 1200 µg for adults. The range between shortage and too much vitamin A is narrow even for adult. It is reported that ingesting vitamin A in amounts not much greater than the (RDA) leads to an increase in bone fractures later in life [376]. High doses of vitamin A for long term may increase the risk of lung cancer among smokers [377-379]. High doses taken early in pregnancy have been linked to a greater risk of birth defects [380]. Vitamin A deficiency is common in developing countries but rarely seen in developed countries [381]. The earliest symptom of vitamin A deficiency is night blindness due to the loss of goblet cells in the conjunctiva, a membrane covering the outer surface of the eye leading to weaken dark adaptation [382]. Severe deficiency causes a condition where changes in the cells of the cornea ultimately result in corneal ulcers xerophthalmia, scarring and blindness [383].

According to the World Health Organization (WHO), vitamin A deficiency in developing countries is a significant concern [381].

Beta – carotene chain – breaking antioxidants interfere with chain propagation by trapping the chain – carrying radicals $RO\dot{O}$ or \dot{R} or both due to the large conjugated double bonds in its molecule [347, 384].



The beta – carotene radical has a radical at the center carbon atom which is resonance-stabilized by the conjugated double bonds. Therefore, it ceases the transfer of free radicals to other compounds. Furthermore, it can react with other radicals such as \dot{R} to

terminate the chain propagation. This reaction occurs much faster than the termination reaction among peroxy – peroxy termination reaction [347]. When pressure of oxygen is low more beta – carotene radicals are formed. That reduces the concentration of free radicals in the system.

1.3. Triacetin

Triacetin (MW = 218.2 g/mol), a triester of glycerin and acetic, is prepared by direct esterification reaction with vacuum distillation as a way of purification [385]. It can also be synthesized by the reaction of glycerin and acetic anhydride using phosphoric acid or zinc as a condensing agent [386]. Naturally, it presents in cod-liver oil, butter, and other fats [387]. Triacetin is soluble in aromatic hydrocarbons and most organic solvents. It is insoluble in aliphatic hydrocarbons. Therefore, mineral oil, vegetable oil and animal oil are not the good solvents for triacetin. Triacetin is partially soluble in water with the solubility of 7%. The chemical, physical properties, as well as biological, and animal toxicology of triacetin is presented in the “final report on safety assessment of triacetin” by Fiume and The Cosmetic Ingredient Review Expert Panel [388]. Triacetin is confirmed as a generally recognized as safe chemical for human food and cosmetics use by FDA [389, 390]. It is neither a genotoxicity nor toxin to humans because the hydrolysis products of triacetin are glycerol and acetic acid which are not toxic [388]. Decomposed to glycerol and acetic acid, triacetin is not a good solvent in flavorings because of the vinegar odor. When water solubility is not an issue, or when the flavors are insoluble in ethanol or propylene glycol, triacetin is a good solvent candidate, particularly in spray-drying when other volatile solvents can cause flavor loss [391]. Vapor pressure of triacetin is very low (about 0.3306 Pa at 25⁰C). It means triacetin almost does not

evaporate at all at room temperature. In gummy candies such as chewing gum, triacetin serves as both flavor and plasticizer. Triacetin is highly capable of forming hydrogen bonding with water due to the rich polar oxygen groups in its molecules. For this reason, it is widely used as a humectant agent in food. The nutritional quality of triacetin was investigated in order to serve astronauts in long term space mission. It was found that animal (rat) can tolerate up to 20% triacetin without the loss of weight [392]. The nutrition quality of triacetin was revised in nineties [393, 394]. The authors confirmed that triacetin does not affect the intestinal mucosa and metabolic substrates in rats while it provides less energy in comparison to medium-chain and long-chain triglyceride fat. Therefore, triacetin is a good candidate for preventing obesity [393]. Recently, Mathew et al [395] suggested that triacetin is a good acetate supplementation for healing canavan disease which causes progressive damage to nerve cells in the brain.

1.4. Surfactant

A surfactant is a substance that lowers the interfacial free energies of an interfacial surface between two immiscible fluids or that of a liquid – solid interface. The interfacial free energy is the minimum amount of work required to create that interface. Surface density is the interfacial surface tension between two phases. The interfacial tension is also a measure of the difference in nature of the two phases meeting at the interface. The greater the dissimilarity in their natures, the greater the interfacial tension between them is. The molecules at a surface have higher potential energies than those in the interior because the cohesion between them and the interior molecules of the substance is larger than the adhesion, which is the interaction between the interfacial molecules with the

exterior molecule of the other substance. Therefore work is required to bring a molecule from the interior to the surface.

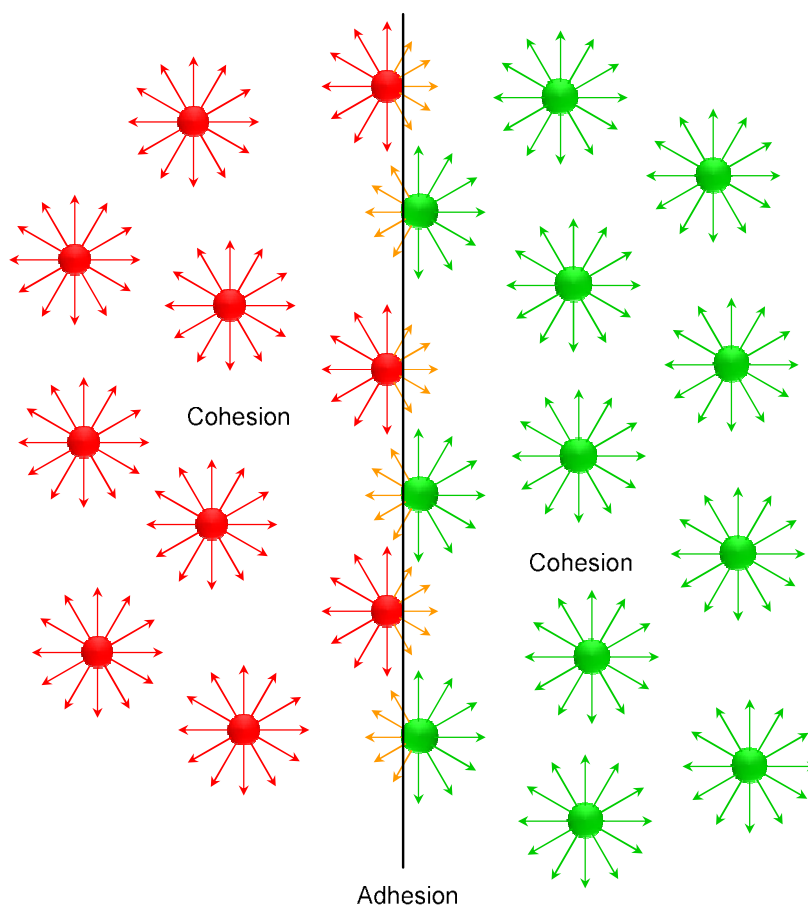


Figure 14: Force acting on the molecules at interface and in the bulk

A surfactant molecule consists of two parts. The head is lyophilic group having strong interaction with water. The tail is a lyophobic a long chain or chains of hydrocarbon having strong interaction with organic phase. Together, they bring amphipathic structure to the surfactant molecule. When surfactants are dissolved in water, the lyophobic tails of the surfactant molecules distort the structure of the water by breaking hydrogen bonds between the water molecules and by structuring the water in the neighborhood of the

hydrophobic group. As a result of this distortion, some of the surfactant molecules are excluded to the interfaces of the system, with their hydrophobic tails oriented so as to minimize contact with the water molecules. Because of the lyophilic heads, surfactant molecules are prevented from being expelled completely from the water as a separate phase. Therefore, the amphiphilic structure of the surfactant causes not only concentration of the surfactant at the surface leading to the decrease in surface tension of the water, but also orientation of the molecule at the surface with its hydrophilic groups in the aqueous phase and its hydrophobic group winged away from it. A similar phenomenon occurs when surfactant is dissolved in an organic solvent but the head groups are expelled.

The chemical structures of combinations suitable as the hydrophobic and hydrophilic group of the surfactant molecule vary with the nature of the solvent and the conditions used. For example, in water, the hydrophobic group can be a hydrocarbon, fluorocarbon, or siloxane chain with proper length, whereas in a less polar solvent only some of these groups may be suitable. Similarly, ionic or highly polar groups may act as lyophilic groups in aqueous media, whereas in a nonpolar solvent like acetone they may act as lyophobic groups. The activities of hydrophobic head and hydrophobic tail of a surfactant vary with temperature and the presence of electrolyte compound. For example, soap is a good surfactant in fresh water but not in marine water. Thus, surfactant molecule must have a suitable chemical structure for its surface activity in a particular system. Depending on the nature of the hydrophilic group, surfactants are classified as:

- If the head group of a surfactant molecule bears a negative charge, the compound is anionic surfactant, for example alkylbenzene sulfonate ($\text{RC}_6\text{H}_4\text{OSO}_2\text{Na}$); sodium dodecyl sulfate ($\text{C}_{12}\text{H}_{25}\text{OSO}_3\text{Na}$).
- When the surface-active portion of a surfactant bears a positive charge, the molecule is cationic surfactant, for example, cetylpyridinium chloride ($\text{C}_{16}\text{H}_{33}\text{C}_5\text{H}_5\text{N}^+\text{Cl}^-$), cetyltrimethylammonium bromide ($\text{C}_{16}\text{H}_{33}\text{N}^+(\text{CH}_3)_3\text{Cl}^-$).
- If the head group of a surfactant molecule consists of both positive and negative charges, the compound is zwitterionic surfactant. The examples for this type of surfactant include dodecyl betaine ($\text{C}_{12}\text{H}_{25}(\text{NH}_2)^+\text{CH}_2\text{COO}^-$) and dodecyl amidobetaine ($\text{C}_{12}\text{H}_{25}\text{CONH}(\text{CH}_2)_3(\text{NH}_2)^+\text{CH}_2\text{COO}^-$).
- If the head group of a molecule does not have apparent ionic charge, the compound is nonionic surfactant, for example tween 20 and tween 80 shown in Figure 13.

Correlations between the chemical structure of surfactants and their emulsifying power are complicated because of the variation in composition of both oil and water phases. Moreover, the concentration at which the emulsifying agent is used determines not only its emulsifying power, but even the type of emulsion (O/W or W/O) formed. As a result, it is necessary to take into consideration the composition of the two phases and the concentration of the emulsifying agent. A frequently used method to characterize the amphiphilic property of a surfactant is the HLB (hydrophilic–lipophilic balance) method by Griffin. A scale of number from 0 to 40 is built based on the hydrophilic head and hydrophobic tail of a surfactant. HLB value indicates where a surfactant is most soluble and will have the strongest interaction. HLB value of a surfactant can be obtained by

experimental emulsification data or calculated from the structure of the molecule with m hydrophilic groups with their HLB H_h and n hydrophobic groups with the HLB H_l as

$$HLB = 7 + mH_h + nH_l . \quad (14)$$

Table 7: The HLB value of some chemical groups

group	HLB value
– O SO ₃ Na	38.7
– COOK	21.1
– COONa	19.9
– N ⁺ (tertiary amine)	9.4
Ester (sorbitan ring)	6.8
Ester (free)	2.4
– COOH	2.1
– OH (sorbitan ring)	0.5
– OH (free)	1.9
– O –	1.3
– CH ₂ – / – CH – / – CH ₃ / = CH –	0.475

The HLB method is useful as a rough guide to select an emulsifier as shown in Table 8. HLB of a mixture is calculated as $HLB = \sum \varphi_i HLB_i$ where φ_i and HLB_i are the corresponding percentage of component i th and its HLB value respectively. HLB value of oil phase is calculated before formulating an emulsion, then, an emulsifier or mixture of emulsifier with the obtained HLB is selected to stabilize the emulsion. HLB has serious limitations because the HLB of a surfactant can vary with the nature of

media[396] . Moreover, a single surfactant can produce either O/W or W/O emulsions depending on conditions such as the shear rate, temperature, ratio of surfactant to oil [397]. Furthermore, many O/W emulsions undergo phase inversion to W/O at critical temperature for nonionic surfactant or salting out electrolytes for ionic surfactants. It is believed the interfacial surface tension of a system is the smallest at the temperature that phase inversion occurs [398, 399]. Therefore, emulsions prepared at phase inversion temperature will have the finest droplet size. Phase inversion temperature method is valid only for emulsions that show inversion at a particular temperature.

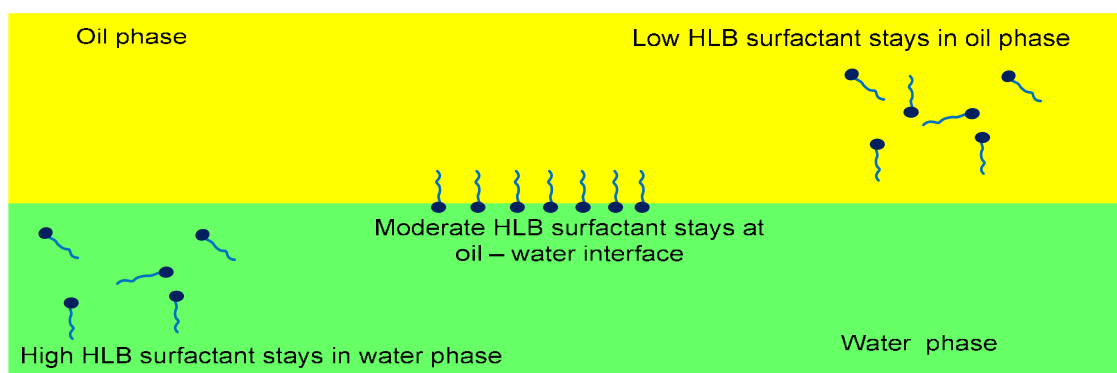


Figure 15: The distribution of surfactant molecules with different HLB values in oil – water mixture

Table 8: The application of emulsifiers based on their HLB value

HLB range	Application	Solubility in water
3 – 6	W/O emulsifier	Poorly soluble or insoluble
7 – 9	Wetting agent	Unstable milky dispersions
8 – 18	O/W emulsifier	Stable milky or translucent dispersions
13 – 15	Detergent	Translucent dispersions
> 15	Solubilizer	Clear solution

1.4.1. Tween 20

Tween 20 (MW = 1227.5 g/mol) is a polysorbate surfactant which is a polyoxyethylene derivative of sorbitan monolaurate and is distinguished from the other members in the polysorbate range by the length of the polyoxyethylene chain. Tween 20 is relative non-toxicity and can be used as a detergent or an emulsifier in a number of domestic, scientific, and pharmacological applications. The HLB of tween 20 is 16.7 indicating that tween 20 tends to move into water phase. In food, tween 20 is used as a wetting agent in flavored mouth drops.

1.4.2. Tween 80

Tween 80 (MW = 1310 g/mol) is common name of polysorbate 80 which is a nonionic surfactant and emulsifier derived from polyethoxylated sorbitan and oleic acid. Similar to tween 20, polysorbate 80 is relatively non-toxic. Tween 80 (HLB =15) is a viscous, water-soluble yellow liquid and often used in food and other products as an emulsifier, particularly in ice cream to make the ice cream smoother and easier to handle, as well as increasing its resistance to melting.

1.4.3. Lecithin

Lecithin soybean is a product extracted from soybean oil. Lecithin (MW = 327.27 g/mol) consists of mainly four types of phospholipids. If the group function connected to phosphorus group is hydrogen the phospholipid is phosphatidic acid (PA); when that group is ethanolamine the lipid is phosphatidylethanolamine (PE); whilst the group function is choline the phospholipids is phosphatidylcholine (PC), and if the group is inositol group the phospholipids is phosphatidylinositol (PI). Rydhag et al. [400] reported that at pH 6-7 the PC and PE compounds are neutral but the PI and PA compounds are partially dissociated. The dissociation of those molecules contributes

negative charge to lecithin. Other researchers [401-403] detailed that the PI and PA form of soy bean lecithin occupy 20 to 30 % of total phospholipids while PE and PC occupy almost 45%. Lecithin is used widely in food or medical application as a natural emulsifier or stabilizer, although the solubility of lecithin in water is low. Because the HLB of lecithin is in the range from 2 to 8, lecithin mainly distributes to oil phase in emulsions.

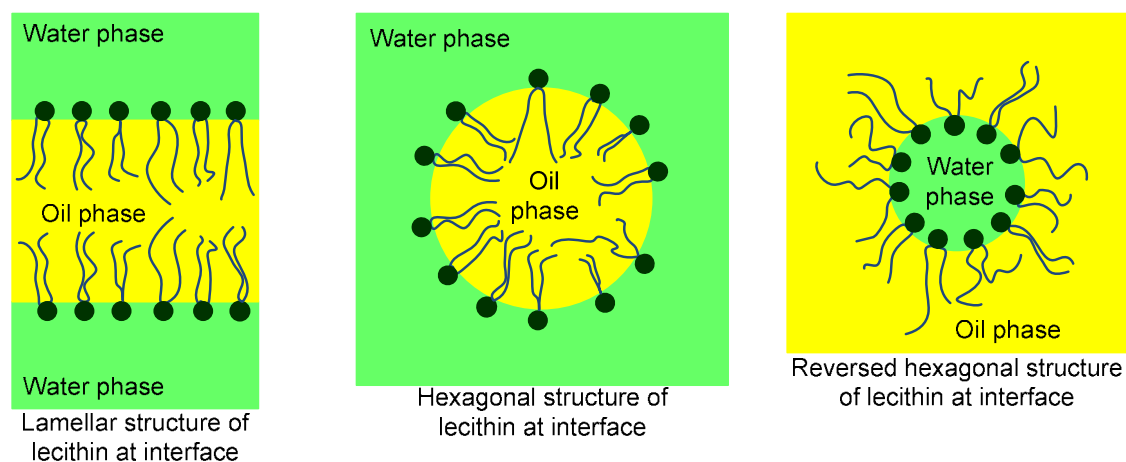


Figure 16: Lamellar structures of lecithin at interface

Similar to other phospholipids, lecithin forms lamellar layer at the oil – water interface as shown in Figure 16. There are three types of lamellae depending on the functional group on the lecithin molecule. According to Nieuwenhuyzen [401] phosphatidylcholine (PC) forms planar lamellar structure, while lysophosphatidylcholine appears as a hexagonal structure at the oil – water interface. Similar to PC, phosphatidylethanolamine (PE) also has both planar lamellar and hexagonal structure. It is suggested that the entire phosphocholine group of the lecithin is in the aqueous inter – bilayer region [404]. The phosphatidylethanolamine (PE) forms a reversed hexagonal structure where the

hydrophilic head groups cluster together to form W/O emulsions [401]. Applying X-ray diffraction analysis, Small [405] calculated the lattice dimensions of hydrated egg lecithin of both dried form and lyotropic lamellar liquid crystalline phase as presented in Table 9. He found that at 240C when from 0 to 7% of water is added, the mixture consists of solid crystalline and waxy phases; when water content occupies from 7 to 12% , the system is waxy birefringence; if water content in the mixture is from 12 to 45 % , the mixture appears as a homogeneous phase of neat soap texture; and the mixture is turbid and there are islands of water due to lamellar structure formation when water content is in the range from 46 to 65%.

Table 9: Dimensions of the lamellar[405]

Mass fraction of lecithin	Distance between molecule (Å)	Surface area of one lecithin molecule (Å ²)	Thickness of lipid layer (Å)	Thickness of water plus phosphoryl layer (Å)	Thickness of “free water zone” (Å)
0.85	51	59.3	35.8	15.2	0
0.8	52.5	61.3	34.7	17.8	1.8
0.7	56.4	65.2	32.6	23.8	7.8
0.62	60.6	68.5	31	29.6	13.6
0.56	64.1	71.7	29.6	34.5	18.5

When the oil phase is absent, lecithin lamellar is formed at 10% of water content at room temperature [406]. It is reported that under heating, a hydrated egg lecithin planar multilaminar structure shows periodic striation instability due to strong attraction of the

lamellar in the structure [406]. Nagel et al. have revealed that the most important molecular energies for the main transition in lecithin bilayers are the hydrocarbon chain interactions and the rotational isomeric energies. They have concluded that the main phase transition from the hexagonal mesophase to the liquid phase of lecithin is similar to the melting transition in the alkanes, but with some modifications. The diffusion within lecithin bilayers was investigated by Wolosin and co-workers. The authors have confirmed that the diffusion within egg lecithin bilayers demonstrates a steep mass dependence representative of diffusion in soft polymers [407]. By varying the chemical potential of water in lipid – water mixtures, Parsegian et al. [408] found that there is no discrete of “bounded water” in lecithin lamellar structures. Moreover, along with the water removal, not only does the lattice distance between the layers decrease but also the molecules rearrange within the layer surface causing layer deformation. Furthermore, when the distance between two layers is 27 Å, the layers start to repel each other. This repulsion force increases exponentially up to 1500 atm when the lattice distance approaches 3 Å. Gottlieb and Eanes [404] investigated the impact of electrolytes on the thickness of the bilayer lamellar lecithin. The authors discovered that impact of the electrolytes examined is in order $\text{CsCl} = \text{KCl} > \text{NaCl} > \text{Na}_2\text{SO}_4 > \text{H}_2\text{O} = \text{LiCl} > \text{CaCl}_2$. The driving force for the swelling of lecithin lamellar phase is the ionic interaction between phosphocholine groups of lecithin molecules and cation in aqueous solution. Moreover, small carbohydrate solutes also cause the lamellar thickness expansion of lecithin [409]. Epanand [410] found that substances expanding the hydrophobic domain promote hexagonal phase formation and lower the bilayer to hexagonal phase transition temperature.

2. Method

2.1. Spectrofotometer for defining the solubility of beta-carotene in triacetin

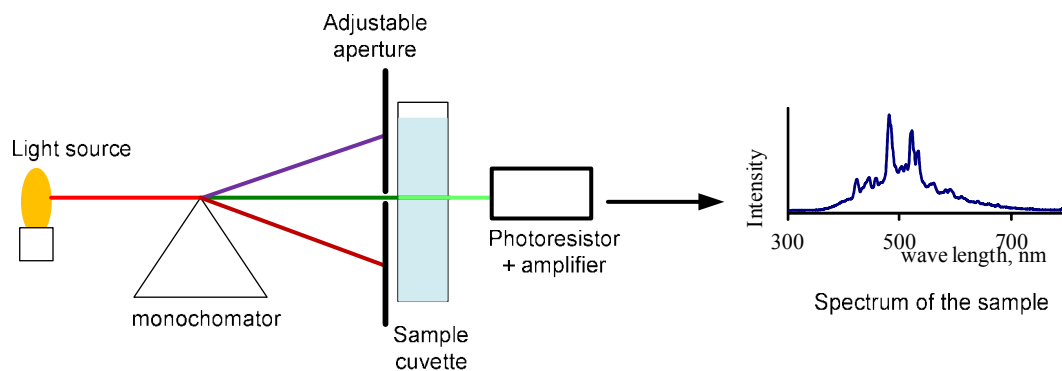


Figure 17: Schematic of a spectrophotometer

The solubility of β -carotene in triacetin is found by using time-resolved UV/Visible spectroscopy. It is the quantitative measurement of the reflection or transmission properties of a material as a function of wavelength. A spectrophotometer consists of a light source, monochromator prism, an adjustable aperture, a cuvette holder, and a photoresistor with an amplifier as shown in Figure 17. The light coming from the light source is scattered by the monochromator to generate several single beams. Those beams pass through the cuvette with sample, then come to the photoresistor. The intensity of the light after the sample is compared to the intensity of the reference beam for transmission at a specific wavelength. The transmission intensity of the beams depends on the chemical structures of the sample and concentration of compounds present in the sample. Therefore, transmission spectrum is the fingerprint of chemical.

The concentration of the chemical present in the sample is quantified by applying Lambert – Beer’s law. According to this law, the transmission intensity, T , of a beam

passing a sample depends on the chemical concentration, C ; the travelling distance of the beam through the sample, l ; and the molar absorption coefficient, ϵ . Mathematically, the relationship among those parameters is $T = 10^{-\epsilon l C}$. Lambert – Beer’s law is validated when the chemical concentration of the investigated sample is low. When the solution approaches saturated condition the molar absorption coefficient is not constant. This is a limitation to Lambert – Beer’s law.

An oversaturated solution of β -carotene in triacetin was prepared and diluted continuously while measuring the transmission of light with the range of wave length from 350 nm to 1300 nm. The wave length with highest transmission intensity value is used to calculate the concentration of β -carotene in triacetin.

2.2. Optical goniometer for surface tension

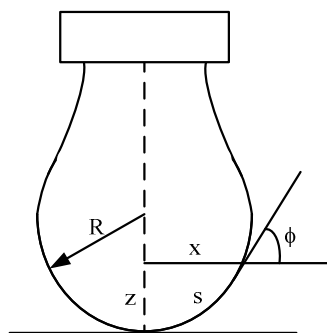


Figure 18 : Geometry of a pendant droplet

The surface tension of the surfactant solution is obtained by using pendant droplet method on an optical Rame-Hart goniometer (software KSV CAM101). In the pendant droplet measurement, a liquid droplet is hanging to the end of a needle as presented in Figure 18. The shape of the drop is determined from the balance of forces which include

the surface tension of that liquid. Therefore, the surface or interfacial tension at the liquid interface can be related to the drop shape through the following equation: $\sigma = \Delta\rho g R^2 / \beta$, where $\Delta\rho$ is the difference in density between the liquid and measuring media; R is the radius of the curvature of the drop at its apex; g is the gravity constant; and β is the shape factor which is the solution of the Young – Laplace equation as detailed by three dimensionless first order equations below

$$\begin{aligned} \frac{dX}{dS} &= \sin \phi \\ \frac{dZ}{dS} &= \cos \phi \\ \frac{d\phi}{dS} &= 2 + \beta X - \frac{\sin \phi}{Z} \end{aligned} \quad , \quad (15)$$

where x is the distance from the axes of the droplet to the interest point, z is the height of the interest point from the bottom of the droplet, s is the length of the curvature from the lowest point of the droplet to the interest point, and ϕ is the angle between the tangent at the interest point and horizontal direction. X , Z and S in equation (15) are the dimensionless parameters obtained by dividing x , z , and s by R respectively. Kutta – Merson's algorithm is applied to solve equation (15) by automatic step length adjustment to generate a large number of theoretical dimensionless profiles corresponding to the whole possible value of β . Each profile was estimated by using cubic interpolation. Thus, curves correlating the parameters β and R with measurable parameters as indicated in the figure were produced, and these curves were fitted with linear polynomials by the method of least squares.

Solutions of varying concentrations of surfactant Tween 20 or soy lecithin are prepared, mixed using a vortex mixer for 2 minutes, and stored for 24 hours. Before testing,

samples are mixed using the vortex mixer for 30 seconds. The critical micelle concentrations of the surfactants are determined from the data curves. This procedure is repeated using surfactant in triacetin solutions.

2.3. Suspension preparation

The effect of emulsification time on β -carotene nanosuspension is tested by applying high shear stress to Tween 20/Tween 80 nanoemulsions for varying periods of time. Coarse emulsions were prepared by mixing 2% (w/w) Tween 20/Tween 80, 14.9% β -carotene/triacetin, and 83.1% deionized water on a magnetic stirrer at 1,000 rpm for 1 hours. For lecithin, the recipe is 4% lecithin/ 14.9% β -carotene/triacetin solution/ 81.1% DI water. High shear stress was applied to 7 ml of the coarse emulsions using a Tekmar Ultra-Turrax Homogenizer at 20,000 rpm for 2,4,6,8, and 10 minutes. After homogenization, 7 ml of nanoemulsion was immediately added to 63 ml of water on a magnetic stirrer. The resulting nanosuspension was stirred for 10 minutes at 600 rpm on a magnetic stirrer. Each sample was sonicated using a Fisher Scientific 550 Sonic Dismembrator at 20 kHz for 4 minutes at 1-minute intervals and 30 seconds between each interval. The particle size, polydispersity index, and zeta-potential of each sample were tested using dynamic light scattering by a Delsa NanoC Particle Analyzer.

2.4. Dynamic light scattering technique for particle size and zeta potential

Particles suspended in liquids with viscosity, μ , are in Brownian motion due to random collisions with solvent molecules. This motion causes the particles to diffuse through the medium. The diffusion coefficient, \mathcal{D} , is inversely proportional to the particle size according to the Stokes – Einstein equation

$$\mathcal{D} = \frac{k_B T}{3\pi\mu d}, \quad (16)$$

where k_B is the Boltzmann's constant, T is the absolute temperature, and d is the hydrodynamic diameter of the particles. The Stoke – Einstein equation above implies that \mathcal{D} will be relatively small for large particles, and large for small ones. That means the large particles will move slowly while smaller particles will move more rapidly. Therefore, it is possible to determine the size of particles based on observing the motion and determining the diffusion coefficient of them in liquid media.

When a laser is sent to particles suspended in a liquid medium, the light is scattered in all direction because of its interaction with the particles. The scattered light that is collected comes from a group of scattering elements within a scattering volume defined by the scattering angle and detection apertures. The observed intensity of the scattered light at any instant will be a result of the interference of light scattered by each element; and thus, will depend on the relative positions of the elements. Because particles move about randomly in Brownian motion, the scattered intensity fluctuations are random, the fluctuations in time of the scattered light intensity will be observed. The fluctuations will occur rapidly for smaller, faster moving particles and more slowly for larger, slower moving particles as shown in Figure 19. The fluctuations of the scattered light are analyzed using the autocorrelation function

$$g^{(*)}(\tau) = \frac{\langle I(t)I(t+\tau) \rangle}{\langle I(t) \rangle^2}. \quad (17)$$

If the particles in the sample have the same size, the autocorrelation function is

$$g^{(1)}(\tau) = B e^{-(\Gamma\tau)}. \quad (18)$$

On the other hand, the autocorrelation function for sample loading particles with different size is

$$g^{(2)}(\tau) = |g^{(1)}(\tau)|^2 + 1. \quad (19)$$

In equation (18), B is a constant dependant on instrumental parameter such as aperture size, Γ , the decay constant which is a function of the diffusion coefficient of the particles, the scattering angle, θ , the refractive index, n , of the medium, and wave length of the beam as

$$\Gamma = \frac{4\pi n \mathcal{D} \sin(0.5\theta)}{\lambda}. \quad (20)$$

The dynamic light scattering will collect the fluctuation signal as a data train of photon pulse per sampling time $\Delta\tau$ to calculate the autocorrelation function $g^{(2)}(\tau)$, then Γ is calculated based on $g^{(1)}(\tau)$. After that, the diffusion coefficient of a particular particle is quantified and the Stokes – Einstein equation is utilized for the size of the particle.

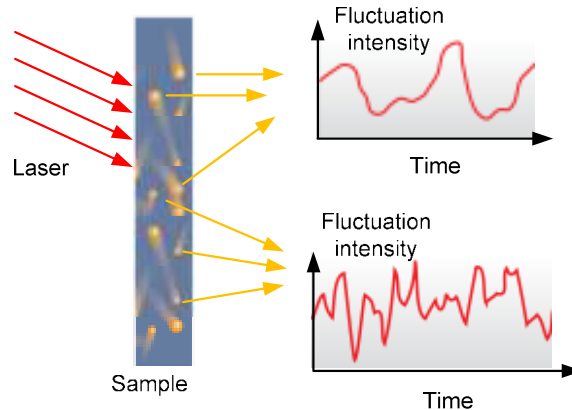


Figure 19: The fluctuation of scattering light from particles in a liquid medium

The surface of particles bears a charge due to chemical of the defects. When the particles are suspended in an aqueous medium, there is a layer of counter charge adsorbed on the surface of the particles. This layer, then, brings other ionized layers with opposite charge surrounding the surface of the particles. That makes the distribution of ions decay with the distance from the particle surface. Typically, the ions adsorbed on the surface of the particles are immovable. They form the Stern layer. The other ions outside of Stern layer can move under thermal diffusion. This layer is known as the diffusive layer. Because the ions in Stern layer attach strongly with the particles, these ions participate in the Brownian movement of the particles. Moreover, some ions in the diffusive layer also take part in the movement of the particles. Together with ions in Stern layer, those ions form a field referred to as the slipping plane where the movement occurs. Zeta potential is the potential at the slipping plane of a particle and the potential at a location far from the particle surface is considered zero. High zeta potential means strong electrostatic repulsive energy among particles. On the contrary, a low absolute value of zeta potential (approaching zero) increases the probability of particles colliding; therefore, forming particle aggregates. Thus, zeta potential implies the dispersion stability of particles.

When an electric field is applied to charged particles in the suspension, particles move toward an electrode opposite to its surface charge. Because the velocity is proportional to the amount of charge of the particles, zeta potential can be estimated by measuring the velocity of the particles. To determine the speed of the particle movement, the particles are irradiated with a laser light, and the scattered light emitted from the particles is detected. Because the frequency of the scattered light is shifted from the incident light in proportion to the speed of the particles movement, the electrophoretic mobility of the

particles can be measured from the frequency shift of the scattered light based on the Doppler effect. The amount of frequency shift ν_D of scattered light is a function of the velocity u of particles, scattering angle θ , the wave length of the scattered light, and the refractive index of the medium as following:

$$\nu_D = u \frac{n \sin \theta}{\lambda}. \quad (21)$$

The zeta potential of particles suspended in an aqueous medium containing electrolytes are calculated from Smoluchowski equation

$$Z = \frac{u\mu}{\varepsilon\varepsilon_0}, \quad (22)$$

where ε and ε_0 are the dielectric constant of vacuum and the medium respectively. The machine applies a static electric field on the sample cell, measures the amount of frequency shift of particles, then calculates particle velocity u using equation (21). The zeta potential of the particles is estimated by Smoluchowski equation.

2.5. Differential scanning calorimetry

The crystallinity of beta-carotene nanosuspensions was characterized by differential scanning calorimetry (DSC) using Perkin Elmer DSC 7 at the rate of 10⁰C per minute and wide angle X-ray diffraction. The DSC analyzer measures the flow of heat into or out of the investigated sample as function of temperature or time. The relationship between the heat flow, scanning temperature and time is in the form

$$\frac{dq}{dt} = \frac{dq}{dT} \frac{dT}{dt} + H(T,t) \quad (23)$$

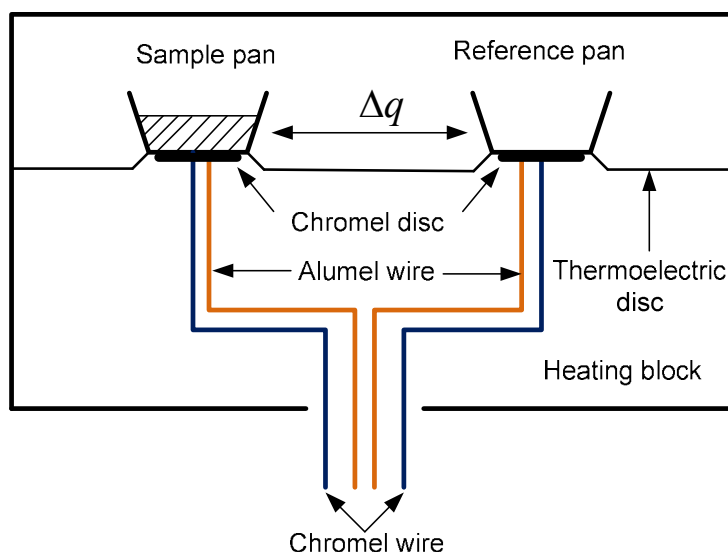


Figure 20 : Schematic diagram of heat flux differential scanning calorimetry cells

In equation (23), the term dq/dt was the heat flow; dq/dT was heat capacity of the sample; dT/dt was the scanning rate, the rate of heating or cooling; and $H(T, t)$ was the heat of thermal incident for example glass transition or solid – liquid transition. Phase transitions of a particular material generates the deviation in heat flow which could be captured by DSC analyzer. By measuring the heat flow, we could characterize not only the crystallinity but also the thermal properties of a material. Figure 20 presents the schematic diagram of heat flux differential scanning calorimetry cells. Figure 21 presents the glass transition T_g ; recrystallization exotherm temperature T_c and enthalpy ΔH_c ; melting endotherm onset melting temperature T_m^0 ; the extrapolation onset crystallization T_m^e ; the peak of melting temperature T_m and heat of fusion, ΔH_m .

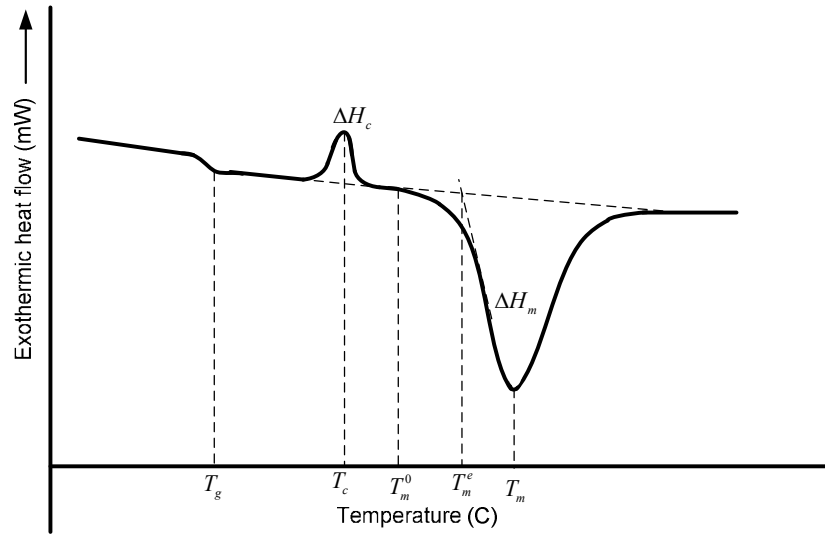


Figure 21: A typical DSC thermogram of a material

The DSC equipment collects the heat flow into/out of the sample pan and the reference pan as a function of pre-programmed temperature. This is accomplished via thermocouples mounted beneath the pans in the heating block. The device then compares the heat flows between those pans and plots the heat flow differences as function of temperature as shown in Figure 21. The heat capacity of the sample is quantified by the slope of the baseline, and the phase transition of a material can be detailed by the change in disorder via Boltzmann relation

$$S = k \ln W, \quad (24)$$

where k is the Boltzmann constant, and W is the complexion. The first-order phase transition caused by the crossing of the Gibbs energy of two phases at a specific transition temperature T_{tran} with different slopes $\left. \frac{\partial G}{\partial T} \right|_p$ when crystal melts or crystal

forms, is defined by a peak in the heat flow trace. The area of this peak provides heat of fusion of the considering material as shown in Figure 21. If material has different forms

of molecular arrangement when it crystallizes, there will be several melting peaks corresponding to each form of these crystals shown in the DSC curve. The second phase transition is glass transition which is defined by the change in heat capacity of the sample. From Figure 21 the glass transition temperature is characterized by the change in the baseline of the heat flow. When the sample contains many miscible components at amorphous forms, the glass transition temperature of the mixture can be calculated from Gordon – Taylor formula

$$T_g^{mix} = \frac{\varphi_1 T_g^1 + K \varphi_2 T_g^2}{\varphi_1 + K \varphi_2}, \quad (25)$$

where φ_i is the mass fraction of component i^{th} corresponding to glass transition temperature T_g^i ; and $K = \frac{\rho_1 T_g^1}{\rho_2 T_g^2}$ where ρ_i is the density of component i^{th} . There is another

equation which is simpler to characterize the glass transition temperature of the mixture mentioned above known as Fox – Flory equation

$$\frac{1}{T_g^{mix}} = \frac{1}{T_g^1} + \frac{1}{T_g^2}. \quad (26)$$

Therefore, by measuring glass transition temperature of an amorphous mixture, we can determine the miscibility of components presented in the mixture as well as mass their fraction.

2.6. X-ray diffraction for characterizing crystallinity

Most solid materials can be described as crystalline where the atoms are arranged in a regular pattern which is positioned to the point of a lattice. The smallest volume element which is repetition in three dimensions describes the crystal and is called a unit cell. The

length of the edges of the cell and the angle between them are the lattice parameters. There are seven crystal systems which are combinations of crystal structures described in Table 10. When the incident X-ray beam is sent to a sample having interplanar spacing d of atomic plane, diffraction occurs only if Bragg's Law is fulfilled. The relationship among interplanar distance, d , incident angle, θ , and wave length, λ , is $n\lambda = 2d\sin\theta$ where n is integers.

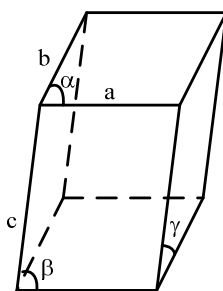


Figure 22: Unit cell

Table 10 : Seven crystal systems

Crystal class	Axis system
Cubic	$a = b = c ; \alpha = \beta = \gamma = 90^0$
Tetragonal	$a = b \neq c ; \alpha = \beta = \gamma = 90^0$
Hexagonal	$a = b \neq c ; \alpha = \beta = 90^0 ; \gamma = 120^0$
Rhobohedral	$a = b = c ; \alpha = \beta = \gamma \neq 90^0$
Orthorhobic	$a \neq b \neq c ; \alpha = \beta = \gamma = 90^0$
Monoclinic	$a \neq b \neq c ; \alpha = \gamma = 90^0 ; \beta \neq 90^0$
Triclinic	$a \neq b \neq c ; \alpha \neq \beta \neq \gamma \neq 90^0$

In most diffractometers, the X-ray wavelength λ is fixed. As a result, a family of planes produces a diffraction peak only at a specific angle 2θ . In addition, d is the perpendicular

vector drawn from the origin of the unit cell to intersect the crystallographic plane. The intensity of the diffraction peaks is determined by the organization of atoms in the whole crystal. Therefore, from the XRD spectrum, the unit cell parameters are determined by the peak locations; the baseline characterizes the amorphous phase; and the peak intensity represents the arrangement of the atoms in the unit cell. Figure 23 shows a schematic diagram of a typical XRD. Both X-ray tube and detector can slide on the surface of a sphere named Ewald sphere. The incident angle which is the angle between the incident beam and the sample determines the detector angle. For every set of planes, there will be a small percentage of crystallites that are perpendicular to bisect the incident and the diffraction beams to diffract. Basic assumptions of powder diffraction are that for every set of planes there is an equal number of crystallites that will diffract and that there is a statistically relevant number of crystallites. The Scattered X-ray beams from the sample are detected by the detector, processed and counted. By scanning the sample through a range of 2θ angles, all possible diffraction directions of the lattice can be attained due to the random orientation of the powdered material. Conversion of the diffraction peaks to interplanar distance, d , allows identification of the sample because the crystal structure of a material has a unique set of lattice parameters. Typically, this is achieved by comparison of interplanar length with the standard reference patterns. Therefore, the lattice constants and angles among them of an unknown crystal structure can be calculated from X-ray diffraction spectrum.

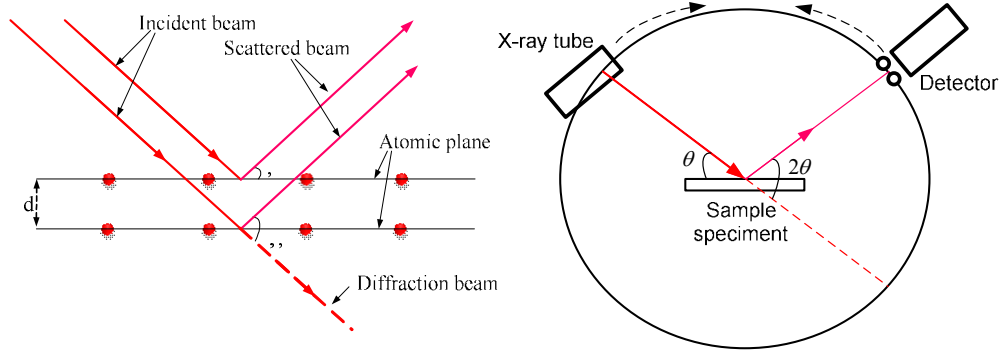


Figure 23: X-ray diffraction on a crystal (left) and the schematic of an X-ray diffraction (right)

2.7. Diffusing wave spectroscopy for nano-rheology of gels

The diffusing wave spectroscopy technique utilizes probes imbedded in the sample to measure rheology of soft materials. Basically, the thermal motion of the probe in a homogeneous elastic medium depends on the stiffness of the local microenvironment. The relationship among the thermal energy density of a bead of radius r to the elastic energy needed to deform a material with an elastic modulus G' a length L yields

$$\frac{k_B T}{r^3} = \frac{G' L^2}{r^2}. \quad (27)$$

The temperature of soft materials rarely changes significantly. Thus, elastic modulus depends on both the size of the embedded probes and on the displacements of small particles L . For micron sphere particles imbedded in a purely viscous medium, the time dependant position correlation function of individual tracers exposes the dynamic of particle motions. This correlation function is known as the mean square displacement (MSD)

$$\langle \Delta \bar{X}^2(\tau) \rangle = \langle |\bar{X}(t+\tau) - \bar{X}(t)|^2 \rangle, \quad (28)$$

where \vec{X} is the n – dimensional particle position, τ is the lag time, and the bracket means an average overall time t . Assuming that the material is always at thermal equilibrium all the time t , the diffusion coefficient, \mathcal{D} , of the particles can be quantified from the diffusion equation

$$\langle \Delta \vec{X}^2(\tau) \rangle = 2n\mathcal{D}\tau. \quad (29)$$

Therefore, the relationship among the viscosity η of the medium, the radius r of the embedded particles, and the diffusion coefficient \mathcal{D} of the particle becomes

$$\mathcal{D} = \frac{k_B T}{6\pi\eta r}. \quad (30)$$

Many soft materials are more complex, demonstrating both viscous and elastic behavior. The MSDs of the embedded tracers reflects both the viscous and elastic contributions. Moreover, the responses are typically frequency dependent and depend on the time and length scale probed by the measurement. As a result, the MSD of tracers in a complex fluid can scale differently with the lag time τ as $\langle \Delta \vec{X}^2(\tau) \rangle \sim \tau^\alpha$ where $0 < \alpha < 1$.

When the considering material is a homogeneously pure elastic, the MSD approaches its plateau when the thermal energy density of the particles equal the elastic energy density of the material

$$\langle \Delta \vec{X}^2(\tau \rightarrow \infty) \rangle = \frac{k_B T}{\pi r G}. \quad (31)$$

The relationship between the force acting on a small particle of mass m and its velocity $u(t)$ in a complex fluid is characterized by a generalized Langevin equation

$$m\dot{u}(t) = f_R(t) - \int_0^t \xi(t-\tau)u(\tau)d\tau, \quad (32)$$

where $f_R(t)$ stands for all the force acting on the particle including the interparticle forces and stochastic Brownian forces. The integral represents the viscous depressing of the fluid with a time dependent memory function $\xi(t)$ to characterize the elasticity in the network. Applying Laplace transform to generalized Langevin equation, the viscoelastic memory function of a complex material can be associated with the velocity autocorrelation function $\langle u(s)u(0) \rangle$

$$\langle u(s)u(0) \rangle = \frac{k_B T}{ms - \xi(s)}, \quad (33)$$

where s is the frequency in the Laplace domain. Replacing the velocity autocorrelation function by the Laplace transform MSD in to equation (33), we obtain

$$\tilde{\xi}(s) = \frac{6k_B T}{s^2 \langle \Delta \tilde{r}^2(s) \rangle} \quad (34)$$

Furthermore, in Laplace domain, the complex shear modulus $\tilde{G}(s)$ can be expressed as function of the memory function $\tilde{\xi}(s)$ as

$$\tilde{G}(s) = \frac{s \tilde{\xi}(s)}{6\pi r}. \quad (35)$$

Combining equation (34) and (35), we come to the direct relationship between complex shear modulus and the Laplace transform mean square displacement of the particles imbedded in the material.

$$\tilde{G}(s) = \frac{k_B T}{\pi s r \langle \Delta \tilde{r}^2(s) \rangle} \quad (36)$$

Equation (36) is known as the Generalized Stokes –Einstein equation for complex fluids. The relationship between diffusion coefficients of the embedded particles and the

Laplace transform mean square displacement is $\langle \Delta \tilde{r}^2(s) \rangle = \frac{6\mathcal{D}}{s^2}$, and the frequency

independent viscosity can be expressed as $\eta = \frac{k_B T}{6\pi r \mathcal{D}}$. Thus, the rheology of any soft

material can be calculated by the mean square displacement of embedded particles.

When a laser elucidates sample loaded particles, the photons penetrate into the sample and are backscattered by the particles. If a video camera is used as detector of the backscattered waves, an interference image called ‘speckle’ is displayed. The dark and bright spots on the speckle image result from respectively destructive and constructive interferences between the backs scattered waves. For viscoelastic sample, particles are mobile due to Brownian motion. This motion of scatterers induces light intensity fluctuations on the speckle image, and an overall deformation of the speckle pattern. Depending on the structure of the media, the speed of motion of particles is different, due to elasticity and viscosity. As a consequence, the speed of intensity fluctuations on the speckle image is different as well, i.e. the speckle pattern deformation speed allows characterization of the structural properties of the product. Due to the Brownian motion of the scatterers in the sample, the speckle image changes as a function of time, and gives information on the viscoelastic properties of the product being studied. In order to quantify this speed of change, a patented decorrelation function is used. This decorrelation is the inter-image distance between two images; it consists in the pixel to pixel difference of intensity.

$$d_2 = \sqrt{\sum_{x=0}^{\text{dim}_x-1} \sum_{y=0}^{\text{dim}_y-1} [I_2(x,y) - I_1(x,y)]^2}, \quad (37)$$

where $dimx$ and $dimy$ are the number of pixels horizontally and vertically respectively. By applying a patented algorithm, it is possible to compute the Mean Square Displacement (MSD) of the scatterers contained in the product from the decorrelation curve above. This parameter depends on the surface explored by the particles at a given decorrelation time. The MSD quantifies the motion of the particles inside the sample, from 0.1 nanometers up to 1000 nanometers. The Mean Square Displacement of particles inside a media is directly linked to Viscoelastic properties of the sample, and gives access information which can be used to compute characteristics of the product. The slope of the third part of MSD curve gives the diffusion coefficient of the particles in the sample. The relaxation time of the sample is defined as $t_R = \mathcal{D} / \delta^2$. Elastic modulus is estimated from the height of the plateau $6\delta^2$ of the MSD and the size r of the particles as

$$G' = \frac{k_B T}{6\delta^2 \pi r} \quad (38)$$

The frequency independent viscosity of the sample is

$$\eta = \frac{k_B T}{6\mathcal{D}\pi r} \quad (39)$$

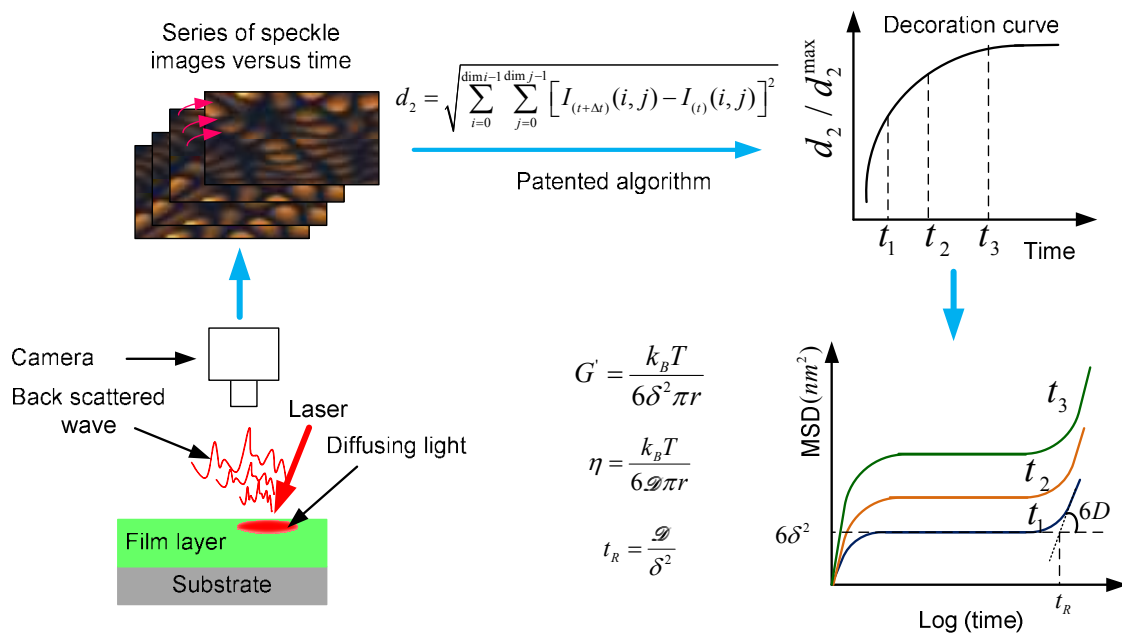


Figure 24: Schematic of DWS technique

PHYSICAL CHEMISTRY OF TRIACETIN – BETA CAROTENE SYSTEM

1. The formation of emulsion droplet in triacetin –water system

1.1. Definition of emulsion

An emulsion is a heterogeneous system consisting of two immiscible liquids, with one of the liquids dispersed as small spherical droplets in the other and stabilized by surfactant. If dispersed phase is oil, it is oil – in – water (O/W) emulsion for example milk is a typical O/W emulsion. On the other hand, if the dispersed phase is water, it is water – in – oil (W/O) emulsion such as margarine. Besides these two fundamental emulsions, there are multiple emulsions such as W/O/W or O/W/O emulsions. Emulsion is normally stabilized by surfactant due to electrostatic repulsion. However, polymer or small particles can be used to stabilize emulsion.

According to Clements [411] emulsions prepared from water and oil phases can be classified based on their size. Macroemulsion with their size in the range from 100 nm to 0.1mm is thermodynamically unstable. It tends to be optically turbid or opaque because the droplets size is similar to the wavelength of visible light leading to strongly scattered light. The size of nanoemulsion is from 20 nm to 100 nm. Although the small droplet size brings advantage to the stability of nanoemulsion because of small gravitational separation[411], this emulsion is only kinetically stable not thermodynamically stable [412] due to its large interfacial surface leading to high free energy. Because its size is smaller than the wavelength of visible light, nanoemulsion tends to be transparent or

slightly turbid. The third type of emulsion based on size classification is microemulsion with diameters somewhere in the 5 nm to 50 nm range. Microemulsion is a thermodynamically stable system [413]. Because the size of microemulsion is much smaller than the wavelength of visible light, this emulsion is transparent.

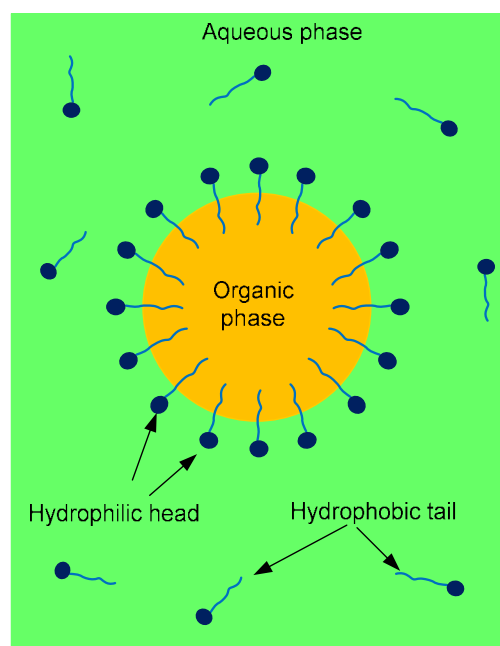


Figure 25: A typical Oil/Water emulsion system

1.2. Formation of emulsion droplets

The preparation of an emulsion causes the formation of a very large amount of interfacial surface between two immiscible phases, because the interfacial surface will increase 100 times if the size reduces 100 times. The work required to create new interface is $W = \sigma \Delta A$, where σ is the interfacial tension between the two liquid phases, and ΔA is the increase in interfacial surface. Figure 26 presents the physicochemical process involved in the mini-emulsification process. The total free energy of formation of an emulsion, ΔG is

$$\Delta G = \sigma\Delta A - T\Delta S \quad (40)$$

ΔG in equation (40) is positive. Therefore, emulsion formation is non-spontaneous and energy is required to produce the droplets. The high energy required for formation of nano-emulsions can be understood from a consideration of the Laplace pressure P which is the difference in pressure between inside and outside the droplet [414]

$$P = \sigma \left(\frac{1}{R_1} + \frac{1}{R_2} \right), \quad (41)$$

where R_1 and R_2 are the primary radii of curvature of the drop, for spherical droplet $R_1 = R_2$. Equation (41) indicates that the smaller droplet is the higher Laplace pressure is. The presence of surfactant in emulsion system reduces interfacial surface tension leading to the decrease in Laplace pressure and brings advantage to the droplet formation. According to Manea [415], during the droplet formation, the droplet size is the result of two consecutive processes: droplet break-up presumably occurring in the homogenizer valve, and coagulation of newly formed droplets insufficiently covered by the emulsifier likely occurring in the bulk after droplet breaks. At low pressures and high emulsifier concentrations, the amount of emulsifier is enough to stabilize the emulsions. As pressure increases, the size of the droplets decreases after passing the homogenizer valves. At one point, the concentration of emulsifier is not enough to efficiently cover the surface leading to coagulation until the surface area of the droplets decreases to a level that could be stabilized by the available emulsifier in the system. Therefore, the size of the emulsion droplets is determined by both the amount of energy added to the system and the emulsifier concentration. The impact of surfactant on the emulsion droplet size is dominant at low emulsifier concentrations no matter how much pressure is applied to the

system, because the surface area generated by homogenizer cannot be stabilized by the emulsifier available in the system. Therefore, the droplet size is governed by the mechanism droplet break-up vs. stabilization giving the largest droplet size [415].

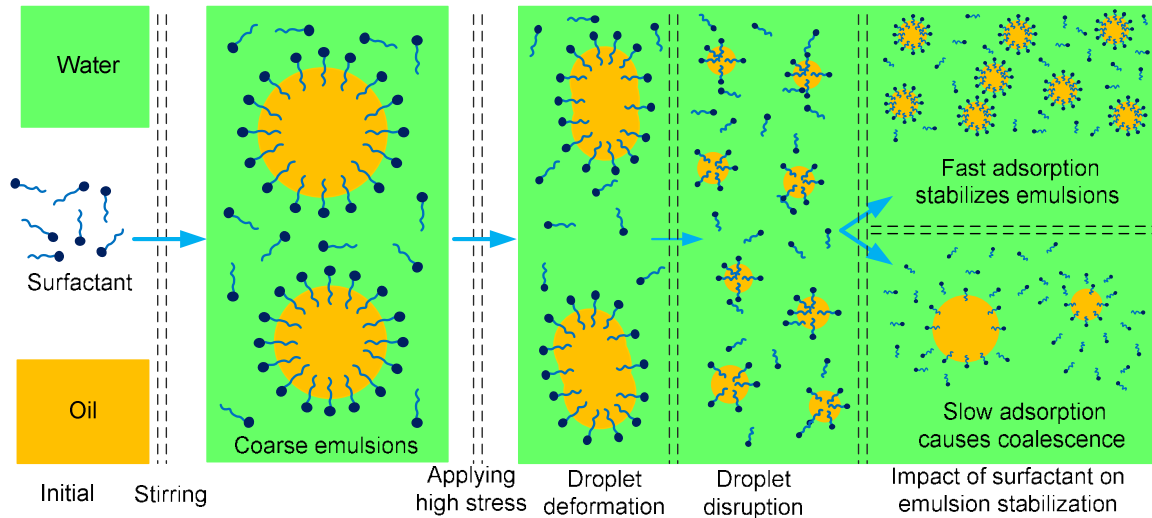


Figure 26: Physicochemical process of emulsification [416]

2. Droplet breakup mechanism

As mentioned earlier, the energy required to break emulsion droplet transmits from the fluid surrounding the droplet via agitation. Thus the flow regime of the bulk determines the disruption force acting on the droplet. There are two main types of flow including turbulence flow which is chaotic nature, and laminar flow, known as well-defined streamlines. These flows are characterized by Reynolds number

$$\text{Re} = \frac{\rho \bar{u} l}{\eta}, \quad (42)$$

where ρ is density of the fluid, \bar{u} is the average velocity, η is viscosity, and l is the characteristic length scale of the flow. For example, if the fluid flows in a channel such as

a pipe, l is the diameter of the pipe; on the other hand, it is the length of the solid object surrounding by the fluid. The Reynolds number of laminar flow is not larger than 2000, in contrast to turbulent flow having Reynolds number larger than 4000. Any flow with Reynolds number in between these two values is transition flow. Figure 27 presents the general breakup mechanism of a droplet depending on the flow characteristic.

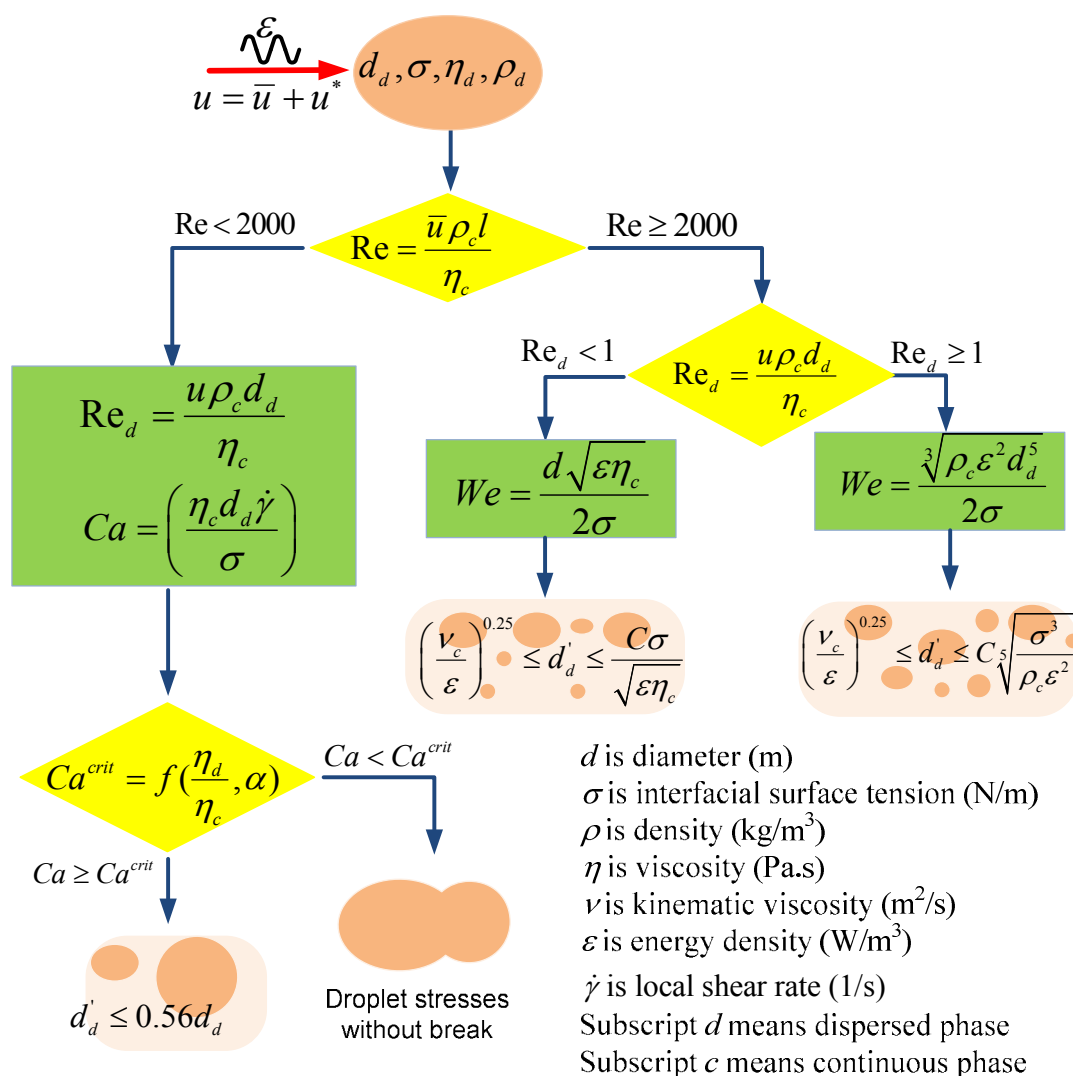


Figure 27: The droplet breakup mechanism

2.1. Droplet breakup mechanism in laminar flow

While investigating the droplet breakup in laminar flow, Taylor [417] has found that in laminar flow, drops deform into prolate spheroids where the longest axis of the drop is initially aligned with the principal axis of strain for both irrotational and simple shear flows. The breakup of a drop in laminar flow depends on the viscosity ratio of the droplet and the bulk. It requires large shear rate to break the drop if the viscosity of the drop is relative high in comparison with that of the bulk and vice versa. The deformation of a droplet in laminar flow depends on the ratio of the external stress (or viscous force) over Laplace pressure (or interfacial force) known as capillary number shown in Figure 27.

When the Reynolds number of macro-flow is smaller than 2000, the flow is laminar. The local flow surrounding the droplet can be considered as stoke flow since

$Re_d = \frac{\bar{u} \rho_d d_d}{\eta_d} \ll 1$. The viscosity of both continuous and dispersion phases plays an

important role in droplet break up. According to Bentley et al. [418] when the density of both phases is the similar, the velocity-gradient tensor is characterized by a single parameter α , which specifies the relative strength of the strain rate and vorticity in the flow. This parameter is defined by

$$\nabla u = 0.5G \begin{bmatrix} 1+\alpha & 1-\alpha & 0 \\ -1+\alpha & -1-\alpha & 0 \\ 0 & 0 & 0 \end{bmatrix}, \quad (43)$$

where G is the velocity – gradient tensor. $\alpha = 1$ for pure-straining flow while $\alpha = 0$ for simple shear flow. The streamline of the flow for $0 \leq \alpha \leq 1$ is in Figure 28.

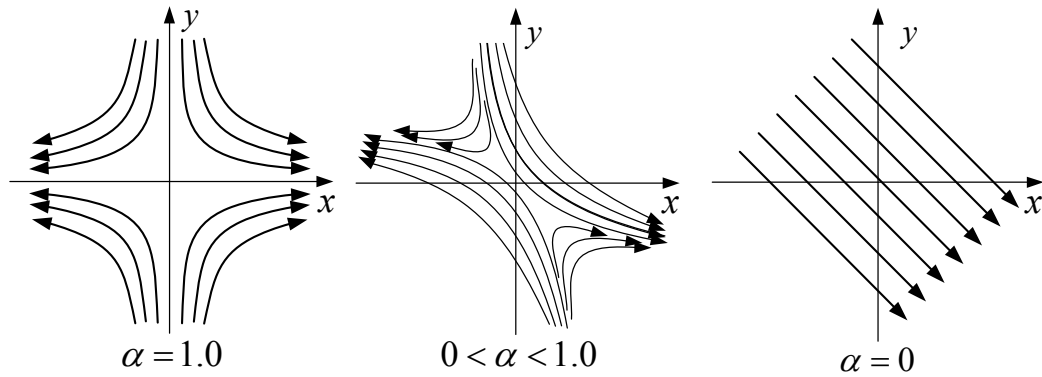


Figure 28: The streamlines of laminar flow field for $1 \geq \alpha \geq 0$

Bentley et al. [418] has suggested that the critical capillary number is a function of viscosity ratio $\varphi = \frac{\eta_d}{\eta_c}$ and α . The drop breaks when its capillary number is larger than the critical capillary number. The value of critical capillary number found by experimental work in [418] reaches its minimum in the neighborhood of $\varphi = 1$. Thus, the droplet breakup falls in viscous regime when critical capillary number is function of viscosity ratio φ , and flow parameter α . Renardy et al. [419] believe that when there is no difference in density, and the Reynolds number of laminar flow is large, the critical capillary number $Ca_{crit} = Re^{-1}$. By modeling the laminar flow with different Reynolds numbers, the authors have recognized that Laplace pressure also causes vortical swirl inside the droplet. They have claimed that number of the swirls within the droplet increases with the value of Reynolds number. Therefore, the breakup mechanism shifts from viscous regime to inertial regime (internal force causes breakup) at large Reynolds number. Cristini *et al.* [420] claimed that for the flow with Reynolds number smaller than 100 the critical capillary number was around 0.154 and 0.155. The volume of daughter droplet is roughly around 50 to 60% of its mother. The authors also claimed that when

the flow has larger Reynolds number the secondary droplet volume was approximately 57% its mother droplet.

2.2. Droplet breakup mechanism in turbulence flow

When the Reynolds number of the flow is larger than 2100, an important parameter that describes droplet deformation is the Weber number, W_e , which gives the ratio of the external stress over the Laplace pressure [421]. Turbulent flow with Reynolds number value around 10000 or more is characterized by the presence of eddies. Thus, the local velocity, u , in a turbulence flow consists of the time average velocity, \bar{u} , and the oscillation velocity, u^* , as following

$$u = \bar{u} + u^* \quad (44)$$

The oscillation velocity, u^* , represents the energy which dissipates by the turbulent flow through the environment. Turbulent flow generates the construction of eddies with different length scales. Among these structures, large eddies in turbulent flow have large u^* . These eddies transfer a part of their energy to the smaller structures, which have small u^* but a large velocity gradient, by inertial and inviscid mechanism. This process continues to generate smaller and smaller structures to form a hierarchy of eddies. The energy cascade process in turbulent flow mentioned above finishes when the smallest eddies at which the molecular diffusion becomes important and viscous dissipation of energy occurs to transfer energy into heat are formed. The smallest scale of the eddy is the Kolmogorov scale. For a liquid with kinematic viscosity, ν , this scale is defined as $l = (\nu^3/\varepsilon)^{0.25}$. Among the hierarchical eddies, the ones which cause the deformation of emulsion droplet with density, ρ_d , are called energy carrying eddies. The relationship of

their size, l , their fluctuation velocity, u^* , density of continuous phase, ρ_c , and the power density in the flow, ε , is

$$u^* = C\sqrt[3]{l\varepsilon / \rho_c} . \quad (45)$$

According to Davies [422], the density power, ε , is directly estimated from the power applied to the homogenizer and the volume of mixing head. Brocart *et al.* [423, 424] believe that for a toothed rotor-stator homogenizer with tip velocity V and tooth spacing a , the density power ε is

$$\varepsilon = \frac{\rho_c V^3}{4a} . \quad (46)$$

Furthermore, the Reynolds number, Re_d , which is the ratio of inertial force and viscous force, of an emulsion droplet is defined as

$$Re_d = \frac{u\rho_c d}{\eta_c} . \quad (47)$$

When $Re_d > 1$, the droplet is in inertial regime and its deformation is governed by the local oscillation pressure caused by the energy carrying eddies. The droplet will break if the local pressure difference, $\Delta p(x) = \rho_c [u^*(x)]^2 = \sqrt[3]{\varepsilon^2 x^2 \rho_c}$, is larger than Laplace pressure, $2\sigma / d$, of the droplet. This relationship is described by Weber number, We , where the scale x is replaced by the maximum diameter of the droplet

$$We = \frac{\sqrt[3]{\rho_c \varepsilon^2 d_{\max}^5}}{2\sigma} . \quad (48)$$

Thus, from equation (47) and (48), we obtain the maximum droplet diameter in inertial regime as:

$$d_{\max} = C \sqrt[5]{\frac{\sigma^3}{\rho_c \varepsilon^2}}. \quad (49)$$

Sprow [425] suggested that the value of constant C is between 0.126 and 0.15.

When $Re_d < 1$, the breakup driving force is viscous force. Suppose that G is the local velocity gradient between droplet and a point with distance x . From Bernoulli equation, the local different pressure Δp is defined as

$$\Delta p = \frac{1}{2} \rho_c u^2 = \rho G x \bar{u}. \quad (50)$$

The shear stress which deforms droplet is $\eta_c G$. Since the viscous force is dominant, $\eta_c G > \rho G x \bar{u}$ that causes $Re_d = \bar{u} \rho x / \eta_c < 1$, the local gradient velocity, G , is derived from local velocity, u^* , with scale much smaller than the energy carrier eddies. Under this condition,

$$u^* = x \sqrt{\frac{\varepsilon}{\eta_c}}, \quad \forall x \ll l \quad (51)$$

The Weber number in this case is the ratio of shear stress over Laplace pressure

$$We = \frac{G \eta_c d_{\max}}{2\sigma} \quad (52)$$

Equation (51) and (52) give us the maximum size of a droplet that will never break

$$d_{\max} = \frac{\sigma We_{crit}}{\sqrt{\varepsilon \eta_c}}. \quad (53)$$

P. Walstra *et al.* [426] suggested that the value of We_{crit} is rarely larger than unity. Thus, the maximum size of children droplet is

$$d_{\max} = \frac{C\sigma}{\sqrt{\varepsilon\eta_c}}. \quad (54)$$

Lagisetty *et al.* [427] proposed that the constant C in viscous regime is 0.125.

Table 11: High shear mixer properties and maximum particle size for triacetin – lecithin system

Rotation speed (rpm)	Rotor diameter (m)	Tooth distance (m)	V (m/s)	ε (W/m ³)	Re	u^* (m/s)	l (μm)
20000	0.0127	0.002	13.293	29.36×10^7	2.9×10^4	0.05	0.22

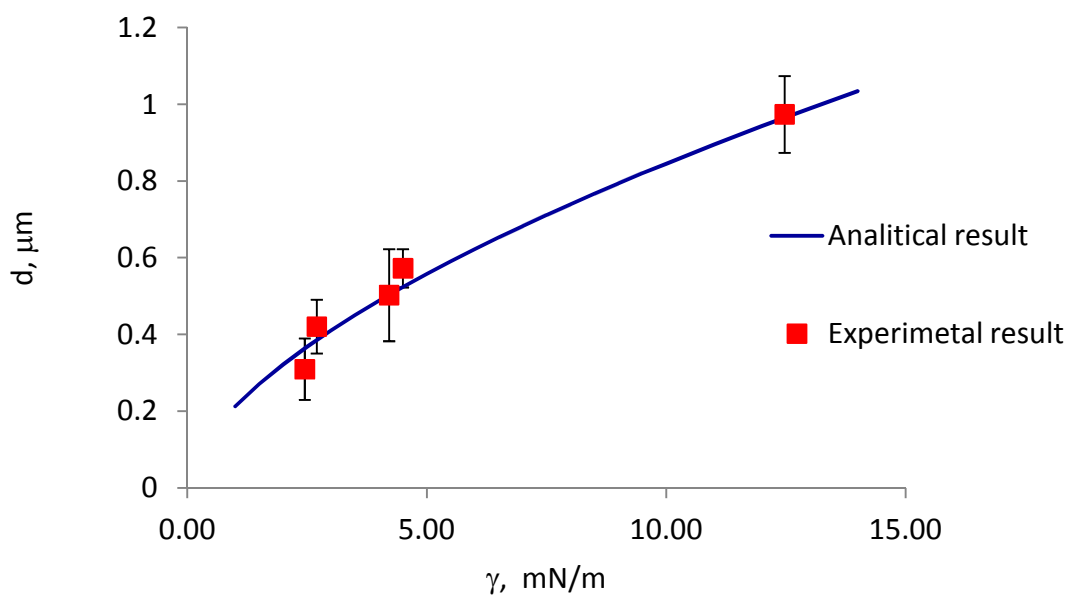


Figure 29: Emulsion droplet size versus surface tension

The operation parameters of the high shear mixer used for preparing beta-carotene nanoemulsion are shown in Table 11. At this flow condition, the Reynolds number of emulsion droplets larger than 70 nm is greater than 1. Thus, the breakup regime of all

micron size emulsion droplets is inertial. Figure 29 demonstrates the maximum diameter of the secondary emulsion droplets as function of the interfacial surface tension estimated by Kolmogorov theory and the experimental result. It is clear that the emulsion droplet size from experimental result fit very well with the analytical result of the model.

2.3. Impact of surfactant on emulsion droplet size

Surfactant plays an important role in droplet breakup. The surfactant occupies the interphase leading to the decrease of surface tension that makes droplet easier to break. Therefore, the attendance of surfactant helps producing emulsions with smaller droplet size. Table 12 shows the interfacial surface tension of triacetin – surfactant – water systems at the concentration of surfactant used for nanoemulsion preparation and the corresponding maximum emulsion droplet size estimated by Kolmogorov theory. It is clear that tween 20 is the best surfactant while lecithin is the worst among the investigating surfactants. The next issue to address how much surfactant is enough for maintaining good emulsion droplet size. The concentration of surfactant has a close relationship with interfacial surface tension given by Gibbs equation $d\sigma = -RT\Gamma \ln a$ where Γ is the surface excess, and a is the activity of the surfactant used. Interfacial surface tension decreases with the increase in concentration of surfactant until CMC. After CMC is reached there is not a significant surface tension reduction.

Table 12: The surface tension of triacetin – surfactant – water system and the maximum emulsion droplet size estimated by Kolmogorov theory

	Triacetin	Triacetin - lecithin	Triacetin – tween 80	Triacetin – tween 20
γ (mN/m)	4.72	4.21	2.7	2.45
d_{\max} (μm)	0.54	0.50	0.36	0.39

Another role of surfactant in emulsion formation is that surfactant prevents emulsion droplets from coagulation. The disruption of emulsion droplet decreases surface concentration of surfactant. If surfactant slowly adsorbs on the droplet surface or amount of surfactant is not enough to build protective layer on the new born droplets, coagulation will occur quickly after flocculation. According to McClements [428], the minimum size of stable droplets that can be produced during homogenization (assuming monodisperse droplets) is therefore governed by the type and concentration of emulsifier present:

$$r = \frac{3\Gamma_{\text{sat}}\phi}{C}, \quad (55)$$

where Γ_{sat} is the excess surface concentration of surfactant at saturated condition (kg/m^2), ϕ is the volume fraction of the dispersed phase, and C is the concentration of surfactant in the bulk (kg/m^3). There is another way to estimate the amount of surfactant based on the area covered by one surfactant molecule, α , which can be determined from the Gibb – Langmuir adsorption isotherm. Supposing that volume of dispersed phase is V , the volume is broken down to m droplets with radius, r . The total area needed to be

covered is $A = 4m\pi r^2$. Therefore, the number of surfactant molecules required to form a fully layer of surfactant on every emulsion droplet is:

$$n = \frac{3V}{\alpha r}. \quad (56)$$

Although equation (55) and (56) can predict the amount of emulsifier required to stabilize emulsions, the surfactant concentration in the system should be smaller than the critical micelle concentration (CMC) of the emulsifier used. Sometimes, it does not require that much amount of surfactant to stabilize emulsion. Taisne et al. [429] have prepared emulsions stabilized by SDS at low concentration in aqueous electrolyte solutions. The authors have found that there is no coalescence even though the concentration of surfactant is very low. They have come to the conclusion that high concentration of electrolytes decreases electrical double layer while it increases electrostatic repulsion leading to stabilization of the emulsion. At low concentration of both electrolytes and SDS, there is drainage of water between two adjoining droplets. This flow prevents droplets from flocculation. Moreover, the adsorption of surfactant on the interface causes interfacial tension gradient $\Delta\sigma$. That induces the movement of the interface at the velocity given by [430]

$$v = 1.23 \sqrt{\frac{(\Delta\sigma)^2}{\eta\rho\delta}}, \quad (57)$$

where δ is the distance that the interface will move. The movement of interface drags some liquid allocated at its adjacency causing the formation of Gibbs – Marangoni effect to stabilize emulsions.

2.4. Impact of other factors to emulsion droplet size

There are several factors affecting the emulsion droplet size. The homogenizer is the main equipment utilized to prepare emulsions. In order to attain the theoretical minimum droplet size, it must be capable of generating a pressure gradient that is large enough to disrupt any droplets as mentioned in equation (41) (i.e. $P \geq 2\sigma/d^2$). Furthermore, emulsion must also spend sufficient time within the homogenization zone for all of the droplets to be completely disrupted. According to Walstra et al. [421] the deformation time of a droplet under external stress σ_{ext} is $\tau_{deform} = \eta_d/\sigma_{ext}$. If an emulsion passes through a homogenizer too rapidly, some of the droplets may not be disrupted. Viscosity of dispersed phase participates in the droplet deformation time. Therefore, the higher viscosity of the dispersed phase the longer deformation time of the droplet is. Another factor affecting the emulsion droplet size is the volume fraction, ϕ , of dispersed phase. High volume fraction of dispersed phase increases the collision rate among emulsion droplets. Therefore, it enhances the flocculation rate and indirectly raises coalescence rate leading to increase in droplet size. Furthermore, high ϕ increases Reynolds number. That may cause the shift in breakup mechanism leading to the change in emulsion droplet size. There is a general rule regulating volume fraction of phases. Emulsions are most stable when the phase volume ration is near 0.50, i.e. the two phases are nearly equal and neither phase shows a clear dominance. The emulsion stability decreases when the volume fraction of either phase increases to the value which is greater than 0.75.

3. The adsorption of surfactant on triacetin interface

Surfactant not only plays an important role in the stability of nanoparticle by contributing to the repulsion force but is also involved in the nanoparticle formation. By concentrating at the oil-water interface, surfactant decreases interfacial surface tension leading to the change in diffusion flux. The absorption isotherm of surfactant at the interphase has been characterized by Gibbs model [431] as the relationship between the surface excess, Γ , the bulk concentration of surfactant, C , and the interfacial surface tension, γ .

$$\left(\frac{\partial \gamma}{\partial \ln C} \right)_T = -RT\Gamma. \quad (58)$$

By nature of amphiphilic molecules, surfactant tends to concentrate at the interface more than distribute in the bulk. According to Langmuir [432], the excess surface concentration caused by absorption can be estimated from the bulk concentration as

$$\omega\Gamma = \frac{K_{ad}C}{1 + K_{ad}C}, \quad (59)$$

where ω is the cross-sectional area of the surfactant molecules at the interface and K_{ad} is the equilibrium adsorption constant. The surface tension of surfactant solution (γ) at equilibrium condition is described by Szyszkowski [433] from the surface tension of pure solvent (γ_0), bulk concentration and saturated absorption concentration

$$\gamma_0 - \gamma = \frac{RT}{\omega} \ln(1 + K_{ad}C). \quad (60)$$

Therefore, by measuring the interfacial surface tension at different surfactant concentration, we can estimate the cross-section area occupied by surfactant molecules at equilibrium condition. The interfacial surface tension of air – triacetin – surfactant is presented in Figure 30. The experimental data shows that the CMC of lecithin is larger

than that of Tween 20. The large value of adsorption energy of both surfactants indicates that both surfactants adsorb quickly on triacetin surface. This maintains the narrow distribution of emulsion droplets to prevent beta-carotene nanoparticles from Ostwald ripening of beta-carotene nanosuspensions. The coverage area of tween 20 is much larger than that of lecithin showing that it requires less number of tween 20 than lecithin molecules to cover the same area. Table 13 presents the adsorption parameters of these surfactants in triacetin by applying Szyszkowski equation.

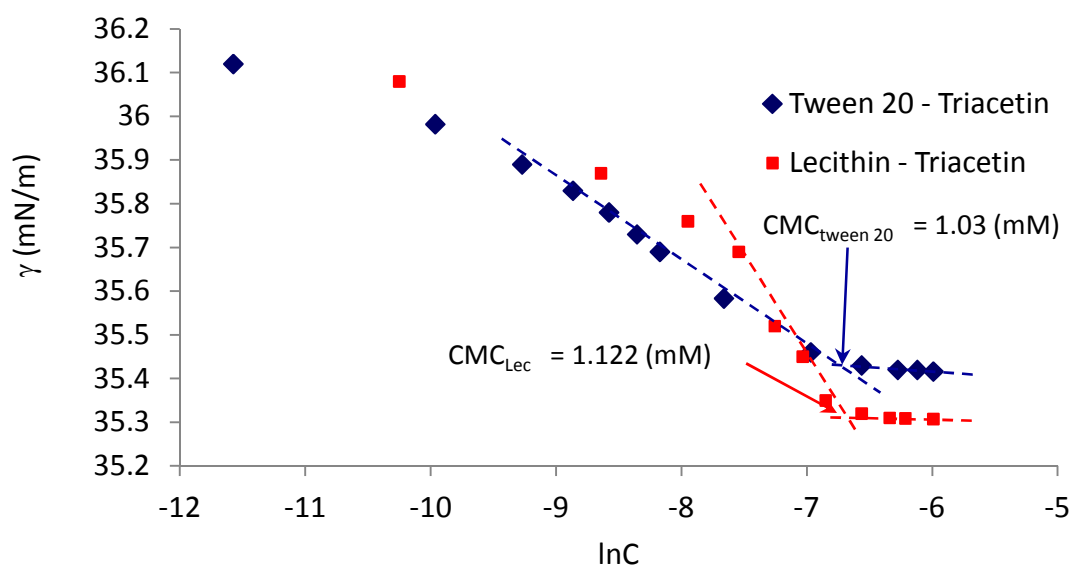


Figure 30 : Surface tension of lecithin and Tween 20 solutions

Table 13: Adsorption parameters of surfactant -triacetin system

	$K_{ad}(M^{-1})$	$\Delta G(J)$	$\omega (m^2 \cdot mole^{-1})$	$\alpha (m^2 \cdot molecule^{-1})$
Tween 20	4.81	-3891.0	22331.70	3.71×10^{-20}
Lecithin	3.46	-3079.33	17456.47	2.90×10^{-20}

(α is the area occupied by a surfactant molecule)

4. Solubility of beta-carotene in triacetin

Solubility of beta-carotene in triacetin is important. It regulates the beta-carotene loading capacity of nanoemulsion. The solubility curve of β -carotene in triacetin can be distinguished by three segments. The first part shows linear relationship between β -carotene concentrations in solution versus transmission intensity. It obeys Beer – Lambert Law for dilute concentration solution. The second segment, where the transmission intensity decays with the increase of solute concentration, corresponds to the solutions with condense concentration of solute. In the last part, the transmission intensity becomes independent of β -carotene concentration showing the over saturation of solute in solution. The solubility of β -carotene in triacetin is determined to be 0.012% or 0.247 mM by intersecting two lines on the transmission intensity vs. $\log(\text{concentration})$ plot in Figure 31. The lines distinguish the concentration ranges where the solution is dilute, and where the solution is saturated or has excess β -carotene.

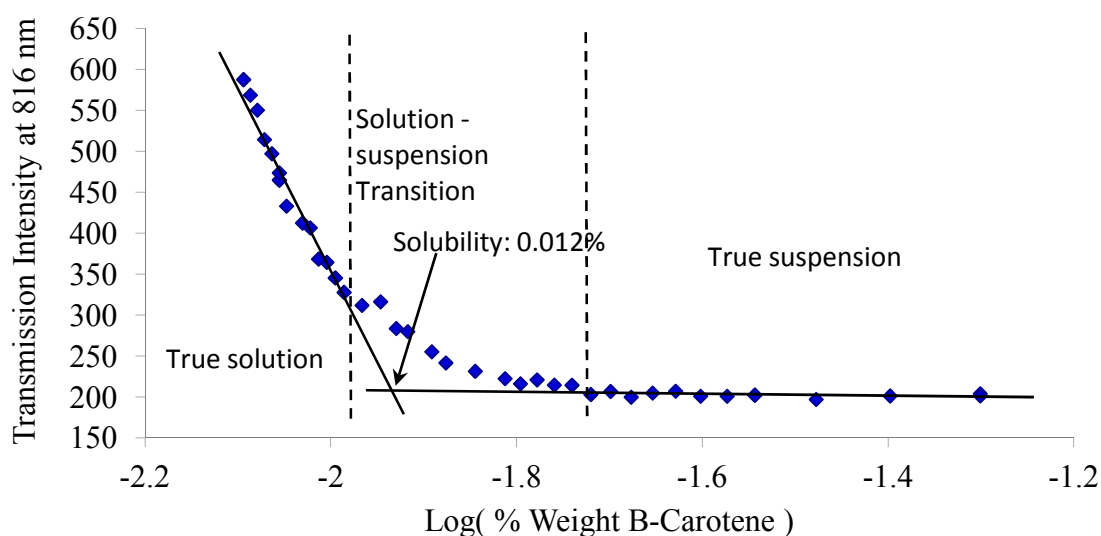


Figure 31: Solubility of β -carotene in Triacetin Curve

NANOSUSPENSION PREPARATION

1. Mathematic model for the diffusion of triacetin from an emulsion droplet

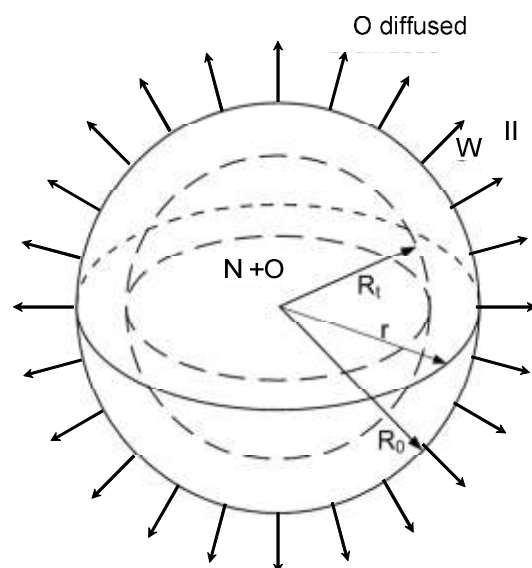


Figure 32: The diffusion of triacetin from an emulsion droplet

For the application of this technique to prepare nanoparticles of hydrophobic nutraceuticals it is important to understand the fundamentals governing the process of nanoparticle formation in order to produce the smallest particles possible in a controlled manner. A simple analytical model is developed utilizing a single droplet to represent the overall process. An image of the system is shown below as Figure 32. The background of the system is as follows: The system consists of two regions, Region I and II. Region I is the dispersed phase droplet constructed from a saturated concentration of a hydrophobic nutraceutical N soluble in oil O. The droplet is immersed in aqueous medium W. N is insoluble in W while O is partially soluble. The concentration of N and

O in the droplet is A and B respectively. It is hypothesized that W is homogeneous and isotropic. Initially, when the diffusion does not occur, the radius of the droplet is R_0 . And then, O suddenly diffuses out of the droplet leading to the shrinkage of the droplet when $t > 0$. Thus at time $t = \tau$, the droplet has radius $R' = R(t)$ and its surface is denoted by the dotted surf in Figure 32. We suppose that the droplet is homogeneous at beginning and isotropic during the diffusion process. It is also assumed that the diffusion coefficient of N and O inside the droplet is much larger than that of O in W and W cannot penetrate into I or $\mathcal{D}_N^I = \mathcal{D}_O^I = \infty$ and $\mathcal{D}_W^I = 0$. Furthermore, the concentration differs on radius only and the droplet shape remains spherical during diffusion process. That means $\frac{\partial C_i}{\partial \phi} = \frac{\partial C_i}{\partial \theta} = 0$ where C_i is mass fraction of component i^{th} in the system. The diffusion of component i^{th} in the media can be presented as

$$\frac{\partial C_i}{\partial t} = -\mathcal{D}_i \nabla^2 C_i. \quad (61)$$

For spherical co-ordinate and using isotropic condition, equation (61) for oil O becomes

$$\frac{\partial C}{\partial t} = -\mathcal{D} \left[\frac{1}{r^2} \frac{\partial}{\partial r} \left(r^2 \frac{\partial C}{\partial r} \right) \right] \quad (62)$$

The boundary conditions and initial condition for equation (62) are

$$\begin{aligned} C(r, 0) &= \begin{cases} C_0 & -R < \forall r < R \\ 0 & \forall r < -R \text{ or } \forall r > R \end{cases} \\ C(R(t), t) &= C^S \quad \forall t > 0 \\ C(\infty, t) &= C^\infty = 0 \quad \forall t \geq 0 \end{aligned} \quad (63)$$

In order to make the problem simpler, a new variable $\mathcal{C} = r(C^\infty - C^s) = -rC^s$ is introduced into equation (62). Thus that equation now becomes

$$\frac{\partial \mathcal{C}}{\partial t} = \mathcal{D} \frac{\partial^2 \mathcal{C}}{\partial r^2} \quad (64)$$

It is subjected to the following boundary conditions and initial conditions

$$\begin{aligned} \mathcal{C}(r, 0) &= -rC^s \\ \mathcal{C}(R, t) &= 0 \end{aligned} \quad (65)$$

It is noticed that the droplet shrinks while O is diffusing into W. Thus, another variable $\xi = r - R(t)$ is introduced to represent the movement of the droplet surface and make equation (64) identical with a one dimensional heat conduction problem which has the solution as shown in [434]

$$\mathcal{C}(r, t) = \frac{C^s}{2\sqrt{\pi \mathcal{D} t}} \int (R(t) - \xi') \left\{ \exp\left[-\frac{(\xi - \xi')^2}{4\mathcal{D} t}\right] - \exp\left[-\frac{(\xi + \xi')^2}{4\mathcal{D} t}\right] \right\} d\xi'. \quad (66)$$

The modified concentration gradient at the droplet surface can be found from equation (66) as

$$\left. \frac{\partial \mathcal{C}}{\partial r} \right|_{r=R(t)} = C^s \left(1 + \frac{R(t)}{\sqrt{\pi \mathcal{D} t}} \right), \quad (67)$$

because $\left. \frac{\partial C}{\partial r} \right|_{r=R(t)} = \frac{1}{R(t)} \left. \frac{\partial \mathcal{C}}{\partial r} \right|_{r=R(t)}$ we obtain the concentration gradient at the interface

$$\left. \frac{\partial C}{\partial r} \right|_{r=R(t)} = C^s \left[\frac{1}{R(t)} + \frac{1}{\sqrt{\pi \mathcal{D} t}} \right]. \quad (68)$$

Therefore, the mass flux of species O out of the droplet per unit of time is now

$$\dot{m} = \frac{dm}{dt} = -4\pi R^2(t) \mathcal{D} \left. \frac{\partial C}{\partial r} \right|_{r=R} = -4\pi R^2(t) C^S \left(\frac{1}{R} + \frac{1}{\sqrt{\pi \mathcal{D} t}} \right). \quad (69)$$

The mass conservation for the droplet gives

$$\frac{dm}{dt} = 4\pi R^2(t) \rho_O \frac{dR(t)}{dt}, \quad (70)$$

where ρ_O is the density of oil O. Thus, the droplet evolution from equation (69) and (70) can be represented as

$$\frac{dR}{dt} = -\frac{\mathcal{D} C^S}{\rho_O} \left(\frac{1}{R} + \frac{1}{\sqrt{\pi \mathcal{D} t}} \right). \quad (71)$$

Because the diffusion coefficients of both N and O in the droplet is significantly very large as compared to the size of the drop, the droplet maintains homogeneous concentration distribution and isotropic during the diffusion process. C^S can be estimated from the volume fraction of the N-O binary system.

$$C^S = \frac{1}{v_O} \left(1 - \frac{n_N v_N}{\frac{4}{3} \pi R^3} \right), \quad (72)$$

where v_N and v_O are the volume of one mole of the nutraceutical N and oil O respectively. n_N is the number of mole N inside the droplet. However, the solubility of N in O is quite small. As a result, we can ignore the second term in equation (72). Thus,

$C^S = \frac{1}{v_O}$. Submitting this term in to equation (71), we have

$$\frac{dR}{dt} = -\frac{\mathcal{D}}{\rho_o v_o} \left(\frac{1}{R} - \frac{1}{\sqrt{\pi \mathcal{D} t}} \right) = -\frac{\mathcal{D}}{Mw_o} \left(\frac{1}{R} - \frac{1}{\sqrt{\pi \mathcal{D} t}} \right), \quad (73)$$

where Mw_o is the molecular weight of oil O. To solve equation (73) two dimensionless variables are introduced. Let $y = \frac{R}{R_0}$ is dimensionless length and $x^2 = \frac{2\mathcal{D}t}{R_0^2}$ is the dimensionless diffusion length variable, equation (73) becomes

$$\frac{dy}{dx} = -\frac{1}{Mw_B} \left(\frac{x}{y} - \sqrt{\frac{2}{\pi}} \right) \quad (74)$$

Solution to equation (74) in form of x series is $y = y_0 - \frac{x}{Mw_o \sqrt{\pi/2}} - \frac{x^2}{2Mw_o^2 y_0} - O(x^3)$.

Therefore, the solution to the equation (73) is

$$R = R_0 - \frac{2\sqrt{\mathcal{D}t}}{Mw_o \sqrt{\pi}} - \frac{\mathcal{D}t}{Mw_o^2 R_0}. \quad (75)$$

The development of this model enlightens several key parameters for the optimizing of minimizing particle size. According to the model, the key factor most significant to control the particle size is the initial droplet size, which has been generated by homogenization. Additionally, density of the oil phase, and the diffusion coefficient of the partially miscible oil into the continuous aqueous phase are also important. The evolution of droplet size is presented in Figure 33 with different initial radius. It is clear that the smaller the droplet is the faster diffusion is. Moreover, initial droplet size determines the size of final suspension particles.

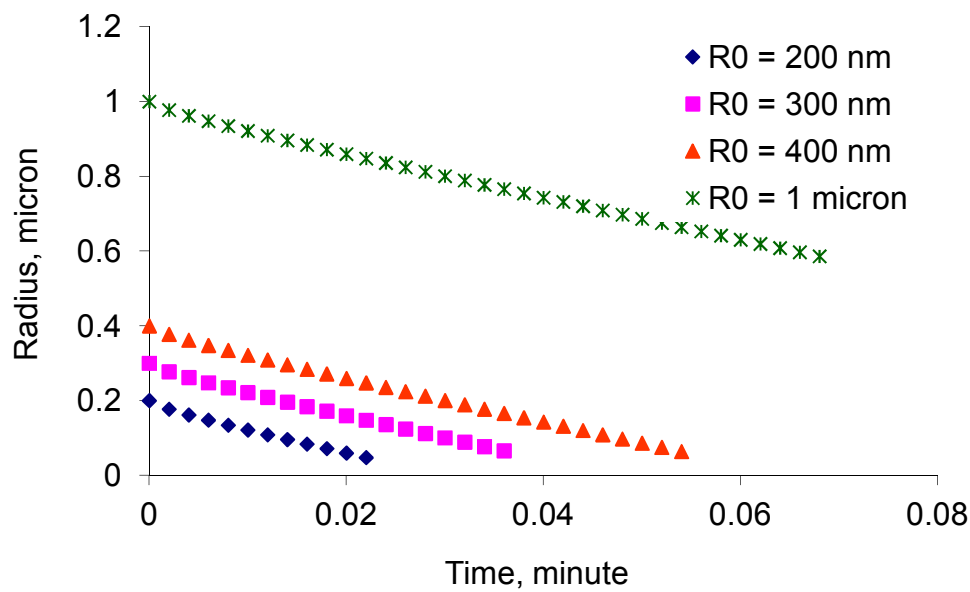


Figure 33: The evolution of droplet radius over time

In equation (75), \mathcal{D} is the diffusivity of Triacetin and can be estimated by utilizing the Stokes – Einstein equation

$$\mathcal{D} = \frac{k_B T}{6\pi\mu r}, \quad (76)$$

where k_B is Boltzmann constant, μ is the viscosity of water at room temperature, and r is the molar radius of Triacetin shown in Table 14. The diffusion flux of triacetin from an emulsion droplet is defined as

$$f = \frac{d}{dt} \left(\frac{V_{droplet}}{A_{droplet}} \right). \quad (77)$$

Table 14: Molar factor of Triacetin

Mw (g mole ⁻¹)	Molar volume (m ³ mole ⁻¹)	Molar radius (m)	Diffusivity (m ² s ⁻¹)	Solubility (g/100 ml)
218.21	0.033 x 10 ⁻²³	0.429x10 ⁻⁹	4.96x10 ⁻⁹	7

Figure 34 shows the both the analytical diffusion flux coming from solution combining equation (75) with equation (77), and the experimental flux measured from a pendant droplet suspended in water. The experimental data shows that after introduction time of 90 seconds, the flux of triacetin from the droplet is in high agreement with the analytical solution of the model. It is noted that when solving for analytical solution, we hypothesize that the triacetin concentration at the water layer in contact with the droplet surface is at saturated condition. The experiment observation reveals that it takes 90 seconds to reach the hypothetical condition. The high agreement between experimental observation and analytical solution validates the solidification of the model developed.

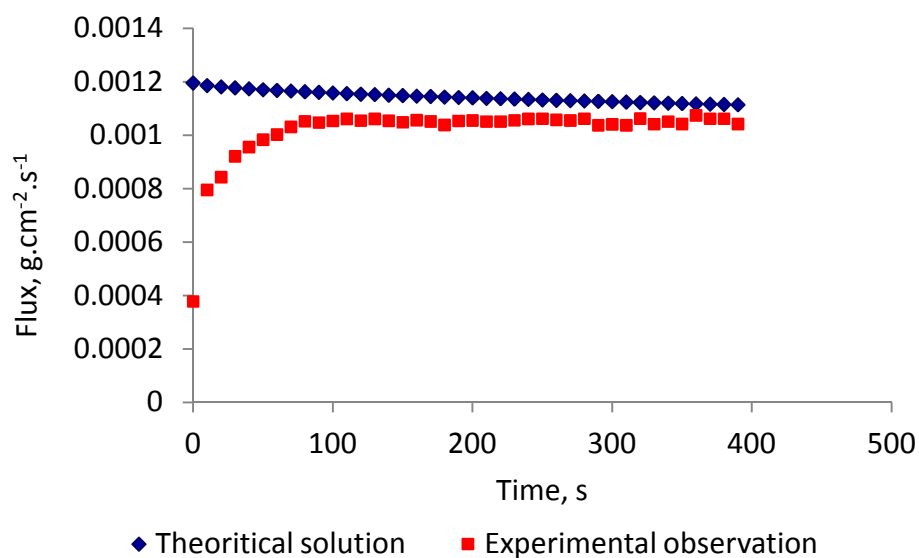


Figure 34: The diffusion flux of triacetin from a pendant droplet

2. The crystallization of beta-carotene in emulsion droplet

Generally, the crystallization of a material starts with nucleation and is followed by crystal growth. There are two types of nucleation. They are (1) homogeneous nucleation

where cluster of molecules forms nucleus and (2) heterogeneous nucleation where interface forms the nucleus. In homogeneous nucleation, the solute molecules must interact in order to form a cluster. At low concentration, the distance among molecules is large. Furthermore, solute molecules have high motion because of Brownian walk. Thus, there is no chance for molecules to interact. When the solution is at supersaturated concentration, the solute molecules not only have low motion but also are tightly packaged. Moreover, supersaturated concentration drives the solution possessing high Gibbs free energy. Therefore, the system reacts by excluding solute molecules to recover the thermodynamic equilibrium. This reduction of Gibbs free energy is the driving force for both nucleation and growth. The change of Gibbs free energy per unit volume of the solid phase, Δg_v , is dependent on the concentration C of the solute and temperature T :

$$\Delta g_v = -\frac{k_B T}{\Omega} \ln \frac{C}{S}, \quad (78)$$

where k_B is the Boltzmann constant, S is the solubility (mole per liter) of solute in the solution, and Ω is the atomic volume. Equation (78) means that when the concentration of the solution is not larger than the solute solubility $\Delta g_v \geq 0$, consequently, no nucleation occurs. On the other hand $\Delta g_v \leq 0$ and nucleation occurs spontaneously. By chance, molecules interact then form clusters of metastable solid phase. The existence of the globule leads to the formation of a new phase and causes the change in Gibbs free energy $\Delta G_v = (4/3)\pi r^3 \Delta g_v$, due to volume formation. However, the system also spend energy, $\Delta G_s = 4\pi r^2 \gamma$, for the formation of new surface. Therefore, the Gibb free energy of a metastable solid phase is

$$\Delta G(r) = \frac{4}{3} \pi r^3 \Delta g_V + 4\pi r^2 \sigma \quad (79)$$

where r is the radius of the metastable solid phase; σ is the interfacial surface tension. Initially, the total energy increases with the addition of molecules to the embryo until it passes the maximum value, ΔG^* , where the volume formation energy becomes dominant as shown in Figure 35. The radius where the free energy value is maxima is the critical radius for a cluster to be a nucleus. The critical radius is

$$r^* = -\frac{2\sigma}{\Delta g_V}, \quad (80)$$

and the critical Gibbs free energy to be a nucleus is

$$\Delta G^* = \frac{16\sigma^3}{3(\Delta g_V)^2}. \quad (81)$$

For heterogeneous nucleation, the solute molecules interact with preferential sites for the cluster formation. The preferential sites can be impurities or the defections on the wall container. The participation of the preferential sites changes the nucleation mechanism because the aggregation of solute molecules on impurities replaces impurity – liquid interface by impurity – solid interface. Therefore, the Gibbs free energy for surface formation becomes

$$\Delta G_S = 2\pi r^2 (1 - \cos \theta) \gamma_{S-L} + \pi r^2 (1 - \cos^2 \theta) (\gamma_{I-S} - \gamma_{I-L}) \quad (82)$$

The first term in equation (82) is the energy for new solid – liquid interface while the second term is the energy for the replaced interface of impurity – liquid by impurity – solid; γ , γ_{I-S} , γ_{I-L} are the interfacial surface tension of solid – liquid, impurity – solid,

and impurity – liquid respectively. These surface tensions define the wet contact angle, θ , in both equation above

$$\cos \theta = \frac{\gamma_{I-L} - \gamma_{I-S}}{\gamma_{S-L}} \quad (83)$$

The Gibbs free energy of volume formation, ΔG_V , is now

$$\Delta G_V = \frac{4}{3} \pi r^3 \Delta g_V \frac{(2 + \cos \theta)(1 - \cos \theta)^2}{4}. \quad (84)$$

The critical radius for an embryo to be a nucleus is similar to that of homogeneous nucleation but the critical Gibbs free energy becomes

$$\Delta G^* = \frac{16\gamma^3}{3(\Delta g_V)^2} \frac{(2 + \cos \theta)(1 - \cos \theta)^2}{4} \quad (85)$$

Thus, the preferential sites contribute to the decrease of critical Gibbs free energy by shape factor. The nanoemulsion droplets contain surfactant molecules which serve as impurity. Therefore, the nucleation of beta – carotene in the droplets is mainly heterogeneous nucleation. Besides these two types of nucleation mentioned above, there is another type of nucleation occurring at lower supersaturated concentration than needed in spontaneous nucleation. It is secondary nucleation which causes tiny crystals on the surface of seed crystals.

Equation (80), and (81) indicate that the critical size and critical Gibbs free energy are strongly dependent on interfacial surface tension, and volume formation Gibbs free energy. According to Eötvös' rule, the surface tension decreases linearly with the increasing of temperature

$$\sigma = \frac{K_E}{\sqrt[3]{V^2}}(T_C - T) \quad (86)$$

where $K_E = 2.1 \times 10^{-7} JK^{-1} mol^{-2/3}$ is the Eötvös' constant, V is the molar volume, and T_C is the critical temperature. Therefore, the higher the crystallization temperature is the smaller interfacial surface tension is. Another way to decrease the critical size of the embryo is increasing the volume formation Gibbs free energy. Because it is a function of the initial concentration C of the supersaturated solution, increasing supersaturated ratio which is the ratio between solution concentration and the solubility, can drive the system to achieve high value of Δg_v . High supersaturated condition of a system can be obtained by dissolving solute at high temperature then cool it down. High supersaturated ratio can also be achieved by extracting solvent out of the system. In case of beta-carotene – triacetin system, the diffusion of triacetin from the emulsion droplets to aqueous phase may increase the supersaturated ratio in the emulsion droplets during the formation of nanosuspensions.

According to Markov [435] the rate of homogeneous nucleation can be expressed as

$$J_{\text{homo}} = \omega \Gamma S \exp\left(-\frac{\Delta G^*}{k_B T}\right) \quad (87)$$

where Γ is the Zeldovich factor which has value in the range from 0.01 to 1, ω is the frequency of attachment of atoms to the critical embryo. Value of ω in homogeneous nucleation is much smaller than in heterogeneous nucleation.

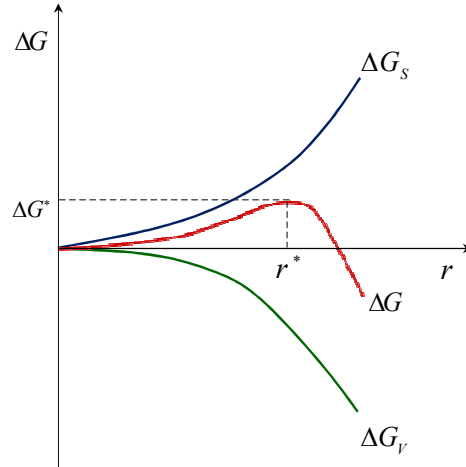


Figure 35: Nucleation energy

When nuclei are formed, solute molecules diffuse from liquid phase to the surface of nuclei to interact. The growth of a crystal consists of diffusion and reaction steps. Supposing that the concentration of solute in the bulk is C_b , that at the solid – liquid interface is C_i , and at the solid surface is C_s , the rate of diffusion step, R_D , and that of reaction step, R_r can be expressed as following:

$$R_G = k_D (C_B - C_i), \quad (88)$$

$$R_G = k_R (C_i - C_s)^\alpha. \quad (89)$$

When there are no of extreme conditions, it is possible to find an analytical relation between reaction rate and the overall concentration variation $\Delta C = C_B - C_s$ [436]. Thus the unknown concentration at the solid – liquid interfacial can be eliminated by combining the two equations (88) and (89). The growth rate becomes

$$R_G = k_R \left(\Delta C - \frac{R_G}{k_D} \right)^\alpha. \quad (90)$$

By introducing “Damköhler number” [437, 438], $h = \frac{k_R}{k_D} \Delta C^{\alpha-1}$, equation (90) becomes

$$\psi_c = [1 - h\psi_c]^\alpha \quad (91)$$

The so-called “two-step model” has found great application for chemical engineering purposes. It offers a simple and instinctive arrangement of the processes involved in the crystal growth. Despite that, difficulties in the scale up of crystallizers are often reported, due to uncertainties in the prediction of growth rates [439].

High reaction rate brings disadvantages to the arrangement of solute molecules at the surface of the crystal. In addition, small diffusion rates give more chance for impurity to be captured inside the crystal. This phenomenon has been well discussed by several researchers [440-443]. When the rate of diffusion is dominant, solute molecules become abundant at the surrounding of the crystal. Besides, a large diffusion rate brings the advantage of enabling the solvent to escape from the development of crystal. Furthermore, small reaction rate helps solute molecules rearrange themselves at activation sites on the crystal surface. In spite of the advantages of large diffusion rate, in some cases, a too large diffusion rate induces high reaction rate leading to amorphous formation. For example in precipitation using spray, the large evaporation rate of solvent disturbs the arrangement of solute molecules at the solid – liquid interface breaks the crystal lattice formation leading to the formation of amorphous structure. In the case of β -carotene – triacetin – water system, triacetin removal from emulsion droplets induces the droplet shrinkage. That squeezes β -carotene molecules in the oil phase towards the beta-carotene crystals. The convection caused by droplet size reduction increases diffusion rate dramatically. That may be a reason for amorphous structure formation of

beta-carotene nanoparticles. High convection can also causes impurity trapped in amorphous beta-carotene nanoparticles.

The initial amount of beta carotene in an emulsion droplet is $m_\beta = \frac{4}{3}\pi R_0^3 \rho_T S$, where S is the solubility of beta-carotene in triacetin in weight percent and ρ_T is the density of triacetin. Supposed that the concentration of beta-carotene in the emulsion droplets during the diffusion of triacetin is aS (where $a > 1$) and the size of solid beta-carotene is too small to be ignored, the mass fraction of solid beta-carotene in the emulsion droplet as function of the droplet size can be expressed as

$$\phi = \frac{S [R_0^3 - a(R(t))^3]}{SR_0^3 + [R(t)]^3}. \quad (92)$$

Figure 36 presents the evolution of solid beta-carotene in an emulsion droplet where $a = 1.2$ during the diffusion of triacetin.

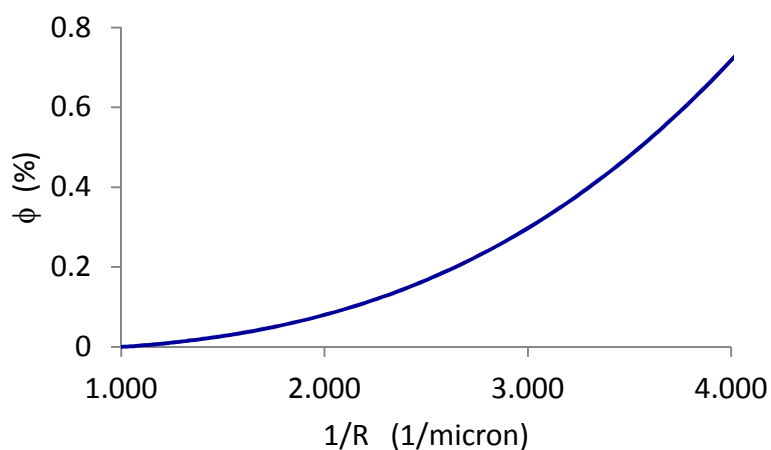


Figure 36 : The mass fraction of solid beta-carotene versus emulsion droplet size during the diffusion of triacetin

3. The diffusion of triacetin from a droplet

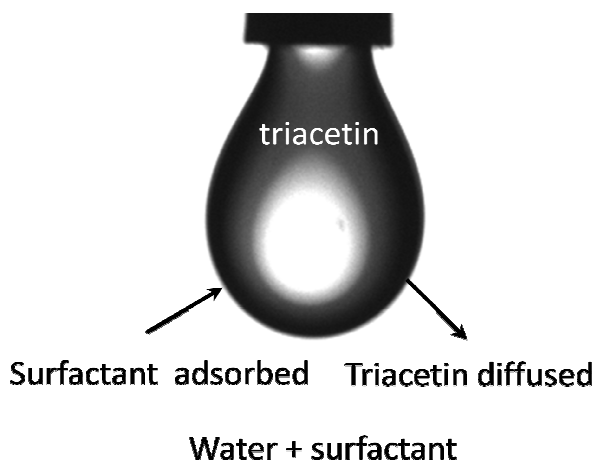


Figure 37: Triacetin diffused from a pendant droplet

The flux of triacetin from a droplet was estimated by measuring the volume of a triacetin droplet suspended in different surfactant solutions over time. The experimental set up is described in Figure 37. A triacetin droplet is mounted at the end of a needle and suspended in water or a surfactant solution at dilute concentration. Initially, the droplet is pended at its maximum volume. The triacetin in the droplet starts diffusing into the aqueous phase to decrease the volume of the droplet. The diffusion flux of triacetin is defined as the derivative of droplet size over time and is shown in Figure 38. It can be seen that the flux of triacetin from the droplet in surfactant solutions is higher than that in water. The order of the diffusion flux in the investigated media is tween 20 > tween 80 > lecithin > water. The diffusion flux from the triacetin droplets contains two stages distinguished by the change in the slope of the curves.

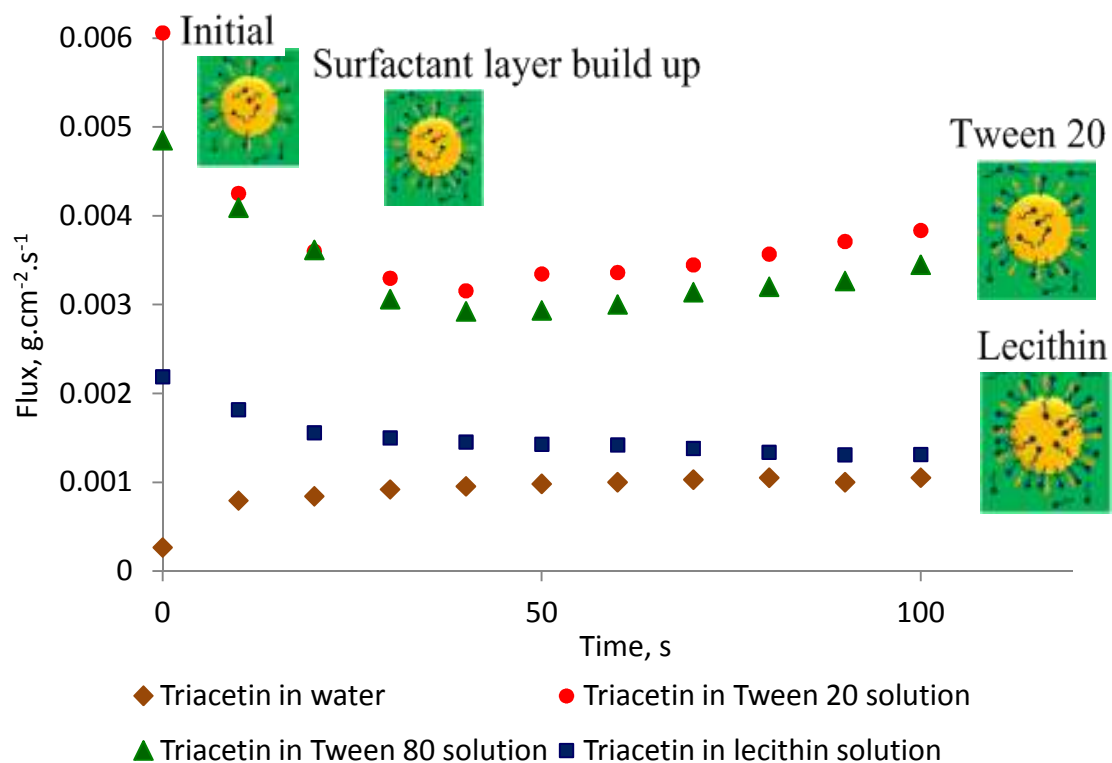


Figure 38 : The flux of triacetin in different surfactant solutions

The diffusion of triacetin from the pendant droplet consists of two steps. It starts with the mass transfer of triacetin crossing the water – oil interfacial to water phase and is followed by the diffusion of triacetin in water. The mass transportation across immiscible liquid-liquid interface has been investigated by applying molecular dynamics simulation [444-448]. It has been documented that the driving force for the mass transfer of solute at the interface are the combinations of the fluctuation at liquid-liquid interface [449] and capillary force[447]. Along with the migration of triacetin through the interface, water penetrates the interfacial [450]. That forms a layer of triacetin adjacent to the droplet and creates a driving force for the diffusion of triacetin in water. Thus the overall diffusion flux of triacetin is controlled by the concentration of triacetin in the layer adjoining the suspended droplet. The concentration of triacetin in this layer is increasing gradually

causing the increase of diffusion flux at the beginning. According to the Ostwald–Freundlich equation the solubility of triacetin in the layer is proportional to interfacial surface tension and reversely proportional to the droplet size. That sets a limitation of concentration that triacetin can reach in the layer and indirectly defines the plateau of diffusion flux of triacetin from the droplet when no surfactant is used. Thus, the introduction stage of the diffusion finishes when the concentration of triacetin in the layer adjoining the droplet is saturated.

When surfactant is used, surfactant molecules adsorb on the oil – water interface to decrease the interfacial surface tension leading to high flux of triacetin both from the droplet to the film adjacent and in water phase. The smaller the surface tension is the larger diffusion flux is. That corresponds to the order of interfacial surface tension of triacetin – surfactant – water shown in Table 12. Along with the diffusion of triacetin, surfactant molecules accumulate at the droplet interface to form a surfactant layer which interferes with the mass transfer causing the decrease in mass flux. Thus, the mass flux of triacetin from the droplets with surfactant is governed by the formation of surfactant layer at the oil-water interface during introduction stage. The triacetin flux from the droplet with surfactants in second stage is very interesting. While the diffusion flux of triacetin from droplet with lecithin is almost constant, the diffusion flux from the droplet with tween 20 and tween 80 increases. The phenomena can be explained based on the nature of surfactants used. The solubility of lecithin in water is very small, for example the solubility of Di-Palmitoyl Phosphatidylcholine is 4.6×10^{-10} M [451]. In oil-water system, lecithin mainly distributes in oil phase. Lecithin has been well documented to form a bi-layered structure [405, 452-455]. In addition, Gennis [456] has suggested that

there are several type of packaging in the bi-layered structure of lecithin depending on the head group and lecithin concentration. For instance, phosphatidylcholine with large head group can shift from straight arrangement to tilted arrangement which allows tighter packing. LeNeveu et al. [452] has documented that the inter-bilayer distance of bi-layered lecithin is 28 Å. This gap is much larger than the size of triacetin (around 4.3 Å). The accumulation of lecithin at the interface of triacetin-water will lead to the formation of a stable bi-layered structure and may cause the stable barrier for the transfer of triacetin from the pendant droplet. As a result, beta-carotene is encapsulated by layer of lecithin. In case of tween 20 and tween 80, high solubility in water of these compounds leads to desorption of surfactant layer on the pendant droplets that makes the diffusion flux increases.

We hypothesis that at dilute concentration of surfactant the number of adsorption sites on the triacetin – media interface is a function of surfactant concentration only. Using Gibbs adsorption isotherm we can estimate the number of adsorption sites on the triacetin droplet surface as function of surfactant concentration. These values are also the number of surfactant molecules adsorbed at the interface as a function of surfactant concentration. Therefore, we can estimate the distance among surfactant molecules adsorbed on triacetin droplet surface when the droplet is pended in surfactant solutions. During the diffusion of triacetin, the surface of the droplet decreases. This reduces the distance among surfactant molecules adsorbed on the interface. As a result, there is the overlap of area occupied by a surfactant molecule at certain time. The overlap of occupied area causes desorption of tween 20. On the other hand, it brings advantage for lecithin to form double layer. Table 15 presents the initial and the shortest distances among surfactant molecules on the

surface of triacetin droplet with different type of surfactant. The shortest distances among surfactant molecules are estimated when the diffusion flux from the droplets becomes smallest of approaches plateau. It is clear that the obtain values highly agree with the occupied area in Table 13. The shortest distance among lecithin molecule in our results is much smaller than found by Small [405] but still larger than the hydrodynamic size of triacetin.

Table 15: Distance among surfactant molecules adsorbed on triacetin surface

Surfactant	Number of molecules adsorbed at interfacial ($mole.m^{-2}$)	Initial distance among molecules (m)	Shortest distance among molecules (m)
Tween 20	2.03×10^{13}	13×10^{-10}	10.5×10^{-10}
Lecithin	5.03×10^{13}	10.9×10^{-10}	9.45×10^{-10}

4. Impact of surfactant on the particle size

Figure 39 shows the impact of surfactant on the distribution of particle size. The blue lines represent the particles made from triacetin – lecithin system while the green and the red lines symbolize particles made from triacetin – Tween 20 and triacetin – Tween 80 systems respectively. It is surprised that soy lecithin yielded the smallest particles. According to the estimated proposed in Table 12, emulsion droplet size is in order tween 20 < tween 80 < lecithin. We expected that the size of nanosuspensions follows this order. The disagreement between experimental results and the expectation could be explained by the aggregation of emulsion droplets during the diffusion of triacetin. By

adding water to create diffusion driving force for triacetin, we dilute concentration of surfactants. It is noticed that tween 20 and tween 80 are more available in water phase than oil phase. On the other hand, lecithin favors oil phase more than water. As mentioned earlier, when either tween 20 or tween 80 is used, surfactant desorbs from the oil – water interface during the formation of the nanosuspensions. Desorption causes the shortage of surfactant at the particle surface leading to aggregation. For lecithin, the low solubility in water interferes with its migration from the oil –water interface to aqueous medium leading to the formation of a strong lecithin layer at the interface to prevent the aggregation of nanoparticles. As shown in Table 13, the coverage area of tween 20 and lecithin is 0.037 nm² and 0.029 nm² per molecule respectively. It requires approximately 3.4×10^6 molecules of tween 20 to fully cover the surface of a particle with its size of 200 nm. It seems impossible to approach that value when solubility of tween 20 in water is high and the concentration of tween 20 in the suspension is quite small. However, the number of lecithin molecules needed to cover the surface of the similar particle is 4.3×10^6 . Furthermore, the solubility of lecithin in water is very small. Therefore, there are enough lecithin molecules adsorbed on the surface of the nanosuspension to prevent particles from aggregation. We have not seen any improvement of particle size when the amount of lecithin is larger than 5% of weight in emulsion preparation.

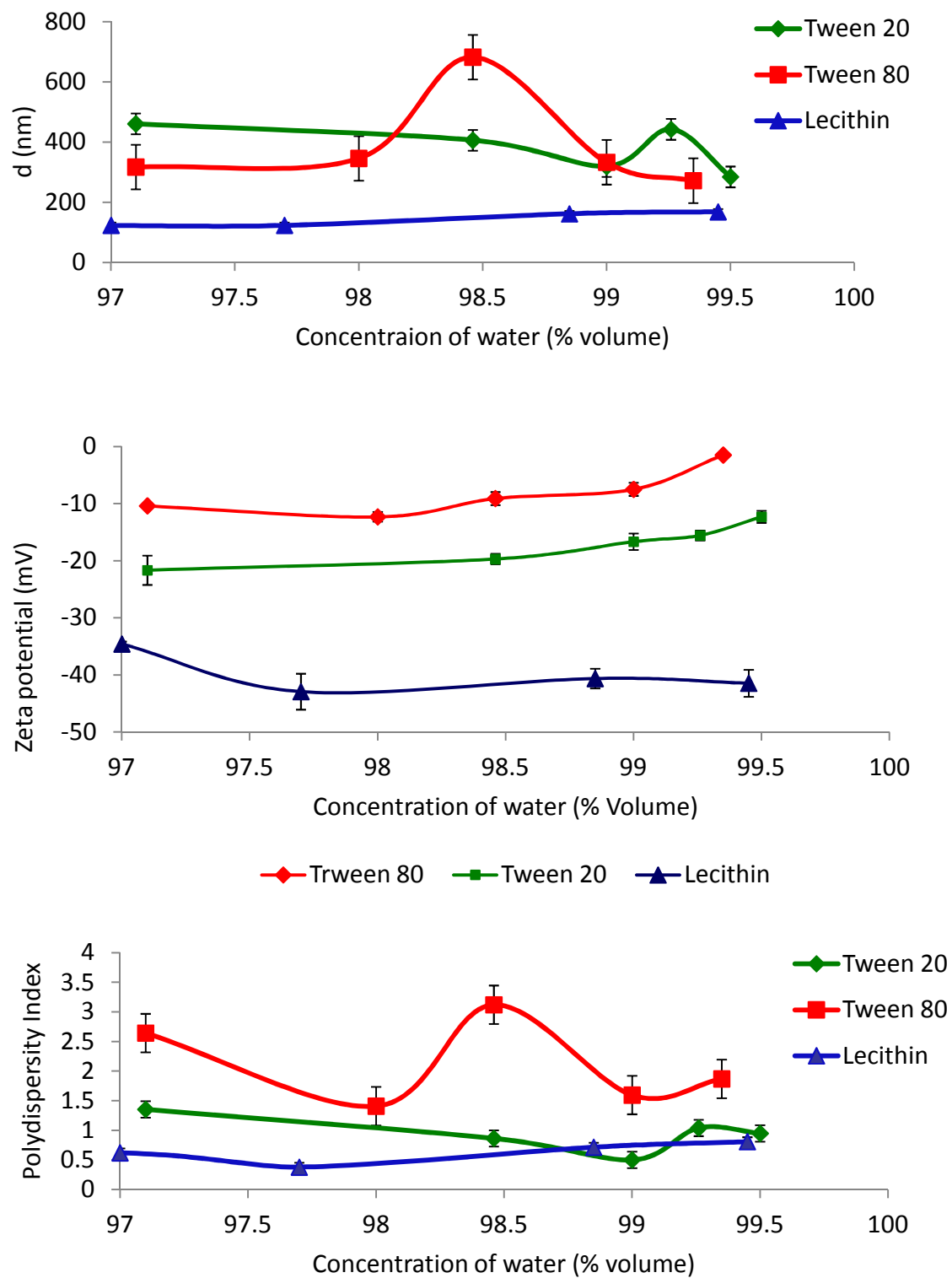


Figure 39: Impact of surfactant on the particle size

5. Impact of operation parameters on the particle size and stability of nanosuspension

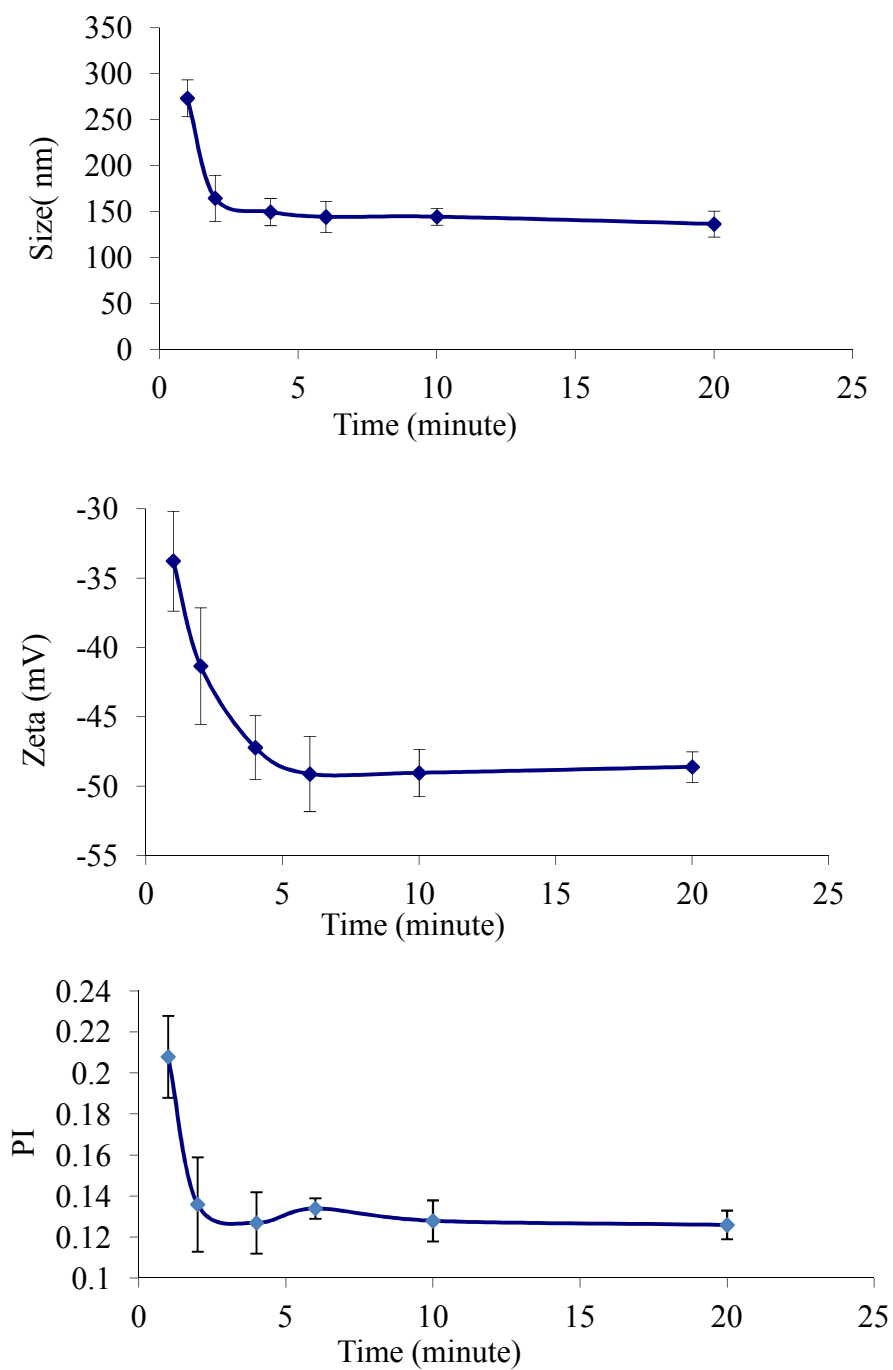


Figure 40: impact of homogenization time on particle size

The impact of emulsification time has been investigated on the emulsions using lecithin at 5% concentration. Emulsification time corresponds to the energy spent for preparing nanosuspension. Longer emulsification time means more energy cost. The effects of homogenization time on nanoparticle properties are presented in Figure 40. The results show that there is not any improvement on the particle diameter after 4 minutes. Similar to particle size, the zeta potential and the polydispersity index of the nanoparticles approached plateau after 6 minutes.

The effects of water content on nanoparticle properties are presented in Figure 41. There is optimal water content that minimizes particle size, and maximizes the absolute value of zeta-potential. The water content can affect Ostwald ripening effects, electrostatic repulsion, and flocculation. Low water concentrations can bring advantages to electrostatic repulsion due to high concentration of surfactant and brings disadvantage to Ostwald ripening effects. However, it increases the flocculation when particles are close together. On the other hand, high water concentration decreases the flocculation resulting in nanosuspension stability. High water content increases the Ostwald ripening effects and causes the migration of surfactant molecules from the particle interface to aqueous medium decreasing the electrostatic repulsive force and leading particle aggregation. The optimal water content for soy lecithin suspensions, which has a noticeable trend as shown in Figure 41, is approximately 97.7%, or can range between 97 and 98%. At this concentration, the average particle diameter is at a minimum of approximately 100 nm, and the absolute value of zeta-potential is at a maximum of approximately 43 mV. The obtained absolute value zeta potential is sufficiently larger than the minimum value required for a nanosuspension to be stable (25 mV). In addition, the standard deviation is

the lowest at 97.7% water. Figure 41 also shows the effect of water content on particle size for short storage time where the ongoing diffusion of triacetin trapped in the nanosuspension may occur. It is evident that particle size decreases at lower water concentrations due to the diffusion of triacetin trapped in the particle. The increase in particle size at higher water concentrations over time can be explained by the electrostatic repulsive force shortage. High water content results in lower surfactant concentrations leading to the decrease of repulsion among particles.

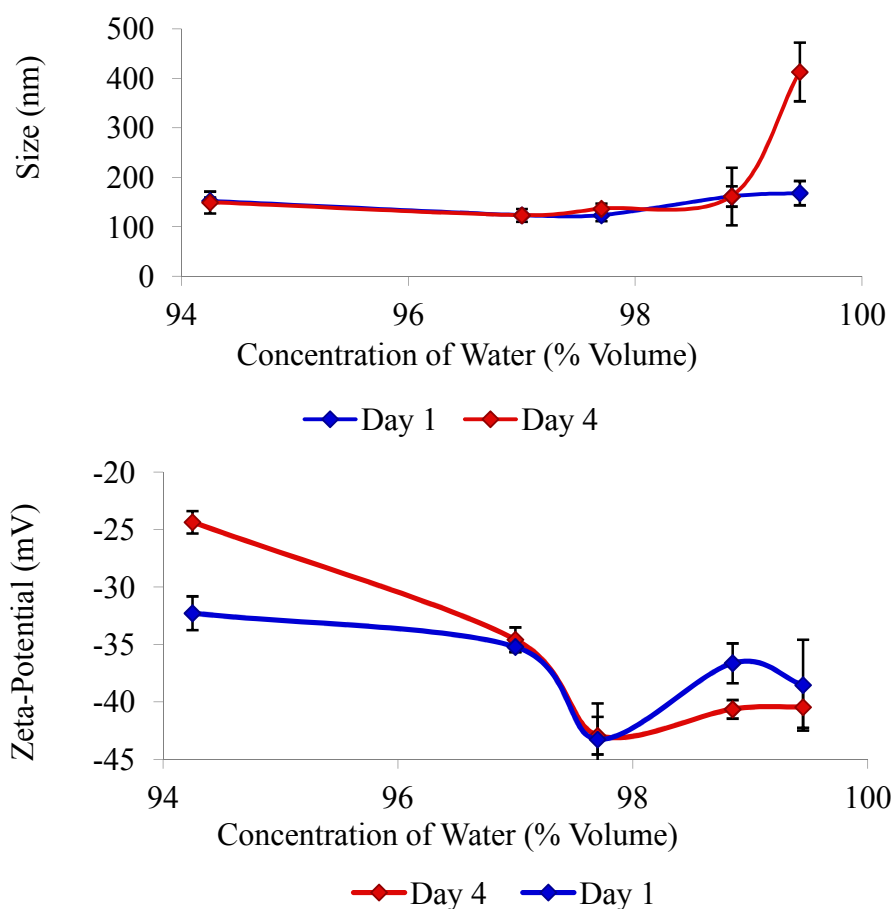


Figure 41: Particle size and zeta potential as function of water content and time

6. Shelf life of beta-carotene nanoparticles

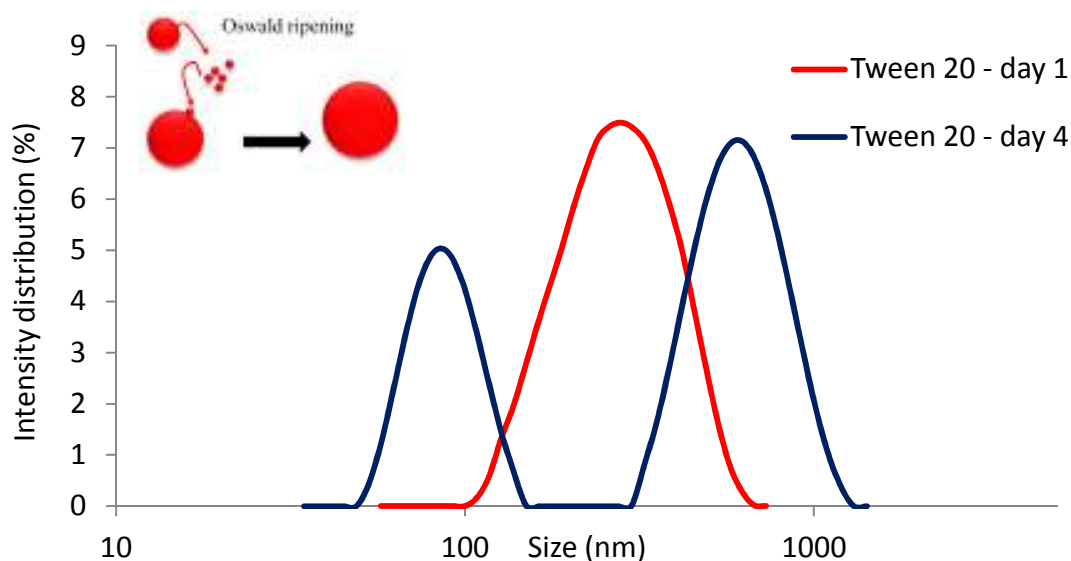


Figure 42 : The impact of Oswald ripening on particle size distribution

Figure 42 represents the evolution of beta-carotene nanoparticles of the suspension samples with 99.5% water content after 4 days from preparation. The particle size distribution of the particles with lecithin slightly broadens due to flocculation while that of the particles with tween 20 definitely separates into two regions. The change in particle size distribution of the particles with tween 20 shows evidence of Oswald ripening. Oswald ripening occurs when beta-carotene diffuses out of particles due to a large Laplace pressure then transfers into more thermodynamically stable larger particles. That makes small particles become smaller gradually while large particles are continually larger leading to the separate particle size distributions.

Oswald ripening is the process by which larger particles grow at the expense of smaller ones. The solubility of small particles is enhanced because of high curvature. This process is a direct consequence of the Kelvin effect [457] and can be quantitative as

$$C(a) = S \exp\left(\frac{\alpha}{a}\right), \quad (93)$$

where $C(a)$ is the solubility of a particle with radius a ; S corresponds to the solubility of a particle with infinite radius, that is the solubility of a flat surface or the bulk solubility; α is the capillary length and is given by

$$\alpha = \frac{2\sigma V_m}{RT} \quad (94)$$

where V_m is the molar volume of the dispersed phase, σ is the interfacial surface tension, R is the universal gas constant, and T is the absolute temperature. Equation (93) indicates that the solubility of small particles is much higher than that of the larger ones. Thus, smaller particles tend to lose their molecules and these molecules diffuse through the continuous phase and re-precipitate onto larger particles. The contribution of dispersed phase molecules to larger particles causes the growing of large particles with time as shown in Figure 42.

The Ostwald ripening in emulsions has been investigated by Hoang et al. [458-460]. According to Hoang and her co-workers, at micron scale, $\alpha \ll a$ or the ratio $\frac{\alpha}{a} \ll 1$.

Therefore, Kelvin equation can be expressed as

$$C(a) = S \left(1 + \frac{\alpha}{a}\right). \quad (95)$$

The diffusion flux of solute across the liquid – solid interface is governed by Fick's law

$$J = -D \left. \frac{\partial C}{\partial r} \right|_{r=a}, \quad (96)$$

where \mathcal{D} is the diffusion coefficient of the dispersed phase. The gradient concentration at the liquid – solid interface is approximated as $\left. \frac{\partial C}{\partial r} \right|_{r=a} = \frac{\bar{C} - C(a)}{a}$. Therefore, the growth rate of the large particles can be detailed as

$$\frac{da}{dt} = \frac{\mathcal{D}}{\rho a} \left[\Delta \mathcal{C}(t) - \frac{\alpha S}{a} \right]. \quad (97)$$

In equation (97), $\Delta \mathcal{C}(t) = \bar{C} - S$ is the time dependent supersaturation of the solution, $\Delta \mathcal{C}(t) = 0$ when $t \rightarrow \infty$ as the average concentration \bar{C} approaches the solubility S . Consequently, at every value of the supersaturation there is a critical radius $a_c = \alpha S / \Delta \mathcal{C}(t)$ that separates the particles into growing group and destroying group. The particles with their size larger than critical radius will grow with the expense of the group of particles which have the size smaller than the critical radius. The critical radius was proved to be the same with a_c by Finsy[461]. A quantitative description of Ostwald ripening in a two-phase system is given by the Lifshitz – Slyozof – Wagner (LSW) theory [462-464]. With a series of assumptions and by using Fick's first law [465], the mass balance, and the continuity equation for the particle size distribution, the Ostwald ripening rate v is derived as

$$v = \frac{d\bar{r}^3}{dt} = \frac{4\alpha \mathcal{D} S}{9}. \quad (98)$$

The Ostwald ripening of beta-carotene nanoparticles has been investigated by Liu et al [466]. The authors have reported that the lower solubility is the smaller particle growth rate is. Ostwald ripening can be strongly reduced by using co-surfactant (low-molecular-weight highly water insoluble compounds [467, 468]. In addition, the combination of co-

surfactant with polymers can be a very efficient way of minimizing Ostwald ripening [469].

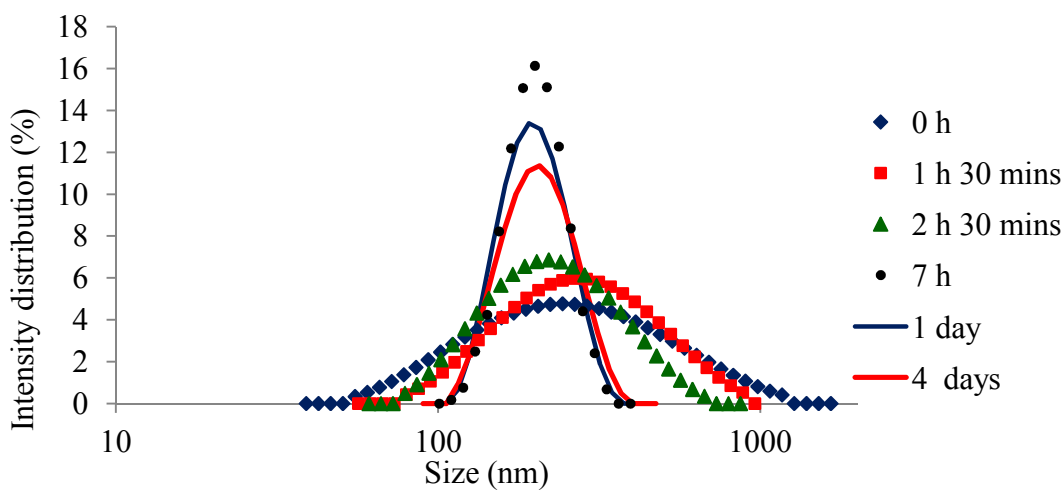


Figure 43: The evolution of particle size distribution during short storage time

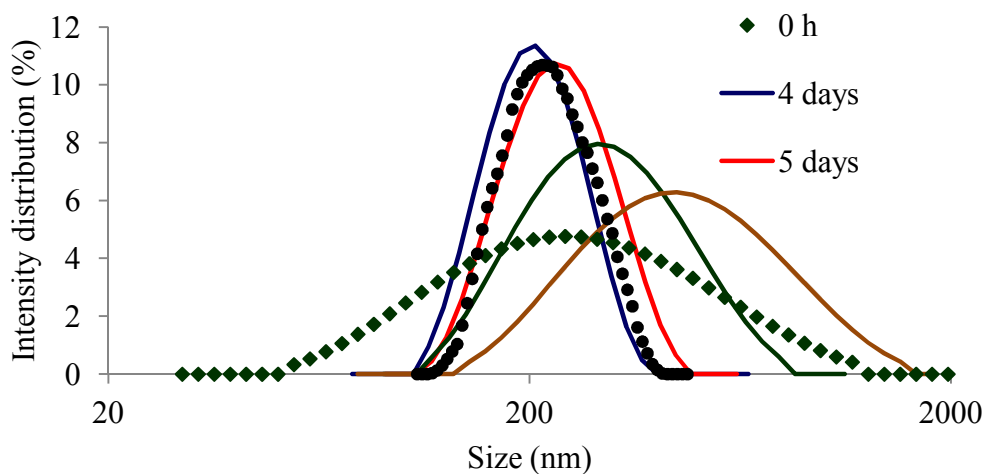


Figure 44: The shelf life of beta-carotene nanoparticles during long time storage

The kinetic stability of nanosuspensions prepared by lecithin has been monitored over time and is represented in Figure 43 and Figure 44. It details the evolution of particle size during short storage time. The size evolution of beta-carotene nanosuspension particles contains two stages. The first 7 hours after preparation is the fast ongoing diffusion of the

remaining triacetin in suspension particles along with the dissolution of small particles. This leads to a change in particle size distribution as can be seen in Figure 43. The change in particle size distribution indicates that the amount of triacetin trapped in the particles is quite large. It is noted that the distance between two lecithin molecules is much larger than the hydrodynamic size of triacetin molecule as shown in Table 15. Moreover, the internal distance between layers of lecithin is 28 Å[453]. Therefore, layers of lecithin just creates diffusion barrier. It cannot hold triacetin in the particles. Large amount of triacetin in the particles designates that the beta-carotene precipitates too fast to trap triacetin in nanosuspensions. Fast precipitation of beta-carotene may form amorphous beta-carotene nanoparticles. The amorphous particles are later confirmed by XRD and DSC. After 24 hours, the particles run out of trapped triacetin. The particle size distribution does almost not change. After that, the average particle size slightly increases due to flocculation as can be seen in Figure 44. The flocculation happens when electrostatic repulsion force among particles is smaller than their van de Waals attractive force. As phospholipids, lecithin forms lamellar structures due to hydrophobic interaction. That may be the reason for the flocculation of the nanoparticles during long storage time. The longer the storage time is the wider and shorter particle size distribution is. The flocculation but not aggregation of the particles is proven by applying sonication to break down weak interaction among particles. It is clear that the particle size distribution returns almost the same as that of after 4 days. The results show that the beta-carotene nanosuspensions prepared with lecithin are stable for long time.

CHARACTERIZATION OF BETA-CAROTENE NANO PARTICLES

The crystallinity of the nanoparticles plays a role in the bioavailability of beta-carotene nanoparticles. Figure 45 shows the XRD of pure beta-carotene and beta-carotene nanoparticles. The XRD spectrum of pure beta-carotene shows several sharp peaks indicating that pure beta-carotene is high crystallinity while that of the nanoparticles confirms that the obtained beta-carotene nanoparticles are almost in amorphous form. The amorphous structure of beta-carotene nanoparticle increases its solubility because the solubility of amorphous form of a material is higher than its crystalline counterpart [262, 470].

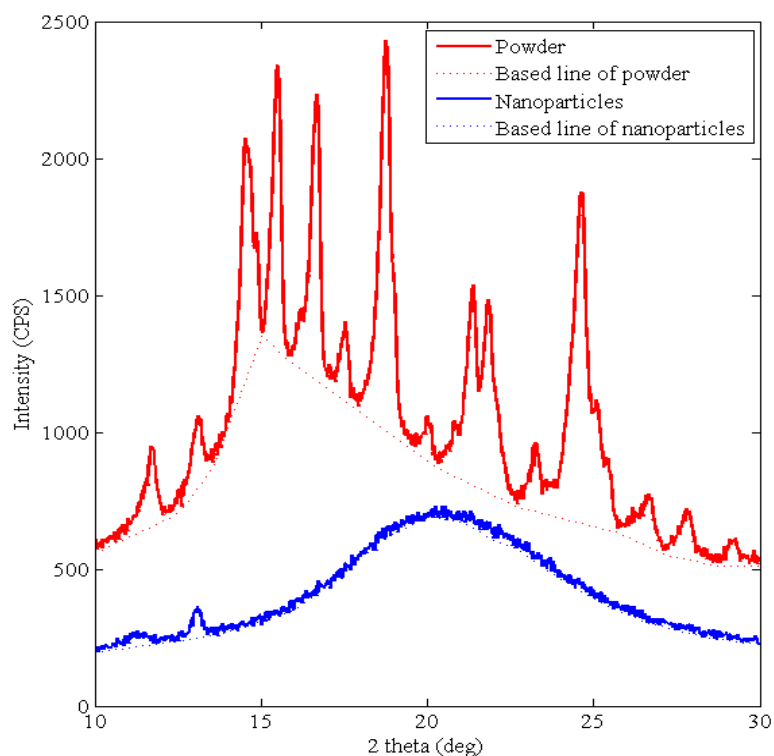


Figure 45 : XRD spectra of pure beta – carotene and beta – carotene nanoparticles

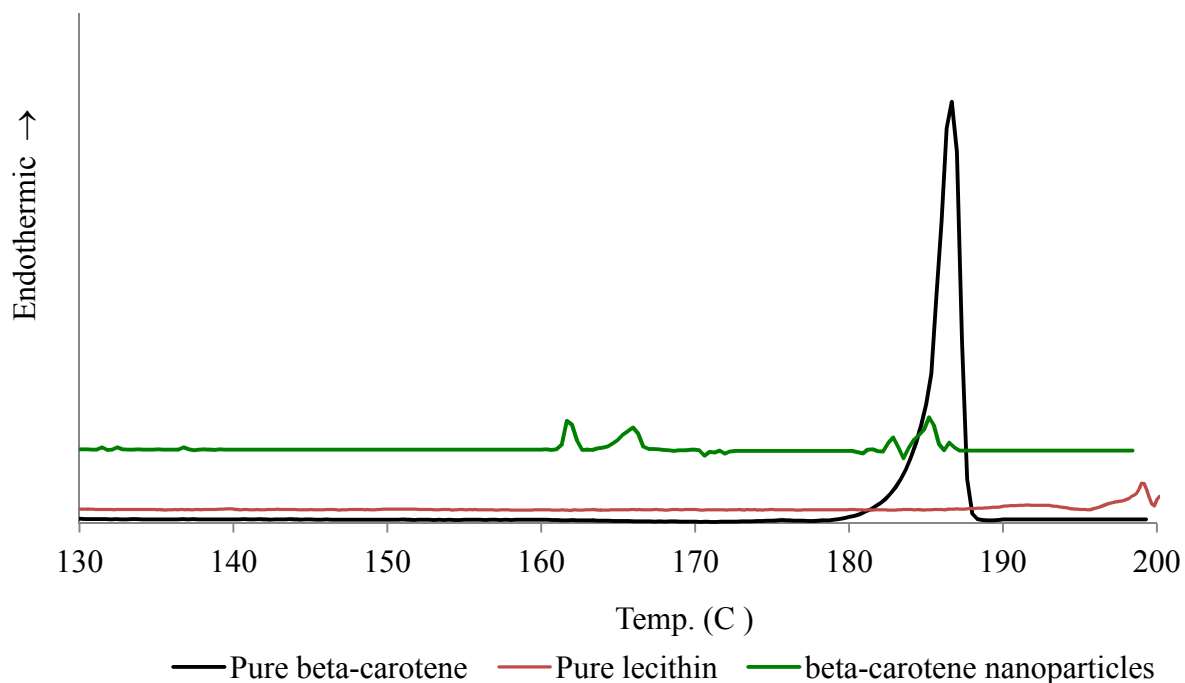


Figure 46: DSC thermograms of pure beta-carotene, lecithin, and beta-carotene nanoparticle

The crystallinity of beta-carotene nanoparticles is also studied by DSC. Phase transition of a material is determined by the change in disorder via Boltzmann relation $S = k_B \ln W$, where k_B is the Boltzmann constant and W is the complexion. When the crystal melts, it causes the crossing of the Gibbs energy of two phases at a specific transition temperature T_{tran} leading to a difference in slopes $\left. \frac{\partial G}{\partial T} \right|_p$ of the heat flow and is defined by a peak in the heat flow trace. Thus, the first-order phase transition corresponds to the solid-liquid transition and the area of this peak provides heat of fusion of the considering material. Figure 46 shows the DSC scan of pure beta-carotene, pure lecithin, and beta-carotene nanosuspension. The thermogram of pure lecithin shows the melting point at 194.260C. The melting point of pure beta-carotene is 186.680C. Its heat of fusion is 92.527 J/g. The

crystal-structure of pure beta-carotene is monoclinic with $\gamma = 105.30^\circ$, $a = 7.55 \text{ \AA}$, $b = 9.51 \text{ \AA}$ and $c = 24.8 \text{ \AA}$ [471]. The thermogram of beta-carotene nanoparticle contains two peaks representing the melting point of beta-carotene nanocrystal at 161.660C and 166.970C. The corresponding heat of fusion to those melting points is 0.3964 J/g and 0.2319 J/g respectively. Another peak at 188⁰C may belong to the lamellar lecithin adsorbed on the particles. The DSC thermogram of beta-carotene nanoparticles specifies that there are two forms of crystal represented in the beta-carotene nanoparticles. These two forms of nanocrystal have been reported by Auweter and his co-workers when they crystallized beta-carotene from its solutions [472]. The authors confirmed that nanocrystals of beta-carotene crystallized from high solubility solutions have H- structure where 4 molecules of beta-carotene arrange parallel. On the other hand nanocrystals obtained from low solubility solutions are J-structure where 4 molecules of beta-carotene rearrange head-to-tail in the cell.

In order to test the fortification ability of the prepared nanoparticles, the beta-carotene nanosuspensions are sublimated. Figure 47 presents the particle size distribution of the original beta-carotene nanoparticles and that of the particles after lyophilization. Without sonication, the particle size distribution increases indicating the flocculation of beta-carotene nanoparticles. When sonication is applied, the particle size distribution is almost the same as that of the original. The movement of particle size distribution towards smaller size after sonicating confirms that the particles flocculate not aggregate. It is noticed that the sublimation can only evaporate water. The particle existence indicates that the particles are well protected by lecithin against dissolution by triacetin leftover.

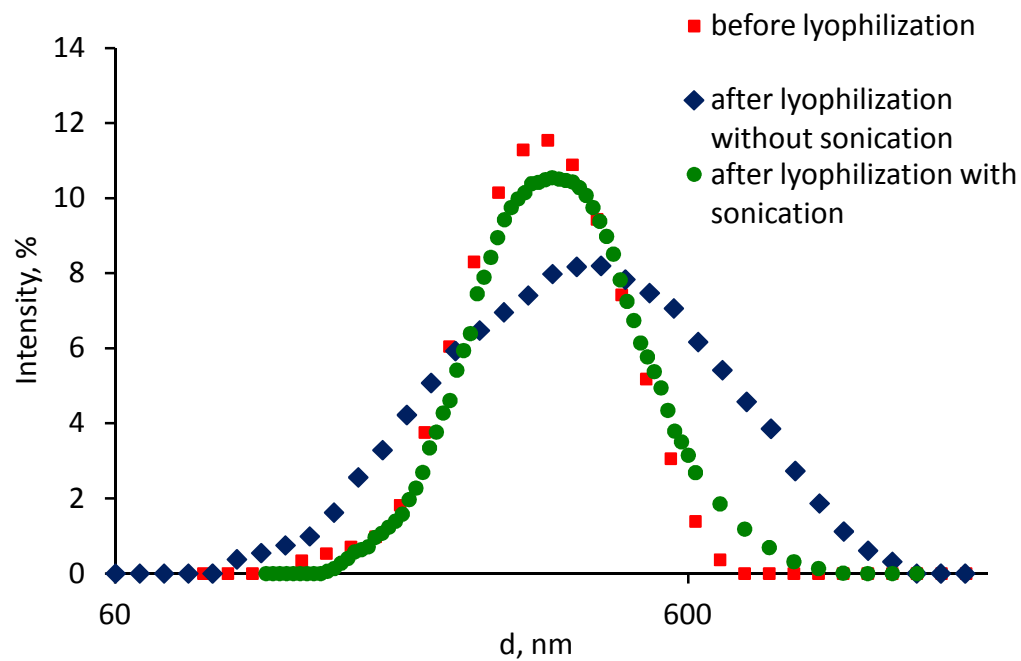


Figure 47: Particle size distribution of beta-carotene nanoparticles before lyophilization and after lyophilization

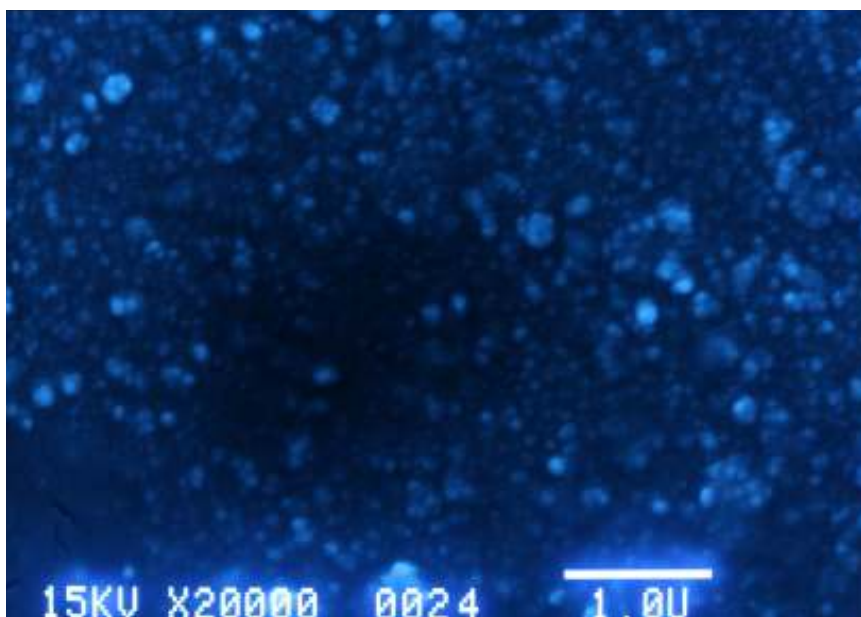


Figure 48: SEM image of the beta-carotene nanoparticles

EDIBLE FILM LOADED BETA-CAROTENE NANOPARTICLES: MODEL OF FOOD FORTIFICATION

1. Hydroxypropyl methylcellulose

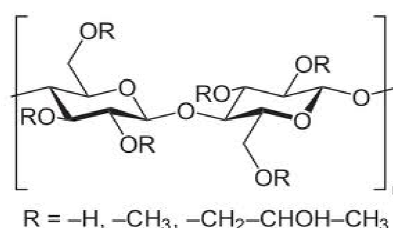


Figure 49: Structure of HPMC

Hydroxypropylmethyl cellulose (HPMC) is a semisynthetic, inert, and viscoelastic polymer derived from cellulose by substituted methyl or hydroxypropyl groups for hydroxyl groups in glucose rings of cellulose molecule (Seen Figure 49). According to the United States Pharmacopeia, HPMC is classified based on the chemical substitution of the ether. The three type of HPMC includes E (hypromellose 2910), F (hypromellose 2906) and K (hypromellose 2208). The major factors that contribute to the chemical differences between these types of HPMC are in the degree of methoxyl substitution, molar degree of hydroxypropoxyl substitution and degree of polymerization which is characterized by measuring the viscosity of aqueous solution of 2% HPMC. The degree of substitution corresponds to the average number of substituted hydroxyl groups, and the molar degree of substitution gives the number of substituents introduced into the glucose ring. The degree of polymerization is related to the average number of monomers in the chains. As other soluble cellulosic derivatives, HPMC is widely used in food as an

emulsifier, thickening, and suspending agent. It is widely used in pharmaceutical industry as the controlled release agent.

In an aqueous solution at lower temperatures, HPMC molecules are hydrated, and there is little polymer – polymer interaction other than simple entanglement. As the temperature increases, the molecules gradually lose their water of hydration as reflected by a decrease in viscosity. Eventually, when a sufficient (but not complete) dehydration of the polymer occurs, a polymer – polymer association takes place, and the system approaches an infinite network structure as reflected by a sharp rise in viscosity. Because different phenomena possibly occur during the heating cycle, the study and understanding of this process is complex [473-475]. It is generally accepted that the thermoreversible gelation of HPMC solutions is due to hydrophobic interactions, and it is sometimes indicated that clouding precedes gelation[476]. Gelation causes a sharp increase in viscosity. Therefore, viscosity is one of the factor that indicates gelatinization of HPMC [477]. The temperature at which gelatinization occurs is influenced by the type of cellulose ether. It has been reported that at the same equivalent substitution and molecular weight, methylcellulose has a lower gelation temperature and forms more rigid gels than HPMC. It means that hydroxypropyl groups make the gelation process more difficult [478, 479]. Furthermore, hydroxypropyl cellulose precipitates with at high temperature but does not form a gel. This has been considered as evidence that the exclusion of water from heavily methoxylated regions of the polymer induces the gelation of cellulose derivatives [476, 480]. Similar to polyethyleneoxide, the hydrophobicity of HPMC increases with temperature [481]. It is generally accepted that a polymer that provides such properties usually carries two different segments: one hydrophobic and one hydrophilic, distributed

along the polymer chain. In the case of HPMC, the impact of the hydrophobic group is predominant at high temperature [482]. Some authors also believe that not only hydrophobic interaction but also hydrogen bonding may be participated in the gelation mechanism of cellulose derivatives [483].

2. Physical chemistry of aqueous hydroxypropyl methyl cellulose solution

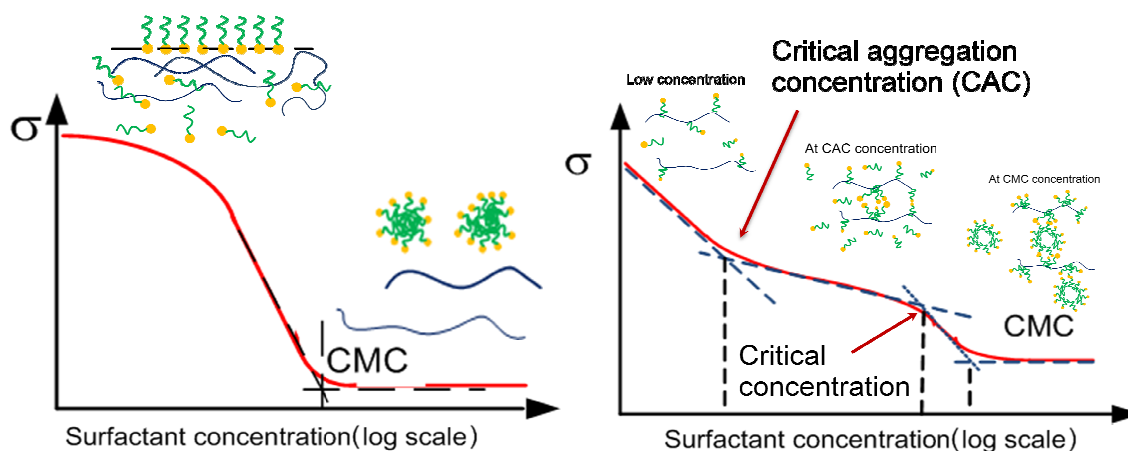


Figure 50: The polymer - surfactant interaction in aqueous media

Interaction of surfactant – polymer may influence the film formation leading to the change in mechanical strength and film performance. Figure 50 represents typical behavior of surfactant – polymer system in aqueous media. Thermodynamically, the adsorption isotherm of surfactant molecules on a molecule or a surface is represented by Gibbs equation

$$\Gamma = -\frac{1}{nRT} \frac{d\sigma}{d(\ln C)}, \quad (99)$$

where Γ is the equilibrium surface excess; $n = 1$ for non-ionic surfactant/neutral molecules or ionic surfactant in the presence of excess electrolyte, $n = 2$ for 1:1 ionic

surfactant; R is gas constant; T is the absolute temperature; σ is surface tension; and C is the concentration of the surfactant in aqueous phase [431].

The interaction of neutral charged polymer and surfactant in aqueous solution can fall into two scenarios (1) no interaction and (2) complex formation. When there is no interaction, the surface tension of polymer – surfactant aqueous solution behaves similar to that of a surfactant solution. That means the surface tension of the mixture decreases with the increase of surfactant concentration until CMC. When concentration of surfactant is larger than CMC, surface tension of the mixture is almost constant as shown in the left of Figure 50. On the other hand, the surface tension of the aqueous polymer – surfactant mixture has four distinguished region [484-486] as on the right of Figure 50. In the first region, adsorption of surfactant at the interface causes a decrease in surface tension. The second region starts at critical aggregation concentration (CAC) of surfactant where the slope surface tension curve disrupts and finishes at the critical concentration C^* , a concentration at which polymer is saturated of surfactant adsorbed. The adsorption of surfactant molecules on polymer molecules causes steep change in the slope of the surface tension curve in the third region. The fourth region starts with the formation of micelle in the bulk. For neutral polymers, the polymer – surfactant interaction can be ion – dipole of the ion head of surfactant and dipole of the hydrophilic part of polymer or hydrophobic interaction between the hydrocarbon tail of surfactant and the back bone of polymer [485]. The micelle in the bulk can serve as a weak bridge among polymer – surfactant complexes leading to the increase of viscosity of the mixture [487]. Therefore, by measuring the surface tension of surfactant – polymer aqueous solution, one can discover the polymer – surfactant interaction in aqueous media. Figure

51 shows the surface tension of lecithin – HPMC aqueous solution. It is clear that the surface tension of this solution is similar to that of a surfactant solution. That indicates lecithin does not interact with HPMC.

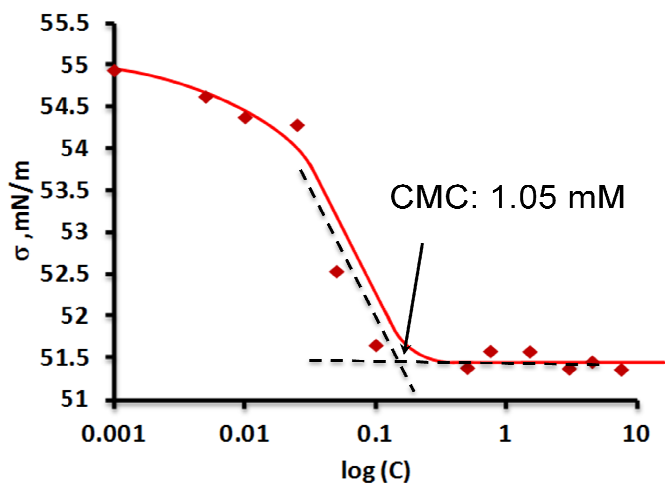


Figure 51: surface tension of lecithin - HPMC aqueous solution

3. Film formation

3.1. Film formation model

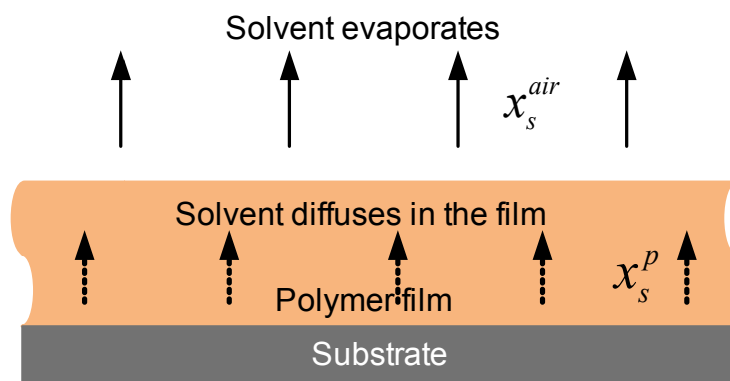


Figure 52: Model of water removal from the polymer solution during film formation

In order to understand the behavior of components during film formation, a model of solvent removal is built. The evaporation of water from a thin film with unlimited length in ambient air is shown in Figure 52. We suppose that the concentration of polymer is homogeneously distributed on horizontal direction. Since the evaporation occurs only at the liquid – air interface, the difference of concentration is a function of vertical direction only. The model becomes 1-D diffusion through a stagnant gas film. The flux of water in the air in contact with the film surface is

$$J_s^{air} = \frac{C^{air} \mathcal{D}^{air} dx^{air}}{(1 - x^{air}) dz}, \quad (100)$$

where C^{air} , \mathcal{D}^{air} and x^{air} are the concentration, the diffusion coefficient, and mole fraction of water in the air respectively. The solvent evaporation generates a concentration gradient which serves as driving force for the diffusion of water in the bulk of the polymer solution layer. The diffusion of water in the bulk of polymer solution is

$$J_s^p = \frac{dC^p}{dt} = - \frac{C^p \mathcal{D}^p dx^p}{(1 - x^p) dz} + J, \quad (101)$$

where C^p , \mathcal{D}^p and x^p are the concentration, the diffusion coefficient, and mole fraction of water in the bulk respectively; J is evaporation flux and defined as $J = J_0 C^p$, where J_0 evaporation flux of pure water. The diffusivity of water in the bulk is estimated by Stokes – Einstein equation

$$\mathcal{D} = \frac{k_B T}{6\pi\eta r} \quad (102)$$

We hypothesis that the viscosity, η , in equation (102) is function of polymer concentration.

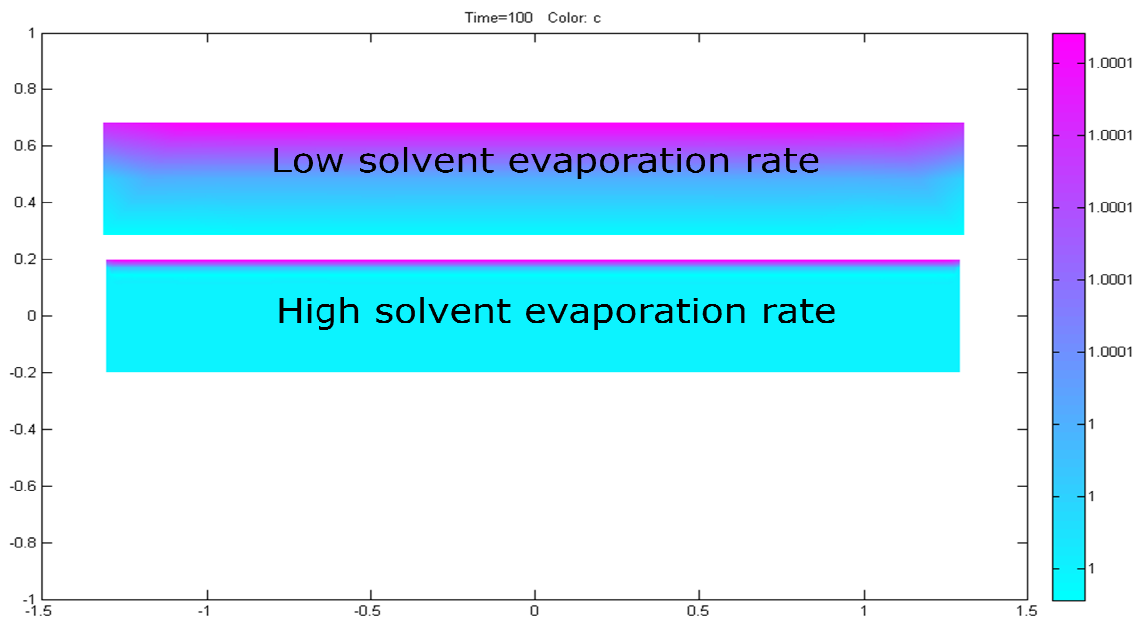


Figure 53: The distribution of polymer concentration in the film at different evaporation rate

Figure 53 shows the distribution of polymer concentration in the film at different evaporation rate. When the evaporation rate is smaller than the diffusion flux of water in the bulk, the mass flux from the film is constant. The concentration of polymer decays through the bulk. The evaporation controls drying process. On the other hand, if the evaporation rate is higher than the flux of diffusion of water in the bulk the diffusion controls the water removal from the film. In this case, there is a thin layer of high polymer concentration at the air – liquid interface. This gel layer influences the drying process of the film and may cause some film defects leading to a decrease in mechanical properties. These drying regimes also present in the film formation at room temperature. The evaporation controlled stage occurs at semi-dilute condition while the diffusion controlled stage happens at high polymer concentration.

Generally, the mass balance of solvent in the film can be formulated from the initial mass of solvent in the air, $m^a W_{ini}^a$, the final mass of solvent in the air, $m^a W_{final}^a$, and the mass of solvent in the film, $m_f W_f$, as

$$m^a (W_{final}^a - W_{ini}^a) = m_f W_f. \quad (103)$$

The flux, J , of evaporation from the films was defined as the amount of solvent escaping from a unit area of the film per unit of time. Thus,

$$J = \frac{d}{dt} \left(\frac{m^a W_{final}^a - m^a W_{ini}^a}{A} \right) = \frac{d}{dt} \left(\frac{m_f W_f}{A} \right) \quad (104)$$

where m^a was the mass of dried air (kg dried air); W_i^a was the amount of solvent in dried air (it was water in our case and has unit of kg/kg dried air); m_f was the mass of dried film (the summation mass of polymer, surfactant, and drug); and W_f was the amount of solvent per unit of dried components (kg solvent/ kg dried film); and A was the film surface. The total mass of the film, $M = m_f (1 + W_f)$, was the summation weight of solvent and dried components. Because there was only solvent evaporated from the film, the second derivative term in equation (104) was replaced by the derivative of total mass M per unit of area

$$J = \frac{d}{dt} \left(\frac{M}{A} \right). \quad (105)$$

Thus, by measuring the total mass evolution of the film, we understood the drying kinetics and explored the phase transition behaviors of HPMC films during solvent evaporation process.

3.2. Factors impact the film formation

During film formation, there are possible relations between the solvent content, viscosity, and the aggregative behavior of nanoparticles in the polymer matrix. By understanding the relationships, we are able to suggest new means of monitoring for the process of gel-formation in the presence of nanoparticles. The water removal from the film consists of mainly two periods which are external convection/diffusion control and internal diffusion control where it is divided into two more sub stages distinguished by the change in the acceleration of evaporation flux. The first transition is so called external-internal transition representing the shift from external convection/diffusion control to internal diffusion control. The second one is named deeply drying transition where the first change in the acceleration of evaporation flux occurs during internal diffusion control state.

Figure 54 shows the comparison of evaporation flux from the pure HPMC, film precursor with lecithin, film precursor with triacetin, and the film precursor with particles. The initial concentration of the film precursor with particles is 2% HPMC, 0.6% lecithin, 1.3% triacetin, and 0.0017% beta-carotene in the form of nanoparticles with the size of 240 nm. It is noticed that the nanoparticles introduced to the film contain lamellar layer of lecithin. The concentration of triacetin and lecithin in the other film is the same as that in the film with particles. The blue curve represents the evaporation flux from the pure HPMC film. During film formation, the HPMC solution passes the external - internal transition at concentration of HPMC of 5.83% and the second transition at 18.5% HPMC. The evaporation rate decreases slightly at the first evaporation stage but dramatically on

the second one because the diffusion of water in the bulk is much smaller at high concentration of polymer.

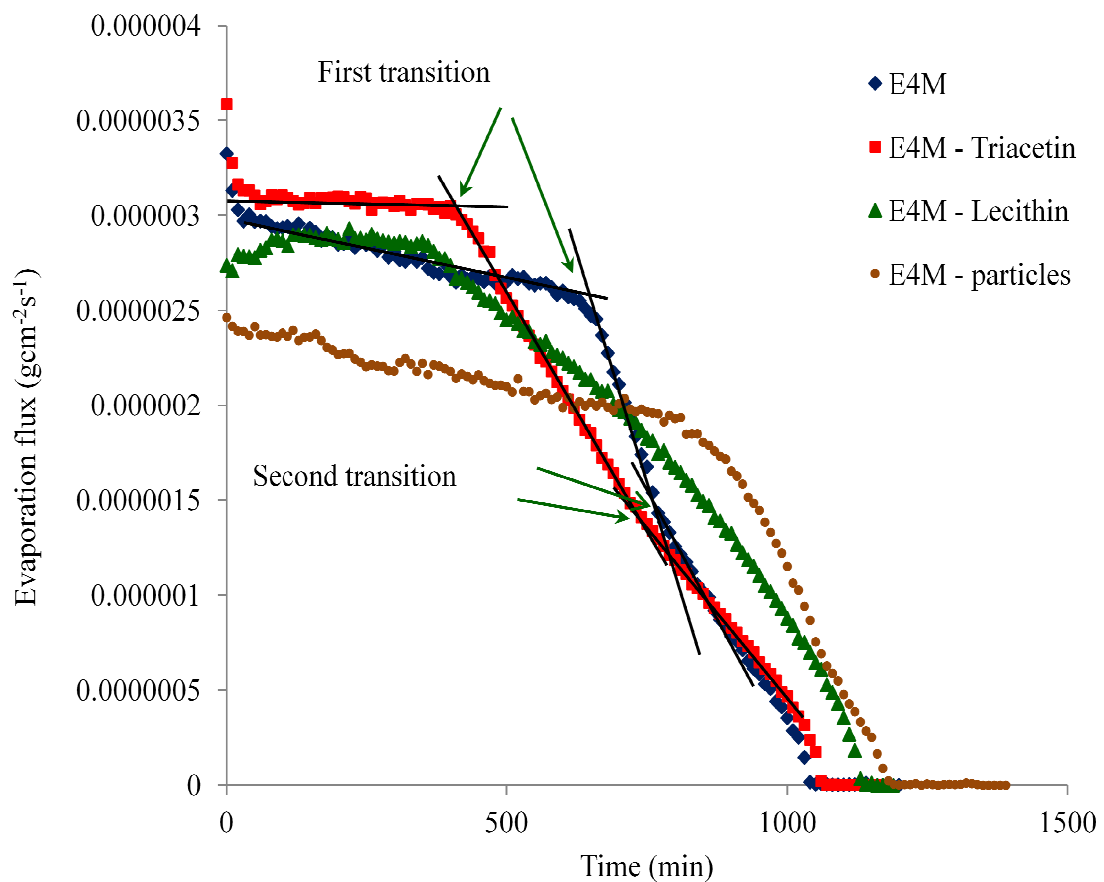


Figure 54: The evaporation flux of the films

The curve represents to the evaporation flux of the film precursor with triacetin and shows that triacetin added into film precursor solution forces those transitions towards lower HPMC concentration of 3.77% and 13% respectively. Moreover, triacetin speeds up the evaporation flux of water from film at low polymer concentration and, subsequently, the flux of evaporation decreases sharply because triacetin forms strong

hydrogen bonding with water. The surface of the film with triacetin in Figure 55 shows numerous of bumps indicating that phase separation occurs in the film.

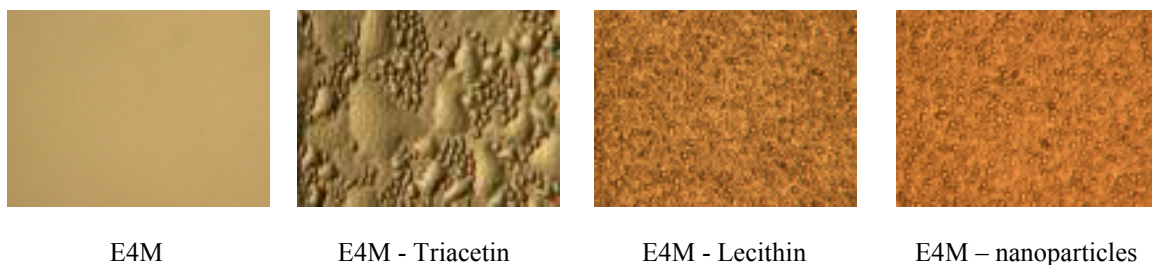


Figure 55 : Surface of the HPMC films under microscope

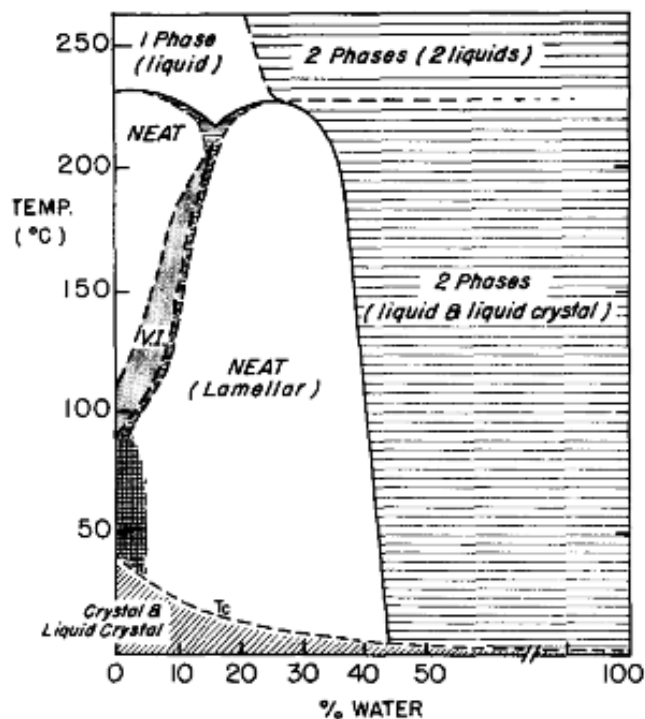


Figure 56: Phase diagram of lecithin -water system

The addition of lecithin to the film precursor drives external – internal transition to even lower concentrations of HPMC. However, the second transition of the system is similar to pure HPMC film precursor solution. Lecithin does not increase the evaporation flux at

semidilute nor at the condense condition but it enhances the rate of water removal at second stage of the film precursor. Furthermore, it requires longer evaporation time in comparison to pure HPMC film precursor solution. We believe that the ability of lamellar structure formation of lecithin causes these changes in water removal from the film precursor. According to Small [405], phosphoryl choline can form several lamellar structures at high water content. Figure 56 where a complicated phase diagram of lecithin – water is presented. In Figure 56, region V.I represents “viscous isotropic” phase; T_c represents the ill-defined boundary of crystal – to – liquid crystal phase transition; the cross-hatched region between 0 to 5% water from 45 to 90⁰C stands for a poorly region where lamellar liquid crystalline phase may coexist with another liquid crystalline phase [405]. Lecithin intermingles with water leading to the liquid crystal formation and then lamellar lecithin in which water is encapsulated. The phase diagram of lecithin – water system shows that at room temperature, the formation of liquid crystal occurs at quite high water content. When the water content in the lecithin – water mixture is around 43% the system consists of liquid crystal and crystal 8, which is mixture of lamellar structures of lecithin. At lower water content (0 to 7%) the lecithin – water mixture becomes a combination of crystalline and waxy birefringence [405]. Small has also calculated and provided an inside view of the lamellar lecithin structure. Figure 57 represents the structure of bilayer lecithin adopted from [405]. D is the repeat distance; d_L is the thickness of lipid bilayer; d_w is the thickness of water layer including the phosphoryl choline zone; d_{w_f} is the thickness of “free water layer”; the hydrophobic tails of lecithin are represented by the wavy lines indicating the partially liquid like state; choline groups of the phospholipid are represented by more or less random away within a zone 8Å thick

[405]. At high water content, the thickness of water layer trapped between two choline head groups of lecithin is around 20 Å. This length starts decreasing when the water concentration in the mixture approaches 45% and becomes negligible when concentration of water is not larger than 15%. Lamellar structures of lecithin occur during film formation leading to isolated bumps as shown in Figure 55.

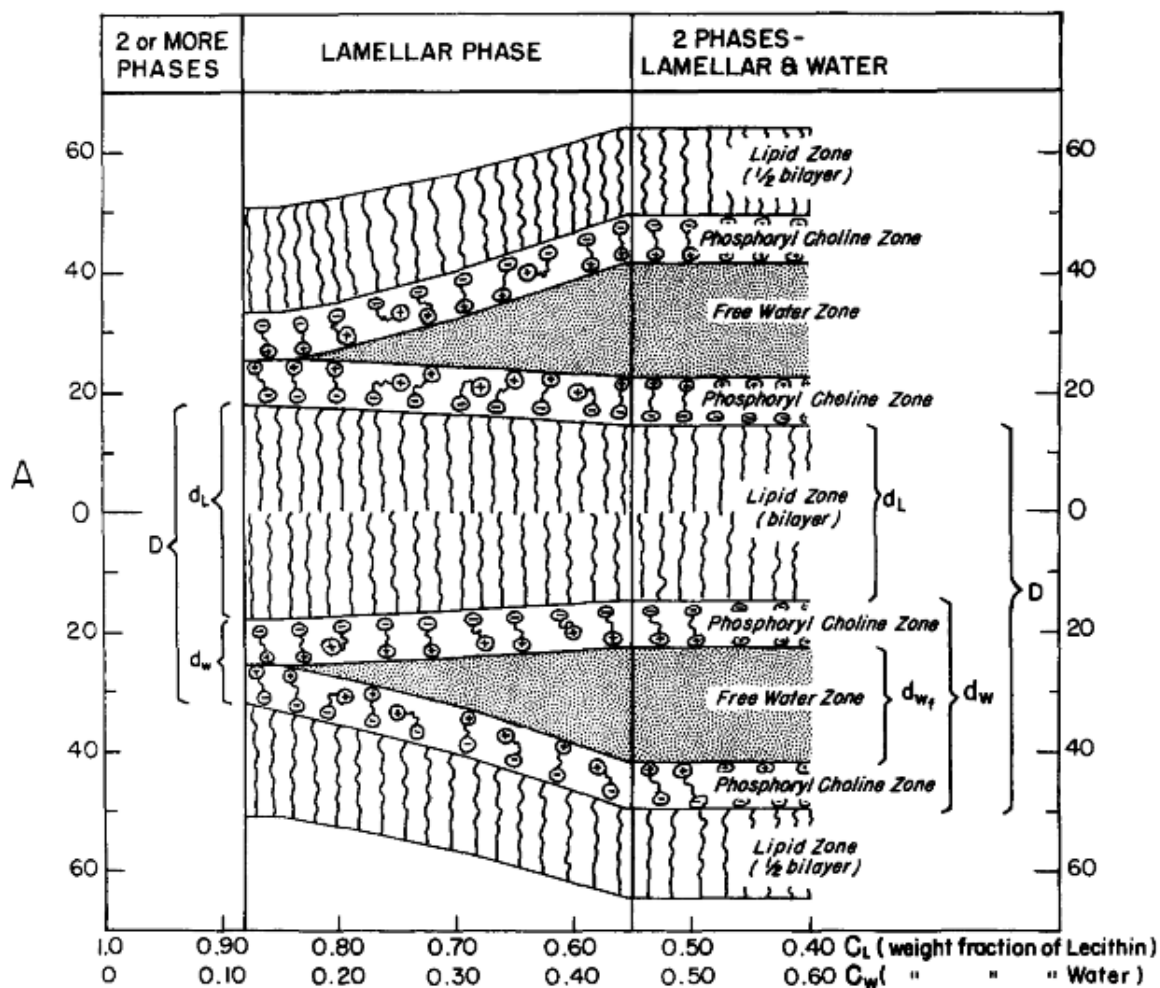


Figure 57: Diagrammatic reconstruction of the bimolecular lecithin leaflet in relation to the amount of water present.

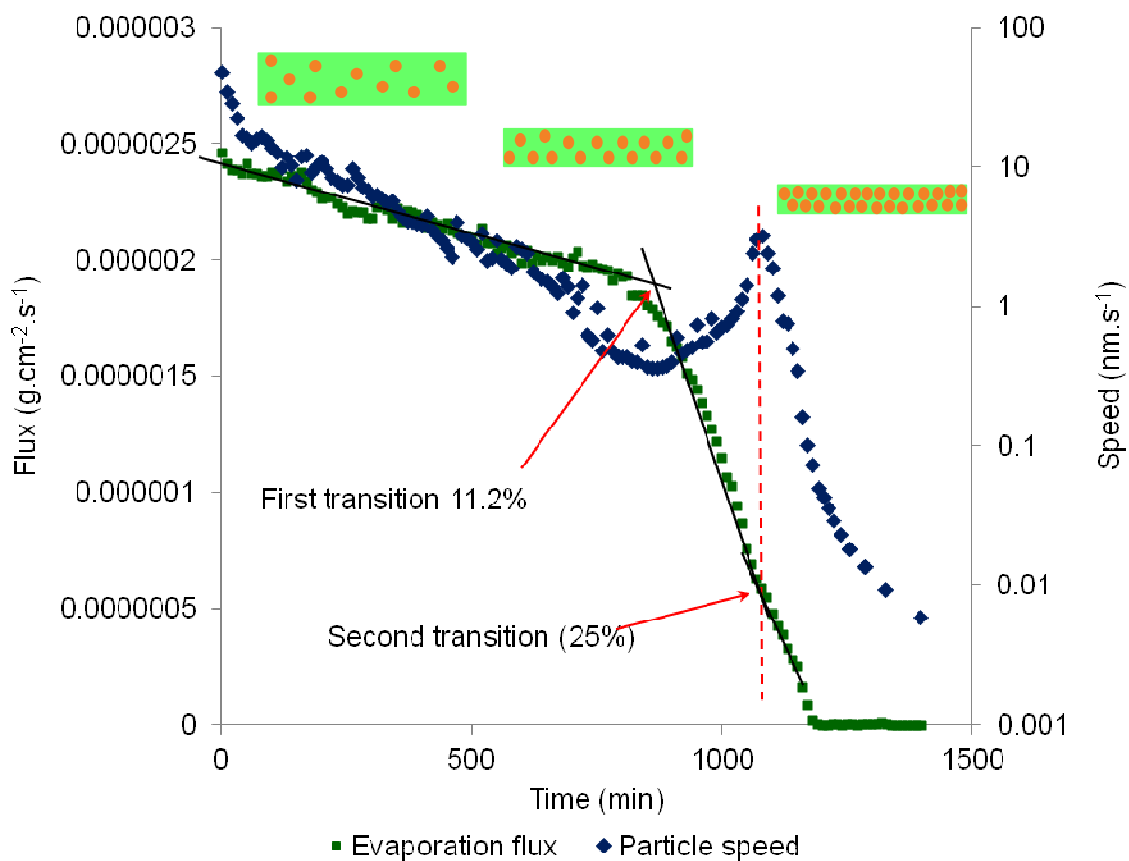


Figure 58: The mobility of particle during film formation

The existence of particles in the film precursor causes the reduction in evaporation flux leading to longer drying time. It is clear that particles cause the delay in the first and second transition. Figure 58 shows the mobility of particles and the evaporation flux as well as a schematic of how particles are packaged during film formation. It is easy to recognize that the velocity of the particles decreases with the increase in the film viscosity. It is interesting that the speed of the particles increases around the first transition until the second transition occurs. These are evidences of the repulsion of particles from the polymeric matrix when the polymer network is formed.

During the film formation, particles pass through three different stages. The first stage is the free movement of Brownian motion where particle concentration is low. Water evaporation induces the increase in concentration of polymer as well as particles. That raises viscosity of the bulk. In the second stage, particles come closer due to volume shrinkage. They interact with each other. In the third stage, particles are well packaged by trapping into gel matrix and later into dried polymer network. Because the film precursor contains surfactant – polymer – particles, there are three different scenarios of surfactant – polymer – particle interactions leading to different packaged types of particles in the polymeric matrix. The impact of surfactant – polymer – particle interaction to the film structure is summarized on Figure 59. The first scenario is described on the left channel where the adsorption of surfactant on polymer is stronger than that on particles leading to the complex construction of surfactant – polymer. Thus, the protective layer of surfactant on surface of the particles is torn off because of complex formation causing depletion aggregation of particles in polymeric matrix. The second scenario is detailed in the middle channel. In this case, both surfactant and polymer adsorb on particles. The particles are partially protected by surfactant while adsorption of polymer causes bridge stabilization in the polymer matrix. The channel on the right of Figure 59 mentions the last scenario where the particles are well protected by surfactant. It happens when surfactant does not interact with polymer but with particles only. That decreases the probability of the polymer adsorbing on the surface of the particles leading to the isolated distribution of single particles trapped in polymeric matrix. Lecithin does not interact with HPMC. It forms a strong protective layer on surface of beta-carotene nanoparticles. Thus, the structure of the film loaded beta-carotene nanoparticles follows channel three.

However, lecithin has high capability of forming lamellar structure. When particles encapsulated with layer of lecithin come in contact, they can flocculate due to the interaction of lecithin layers before being trapped in polymer matrix as shown on the right in Figure 59.

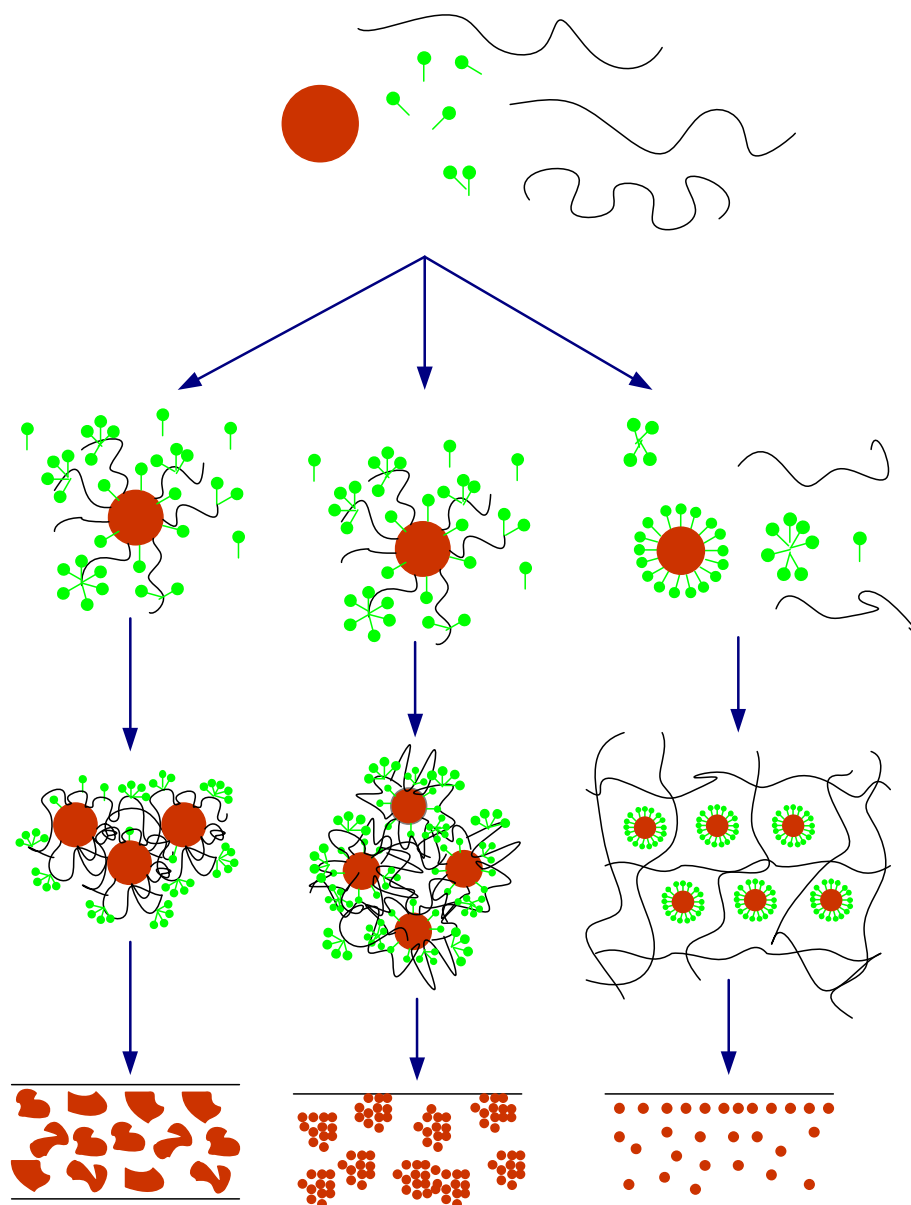


Figure 59: Surfactant - polymer - particle interaction tailors the film structure

4. Nano-rheology of hydroxypropyl methyl cellulose gels

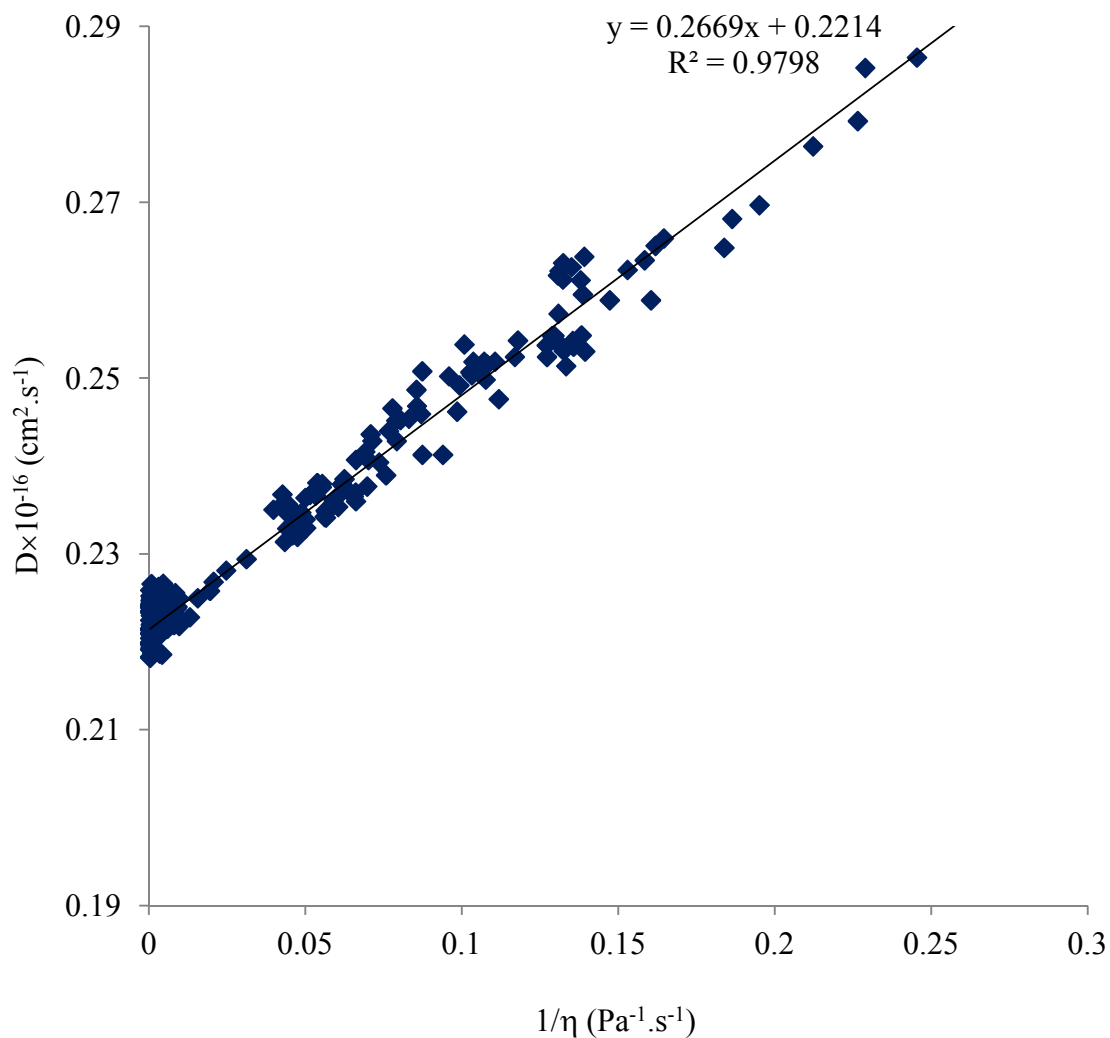


Figure 60: The dynamic diffusion coefficient of the particles during film formation

The dynamic diffusion coefficient of particles represents the evolution of hydrodynamic radius of the particles during the film formation. It provides the length scale that the interaction between particles may occur. Theoretically, the diffusion coefficient \mathcal{D}_s of a particle in a polymer solution with concentration C and molecular weight M is $\mathcal{D}_s = \mathcal{D}_0 \exp(-\alpha C^\nu M^\gamma)$ [488-492], where \mathcal{D}_0 is the diffusion coefficient in pure solvent.

The relationship between the zero shear rate viscosity of a polymer solution and its concentration can be described as $\eta = \eta_0 \exp(aC^\nu M^\gamma)$ [491, 492]. Here a and α are scaling factors, ν and γ are scaling exponential factors and different for each system property, and η_0 is the viscosity of pure solvent. At high concentration of polymer, the viscosity increases and the solution becomes a gel. When the polymer solution gelatinizes, particles cannot migrate freely but in the liquid void phase. They have to travel along the polymer molecule. Therefore, traveling path of the particles is increased and the diffusion coefficient of the particles decreases. Since the particles migrate in the free liquid phase, the viscosity of the gel is not representative for the medium in which the particles travel but the intrinsic viscosity or effective viscosity[493, 494]. Therefore, Stokes – Einstein equation is not valid for particles in a polymeric solution or gel and the diffusion coefficient of a particle is not reversely proportional to the viscosity of the medium that it is embedded.

So far, there are limited tools to quantify the diffusion coefficient of the particles in high concentrated polymer solution in which the viscosity may approach thousands cP. The DWS technique provides a tool to quantify both the viscosity of the bulk and diffusion coefficient of the embedded particles. The dynamic diffusion coefficient of beta-carotene nanoparticles as a function of reverse viscosity of the bulk is presented in Figure 60. It is clear that Stokes – Einstein equation is still valid for small particles because the diffusion coefficient of the particle is reversely proportional to the viscosity of the polymer solution. The phenomenon can be explained by the polymer – particle interaction in high concentrated polymer solutions. The diffusion of particles in a polymeric solution is controlled by Brownian motion and attraction force by the polymer molecule as shown in

Figure 61. The adsorption of polymer on the particles increases the hydrodynamic characteristic length of the particles. If the interaction between polymer and particles is weak, the absorbed polymer molecules may be random coil because of huge surrounding space causing the change in the size of the particles. When the interaction is strong, more and more polymer molecules attach on the surface of the particles and the adsorbents do not have much space for random coil configuration. They have to expand because of high population leading to huge increase in particle size. Sometimes, strong adsorption forms bridge aggregation among particles because one polymer molecule can adsorb on more than one particle. According to Pham et al. [495] polymer adsorption on particles not only changes the particle hydrodynamic size but also decrease the viscosity of the bulk. Moreover, the polymer molecules adsorbing on the particles can interact with other molecule in the network. Therefore, the diffusion coefficient of the particles is not reversely proportional to the bulk viscosity. When there is no interaction between particles and polymer, the hydrodynamic size of the particles does not change. Particles travel in the liquid void space in polymeric matrix. If the size of the particles is much smaller than the void space, the diffusion coefficient of the particles is still governed by Stokes –Einstein equation. On the other hand, particles may be stuck in the network or their diffusion coefficient is not linearly proportional to the inverse of the bulk viscosity.

Rheology is the study of the deformation and flow of a material when stress is applied. A simple solid subject stores energy and behaves a spring-like, elastic response, whereas simple liquids dissipate energy through viscous flow. The rheological measurements of other soft, viscoelastic materials, reveal both the solid-and fluid-like responses and

generally depend on the time scale at which the sample is probed [496]. The time-dependent stress of a soft material is linearly proportional to the strain, and is given by

$$\sigma(t) = \gamma_0 [G'(\omega)\sin(\omega t) + G''(\omega)\cos(\omega t)], \quad (106)$$

where γ_0 is the amplitude oscillation shear strain; ω is the frequency oscillation; $G'(\omega)$ is the response in phase with the applied strain and known as the elastic or storage modulus which stands for the elastic energy by the sample; $G''(\omega)$ is the response out of phase with the applied strain known as viscous or loss modulus which represents the viscous dissipation of energy by the sample. The complex shear modulus of a soft material is defined as $G^* = G' + iG''$.

The dynamic nano-rheology of the film loaded beta-carotene nano particles is presented in Figure 62. Dynamic rheology of the film precursor has two regions distinguished by an intersection of storage modulus G' and lost modulus G'' . Both moduli increase with the increase in polymer concentration due to water evaporation. In the first region viscous modulus dominates and indicates that the film is a true polymeric solution. The other where elastic modulus dominates indicates gelatinization state of the film. The sol – gel transition of the mixture is at 6.9% of HPMC.

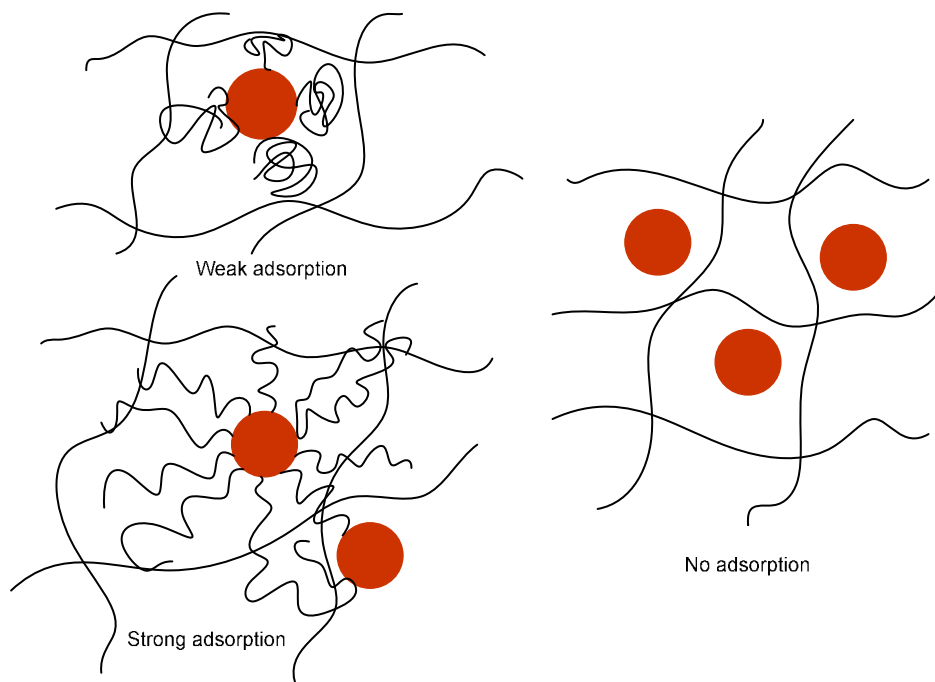


Figure 61: The polymer - particle interaction

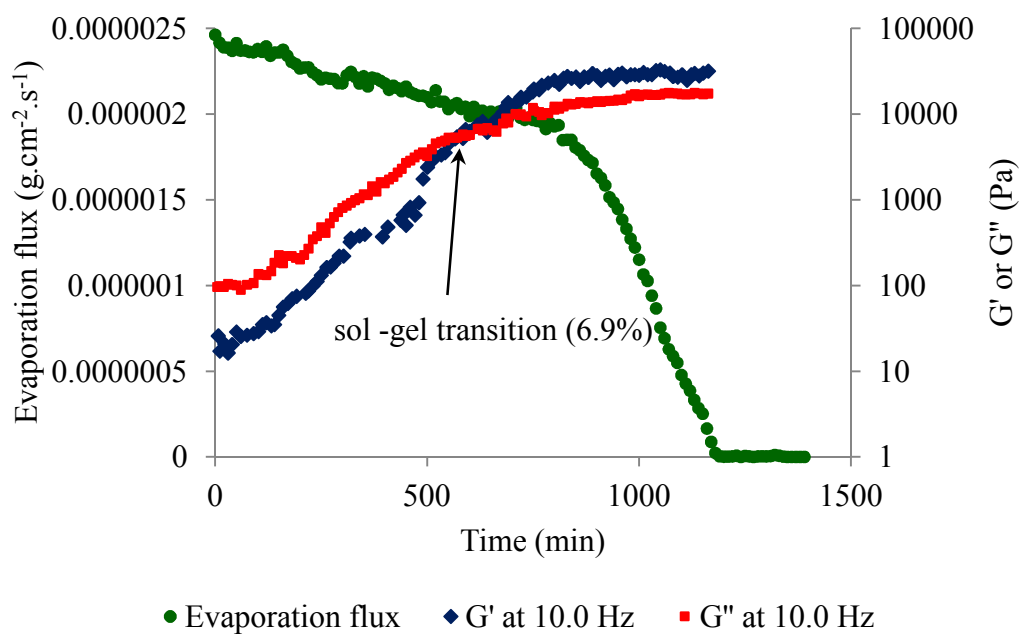


Figure 62 : Dynamic storage and lost modulus of the film

5. Moisture adsorption of the films

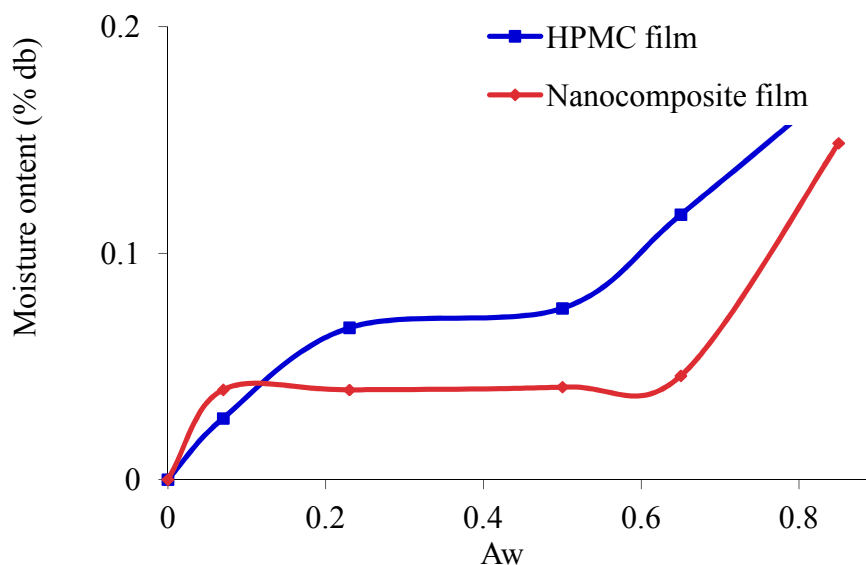


Figure 63: Moisture isotherm of the films

The moisture adsorption isotherm of the films at room temperature is shown in Figure 63. Both films require 96 hour encountering the equilibrium. The red line represents the sorption isotherm of the HPMC film with particles while the blue line stands for the sorption isotherm of the HPMC film. They both belong to Type II sigmoid as classified by Brunauer [497]. Generally, the moisture content of the films is strongly dependent on the environment humidity. The moisture adsorption of both films is very similar in low humidity environment. However, when the humidity increases, the sorption isotherm of the films becomes different. The water content in the HPMC film increases with the increase of relative humidity. But, the water content of the nanocomposite film is almost

stable for a wide range of relative humidity until the humidity approaches 75%. The obtained data are fitted to five different sorption models widely used for edible films [498]. The regression statistical analyses of the fitting are in Table 16. The moisture adsorption isotherm of the HPMC film fits the Smith model while that of the composite film fits the BET model.

Table 16: The sorption isotherm model confidence fit of the films

Model	Regression parameters	HPMC film	Nanocomposite film
Smith	S(B)	-0.0760	-0.0580
	I(A)	0.0320	0.0168
	r^2	0.9640	0.7660
Oswin	S(B)	0.4110	0.2530
	I(A)	-2.4320	-2.8560
	r^2	0.9550	0.5390
Hasley	S(B)	-0.6180	-0.4330
	I(A)	-2.7620	-3.0730
	r^2	0.9130	0.6690
GAB	m_0	0.0540	0.0180
	k	0.8190	1.0040
	c	19.8580	-16.1200
	r^2	0.8670	0.8940
BET	S	39.0320	61.760
	I	-3.4330	-4.6600
	m_0	0.0280	0.0180
	r^2	0.8100	0.9270

CONCLUSIONS

Nanoparticles of β -carotene are successfully formulated by using high-shear stress based on emulsion template where only GRAS materials were applied. Lecithin is the best surfactant among the emulsifiers investigated. The optimal surfactant concentration of lecithin is 5% based on the mass of emulsion. The optimal emulsification time is 4 minutes. The obtained particles have the most stability when the water content is approximately 98%. There is evidence that Oswald ripening and shortage of surfactant adsorbed on the particles are the main reasons for the change in particle size when tween 20 is used. The particles created using lecithin are stable for long time of storage. The shelf life of the nanosuspensions consists of two stages. The first stage is the ongoing diffusion of triacetin trapped in the particles causing the decrease in particle size. In the second stage, the particle size increases due to flocculation of particles. The proposed method is green, simple, easy to scale up and robust.

The breakup mechanism of emulsion droplet under high shear is built based on Kolmogorov's theory. The calculation shows that emulsion droplets brake under inertial force. The emulsion droplet size from experimental results is highly fitted with the estimated curve from Kolmogorov theory showing the prediction validity of the model. The relationship between droplet radius and mass fraction of solid beta-carotene in an emulsion droplet during the diffusion of triacetin is detailed by solving a mathematic diffusion model. Moreover, the mathematic diffusion model also points out the relationship between emulsion droplet size and its diffusion time. At nano scale, the diffusion is very short. That highly impacts the morphology of the nanoparticles.

The flux of diffusion of triacetin from an emulsion droplet has been investigated using optical goniometer. The diffusion of triacetin from the droplet pended in aqueous media consists of two stages distinguished by the slope of diffusion flux. The diffusion flux of triacetin is highly dependent on the interfacial surface tension. The lower the interfacial surface tension is the higher diffusion flux is. Without surfactant, the diffusion flux approaches plateau after introduction stage in which the diffusion flux increases with the accumulation of triacetin on the film adjacent to the droplet. When surfactants are introduced, they accumulate at the interface to form layer of surfactant and decrease interfacial surface tension leading to high diffusion flux of triacetin. Low HLB surfactant generates a stable layer at the oil-water interface to increase the diffusion barrier leading to the plateau of diffusion flux. High HLB surfactants which are water soluble tend to migrate from the oil – water interface into aqueous media at certain time. The molecular coverage area by one surfactant molecule is calculated based on the interfacial surface tension of surfactant – triacetin system. Gibbs adsorption isotherm is applied to calculate the smallest internal distance between surfactant molecules in the surfactant layer on triacetin surface. The obtained internal distance between two lecithin molecules is 9.45Å which agrees highly with the data calculated by Small [405]. It proves that the triacetin is trapped in the particles due to fast precipitation of beta-carotene. The different adsorption behaviors of those surfactants create different particle size evolution scenario of the nanosuspensions.

Morphology of the particles is characterized by XRD and DSC. The results prove that the beta-carotene nanoparticles are primarily amorphous. The particles prepared by using lecithin are not only stable for long storage time but also can be sublimated without

melting by triacetin residue. It turns out that the obtained nanoparticles are beta-carotene encapsulated by lecithin which causes particle flocculation during storage or lyophilization.

A fortified food model of edible film is investigated in order to characterize the impact of nanoparticles on food matrix. A mass transfer model is built to understand the effects of drying condition to the film formation. Fast solvent removal forms a gel layer at the liquid – air interface leading to poor mechanical properties of the film. The evaporation consists of mainly two stages. External solvent removal controls the constant drying rate while the internal diffusion governs the falling drying rate period. Both triacetin and lecithin reduce the time for the constant drying rate while the particles enlarge it. It is found that phase separation occurs in the film with triacetin although the mass fraction of triacetin used is 33% on dried basic. Lecithin lamellar structure formation in the film with lecithin causes the change in solvent removal behavior. The interfacial surface tension of lecithin – HPMC in aqueous solution reveals that lecithin does not interact with HPMC. This indicates that the particles are well protected by layer of lecithin from the absorption of polymer. However, particle flocculation occurs during film formation due to the interaction between lecithin lamellar structures on the surface of the particles.

During film formation, the particles pass through three periods (1) the freely mobile under Brownian motion, (2) the limited movement stage, and (3) packaged in polymeric matrix stage due to the volume shrinkage. Depending on the particle – polymer – surfactant interaction, three scenarios may occur to form different structures of the film loaded particles. The dynamic nano-rheology of the film discloses that the sol – gel transition of the film loaded particles happens at 6.9% of HPMC. Moreover, the

experiment data shows that the diffusion coefficient of the beta-carotene nanoparticle obeys Stokes –Einstein equation even when in high concentrated polymer solution. The presence of the particles in the film also causes the change in moisture adsorption behavior. Moisture adsorption measurements reveal that the moisture adsorption isotherm of the HPMC film fits the Smith model while that of the film with particles fits the BET model.

Despite the success of the work, there are some small limitations, for example the solubility of nutraceutical in oil is quite low. This restricts the loading capacity of emulsion then causing low loading capacity of nanosuspensions. The residue of short chain triglyceride in the obtained suspensions brings advantage for Ostwald ripening leading to the change in particle size of the nanoparticles. Moreover, the concentration of particles in nanosuspensions is quite low. It may require further steps before introducing particles into food matrix.

FUTURE WORKS

The key factor for the success of the process is the distribution of nutraceutical in emulsion droplets. Unfortunately, triacetin cannot be a good solvent for all nutraceuticals. In order to broaden the application of this technique, we would like to scan other food grade solvents for not only higher nutraceutical loading capacity but also enrichment the recipe for the approach.

The next step after the success of preparing nanoparticles is the *in vitro* and *in vivo* bioavailability testing. These investigations will provide robust evidences for the hypothesis of higher bioavailability of nanoparticles. Furthermore, those tests will supply the feedback information to improve the operation conditions.

Because the fortified food spectrum is large, we would like to investigate the application of the obtained nanoparticles to other food products such as beverage, ready to eat soup, etc. In order to apply particles in a new product, it requires understanding the interaction between particles and other food component.

We also would like to transfer our approach to food industry. Thus, it raises a demand for scale up production at lab scale and small batch. The scale up production will give better understanding of the process for industrial application.

REFERENCES

1. Hasler, C.M., *Functional Foods: Their role in disease prevention and health promotion*. Food Technology, 1998. 52(11): p. 63-70.
2. Hasler, C.M., *The changing face of functional foods*. Journal of American College of Nutrition, 2000. 19(5): p. 499S-506S.
3. Mitchell, E.A., et al., *Clinical characteristics and serum essential fatty acid levels in hyperactive children*. Journal of Clinical Pediatrics, 1987. 26: p. 406-411.
4. Wolfson, W., *Fish oil cookies*. Technology Reviews, 2004: p. 27-27.
5. BCC, R. *Nutraceuticals: Global markets and processing technologies*. 2009; Available from: www.bccresearch.com.
6. Biesalski, H.K., *Nutraceutical: The link between nutrition and medicine*, in *Nutraceuticals in health and disease prevention of Toxicology*, K. Kramer, P.P. Hoppe, and L. Packer, Editors. 2001, Marcel Dekker Inc: New York. p. 1-26.
7. Kris-Etherton, P.M., et al., *Bioactive compounds in foods: Their role in the prevention of cardiovascular disease and cancer*. The American Journal of Medicine, 2002. 113(9B): p. 71S-88S.
8. Kramer, K., P. Hoppe, and L. Packer, *Nutraceuticals in health and disease prevention*. Nutraceuticals in health and disease prevention, ed. Anonymous. 2001, New York: Marcel Dekker Inc.
9. Krauss, W.E., J.H. Erb, and R.G. Washburn, *Studies on the Nutritive Value of Milk. II. The Effect of Pasteurization on Some of the Nutritive Properties of Milk*. Journal of the American Medical Association, 1933. 100(25): p. 2043-2044.
10. Renner, E., *Effects of agricultural practices on milk and dairy products*, in *Nutritional evaluation of food processing*, E. Karmas and R.S. Harris., Editors. 1988, Van Nostrand Reinhold Company: New York p. 203-224.
11. Sadler, G.D., M.E. Perish, and L. Wicker, *Microbial, enzymatic and chemical changes during storage of fresh and processed orange*. Journal of Food Science. , 1992. 57(5): p. 1187-11971.
12. Ilic, D.B. and S.H. Ashoor, *Stability of Vitamins A and C in Fortified Yogurt*. Journal of Dairy Science, 1988. 71(6): p. 1492-1498.
13. Zhu, H. and S. Damodaran, *Effects of Calcium and Magnesium Ions on Aggregation of Whey Protein Isolate and Its Effect on Foaming Properties*. Journal of Agricultural and Food Chemistry, 1994. 42(4): p. 856-862.
14. Tatum, J.H., P.E. Shaw, and R.E. Berry, *Degradation products from ascorbic acid*. Journal of Agricultural and Food Chemistry, 1969. 17(1): p. 38-40.
15. Rouseff, R.L., J.F. Fisher, and S. Nagy, *HPLC separation and comparison of the browning pigments formed in grapefruit juice stored in glass and cans*. Journal of Agricultural and Food Chemistry, 1989. 37(3): p. 765-769.
16. Riberio, H.S., K. Ax, and H. Schubert, *Stability of lycopene emulsions in food systems*. Journal of Food Science, 2003. 68(9): p. 2730-2734.
17. Aguilera, J.M., *Why food microstructure*. Journal of Food Engineering, 2005. 67: p. 3-11.

18. Leser, M.E., Michael, M., Watzke, H. J, *Food goes nano: new horizons for food structure research*, in *Food Colloids: Biopolymers and Materials*, E. Dickinson and T. Vliet, Editors. 2003, Royal Society of Chemistry: Cambridge. p. 3-13.
19. Aguilera, J.M., *Microstructure and food product engineering*. Food Technology, 2000. 54(11): p. 56-65.
20. Gokhale, R., *Food effect on drug formulation performance in vivo*. Drug Delivery Technology, 2006. 6(4): p. 62-72.
21. Allen, L., et al., *guidelines for food fortification with micronutrients*. 2006: WHO - Nutrition Publications
22. Bruno de Benoist, et al., *Iodine status worldwide. WHO Global Database on Iodine Deficiency*. 2004, Geneva: World Health Organization.
23. Verster, A., *Food fortification: good to have or need to have? - East Mediterr Health J*. 2004 Nov;10(6):771-7., (- 1020-3397 (Print)): p. T - ppublish.
24. Hallberg, L., L. Rossander, and A.B. Skanberg, *Phytates and the inhibitory effect of bran on iron absorption in man*. American Journal of Clinical Nutrition, 1987. 45(5): p. 988-996.
25. Hurrell, R.F., et al., *Soy protein, phytate and iron absorption in men*. American Journal of Clinical Nutrition, 1992. 56(3): p. 573-578.
26. Hurrell, R., *How to Ensure Adequate Iron Absorption from Iron-fortified Food*. Nutrition Reviews, 2002. 60: p. S7-S15.
27. Swain, J.H., S.M. Newman, and J.R. Hunt, *Bioavailability of Elemental Iron Powders to Rats Is Less than Bakery-Grade Ferrous Sulfate and Predicted by Iron Solubility and Particle Surface Area*. The Journal of Nutrition, 2003. 133(11): p. 3546-3552.
28. Cook JD, R.M., *Iron fortification: an update*. The American Journal of Clinical Nutrition, 1983. 38(4): p. 648-59.
29. Russell, R.M., *Vitamin and trace mineral deficiency and excess*, in *Harrison's Principles of Internal Medicine*, D.L. Kasper, et al., Editors. 2001, McGraw-Hill: New York.
30. Latham, M.E., *Human Nutrition in the Developing World (Fao Food and Nutrition Paper)*. 1997: Food & Agriculture Organization of the United.
31. Sommer, A., *Vitamin A Deficiency and Its Consequences: A Field Guide to Detection and Control*. 1995: World Health Organization.
32. Dary, O. and J.O. Mora, *Food Fortification to Reduce Vitamin A Deficiency: International Vitamin A Consultative Group Recommendations*. The Journal of Nutrition, 2002. 132(9): p. 2927S-2933S.
33. Mejia, L., R. Hodges, and R. Rucker, *Clinical signs of anemia in vitamin A-deficient rats*. The American Journal of Clinical Nutrition, 1979. 32(7): p. 1439-1444.
34. Oliveros, L.B., et al., *Vitamin A deficiency modifies lipid metabolism in rat liver*. British Journal of Nutrition, 2007. 97: p. 263-272.
35. Allen, L., et al., *Guidelines on food fortification with micronutrients*. 2006: World Health Organization - Food and Agricultural Organization of the United Nations.
36. Krishnaswamy, K. and K.M. Nair, *Importance of folate in human nutrition*. British Journal of Nutrition, 2001. 85: p. S 115 - S 123.

37. Eva Hertrampf, et al., *Consumption of folic acid-fortified bread improves folate status in women of reproductive age in Chile*. *Journal of Nutrition* Cancer, 2003. 133: p. 3166-3169.
38. Villalpando, S., et al., *Vitamins A, and C and folate status in Mexican children under 12 years and women 12-49 years: a probabilistic national survey*. *Salud Pública de México*, 2003. 45: p. 508-519.
39. L.H. Allen and J.E. Casterline-Sabel, *Prevalence and causes of nutritional anemias*, in *Nutritional Anemias*, U. Ramakrishnan, Editor. 2000, CRC Press, Boca Raton, FL. p. 17-21.
40. Hennessy-Priest, K., et al., *Folic acid food fortification prevents inadequate folate intake among preschoolers from Ontario*. *Public Health Nutrition*, 2009. 12(09): p. 1548-1555.
41. Darnton-Hill, I., et al., *Iron and Folate Fortification in the Americas to Prevent and Control Micronutrient Malnutrition: An Analysis*. *Nutrition Reviews*, 1999. 57(1): p. 25-31.
42. McLean, E., B.d. Benoist, and L.H. Allen, *Review of the magnitude of folate and vitamin B12 deficiencies worldwide*. *Food Nutrition Bulletin*, 2008. 29(2): p. 0379-5721.
43. Rosado, J.L., *Zinc and Copper: Proposed Fortification Levels and Recommended Zinc Compounds*. *The Journal of Nutrition*, 2003. 133(9): p. 2985S-2989S.
44. de Romaña, D.L., B. Lönnnerdal, and K.H. Brown, *Absorption of zinc from wheat products fortified with iron and either zinc sulfate or zinc oxide*. *The American Journal of Clinical Nutrition*, 2003. 78(2): p. 279-283.
45. Aro, A., G. Alfthan, and P. Varo, *Effects of supplementation of fertilizers on human selenium status in Finland*. *Analyst*, 1995. 120(3): p. 841-843.
46. Olson, J.A., *Vitamin A*, in *Present knowledge in nutrition*, Ziegler E.E. and F. L.J., Editors. 1996, International Life Sciences Institute Press: Washington, DC. p. 109-119.
47. Dary Omar and M.J. O., *Food Fortification to Reduce Vitamin A Deficiency: International Vitamin A Consultative Group Recommendations*. *The Journal of Nutrition*, 2002. 132(9): p. 2927S-2933S.
48. Commodities, C.o.I.N.-V.C.i.F.A. and I.o. Medicine, *Vitamin C Fortification of Food Aid Commodities: Final Report*. 1997: The National Academies Press.
49. Mona S Calvo, Susan J Whiting, and C.N. Barton, *Vitamin D fortification in the United States and Canada: current status and data needs*. *The American Journal of Clinical Nutrition* 2004. 80: p. 1710S - 1716S.
50. Refsum Helga and S.A. David, *Are we ready for mandatory fortification with vitamin B-12?* *The American Journal of Clinical Nutrition*, 2008. 88(2): p. 253-254.
51. Allen, L.H., *B Vitamins: Proposed Fortification Levels for Complementary Foods for Young Children*. *The Journal of Nutrition*, 2003. 133(9): p. 3000S-3007S.
52. Czeizel, A.E. and Z. Merhala, *Bread fortification with folic acid, vitamin B12, and vitamin B6 in Hungary*. *The Lancet*, 1998. 352(9135): p. 1225.
53. Rosenberg, I.H., *Further evidence that food fortification improves micronutrient status*. *British Journal of Nutrition*, 2007. 97(06): p. 1051-1052.

54. Evelyn M. Hannon, Mairead Kiely, and A. Flynn, *The impact of voluntary fortification of foods on micronutrient intakes in Irish adults*. British Journal of Nutrition, 2007. 97: p. 1177-1186.
55. Best, C., et al., *Can multi-micronutrient food fortification improve the micronutrient status, growth, health, and cognition of schoolchildren? A systematic review*. Nutrition Reviews, 2011. 69(4): p. 186-204.
56. Douglas Jr, F.W., et al., *Color, Flavor, and Iron Bioavailability in Iron-Fortified Chocolate Milk*. Journal of Dairy Science, 1981. 64(9): p. 1785-1793.
57. Disler PB, L.S., Charlton RW, Bothwell TH, Walker RB, Mayet *Studies on the fortification of cane sugar with iron and ascorbic acid*. The British Journal of Nutrition, 1975. 34(1): p. 141-152.
58. Richardson, D.P., *Food Fortification*. Proceedings of the Nutrition Society, 1990. 49(01): p. 39-50.
59. Killeit, U., *The stability of vitamins. A selection of current literature*. 1988, Grenzach-Whylen, Germany: Hoffman-LaRoche AG.
60. Counsell, J.N., *Vitamin fortification of food*, in *Food Technology International Europe*, A. Turner, Editor. 1988, Sterling Publications Ltd: London p. 211-218.
61. Shane, B., *Folate fortification: enough already?* The American Journal of Clinical Nutrition, 2003. 77(1): p. 8-9.
62. Beard, C.M., L.A. Panser, and S.K. Katusic, *Is excess folic acid supplementation a risk factor for autism?* Medical Hypotheses, 2011. 77(1): p. 15-17.
63. William J. Barbaresi, et al., *The Incidence of Autism in Olmsted County, Minnesota, 1976-1997: Results From a Population-Based Study*. Archives of Pediatrics and Adolescent Medicine, 2005. 159(1): p. 37-44.
64. Hathcock, J., *Vitamins and minerals: efficacy and safety*. The American Journal of Clinical Nutrition, 1997. 66(2): p. 427-437.
65. J E Baggott, et al., *Inhibition of folate-dependent enzymes by non-steroidal anti-inflammatory drugs*. Biochemical Journal 1992. 282(1): p. 197-202.
66. Spernath, A. and A. Aserin, *Microemulsions as carriers for drugs and nutraceuticals*. Advances in Colloid and Interface Science, 2006. 128–130(0): p. 47-64.
67. Brigger, I., C. Dubernet, and P. Couvreur, *Nanoparticles in cancer therapy and diagnosis*. Advanced Drug Delivery Reviews, 2002. 54(5): p. 631-651.
68. Gupta, R.B. and U.B. Kompella, *Nanoparticle Technology for Drug Delivery*. 2006: Taylor & Francis.
69. Mainardes, R.M. and L.P. Silva, *Drug delivery systems: past, present and future*. Current Drug Targets, 2004. 5: p. 449-455.
70. Sahoo, S.K. and V. Labhasetwar, *Nanotech approaches to drug delivery and imaging*. Drug discovery today, 2003. 8(24): p. 1112-1120.
71. Bangham, A.D., M.M. Standish, and J.C. Watkins, *Diffusion of univalent ions across the lamellae of swollen phospholipids*. Journal of Molecular Biology., 1965. 13(1): p. 238-252.
72. Sessa, G., Weissmann, G, *Phospholipid spherules (liposomes) as a model for biological membranes*. Journal of Lipid Research, 1968. 9: p. 310–318.

73. Bangham, A.D., Horne, R.W, *Negative staining of phospholipids and their structural modification by surface active agents as observed in the electron microscope*. Journal of Molecular Biology, 1964. 8: p. 660–668.
74. Lasic, D., D, *Liposomes from Physics to Applications*. Liposomes from Physics to Applications, ed. D. Lasic, D. 1993, Amsterdam: Elsevier.
75. Ostro, M., J, *Liposomes from Biophysics to Therapeutics*. Liposomes from Biophysics to Therapeutics, ed. M. Ostro, J. 1987, New York:: Marcel Dekker.
76. Barenholz, Y., *Quality Control of Liposomes*. Chemistry and Physics of Lipids, 1993. 4.
77. Er, Y., C.A. Prestidge, and D. Fornasiero, *Attenuated total reflectance infrared studies of liposome adsorption at the solid-liquid interface*. Colloids and Surfaces B: Biointerfaces, 2004. 36: p. 147-153.
78. Grabielle-Madelmont, C., S. Lesieur, and M. Ollivon, *Characterization of loaded liposomes by size exclusion chromatography*. Journal of Biochemical and Biophysical Methods, 2003. 56: p. 189-217.
79. Kozubek, A., Gubernator, J., Przeworska, E., Stasiuk, M, *Liposomal drug delivery, the novel approach; Plarosomes*. Acta Biochim Polon, 2000. 47: p. 639-649
80. Woodle, W., Papahadjopoulos, D, *Liposome preparation and size characterization*. Methods In Enzymology 1989. 171: p. 193–217.
81. Senior, J.H., *Fate and behavior of liposomes in vivo: a review of controlling factors*. Critical Review of Therapeutic Drug Carrier System, 1987. 3(2): p. 123-193.
82. Allen, T., M, *Liposomes, Opportunities in drug delivery*. Drugs, 1997. 54(4): p. 8-14.
83. Gabizona, A., Gorena, D., Cohenb, R., Barenholz, Y, *Development of liposomal anthracyclines: from basics to clinical applications*. Journal of Control Release, 1998. 53: p. 275-279.
84. Allen, T.M., P. Sapra, and E. Moase, *Use of the post insertion method for the formation of ligand-coupled liposomes*. Cellular and Molecular Biology Letters, 2002. 7(2): p. 217-219.
85. Allen, T.M., *Long-circulating (sterically stabilized) liposomes for targeted drug delivery*. Trends in Pharmacological Sciences, 1994. 15(7): p. 215-220.
86. Hansen, C.B., et al., *Attachment of antibodies to sterically stabilized liposomes: evaluation, comparison and optimization of coupling procedures*. Biochimica Biophysica Acta, 1995. 1239: p. 133-144.
87. Yamazaki, N., K. M, M, and H.J. Gabius, *Neoglycoprotein-liposome and lectin-liposome conjugates as tools for carbohydrate recognition research*. Methods In Enzymology, 1994. 242: p. 56-65.
88. Skeie, S., *Developments in microencapsulation science applicable to cheese research and development. A review* International Dairy Journal, 1994. 4(7): p. 573-595
89. Kirby, C.J., et al., *Stabilization of ascorbic acid by microencapsulation in liposomes*. International Journal of Food Science & Technology, 1991. 26(5): p. 437-449.

90. Lee, D., H., Jin, B. H., Hwang, Y. I., Seung-Cheol-Lee, S. C., *Encapsulation of bromelain in liposome*. Journal of Food Science and Nutrition 2000. 5: p. 81-85.
91. Laridi, R., et al., *Liposome encapsulated nisin Z: optimization, stability and release during milk fermentation*. International Dairy Journal, 2003. 13: p. 325-336.
92. Kirby, C., J., Whittle, C., J., Rigby, N., Coxon, D., T., Law, B., A., *Stabilization of ascorbic acid by microencapsulation in liposomes*. International Journal of Food Science & Technology, 1991. 26(5): p. 437-449.
93. Singh, H., *The milk fat globule membrane- A biophysical system for food applications*. Current Opinion in Colloids and Interface Science, 2006. 11: p. 154-163.
94. Zarif, L., Graybill, Jr., Perlin, D., Mannino, R. J., *Cochleates new lipid based drug delivery system*. Journal of Liposome Research, 2000. 10: p. 523.
95. Papahadjopoulos, D., et al., *Cochleate lipid cylinders: Formation by fusion of unilamellar lipid vesicles*. Biochimica Biophysica Acta, 1975. 394: p. 483-490.
96. Gould-Fogerite, S., et al., *Targeting immune response induction with cochleate and liposome-based vaccines*. Advanced Drug Delivery Reviews, 1998. 32: p. 273-287.
97. Jansen, J.F., et al., *Encapsulation of guest molecules into a dendritic box*. Science, 1994. 266(5188): p. 1226-1229.
98. Joseph, T., Morrison, M., *Nanotechnology in agriculture and food: A nanoforum report*. 2006, Institute of nanotechnology.
99. Etcgroup, *Down on the farm-The Impact of Nano-Scale Technologies on Food and Agriculture*. 2004.
100. Kamath, K. and K. Park, *Biodegradable hydrogels in drug delivery*. Advance Drug Delivery Review, 1993: p. 59-84.
101. Peppas, N.A. and Lowman, *Hydrogels encyclopedia of controlled drug delivery*, ed. E. Mathiowitz. 1999, Wiley.
102. Qiu, Y. and K. Park, *Environment-sensitive hydrogels for drug delivery*. Advanced Drug Delivery Reviews, 2001. 53: p. 321-339.
103. Lee, e.a., *Trends and Future Perspectives in Peptides and Proteins Drug Delivery*. Harwood Chur, 1995.
104. Peppas, N.A., et al., *Hydrogels in pharmaceutical formulation*. European Journal of Pharmaceutics and Biopharmaceutics, 2000. 50: p. 27-46.
105. Fix, J., A., *Oral controlied release technology for peptides: Status and future prospects*. Pharmaceutical Research, 1996. 13: p. 1760-1764.
106. Plate, N., A., Valuev, L.I., Starosel'tseva, L. K., Valueva, T. A., Vanchugova, L. V., Ul'yanova, M. V., Valuev, I. L., Sytov, G. A., Ametov, A. S., Knyazhev, V. A., *Macromolecular systems containing insulin as related to the problem of diabetes*. Polymer Science, 1994. 36: p. 1581-1585.
107. Kopece, J., Kopeckova, P., Omelyanenko, V., *Biorecognizable biomedical polymers: Advanced biomaterials*. In *Biomedical and Drug Delivery Systems*, in Springer, N. Ogata, Kim, S. W., Feijen, J., Okano, T., Editor. 1996: Tokyo. p. 91-95.

108. Park, K., Park, H, *Smart Hydrogels*, in *Concise Polymeric Materials Encyclopedia*, J. Salamone, C, Editor. 1999, CRC Press: Boca Raton. p. 1476–1478.
109. Peppas, N.A., Sahlin, J.J. , *Hydrogels as Muco- and Bioadhesive Materials: A Review*. *Biomaterials*, 1996. 17: p. 1553-1561.
110. Podula, K., F.J. Doyle III, and N.A. Peppas, *Glucose-sensitivity of glucose oxidase containing cationic copolymer hydrogels having poly (ethylene glycol) grafts*. *Journal of Controlled Release*, 2000. 67: p. 9-17.
111. Mitra, S., et al., *Tumour targeted delivery of encapsulated dextran-doxorubicin conjugate using chitosan nanoparticles as carrier*. *Journal of Controlled Release*, 2001. 74: p. 317-323.
112. Sahoo, S.K., et al., *pH and thermosensitive hydrogels nanoparticles*. *Journal of Colloid and Interface Sciences*, 1998. 206: p. 361-368.
113. Hoffman, A.S., *Hydrogels for biomedical applications*. *Advanced Drug Delivery Reviews*, 2002. 54: p. 3-12.
114. Chen, L., G.E. Remondetto, and M. Subirade, *Food protein based materials as nutraceutical delivery systems*. *Trends in Food Science and Technology*, 2006. 17: p. 272-283.
115. Leung, S., V., Remondetto, G., E., Subirade, M, *Cold gelation of β -lactoglobulin oil-in-water emulsions*. *Food Hydrocolloids* 2005. 19: p. 269-278.
116. Kwon, G.S. and T. Okano, *Polymeric micelles as new drug carriers*. *Advance Drug Delivery Review*, 1996. 21: p. 107-116.
117. Trubetskoy, V.S. and T.J. Burke, *Engineered polymeric micelles: A novel tool for solubilization and stabilization of membrane protein target for proteomics and drug discovery*. *American Laboratory*, 2005: p. 19-22.
118. Torchilin, V.P., *Structure and design of polymeric surfactant-based drug delivery systems*. *Journal of Controlled Release*, 2001. 73(2-3): p. 137–172.
119. Attwood, D. and A.T. Florence, *Surfactant systems: Their chemistry, pharmacy and biology*. 1983, London: Chapman and Hall.
120. Rosler, A., G.W.M. Vandermeulen, and H.A. Klok, *Advanced drug delivery devices via self-assembly of amphiphilic block copolymers*. *Advanced Drug Delivery Reviews*, 2001. 53: p. 95-108.
121. Tomalia, D.A., N. Am, A. M, and W.A. Goddard III, *Starburst dendrimers: Molecular-level control of size, shape, surface chemistry, topology, and flexibility from atoms to macroscopic matter*. *Angew.Chem.Int.*, 1990. 102: p. 138-75.
122. Aulenta, F., W. Hayes, and S. Rannard, *Dendrimers: a new class of nanoscopic containers and delivery devices*. *European Polymer Journal*, 2003. 39: p. 1741-1771.
123. Hawker, C.J., Frechet, J. M. J, *Comparison of linear, hyperbranched, and dendritic macromolecules*, in *Step-Growth Polymers for High-Performance Materials*, J. Hedrick and J. Labadie, Editors. 1996, American Chemical Society: Washington D.C. p. 132-144.
124. Liu, S. and S.P. Armes, *Recent advances in the synthesis of polymeric surfactants*. *Current Opinion in Colloid & Interface Science*, 2001. 6: p. 249-256.
125. Kohn, J., *Design, synthesis, and possible applications of pseudo-poly(amino acids)*. *Trend in Polymer Science*, 1993. 17: p. 206-212.

126. Nathan, N., Zalipsky, S., Kohn, J, *Strategies for Covalent Attachment of Doxorubicin to Poly(PEG-Lys), a New Water-Soluble Poly(ether urethane)*. Journal of Bioactive and Compatible Polymers, 1994. 9(3): p. 239-251
127. Purohit, G., T. Sakthivel, and A.T. Florence, *Interaction of cationic partial dendrimers with charged and neutral liposomes*. International Journal of Pharmaceutics, 2001. 214(1-2): p. 71-76.
128. Khopade, A.J., et al., *Effect of dendrimer on entrapment and release of bioactive from liposomes*. International Journal of Pharmaceutics, 2002. 232: p. 157-162.
129. Sarbolouki, M.N., et al., *Dendrosomes: A novel family of vehicles for transfection and therapy*. Journal of Chemical Technology and Biotechnology, 2000. 75: p. 919-922.
130. Couvreur, P., Couarraze, G., Devissaguet, J. P., Puisieux, F, *Nanoparticles: Preparation and Characterization*. Nanoparticles: Preparation and Characterization., ed. P. Couvreur, Couarraze, G., Devissaguet, J. P., Puisieux, F. 1996, New York: Marcel Dekker.
131. Allemann, E., J. Leroux, and R. Gurny, *Polymeric nano- and microparticles for the oral delivery of peptides and peptidomimetics*. Advanced Drug Delivery Reviews, 1998. 34: p. 171-189.
132. Majeti, N.V.R. and N.V. Majeti, *Nano and Microparticles as controlled drug delivery devices*. Journal of Pharmacology and Pharmaceutical Science, 2000. 3(2): p. 234-258.
133. Gref, R., et al., *Biodegradable long-circulating polymeric nanospheres*. Science, 1994. 263(5153): p. 1600-1603.
134. Fattal, E., Vauthier, C., Aynie, I., Nakada, Y., Lambert, G., Malvy, C., Couvreur, P, *Biodegradable polyalkylcyanoacrylate nanoparticles for the delivery of oligonucleotides*. Journal of Controlled Release, 1998. 53(1-3): p. 137-143.
135. Soppimath, K.S., et al., *Biodegradable polymeric nanoparticles as drug delivery devices*. Journal of Controlled Release, 2001. 70: p. 1-20.
136. Barratt, G.M., *Therapeutic applications of colloidal drug carriers*. Pharmaceutical Science & Technology Today, 2000. 3(5): p. 163-171.
137. Delie, F., *Evaluation of nano- and microparticle uptake by the gastrointestinal tract*. Advanced Drug Delivery Reviews, 1998. 34: p. 221-233.
138. Lambert, G., et al., *Polyisobutylcyanoacrylate nanocapsules containing an aqueous core as a novel colloidal carrier for the delivery of oligonucleotides*. Pharmaceutical Research, 2000. 17(6): p. 707-714.
139. Godard, G., et al., *Antisense effects of cholesterol-oligodeoxynucleotide conjugates associated with poly(alkylcyanoacrylate) nanoparticles*. European Journal of Biochemistry, 1995. 232(2): p. 404-410.
140. Schwab, G., et al., *Antisense oligonucleotides adsorbed to polyalkylcyanoacrylate nanoparticles specifically inhibit mutated Ha-ras-mediated cell proliferation and tumorigenicity in nude mice*. Proceedings of the National Academy of Sciences of the United States of America, 1994. 91: p. 10460-10464.
141. Zimmer, A., *Antisense oligonucleotide delivery with polyhexylcyanoacrylate nanoparticles as carriers*. Methods, 1999. 18: p. 286-295.
142. Nishioka, Y. and H. Yoshino, *Lymphatic targeting with nanoparticulate systems*. Advanced Drug Delivery Reviews, 2001. 47: p. 55-64.

143. Storm, G., et al., *Surface modification of nanoparticles to oppose uptake by the mononuclear phagocyte system*. *Advanced Drug Delivery Reviews*, 1995. 17: p. 31-48.
144. Sharma, D., et al., *Novel Taxol formulation: polyvinylpyrrolidone nanoparticle-encapsulated Taxol for drug delivery in cancer therapy*. *Oncology research*, 1996. 7-8: p. 281-286.
145. Stolnik, S., Illum, L., S.S. Davis, S, S, *Long circulating microparticulate drug carriers*. *Advanced Drug Delivery Review*, 1995. 16: p. 195–214.
146. Brigger, I., P. Couvreur, and D. C, *Nanoparticles in cancer therapy and diagnosis*. *Advanced Drug Delivery Reviews*, 2002. 54: p. 631-651.
147. Hans, M.I. and A.M. Lowman, *Biodegradable nanoparticles for drug delivery and targeting*. *Current Opinion in Solid State and Materials Science*, 2002. 6: p. 319-327.
148. Goldstein, I.J., et al., *What should be called a lectin?* *Nature*, 1980. 285: p. 66.
149. Arbos, P., et al., *Quantification of the bioadhesive properties of protein-coated PVM/MA nanoparticles*. *International Journal of Pharmaceutics*, 2002. 242: p. 129-136.
150. Rodrigues, J.S., et al., *Novel core(polyester)-shell(polysaccharide) nanoparticles: protein loading and surface modification with lectins*. *Journal of Controlled Release*, 2003. 92: p. 103-112.
151. Leroux, J.C., et al., *Biodegradable nanoparticles -- From sustained release formulations to improved site specific drug delivery*. *Journal of Controlled Release*, 1996. 39: p. 339-350.
152. Ponchel, G. and J. Irache, *Specific and non-specific bioadhesive particulate systems for oral delivery to the gastrointestinal tract*. *Advanced Drug Delivery Reviews*, 1998. 34: p. 191-219.
153. Duncan, R., *Drug-polymer conjugates: potential for improved chemotherapy* *Anti-Cancer Drugs* 1992. 3(3): p. 175-210.
154. Dickinson, E. and D.J. McClements, *Advances in food colloids*.
155. Coupland, J.N. and D.J. McClements, *Droplet size determination in food emulsions: comparison of ultrasonic and light scattering methods*. *Journal of Food Engineering*, 2001. 50: p. 117-120.
156. Dickinson, E., *Introduction to food colloids*. *Introduction to food colloids*, ed. E. Dickinson, McClements, D. J. 1992, Oxford: Oxford Univ. Press.
157. McClements, D., J, *Food emulsions: principles, practice, and techniques*. *Food emulsions: principles, practice, and techniques.*, ed. D. McClements, J., Decker, E, A, Weiss, J. 2005, Boca Raton: CRC Press.
158. McClements, D., J., Decker, E, A, Weiss, J, *Emulsion-Based Delivery Systems for Lipophilic Bioactive Components*. *Journal of Food Science*, 2007. 72(8): p. 109-124.
159. Muller, R.H., Keck, C. M. , *Challenges and solutions for the delivery of biotech drugs--a review of drug nanocrystal technology and lipid nanoparticles*. *Journal of Biotechnology*, 2004. 113(1-3): p. 151-70.
160. Nakano, M., *Places of emulsions in drug delivery*. *Advance Drug Delivery Review*, 2000. 45: p. 1-4.

161. Benichou, A., A. Aserin, and N. Garti, *Double emulsions stabilized with hybrids of natural polymers for entrapment and slow release of active matters*. *Advances in Colloid and Interface Science*, 2004. 108-109: p. 29-41.
162. Garti, N., Benichou, A, *Double Emulsions for Controlled-release Applications - Progress and Trends*. *Encyclopedic Handbook of Emulsion Technology*, ed. J. Sjoblom. 2001: Marcel Dekker, Inc.
163. Lawson, L.B. and K.D. Papadopoulos, *Effects of a phospholipid cosurfactant on external coalescence in water-in-oil-in-water double-emulsion globules*. *Colloids and Surfaces A: Physicochem.Eng.Aspects*, 2004. 250: p. 337-342.
164. Müller, R.H., Rühl, D., Runge, S.A., Schulze-Forster, K., Mehnert, W, *Cytotoxicity of solid lipid nanoparticles as a function of the lipid matrix and the surfactant*. *Pharmaceutical Research*, 1997a. 14(4): p. 458–462.
165. Müller, R.H., Maaßen, S., Schwarz, C., Mehnert, W, *Solid lipid nanoparticles (SLN) as potential carrier for human use: interaction with human granulocytes*. *Journal of Controlled Release*, 1997b. 47(3): p. 261–269.
166. Gasco, M.R., *Solid lipid nanospheres from warm micro-emulsions*. . *Pharmaceutical Technology Europe*, 1997. 9(52-54): p. 56-58.
167. Heiati, H., Phillips, N, C., Tawashi, R, *Evidence for Phospholipid Bilayer Formation in Solid Lipid Nanoparticles Formulated with Phospholipid and Triglyceride* *Pharmaceutical Research*, 1996. 13(9): p. 1406-1410.
168. Mukherjee, S., Ray, S., Thakur, R, S, *Solid Lipid Nanoparticles: A Modern Formulation Approach in Drug Delivery System*. *Indian Journal of Pharmaceutical Science*, 2009. 71(4): p. 349–358.
169. Mehnert, W. and K. Mader, *Solid lipid nanoparticles: Production, characterization and applications*. *Advanced Drug Delivery Reviews*, 2001. 47: p. 165-196.
170. Muller, R.H., Mehnert, W., Lucks, J. S., Schwarz, C., Zur Muhlena, A., Meyhers, H., Freitas, C., Ruhl, D *Solid lipid nanoparticles (SLN): An alternative colloidal carrier system for controlled drug delivery*. *European Journal of Pharmaceutics and Biopharmaceutics*, 1995. 41(1): p. 62-69.
171. Schwarz, C. and W. Mehnert, *Solid lipis nanoparticle for controlled drug delivery II. drug incorporation and physicochemical characterization*. *Journal of Microencapsulation*, 1999. 16(2): p. 205-213.
172. Tabatta, K., Kneuerb, C., Sametic, M., Olbricha, C., Müllera, R. H., Lehr, C., Bakowsky, U *Transfection with different colloidal systems: comparison of solid lipid nanoparticles and liposomes*. *Journal of Controlled Release*, 2004. 97(2): p. 321-332.
173. Tabatta, K., Sameti, M., Olbrich, C., Müller, R. H., Lehr, C. M, *Effect of cationic lipid and matrix lipid composition on solid lipid nanoparticle-mediated gene transfer*. *European Journal of Pharmaceutics and Biopharmaceutics*, 2004. 57(2): p. 155-162.
174. Uner, M., *Preparation, characterization and physico-chemical properties of solid lipid nanoparticles (SLN) and nanostructured lipid carriers (NLC): their benefits as colloidal drug carrier systems*. *Pharmazie*, 2006. 61: p. 375-386.

175. Muller, R., H., Radtke, M., Wissing, S, A, *Solid lipid nanoparticles (SLN) and nanostructured lipid carriers (NLC) in cosmetic and dermatological preparations*. *Advanced Drug Delivery Review*, 2002. 54: p. S131-155.
176. Radtke, M., Muller, R, H, *Comparison of structural properties of solid lipid nanoparticles (SLN) versus other lipid particles*. *Proceed International Symposium Control Release Bioactive Materials*, 2000. 27: p. 309-210.
177. Müller, R.H., Mäder, K. , Gohla, S. , *Solid lipid nanoparticles (SLN) for controlled drug delivery - a review of the state of the art*. *European Journal of Pharmaceutics and Biopharmaceutics*, 2000a. 50(1): p. 161-177.
178. Müller, R.H., Mäder, K., Lippacher, A., Jennings, V. , *Solid-lipid (semi-solid) liquid particles and method of producing highly concentrated particles dispersions*. 2000b.
179. Olbrich, C., Gessner, A., Kayser, O., Müller, R, H, *Lipid-drug-conjugate (LDC) nanoparticles as novel carrier system for the hydrophilic antitrypanosomal drug diminazenediaceturate*. *Journal of Drug Targeting*, 2002. 10(5): p. 387-396.
180. Bakan, J.A. and A.F. Kydonieus, *Microencapsulation using coacervation/phase separation technique*, in *Controlled release technologies*, Anonymous, Editor. 1980, CRC PRESS: Boca Raton.
181. Carless, D.J. and J.E. Burgess, *Microelectrophoretic studies of gelatin and acacia for the prediction of complex coacervation*. *Journal of Colloid and Interface Science*, 1984. 98: p. 108.
182. Dervichian, D.G., *A comparative study of the flocculation and coacervation of different systems*. *Discussion of the Faraday Society*, 1954. 18: p. 231-239.
183. Dobbetti, L. and V. Pantaleo, *Application of a hydrodynamic model to microencapsulation by coacervation*. *Journal of Microencapsulation*, 2002. 19(2): p. 139-151.
184. Prokop, A., Hunkeler, D., DiMaris, S., Haralsom, M. A., Wang, T. G *Water soluble polymers for immunolisation I: complex coacervation and cytotoxicity*. *Advanced Polymer Science*, 1998. 136: p. 1-51.
185. Korus, J., Tomasik, P., Lii, C. Y. , *Microcapsules from starch granules*. *Journal of Microencapsulation*, 2003. 20(1): p. 47-56.
186. Lamprecht, A., Schäfer, U. F., Lehr, C, M, *Influences of process parameters on preparation of microparticle used as a carrier system for $\dot{U} - 3$ unsaturated fatty acid ethyl esters used in supplementary nutrition*. . *Journal of Microencapsulation* 2001. 18(3): p. 347-357.
187. Dubin, P.L., Muhoberac, B. B., Xia, J, *Preparation of Enzyme-Polyelectrolyte Coacervate Complexes and their Properties*. 1998.
188. Junyaprasret, M., et al., *Effect of Process Variables on the microencapsulation of vitamin and palmitate by gelatin acacia coacervation*. *Drug Delivery and Industrial Pharmacy*, 2001. 26(6): p. 561-566.
189. Strauss, G. and S.M. Gibson, *Plant phenolics as cross-linkers of gelatin gels and gelatin-based coacervates for use as food ingredients*. *Food Hydrocolloids*, 2004. 18: p. 81-89.
190. Yeo, Y., et al., *Complex coacervates for thermally sensitive controlled release of flavor compounds*. *Journal of Agriculture and Food Chemistry*, 2005. 53: p. 7518-7525.

191. Gouin, S., *Micro encapsulation industrial appraisal of existing technologies and trends*. Trends in Food Science and Technology, 2004. 15: p. 330-347.
192. Rabinow, B.E., *Nanosuspensions in drug delivery*. Nature Reviews, 2004. 3: p. 785-796.
193. Muller, R.H., C. Jacobs, and O. Kayser, *Nanosuspensions as particulate drug formulations in therapy: Rationale for development and what we can expect for the future*. Advanced Drug Delivery Reviews, 2001. 47: p. 3-19.
194. Liversidge, G.C. and K.C. Cundy, *Drug nanocrystals for improved drug delivery in*. Control Release Bioact, 1996. 23.
195. Liversidge, G., G., Cundy K, C, *Particle size reduction for improvement of oral bioavailability of hydrophobic drugs. I. Absolute oral bioavailability of nanocrystalline danazol in beagle dogs*. International Journal of Pharmaceuticals, 1995. 125: p. 91-97.
196. Merisko-Livresidge, E., L.G. G, and E.R. Cooper, *Nanosizing a formulations approach for poorly water soluble compounds*. European Journal of Pharmaceutical Sciences, 2003. 18: p. 113-120.
197. Sarkari, M., Brown, J., Chen, X. X., Swinnea, S., Williams, R. O., Johnston, K. P, *Enhanced drug dissolution using evaporative precipitation into aqueous solution*. International Journal of Pharmaceuticals, 2002. 243: p. 17-31.
198. Grau, M.J., O. Kayser, and R.H. Muller, *Nanosuspensions of poorly soluble drugs -- reproducibility of small scale production*. International Journal of Pharmaceutics, 2000. 196(2): p. 155-159.
199. Jia, L., et al., *Effect of nanonization on absorption of 301029: ex vivo and in vivo pharmacokinetic correlations determined by liquid chromatography/mass spectrometry*. Pharmaceutical Research 2002. 19(8): p. 1091-1096.
200. Spicer, P., *T Cubosomes: Bicontinuous Liquid Crystalline Nanoparticles*, in *Dekker Encyclopedia of Nanoscience and Nanotechnology*, C. Contescu, I., Putyera, K Editor. 2009, CRC Press. p. 1018–1028.
201. Borne, J., Naylander, T., Khan, A, *Effect of lipase on olein-based cubic phase dispersion (cubosomes) and vesicles*. Journal of Physical Chemistry B, 2002. 106(40): p. 10492–10500.
202. Sukhorukov, G.B., Rogach, A. L., Zebli, B., Liedl, T., Skirtach, A. G., Köhler, K., Antipov, A. A., Gaponik, N., Susha, A. S., Winterhalter, M., Parak, W. J, *Nanoengineered polymer capsules: tools for detection, controlled delivery and site-specific manipulation*. Small, 2005. 1(2): p. 194-200.
203. Biesalski, H.K., *Nutraceutical: The link between nutrition and medicine*. Journal of Toxicology, 2002. 2(1): p. 9-30.
204. Clemens, R. and J. Coughlin, *Coffee and Health: surprisingly good news*. Food Technology, 2007. 1(1): p. 17-17.
205. Mitchell E. A., A.M.G., Turbott S. H., Manku M., *Clinical characteristics and serum essential fatty acid levels in hyperactive children*. Journal of Clinical Pediatrics, 1987. 26: p. 406-411.
206. Burgess J. R, S.L., Zhang W., Peck L., *Long-chain polyunsaturated fatty acids in children with attention deficit hyperactivity disorder*. American Journal of Clinical Nutrition, 2000. 71: p. 327S-330S.

207. Murphy, D.J. and M.I. Underhill, *Omega-3 fatty acid in pregnant women and infants*. The American Chiropractor, 2007. 24(2).
208. Schacky V. C., A.P., Kothny W., Theisen K., Mudra H., *The effect of dietary omega-3 fatty acids on coronary atherosclerosis*. Annals of Internal Medicine, 1999. 130(7): p. 554-562.
209. Agus D. B., G.S.S., Pardridge W. M., Spielholz C., Baselga J., Vera J. C., Golde D. W., *Vitamin C crosses the blood brain barrier in the oxidized form through the glucose transporters*. Journal of Clinical Investigation, 1997. 100(11): p. 2842-2848.
210. Meydani, M., *Antioxidants in the prevention of chronic diseases*. Nutrition Clinical Care, 2002. 5(2): p. 47-49.
211. Evans, R.C., R.J. Miller, and G. Paganga, *Structure antioxidant activity relationships of flavonoids and phenolic acids*. Free Radical Biology Medicine, 1996. 20: p. 933-956.
212. Hertog, M.G.L., *Epidemiological evidences on potential health properties of flavonoids*. Proceeding of Nutrition Society, 1996. 55.
213. Richardson, D.P. and P.B. Ottaway, *Food Fortification*, in *The technology of vitamin in food*. 1993, Blackie Academic and Professional: Glasgow Scotland. p. 233-244.
214. Ottaway, P.B., *Stability of vitamin in food*, in *The technology of vitamins in foods*. 1993, Blackie Academic and Professional: Glasgow Scotland. p. 90-112.
215. Fennema, O.R., *Food Chemistry*, ed. Anonymous. 2004.
216. Xianquan, S., Shi, J, Kakuda, Y., Yueming, J, *Stability of lycopene during food processing and storage*. Journal of Medicinal Foods, 2005. 8(4): p. 413-422.
217. Heinonen, M., Haila, K., Lampi, A, M., Piironen, V, *Inhibition of oxidation in 10% oilin- water emulsions by beta-carotene with alpha- and gamma-tocopherols*. Journal of American Chemical Society, 1997. 74(9): p. 1047-1052.
218. Patrasa, A., Bruntona, N. P., O'Donnellb, C., Tiwari, B, K *Effect of thermal processing on anthocyanin stability in foods; mechanisms and kinetics of degradation* Trends in Food Science & Technology, 2010. 21(1): p. 3-11.
219. Sua, Y.L., Leunga, L. K., Huangb, Y., Chen, Z, *Stability of tea theaflavins and catechins* Food Chemistry, 2003. 83(2): p. 189-195.
220. Chan, H.W.S., *The mechanism of autoxidation*, in *In autoxidation of unsaturated lipids*, Anonymous, Editor. 1987, Academic Press: London, UK. p. 1-16.
221. Frankel, E., N, *Lipid Oxidation: Mechanisms, Products and Biological Significance*. Journal of the American Oil Chemists' Society, 1984. 61(12): p. 1908-1917.
222. Halliwell, B. and S. Chirico, *Lipid peroxidation: its mechanism, measurement, and significance*. The American Journal of Clinical Nutrition 1993. 57: p. 715S - 725S.
223. Droge, W., *Free Radicals in the Physiological Control of Cell Function*. Physiological Reviews, 2002. 82: p. 47-95.
224. Chen, C.C. and G. Wagner, *Vitamin E nanoparticle for beverage applications*. Chemical Engineering and Research Design, 2004. 82(A11): p. 1432-1437.

225. Gomes D. C. F., A.L.V., Leon L. I., de Lima M. E. F, *Total synthesis and anti-leishmanial activity of some curcumin analogues*. *Arzneim-Forsch*, 2002. 52: p. 695-698.
226. Vijayakumar, G.R. and S. Divakar, *Synthesis of guaiacol-alpha-D-glucoside and curcumin-bis-alpha-D-glucoside by an amyloglucosidase from Rhizopus*. *Biotechnology Letter*, 2005. 27: p. 1411-1415.
227. Blot, W.J., W.H. Chow, and J.K. McLaughlin, *Tea and cancer: a review of the epidemiological evidence*. *European Journal of Cancer Prevention*, 1996. 5: p. 425-438.
228. Kohlmeier, L., et al., *Tea and cancer prevention an evaluation of epidemiological literature*. *Journal of Nutrition Cancer*, 1997. 27: p. 1-13.
229. Gomes, D.C.F., et al., *Total synthesis and anti-leishmanial activity of some curcumin analogues*. *Arzneim-Forsch*, 2002. 52: p. 695-698.
230. Olthof, M.R., et al., *Bioavailabilities of quercetin-3-glucoside and quercetin-4-glucoside do not differ in humans*. *American Society of Nutritional Sciences*, 2000: p. 1200-1203.
231. Xu, J.Z., et al., *Comparison of antioxidant activity and bioavailability of tea epicatechins with their epimers*. *British Journal of Nutrition*, 2004. 91: p. 873-881.
232. Lee, M., J., Maliakal, ., Chen, L., Meng, X., Bondoc, F, Y., Prabhu, S., Lambert, G., Mohr, S., Yang, C, S, *Pharmacokinetics of tea catechins after ingestion of green tea and (-)-epigallocatechin-3-gallate by humans: formation of different metabolites and individual variability*. *Cancer Epidemiology Biomarkers Prevention*, 2002. 11(1): p. 1025-1032.
233. Hix, L.M., S.F. Lockwood, and J.S. Bertram, *Bioactive carotenoids: potent antioxidants and regulators of gene expression*. *Redox Reports*, 2004. 9(4): p. 181-191.
234. Fielding, J., M., Li, D., Stockmann, R., Sinclair, A, J, *The effect of different plant oils used in preparing tomato sauces on plasma concentrations of lycopene and oxidative status: a dietary intervention study*. *Asia Pacific Journal of Clinical Nutrition*, 2004. 13(S49): p. 1-5.
235. Bryant, J., D., McCord, J, D., Unlu, L, K., Erdman, J, W., *The isolation and partial characterization of alpha and beta-carotene carotenoprotein(s) from carrot (*Dacus carota L*) root chromoplasts*. *Journal of Agricultural and Food Chemistry*, 1992. 40: p. 545-549.
236. Kuhlbrandt, W., Wang, D, N., Fujiyoshi, Y, *Atomic model of plant light-harvesting complex by electron crystallography*. *Nature*, 1994. 367: p. 614-621.
237. Zhou, J., R., Gugger, E, T., Erdman, J, W *The crystalline form of carotenes and the food matrix in carrot root decrease the relative bioavailability of beta- and alpha-carotene in the ferret model*. *Journal of the American College of Nutrition*, 1996. 15: p. 84-91.
238. Lichtenstein, A.H., Jones, P. J *Lipids: absorption and transport*, in *Present Knowledge in Nutrition. Present Knowledge in Nutrition*, B.A. Bowman and R.M. Russel, Editors. 2001, ILSI Press, International Life Sciences Institute, Washington, D. C. p. 93-103.

239. Donovan, J.L., et al., *Catechin is metabolized by both the small intestine and liver of rats*. American Society for Nutritional Sciences, 2001. 131: p. 1753-1757.
240. Manach, C., et al., *Polyphenols: food sources and bioavailability*. American Journal of Clinical Nutrition, 2004(79): p. 5-727.
241. Petri, N., et al., *Absorption/Metabolism of sulforaphane and quercetin and regulation of phase II enzymes in human jejunum in vivo*. Drug Metabolism and Disposition, 2003. 31(6): p. 805-813.
242. Walle, U.K., et al., *High absorption but very low bioavailability of oral resveratrol in humans*. Drug Metabolism and Disposition, 2004. 32(12): p. 1377-1382.
243. Weiss, J., P. Takhistov, and J. McClements, *Functional materials in food nanotechnology*. Journal of Food Science, 2006. 71(9): p. 107-116.
244. Yokoyama, M., et al., *Characterization and anticancer activity of micelle-forming polymeric anticancer drug adriamycin-conjugated poly(ethylene glycol)-poly(aspartic acid) block copolymer*. Cancer Research, 1990. 50: p. 1693-1970.
245. Yokoyama, M., et al., *Toxicity and antitumor activity against solid tumors of micelle-forming polymeric anticancer drug and its extremely long circulation in blood*. Cancer Research, 1991. 51: p. 3229-3236.
246. Kwon, G.S., et al., *Physical entrapment of adriamycin in AB block copolymer micelles*. Pharmaceutical Research, 1995. 12(2): p. 192-195.
247. Peracchia, M.T., et al., *PEG-coated nanospheres from amphiphilic diblock and multiblock copolymers: investigation of their drug encapsulation and release characteristics*. Journal of Controlled Release, 1997. 46: p. 223-231.
248. Trotta Michele, G.M., Carlotti Maria Eugenia, Morel Silvia, *Preparation of griseofulvin nanoparticles from water-dilutable microemulsions*. International Journal of Pharmaceutics, 2003. 254(2): p. 235-242.
249. Brunner, E., *Theorie der Reaktionsgeschwindigkeit in heterogenen systemen*. Z. Phys. Chem, 1904. 47: p. 56-102.
250. Nernst, W., *Theorie der Reaktionsgeschwindigkeit in heterogenen Systemen*. Z. Phys. Chem, 1904. 47: p. 52-55.
251. Noyes, A.A. and W.R. Whitney, *The rate of solution of solid substances in their own solutions*. Journal of the American Chemical Society, 1897. 19(12): p. 930-934.
252. Kocbek, P., S. Baumgartner, and J. Kristl, *Preparation and evaluation of nanosuspensions for enhancing the dissolution of poorly soluble drugs*. International Journal of Pharmaceutics, 2006. 312(1-2): p. 179-186.
253. Wu, W. and G.H. Nancollas, *A New Understanding of the Relationship Between Solubility and Particle Size*. Journal of Solution Chemistry, 1998. 27(6): p. 521-531.
254. Godec, A., M. Gaberšček, and J. Jamnik, *Comment on the Article "A New Understanding of the Relationship between Solubility and Particle Size" by W. Wu and G.H. Nancollas*. Journal of Solution Chemistry, 2009. 38(1): p. 135-146.
255. Kipp, J.E., *The role of solid nanoparticle technology in the parenteral delivery of poorly water-soluble drugs*. International Journal of Pharmaceutics, 2004. 284(1-2): p. 109-122.

256. Müller, R.H. and C.M. Keck, *Challenges and solutions for the delivery of biotech drugs* "a review of drug nanocrystal technology and lipid nanoparticles. *Journal of Biotechnology*, 2004. 113(1-3): p. 151-170.
257. Patravale, V.B., A.A. Date, and R.M. Kulkarni, *Nanosuspensions: a promising drug delivery strategy*. *Journal of Pharmacy and Pharmacology*, 2004. 56(7): p. 827-840.
258. Jinno, J.-i., et al., *Effect of particle size reduction on dissolution and oral absorption of a poorly water-soluble drug, cilostazol, in beagle dogs*. *Journal of Controlled Release*, 2006. 111(1-2): p. 56-64.
259. Nicolas, A., B. Jean-Pierre, and S. Patrick, *Design and production of nanoparticles formulated from nano-emulsion templates-A review*. *Journal of Controlled Release*, 2008. 128(3): p. 185-199.
260. Acosta, E., *Bioavailability of nanoparticles in nutrient and nutraceutical delivery*. *Current Opinion in Colloid & Interface Science*, 2009. 14(1): p. 3-15.
261. Krishnaiah, Y.S.R., *Pharmaceutical Technologies for Enhancing Oral Bioavailability of Poorly Soluble Drugs*. *Journal of Bioequivalence and Bioavailability*, 2010. 2(2): p. 28-36.
262. Hancock, B.C. and M. Parks, *What is the True Solubility Advantage for Amorphous Pharmaceuticals?* *Pharmaceutical Research*, 2000. 17(4): p. 397-404.
263. Niebergall, P.J., G. Milosovich, and J.E. Goyan, *Dissolution rate studies II. Dissolution of particles under conditions of rapid agitation*. *Journal of Pharmaceutical Sciences*, 1963. 52(3): p. 236-241.
264. Bisrat, M. and C. Nyström, *Physicochemical aspects of drug release. VIII. The relation between particle size and surface specific dissolution rate in agitated suspensions*. *International Journal of Pharmaceutics*, 1988. 47(1-3): p. 223-231.
265. Mosharraf, M. and C. Nyström, *The effect of particle size and shape on the surface specific dissolution rate of micro-sized practically insoluble drugs*. *International Journal of Pharmaceutics*, 1995. 122(1-2): p. 35-47.
266. Panyam, J. and V. Labhasetwar, *Biodegradable nanoparticles for drug and gene delivery to cells and tissue*. *Advanced Drug Delivery Reviews*, 2003. 55: p. 329-347.
267. Mbela, T.K.M., J.H. Poupaert, and P. Dumont, *Poly(diethylmethylenedimaleonate) nanoparticles as primaquine delivery system to liver*. *International Journal of Pharmaceutics*, 1992. 79(1-3): p. 29-38.
268. Kreuter, J., *Nanoparticulate systems for brain delivery of drugs*. *Advanced Drug Delivery Reviews*, 2001. 47: p. 65-81.
269. Moghimi, S.M., J.C. Murray, and A.C. Hunter, *Long-circulating and target specific nanoparticles: theory to practice*. *Pharmacological reviews*, 2001. 53(2): p. 283-318.
270. Lockman, P.R., et al., *Nanoparticle technology for drug delivery across the blood brain barrier*. *Drug Development and Industrial Pharmacy*, 2002. 28(1): p. 1-13.
271. Couvreur, P. and C. Vauthier, *Nanotechnology: Intelligent Design to Treat Complex Disease*. *Pharmaceutical Research*, 2006. 23(7): p. 1417-1450.
272. Davda, J. and V. Labhasetwar, *Characterization of nanoparticle uptake by endothelial cells*. *International Journal of Pharmaceutics*, 2002. 233: p. 51-59.

273. Florence, A.T. and N. Hussain, *Transcytosis of nanoparticle and dendrimer delivery systems: evolving vistas*. *Advanced Drug Delivery Reviews*, 2001. 50: p. S69-S89.
274. Lambert, G., E. Fattal, and P. Couvreur, *Nanoparticulate systems for the delivery of antisense oligonucleotides*. *Advanced Drug Delivery Reviews*, 2001. 47: p. 99-112.
275. Mundargi, R., C., Babu, V. R., Rangaswamy, V., Patel, P., Aminabhavi. T, M *Nano/micro technologies for delivering macromolecular therapeutics using poly(D,L-lactide-co-glycolide) and its derivatives*. *Journal of Control Release*, 2008. 125: p. 193-209.
276. Davis, S.S., *Biomedical applications of nanotechnology - implications for drug targeting and gene therapy*. *Trends in biotechnology*, 1997. 15(6): p. 217-224.
277. Kreuter, J., *Drug targeting with nanoparticles*. *European Journal of Drug Metabolism and Pharmacokinetics*, 1994. 19(3): p. 253-256.
278. Gaur, U., Sahoo, S. K., De, T. K., Ghosh, P.C., Maitra, A. N., Ghosh, P. K, *Bio-distribution of fluoresceinated dextran using novel nanoparticles evading reticuloendothelial system*. *International Journal of Pharmaceutics*, 2000. 202(1-2): p. 1-10.
279. Allemann, E., R. Gurny, and E. Doelker, *Drug-loaded nanoparticles preparation method and drug targeting tissues*. *European Journal of Pharmaceuticas and Biopharmaceutics*, 1993. 39(5): p. 173-191.
280. Roberts, M.J., M.D. Bentley, and J.M. Harris, *Chemistry of peptide and protein PEGylation*. *Advanced Drug Delivery Reviews*, 2002. 54: p. 459-476.
281. Douglas, S.J., Davis, S. S., Illum, L, *Nanoparticles in drug delivery*. *Critical Review In Therapeutic Drug Carrier System* 1987. 3(3): p. 233-261.
282. Lacava, L.M., Lacava, Z. G., Da Silva, M. F ., Silva, O ., Chaves, S. B., Azevedo, R. B ., Pelegrini, F., Gansau, C ., Buske, N., Sabolovic, D ., Morais, P. C *Magnetic resonance of a dextran-coated magnetic fluid intravenously administered in mice*. *Biophysics Journal*, 2001. 80(5): p. 2483–2486. .
283. Brannon-Peppas, L. and J.O. Blanchette, *Nanoparticle and targeted systems for cancer therapy*. *Advanced Drug Delivery Reviews*, 2004. 56: p. 1649-1659.
284. Hou, D.Z., et al., *The production and characteristics of solid lipid nanoparticles (SLNs)*. *Biomaterials*, 2003. 24: p. 1781-1785.
285. Gupta, A.K., et al., *Ketorolac entrapped in polymeric micelles: preparation, characterization and ocular anti-inflammatory studies*. *International Journal of Pharmaceutics*, 2000. 209: p. 1-14.
286. Pignatello, R., et al., *Flurbiprofen-loaded acrylate polymer nanosuspensions for ophthalmic application*. *Biomaterials*, 2002. 23: p. 3247-3255.
287. Chen, H., J. Weiss, and F. Shahidi, *Nanotechnology in nutraceuticals and functional foods*. *Food Technology*, 2006: p. 30-36.
288. Varin, R.A., et al., *Fracture toughness of intermetallic compacts consolidated from nanocrystalline powders*. *Materials Science and Engineering: A*, 2001. 300(1–2): p. 1-11.
289. Kim, Y.D., et al., *Formation of nanocrystalline Fe–Co powders produced by mechanical alloying*. *Materials Science and Engineering: A*, 2000. 291(1–2): p. 17-21.

290. Claudio L. De Castro and B.S. Mitchell, *Nanoparticles from Mechanical Attrition*, in *Synthesis, functionalization and surface treatment of nanoparticles*, M.-I. Baraton, Editor. 2002, American Scientific Publishers: Los Angeles. p. 1-16.
291. S. Buchmann, et al. *Aqueous microsuspension, an alternative intravenous formulation for animal studies*. in *42 nd Annual Congress of the International Association for Pharmaceutical Technology (APV)*. 1996. Mainz.
292. Nielsen, K. and T. Malvik, *Grindability enhancement by blast-induced microcracks*. Powder Technology, 1999. 105(1-3): p. 52-56.
293. Skelton, R., A.N. Khayyat, and R.G. Temple, *Fluid energy milling. An investigation of micronizer performance*, in *Fine Particles Processing P*. Somasundaran, Editor. 1980, Society for Mining Metallurgy. p. 113-125.
294. Keck, C.M. and R.H. Müller, *Drug nanocrystals of poorly soluble drugs produced by high pressure homogenisation*. European Journal of Pharmaceutics and Biopharmaceutics, 2006. 62(1): p. 3-16.
295. B. Klinksiek and B. Koglin, in *Technik der mehrphasigen Strömungen nichtmischbarer fluider Phasen - Schäume, Emulsionen, CVC*, Editor. 1992, Köln: Vortrags- und Diskussionstagung.
296. Okuyama, K. and I. Wuled Lenggoro, *Preparation of nanoparticles via spray route*. Chemical Engineering Science, 2003. 58(3-6): p. 537-547.
297. Hu, J., et al., *Improvement of Dissolution Rates of Poorly Water Soluble APIs Using Novel Spray Freezing into Liquid Technology*. Pharmaceutical Research, 2002. 19(9): p. 1278-1284.
298. Dixon, D.J., K.P. Johnston, and R.A. Bodmeier, *Polymeric materials formed by precipitation with a compressed fluid antisolvent*. AIChE Journal, 1993. 39(1): p. 127-139.
299. Reverchon, E. and G. Della Porta, *Production of antibiotic micro- and nanoparticles by supercritical antisolvent precipitation*. Powder Technology, 1999. 106(1-2): p. 23-29.
300. Chattopadhyay, P. and R.B. Gupta, *Protein nanoparticles formation by supercritical antisolvent with enhanced mass transfer*. AIChE Journal, 2002. 48(2): p. 235-244.
301. Türk, M., et al., *Micronization of pharmaceutical substances by the Rapid Expansion of Supercritical Solutions (RESS): a promising method to improve bioavailability of poorly soluble pharmaceutical agents*. The Journal of Supercritical Fluids, 2002. 22(1): p. 75-84.
302. Briggs A. R. and M.T. J., *Process for Preparing Powder Blends*. 1973: U.S. Patent 3721725.
303. Adams T. H., Beck J. P., and M.R. C., *Novel Particulate Compositions*. 1982: U.S. Patent 4323478.
304. Lilakos, L., *Method and Apparatus for Cryogenic Crystallization of Fats*. 1990: U.S. Patent 4952224.
305. Hebert P. F. and H.M. S., *Production Scale Method of Forming Microparticles*. 1999: U.S. Patent 5922253.
306. Gombotz W. R., Healy H. S., and B.L. R., *Very Low Temperature Casting of Controlled Release Microspheres* 1991: U.S. Patent 5019400.

307. Young, T.J., et al., *Encapsulation of lysozyme in a biodegradable polymer by precipitation with a vapor-over-liquid antisolvent*. Journal of Pharmaceutical Sciences, 1999. 88(6): p. 640-650.
308. Young, T.J., et al., *Rapid Expansion from Supercritical to Aqueous Solution to Produce Submicron Suspensions of Water-Insoluble Drugs*. Biotechnology Progress, 2000. 16(3): p. 402-407.
309. L. Bayvel and Z. Orzechowski, *Liquid atomization*. 1993, Washington, DC: Taylor & Francis.
310. Österholm, J.E., et al., *Emulsion polymerization of aniline*. Synthetic Metals, 1993. 55(2-3): p. 1034-1039.
311. Kinlen, P.J., et al., *Emulsion Polymerization Process for Organically Soluble and Electrically Conducting Polyaniline*. Macromolecules, 1998. 31(6): p. 1735-1744.
312. Palaniappan, S. and A. John, *Polyaniline materials by emulsion polymerization pathway*. Progress in Polymer Science, 2008. 33(7): p. 732-758.
313. zur Muhlen, A., C. Schwarz, and W. Mehnert, *Solid lipid nanoparticles (SLN) for controlled drug delivery - Drug release and release mechanism*. European Journal of Pharmaceutics and Biopharmaceutics, 1998. 45(2): p. 149-155.
314. R.H. Müller, et al., *Solid lipid nanoparticles (SLN)—an alternative colloidal carrier system for controlled drug delivery*. Eur. J. Pharm. Biopharm, 1995. 41: p. 62-69.
315. Muller, R.H., K. Menher, and S. Gohla, *Solid lipid nanoparticles (SLN) for controlled drug delivery - a review of the state of the art*. European Journal of Pharmaceutics and Biopharmaceutics, 2000. 50(1): p. 161-177.
316. Mehnert, W. and K. Mäder, *Solid lipid nanoparticles: Production, characterization and applications*. Advanced Drug Delivery Reviews, 2001. 47(2-3): p. 165-196.
317. zur Mühlen, A., C. Schwarz, and W. Mehnert, *Solid lipid nanoparticles (SLN) for controlled drug delivery – Drug release and release mechanism*. European Journal of Pharmaceutics and Biopharmaceutics, 1998. 45(2): p. 149-155.
318. Mehnert, W. and K. Mader, *Solid lipid nanoparticles: Production, characterization and applications*. Advanced Drug Delivery Reviews, 2001. 47(2-3): p. 165-196.
319. Bodmeier, R. and J.W. McGinity, *Solvent selection in the preparation of poly(DL-lactide) microspheres prepared by the solvent evaporation method*. International Journal of Pharmaceutics, 1988. 43(1-2): p. 179-186.
320. Sah, H., *Microencapsulation techniques using ethyl acetate as a dispersed solvent: effects of its extraction rate on the characteristics of PLGA microspheres*. Journal of Controlled Release, 1997. 47(3): p. 233-245.
321. Birnbaum, D.T., et al., *Controlled release of β -estradiol from PLGA microparticles: The effect of organic phase solvent on encapsulation and release*. Journal of Controlled Release, 2000. 65(3): p. 375-387.
322. Sah, H., *Ethyl formate — alternative dispersed solvent useful in preparing PLGA microspheres*. International Journal of Pharmaceutics, 2000. 195(1-2): p. 103-113.

323. Trotta, M., et al., *Emulsions containing partially water-miscible solvents for the preparation of drug nanosuspensions*. Journal of Controlled Release, 2001. 76(1-2): p. 119-128.
324. Van Arnum, S.D., *Vitamin A*, in *Kirk-Othmer Encyclopedia of Chemical Technology*. 2000, John Wiley & Sons, Inc.
325. Chug-Ahuja, J.K., et al., *The development and application of a carotenoid database for fruits, vegetables, and selected multicomponent foods*. Journal of the American Dietetic Association, 1993. 93(3): p. 318-323.
326. Mangels, A.R., et al., *Carotenoid content of fruits and vegetables: An evaluation of analytic data*. Journal of the American Dietetic Association, 1993. 93(3): p. 284-296.
327. Block, G., *Nutrient Sources of Provitamin A Carotenoids in the American Diet*. American Journal of Epidemiology, 1994. 139(3): p. 290-293.
328. Gebhardt, S., et al., *USDA National Nutrient Database for Standard Reference, Release 22*, USDA, Editor. 2009.
329. Alfred Sommer, et al., *Vitamin A deficiency, health, survival, and vision*. 1996, New York: Oxford Press
330. Bauernfeind, J.C., *Vitamin A deficiency and its control*. 1986, Orlando: Academic Press.
331. Peto R., D.R., Buckley J. D., Sporn M. B., *Can dietary beta-carotene materially reduce human cancer rates?* Nature, 1981. 290(5803): p. 201-208.
332. Serge Hercberg, P.G., Paul Preziosi, Sandrine Bertrais, Louise Mennen, Denis Malvy, Anne-Marie Roussel, Alain Favier, Serge Briançon, *The SU.VI.MAX Study: A Randomized, Placebo-Controlled Trial of the Health Effects of Antioxidant Vitamins and Minerals* Archives of Internal Medicine, 2004. 164(21): p. 2335-2342.
333. Gerster, H., *Anticarcinogenic effect of common carotenoids*. International Journal for Vitamin and Nutrition Research, 1993. 63(2): p. 93-121.
334. Peto, R., et al., *Can dietary beta-carotene materially reduce human cancer rates?* Nature, 1981. 290(5803): p. 201-208.
335. Giovannucci, E., *Tomatoes, Tomato-Based Products, Lycopene, and Cancer: Review of the Epidemiologic Literature*. Journal of the National Cancer Institute, 1999. 91(4): p. 317-331.
336. Temple, N.J. and T.K. Basu, *Does beta-carotene prevent cancer? A critical appraisal*. Nutrition Research, 1988. 8(6): p. 685-701.
337. Kritchevsky, S.B., *β -Carotene, Carotenoids and the Prevention of Coronary Heart Disease*. The Journal of Nutrition, 1999. 129(1): p. 5-8.
338. Agarwal, S. and A.V. Rao, *Carotenoids and chronic diseases*. Drug metabolism and drug interactions, 2000. 17(1-4): p. 189-210.
339. Paiva, S.A.R. and R.M. Russell, *β -Carotene and Other Carotenoids as Antioxidants*. Journal of the American College of Nutrition, 1999. 18(5): p. 426-433.
340. Riondel J, et al., *The effect of a water-dispersible beta-carotene formulation on the prevention of age-related lymphoid neoplasms in mice*. anticancer research, 2002. 22(2A): p. 883-888.

341. Ames, B.N., M.K. Shigenaga, and T.M. Hagen, *Oxidants, antioxidants, and the degenerative diseases of aging*. Proceedings of the National Academy of Sciences, 1993. 90(17): p. 7915-7922.
342. Rona, C. and E. Berardesca, *Aging skin and food supplements: the myth and the truth*. Clinics in Dermatology, 2008. 26(6): p. 641-647.
343. Epler, K.S., R.G. Ziegler, and N.E. Craft, *Liquid chromatographic method for the determination of carotenoids, retinoids and tocopherols in human serum and in food*. Journal of Chromatography B: Biomedical Sciences and Applications, 1993. 619(1): p. 37-48.
344. Epler, K.S., et al., *Evaluation of reversed-phase liquid chromatographic columns for recovery and selectivity of selected carotenoids*. Journal of Chromatography A, 1992. 595(1-2): p. 89-101.
345. Drewnowski, A., et al., *Serum beta-carotene and vitamin C as biomarkers of vegetable and fruit intakes in a community-based sample of French adults*. The American Journal of Clinical Nutrition, 1997. 65(6): p. 1796-1802.
346. Stryker, W.S., et al., *The relation of diet, cigarette smoking, and alcohol consumption to plasma beta-carotene and alpha-tocopherol levels*. American Journal of Epidemiology, 1988. 127(2): p. 283-296.
347. Burton G. W. and I.K. U., *beta-Carotene: an unusual type of lipid antioxidant*. Science, 1984. 224: p. 569-573.
348. Canfield, L.M., J.W. Forage, and J.G. Valenzuela, *Carotenoids as Cellular Antioxidants*. Proceedings of the Society for Experimental Biology and Medicine. Society for Experimental Biology and Medicine (New York, N.Y.), 1992. 200(2): p. 260-265.
349. Bertram, J. and H. Bortkiewicz, *Dietary carotenoids inhibit neoplastic transformation and modulate gene expression in mouse and human cells*. The American Journal of Clinical Nutrition, 1995. 62(6): p. 1327S-1336S.
350. Bendich, A., *beta-Carotene and the Immune Response* Proceedings of the Nutrition Society, 1991. 50: p. 263-274.
351. Burri, B.J., *Beta-carotene and human health: A review of current research*. Nutrition Research, 1997. 17(3): p. 547-580.
352. Chichili, G.R., et al., *beta-Carotene Conversion into Vitamin A in Human Retinal Pigment Epithelial Cells*. Investigative Ophthalmology & Visual Science, 2005. 46(10): p. 3562-3569.
353. Biesalski, H.K., et al., *Conversion of beta-Carotene to Retinal Pigment*, in *Vitamins & Hormones*, L. Gerald, Editor. 2007, Academic Press. p. 117-130.
354. Olson, J.A., *Provitamin A Function of Carotenoids: The Conversion of beta-Carotene into Vitamin A*. The Journal of Nutrition, 1989. 119(1): p. 105-108.
355. Canfield L.M., Forage J.W., and V. J.G., *Carotenoids as cellular antioxidants*. Proceedings of the Society for Experimental Biology and Medicine, 1992. 200(2): p. 260-265.
356. Ichikawa, F., et al., *The Effects of Lipoxigenase Products on Progesterone and Prostaglandin Production by Human Corpora Lutea*. Journal of Clinical Endocrinology & Metabolism, 1990. 70(4): p. 849-855.
357. Kazuyo Sato, et al., *Effect of the Interaction Between Lipoxigenase Pathway and Progesterone on the Regulation of Hydroxysteroid 11-Beta Dehydrogenase 2 in*

- Cultured Human Term Placental Trophoblasts* Biology of Reproduction, 2008. 78(3): p. 514-520.
358. Moreno, F.S., et al., *Effect of β -carotene on the expression of 3-hydroxy-3-methylglutaryl coenzyme A reductase in rat liver*. Cancer Letters, 1995. 96(2): p. 201-208.
359. Farmer, J.A., *Aggressive lipid therapy in the statin era*. Progress in Cardiovascular Diseases, 1998. 41(2): p. 71-94.
360. Zhang, L.-X., R.V. Cooney, and J.S. Bertram, *Carotenoids Up-Regulate Connexin43 Gene Expression Independent of Their Provitamin A or Antioxidant Properties*. Cancer Research, 1992. 52(20): p. 5707-5712.
361. Frommel, T.O., H. Lietz, and S. Mobarhan, *Expression of mRNA for the gap-junctional protein connexin43 in human colonic tissue is variable in response to β -carotene supplementation*. Nutrition and Cancer, 1994. 22(3): p. 257-265.
362. Zhang, L.-X., R.V. Cooney, and J.S. Bertram, *Carotenoids enhance gap junctional communication and inhibit lipid peroxidation in C3H/10T1/2 cells: relationship to their cancer chemopreventive action*. Carcinogenesis, 1991. 12(11): p. 2109-2114.
363. Britz-Cunningham, S.H., et al., *Mutations of the Connexin43 Gap-Junction Gene in Patients with Heart Malformations and Defects of Laterality*. New England Journal of Medicine, 1995. 332(20): p. 1323-1330.
364. Jiang, X.-y., et al., *Differential expression of connexin 43 in human autoimmune thyroid disease*. Acta Histochemica, 2010. 112(3): p. 278-283.
365. Allard, J., et al., *Effects of beta-carotene supplementation on lipid peroxidation in humans*. The American Journal of Clinical Nutrition, 1994. 59(4): p. 884-890.
366. Jialal, I., et al., *β -Carotene inhibits the oxidative modification of low-density lipoprotein*. Biochimica et Biophysica Acta (BBA) - Lipids and Lipid Metabolism, 1991. 1086(1): p. 134-138.
367. Sies, H. and W. Stahl, *Vitamins E and C, beta-carotene, and other carotenoids as antioxidants*. The American Journal of Clinical Nutrition, 1995. 62(6): p. 1315S-1321S.
368. Dixon, Z.R., et al., *Effects of a carotene-deficient diet on measures of oxidative susceptibility and superoxide dismutase activity in adult women*. Free Radical Biology and Medicine, 1994. 17(6): p. 537-544.
369. Prabhala, R.H., et al., *The effects of 13-cis-retinoic acid and beta-carotene on cellular immunity in humans*. Cancer, 1991. 67(6): p. 1556-1560.
370. Chew, B.P., *Role of Carotenoids in the Immune Response*. Journal of Dairy Science, 1993. 76(9): p. 2804-2811.
371. Bendich, A. and S.S. Shapiro, *Effect of beta-carotene and canthaxanthin on the immune responses of the rat*. The Journal of Nutrition, 1986. 116(11): p. 2254-62.
372. Burri, B.J., *Serum thyroid hormone concentrations may increase during carotenoid depletion of healthy adult women*. Journal of Nutritional Biochemistry, 1995. 6(11): p. 613-617.
373. Hemken, R.W. and D.H. Bremel, *Possible Role of Beta-Carotene in Improving Fertility in Dairy Cattle*. Journal of Dairy Science, 1982. 65(7): p. 1069-1073.
374. Aréchiga, C.F., et al., *Effect of injection of β -carotene or vitamin E and selenium on fertility of lactating dairy cows*. Theriogenology, 1998. 50(1): p. 65-76.

375. Folman, Y., et al., *Adverse Effect of β -Carotene in Diet on Fertility of Dairy Cows*. Journal of Dairy Science, 1987. 70(2): p. 357-366.
376. Diane Feskanich, et al., *Vitamin A Intake and Hip Fractures Among Postmenopausal Women* The journal of the American Medical Association, 2002. 287(1): p. 47-54.
377. Albanes, D., et al., *α -Tocopherol and β -Carotene Supplements and Lung Cancer Incidence in the Alpha-Tocopherol, Beta-Carotene Cancer Prevention Study: Effects of Base-line Characteristics and Study Compliance*. Journal of the National Cancer Institute, 1996. 88(21): p. 1560-1570.
378. *Beta Carotene, Vitamin E, and Lung Cancer*. New England Journal of Medicine, 1994. 331(9): p. 611-614.
379. Omenn, G.S., et al., *Effects of a Combination of Beta Carotene and Vitamin A on Lung Cancer and Cardiovascular Disease*. New England Journal of Medicine, 1996. 334(18): p. 1150-1155.
380. Werler, M.M., et al., *Maternal vitamin A supplementation in relation to selected birth defects*. Teratology, 1990. 42(5): p. 497-503.
381. WHO, *WHO. Global prevalence of vitamin A deficiency in populations at risk 1995–2005. WHO Global Database on Vitamin A Deficiency*. 2009: Geneva.
382. Underwood, B.A., *Vitamin A Deficiency Disorders: International Efforts to Control A Preventable "Pox"*. The Journal of Nutrition, 2004. 134(1): p. 231S-236S.
383. Tielsch, J.M. and A. Sommer, *The Epidemiology of Vitamin A Deficiency and Xerophthalmia*. Annual Review of Nutrition, 1984. 4(1): p. 183-205.
384. Burton, G.W., *Antioxidant Action of Carotenoids*. The Journal of Nutrition, 1989. 119(1): p. 109-111.
385. Lewis, R.J., Sr, *Hawley's Condensed Chemical Dictionary* 12th ed. 1993, New York: Van Nostrand Reinhold Co.
386. Opdyke, D.L.J., *Monographs on fragrance raw materials*. Food and Cosmetics Toxicology, 1975. 13(4): p. 449-457.
387. Grant, J., *Hackh's chemical dictionary*. 4th ed. 1972, New York, NY: McGraw-Hill Book Co.
388. M.Z. Fiume and C.I.R.E. Panel, *Final report on the safety assessment of triacetin*. International Journal of Toxicology 2003. 22(Suppl 2): p. 1-10
389. FDA, *Certain glycerides; affirmation of GRAS status. Final rule*. 1983, Fed Register 54:7401-7404.
390. FDA, *Frequency of use of cosmetic ingredients. FDA database*. 1998, FDA.: Washington, DC:.
391. Wright, J., *Creating and Formulating Flavours, in Food Flavour Technology*. 2010, Wiley-Blackwell. p. 1-23.
392. Jacob Shapira, et al., *Current Research On Regenerative Systems, in Eleventh Annual Meeting, C.O.S. Research, Editor*. 1968, NASA: Tokyo.
393. Lynch, J.W. and J.W. Bailey, *Dietary Intake of the Short-Chain Triglyceride Triacetin vs. Long-Chain Triglycerides Decreases Adipocyte Diameter and Fat Deposition in Rats*. The Journal of Nutrition, 1995. 125(5): p. 1267-1273.

394. Bailey, J., J. Miles, and M. Haymond, *Effect of parenteral administration of short-chain triglycerides on leucine metabolism*. The American Journal of Clinical Nutrition, 1993. 58(6): p. 912-916.
395. Mathew, R., et al., *Progress toward Acetate Supplementation Therapy for Canavan Disease: Glyceryl Triacetate Administration Increases Acetate, but Not N-Acetylaspartate, Levels in Brain*. Journal of Pharmacology and Experimental Therapeutics, 2005. 315(1): p. 297-303.
396. Shinoda, K. and H. Takeda, *The effect of added salts in water on the hydrophile-lipophile balance of nonionic surfactants: The effect of added salts on the phase inversion temperature of emulsions*. Journal of Colloid and Interface Science, 1970. 32(4): p. 642-646.
397. Vander Kloet, J. and L. Schramm, *The effect of shear and oil/water ratio on the required hydrophile-lipophile balance for emulsification*. Journal of Surfactants and Detergents, 2002. 5(1): p. 19-24.
398. Shinoda, K. and H. Arai, *The Correlation between Phase Inversion Temperature In Emulsion and Cloud Point in Solution of Nonionic Emulsifier*. The Journal of Physical Chemistry, 1964. 68(12): p. 3485-3490.
399. Shinoda, K. and H. Arai, *Solubility of nonionic surface-active agents in hydrocarbons*. Journal of Colloid Science, 1965. 20(1): p. 93-97.
400. Rydhag, L. and I. Wilton, *The function of phospholipids of soybean lecithin in emulsions*. Journal of the American Oil Chemists' Society, 1981. 58(8): p. 830-837.
401. van Nieuwenhuyzen, W., *Lecithin and Other Phospholipids*, in *Surfactants from Renewable Resources*, John Wiley & Sons, Ltd. p. 191-212.
402. Bueschelberger, H.-G., *Lecithins*, in *Emulsifiers in Food Technology*. 2007, Blackwell Publishing Ltd. p. 1-39.
403. van Nieuwenhuyzen, W. and M.C. Tomás, *Update on vegetable lecithin and phospholipid technologies*. European Journal of Lipid Science and Technology, 2008. 110(5): p. 472-486.
404. Gottlieb, M.H. and E.D. Eanes, *Influence of Electrolytes on the Thicknesses of the Phospholipid Bilayers of Lamellar Lecithin Mesophases*. Biophysical Journal, 1972. 12(11): p. 1533-1548.
405. Small, D.M., *Phase equilibria and structure of dry and hydrated egg lecithin*. Journal of Lipid Research, 1967. 8(6): p. 551-557.
406. Petrov, A.G. and G. Durand, *Thermal instability in lamellar phases of lecithin : a planar undulation model* Journal de Physique Lettres, 1983. 44(18): p. 793-798.
407. Wolosin, J.M., et al., *Diffusion within egg lecithin bilayers resembles that within soft polymers*. The Journal of General Physiology, 1978. 71(1): p. 93-100.
408. V. A. Parsegian, N. Fuller, and R.P. Rand. *Measured work of deformation and repulsion of lecithin bilayers*. in *Proceedings of the National Academy of Sciences of the United States of America*. 1979.
409. Bruno Demé, Monique Dubois, and T. Zemb, *Swelling of a Lecithin Lamellar Phase Induced by Small Carbohydrate Solutes*. Biophysical Journal, 2002. 82(1): p. 215-255.

410. Epand, R.M., *Diacylglycerols, lysolecithin, or hydrocarbons markedly alter the bilayer to hexagonal phase transition temperature of phosphatidylethanolamines*. *Biochemistry*, 1985. 24(25): p. 7092-7095.
411. McClements, D.J., E.A. Decker, and J. Weiss, *Emulsion-Based Delivery Systems for Lipophilic Bioactive Components*. *Journal of Food Science*, 2007. 72(8): p. R109-R124.
412. Tadros, T., et al., *Formation and stability of nano-emulsions*. *Advances in Colloid and Interface Science*, 2004. 108–109(0): p. 303-318.
413. Izquierdo, P., et al., *Formation and Stability of Nano-Emulsions Prepared Using the Phase Inversion Temperature Method*. *Langmuir*, 2001. 18(1): p. 26-30.
414. Tadros, T., et al., *Formation and stability of nano-emulsions*. *Advances in Colloid and Interface Science*, 2004. 108-109: p. 303-318.
415. Manea, M., et al., *Miniemulsification in high-pressure homogenizers*. *AIChE Journal*, 2008. 54(1): p. 289-297.
416. Weiss, J., *Emulsion Processing: Homogenization*. 2008: Amherst.
417. Taylor, G.I. *The formation of emulsions in definable fields of flow in Proceedings of the Royal Society of London A*. 1934: Royal Society Publishing.
418. Bentley, B.J. and L.G. Leal, *An experimental investigation of drop deformation and breakup in steady, two-dimensional linear flows*. *Journal of Fluid Mechanics*, 1986. 167: p. 241-283.
419. Renardy, Y.Y. and V. Cristini, *Effect of inertia on drop breakup under shear*. *Physics of Fluids*, 2001. 13(1): p. 7-13.
420. Yuriko, Y.R. and C. Vittorio, *scalings for fragments produced from drop breakup in shear flow with inertia*. *Physic of fluids*, 2001. 13(8): p. 2161-2164.
421. P. Walstra and P.E.A. Smoulers, *Emulsion formation*, in *Modern Aspects of Emulsion Science*, B.P. Binks, Editor. 1998, The Royal Society of Chemistry: Cambridge.
422. Davies, J.T., *Drop sizes of emulsions related to turbulent energy dissipation rates*. *Chemical Engineering Science*, 1985. 40(5): p. 839-842.
423. Brocart, B., et al., *Design of In-Line Emulsification Processes for Water-in-Oil Emulsions*. *Journal of Dispersion Science and Technology*, 2002. 23(1): p. 45 - 53.
424. Brocart Benjamin, T.P.A., Magnin Cesar, Bousquet Jacques, *Design of In-Line Emulsification Processes for Water-in-Oil Emulsions*. *Journal of Dispersion Science and Technology*, 2002. 23(1): p. 45 - 53.
425. Sprow, F.B., *Distribution of drop sizes produced in turbulent liquid--liquid dispersion*. *Chemical Engineering Science*, 1967. 22(3): p. 435-442.
426. Binks, B.P., *modern aspects of emulsion science*. 1998: Royal Society of Chemistry.
427. Lagisetty J. S., D.P.K., Kumar R., Gandhi K. S., *Breakage of viscous and non-Newtonian drops in stirred dispersions*. *Chemical Engineering Science*, 1986. 41(1): p. 65-72.
428. McClements, D.J., *food emulsions principles practices and techniques* 2ed. 2004: CRC Press.
429. Taisne, L., P. Walstra, and B. Cabane, *Transfer of Oil between Emulsion Droplets*. *Journal of Colloid and Interface Science*, 1996. 184(2): p. 378-390.

430. Lucassen, J., *Longitudinal capillary waves. Part 1.-Theory*. Transactions of the Faraday Society, 1968. 64: p. 2221-2229.
431. Gibbs, J.W., in: *H.A. Burnstead, R.G. van Name (Eds)*. Paper of J. Willard Gibbs. 1906, London: Longmans Green (Reprinted by Dove, New York, 1996).
432. Langmuir, I., *The constitution and fundamental properties of solids and liquids. Part I. Solids*. Journal of the American Chemical Society, 1916. 38(11): p. 2221-2295.
433. Szyszkowski, B.V., *Experimentelle studien über kapillare eigenschaften der wässerigen lösungen von fettsäuren*. Z. Phys. Chem, 1908(64): p. 385 - 414.
434. H.S.Carslaw, *introduction to the mathematical theory of the conduction of heat in solid*. 1945: Dover Publication, New York 158.
435. Markov, I.V., *Nucleation at surfaces*, in *Springer Handbook of Crystal Growth*, G. Dhanaraj, et al., Editors. 2010, Springer.
436. Garside, J., *The concept of effectiveness factors in crystal growth*. Chemical Engineering Science, 1971. 26(9): p. 1425-1431.
437. Garside, J., et al. *Advances in industrial crystallization*. Oxford; Boston: Butterworth Heinemann.
438. Mullin, J.W., *Crystallization*. 1992, Oxford Butterworth-Heinemann
439. Martins, P.M. and F. Rocha, *A new theoretical approach to model crystal growth from solution*. Chemical Engineering Science, 2006. 61(17): p. 5696-5703.
440. Keith, H.D. and F. J. Padden, Jr., *Spherulitic Crystallization from the Melt. II. Influence of Fractionation and Impurity Segregation on the Kinetics of Crystallization*. Journal of Applied Physics, 1964. 35(4): p. 1286-1296.
441. Glasner, K., *Solute trapping and the non-equilibrium phase diagram for solidification of binary alloys*. Physica D: Nonlinear Phenomena, 2001. 151(2-4): p. 253-270.
442. Danilov, D. and B. Nestler, *Phase-field modelling of solute trapping during rapid solidification of a Si-As alloy*. Acta Materialia, 2006. 54(18): p. 4659-4664.
443. Galenko, P., *Solute trapping and diffusionless solidification in a binary system*. Physical Review E (Statistical, Nonlinear, and Soft Matter Physics), 2007. 76(3): p. 031606.
444. Schulten, K., Z. Schulten, and A. Szabo, *Dynamics of reactions involving diffusive barrier crossing*. The Journal of Chemical Physics, 1981. 74(8): p. 4426-4432.
445. Hayoun, M., M. Meyer, and P. Turq, *Molecular dynamics study of self-diffusion in a liquid-liquid interface*. Chemical Physics Letters, 1988. 147(2-3): p. 203-207.
446. Benjamin, I., *Dynamics of ion transfer across a liquid-liquid interface: A comparison between molecular dynamics and a diffusion model*. The Journal of Chemical Physics, 1992. 96(1): p. 577-585.
447. Nakatani, K., M. Sudo, and N. Kitamura, *Intrinsic Droplet-Size Effect on Mass Transfer Rate across a Single-Micdroplet/Water Interface: Role of Adsorption on a Spherical Liquid/Liquid Boundary*. The Journal of Physical Chemistry B, 1998. 102(16): p. 2908-2913.

448. Gupta, A., A. Chauhan, and D.I. Kopelevich, *Molecular transport across fluid interfaces: Coupling between solute dynamics and interface fluctuations*. Physical Review E, 2008. 78(4): p. 041605.
449. Daikhin, L.I., et al., *ITIES fluctuations induced by easily transferable ions*. Chemical Physics, 2005. 319(1-3): p. 253-260.
450. Chowdhary, J. and B.M. Ladanyi, *Water-Hydrocarbon Interfaces: Effect of Hydrocarbon Branching on Interfacial Structure*. The Journal of Physical Chemistry B, 2006. 110(31): p. 15442-15453.
451. Small, D.M., *The physical chemistry of lipids: from alkanes to phospholipid*. 1986, New York: Plenum Press.
452. LeNeveu D. M., R.R.P., Gingell D., Parsegian V. A., *Apparent modification of forces between lecithin bilayers*. Science, 1976. 191(4225): p. 399-400.
453. Leneveu, D.M., R.P. Rand, and V.A. Parsegian, *Measurement of forces between lecithin bilayers*. Nature, 1976. 259(5544): p. 601-603.
454. Nagle J. F., W.D.A., *Lecithin bilayers. Density measurement and molecular interactions*. Biophysical journal, 1978. 23(2): p. 159-175.
455. Rydhag L., W.I., *The function of phospholipids of soybean lecithin in emulsions*. Journal of the American Oil Chemists' Society, 1981. 58(8): p. 830-837.
456. Gennis, R.B., *Biomembranes: Molecular structure and function*. 1989, Heidelberg: Springer Verlag.
457. Adamson, A. W., and Gast, *Physical chemistry of surfactes*. 1997, New York. 53.
458. Hoang, T.K.N., et al., *Monitoring the Simultaneous Ostwald Ripening and Solubilization of Emulsions*. Langmuir, 2004. 20(21): p. 8966-8969.
459. Hoang, T.K.N., et al., *Ostwald Ripening of Alkane Emulsions Stabilized by Polyethylene Glycol Monolaurate*. Langmuir, 2001. 17(17): p. 5166-5168.
460. Hoang, T.K.N., et al., *Ostwald Ripening of Alkane in Water Emulsions Stabilized by Hexaethylene Glycol Dodecyl Ether*. Langmuir, 2003. 19(15): p. 6019-6025.
461. Finsy, R., *On the Critical Radius in Ostwald Ripening*. Langmuir, 2004. 20(7): p. 2975-2976.
462. Lifshitz, I.M. and V.V. Slyozov, *The kinetics of precipitation from supersaturated solid solutions*. Journal of Physics and Chemistry of Solids, 1961. 19(1-2): p. 35-50.
463. Kabalnov, A.S. and E.D. Shchukin, *Ostwald ripening theory: applications to fluorocarbon emulsion stability*. Advances in Colloid and Interface Science, 1992. 38: p. 69-97.
464. Taylor, P., *Ostwald ripening in emulsions*. Advances in Colloid and Interface Science, 1998. 75(2): p. 107-163.
465. Vold, R.D., *Colloid and interface chemistry*. 1983, London: Addison-Wesley. 186.
466. Liu, Y., et al., *Ostwald Ripening of β -Carotene Nanoparticles*. Physical Review Letters, 2007. 98(3): p. 036102.
467. Higuchi, W.I. and J. Misra, *Physical degradation of emulsions via the molecular diffusion route and the possible prevention thereof*. Journal of Pharmaceutical Sciences, 1962. 51(5): p. 459-466.

468. Ugelstad, J., et al., *Swelling of oligomer-polymer particles. New methods of preparation*. *Advances in Colloid and Interface Science*, 1980. 13(1-2): p. 101-140.
469. Miller, C.M., et al., *Effect of the presence of polymer in miniemulsion droplets on the kinetics of polymerization*. *Journal of Polymer Science Part A: Polymer Chemistry*, 1994. 32(12): p. 2365-2376.
470. Gupta, P., G. Chawla, and A.K. Bansal, *Physical Stability and Solubility Advantage from Amorphous Celecoxib: The Role of Thermodynamic Quantities and Molecular Mobility*. *Molecular Pharmaceutics*, 2004. 1(6): p. 406-413.
471. Sterling, C., *Crystal structure analysis of [beta]-carotene*. *Acta Crystallographica*, 1964. 17(10): p. 1224-1228.
472. Auweter, H., et al., *Supramolecular Structure of Precipitated Nanosize β -Carotene Particles*. *Angewandte Chemie International Edition*, 1999. 38(15): p. 2188-2191.
473. Hussain, S., C. Keary, and D.Q.M. Craig, *A thermorheological investigation into the gelation and phase separation of hydroxypropyl methylcellulose aqueous systems*. *Polymer*, 2002. 43(21): p. 5623-5628.
474. Sarkar, N., *Kinetics of thermal gelation of methylcellulose and hydroxypropylmethylcellulose in aqueous solutions*. *Carbohydrate Polymers*, 1995. 26(3): p. 195-203.
475. Kita, R., et al., *Pinning of phase separation of aqueous solution of hydroxypropylmethylcellulose by gelation*. *Physics Letters A*, 1999. 259(3-4): p. 302-307.
476. Sammon, C., et al., *The application of attenuated total reflectance Fourier transform infrared spectroscopy to monitor the concentration and state of water in solutions of a thermally responsive cellulose ether during gelation*. *Polymer*, 2006. 47(2): p. 577-584.
477. Sarkar, N., *Thermal gelation properties of methyl and hydroxypropyl methylcellulose*. *Journal of Applied Polymer Science*, 1979. 24(4): p. 1073-1087.
478. Haque, A. and E.R. Morris, *Thermogelation of methylcellulose. Part I: molecular structures and processes*. *Carbohydrate Polymers*, 1993. 22(3): p. 161-173.
479. Haque, A., et al., *Thermogelation of methylcellulose. Part II: effect of hydroxypropyl substituents*. *Carbohydrate Polymers*, 1993. 22(3): p. 175-186.
480. Ibbett, R.N., K. Philp, and D.M. Price, *^{13}C n.m.r. studies of the thermal behaviour of aqueous solutions of cellulose ethers*. *Polymer*, 1992. 33(19): p. 4087-4094.
481. Karlstroem, G., A. Carlsson, and B. Lindman, *Phase diagrams of nonionic polymer-water systems: experimental and theoretical studies of the effects of surfactants and other cosolutes*. *The Journal of Physical Chemistry*, 1990. 94(12): p. 5005-5015.
482. Aguilar, M.R., et al., *Smart polymers and their applications as biomaterials*, in *Topics in Tissue Engineering*, N. Ashammakhi, R. Reis, and E. Chiellini, Editors. 2007. p. 1.
483. Sekiguchi, Y., C. Sawatari, and T. Kondo, *A gelation mechanism depending on hydrogen bond formation in regioselectively substituted O-methylcelluloses*. *Carbohydrate Polymers*, 2003. 53(2): p. 145-153.

484. Jones, M.N., *The interaction of sodium dodecyl sulfate with polyethylene oxide*. Journal of Colloid and Interface Science, 1967. 23(1): p. 36-42.
485. Goddard, E.D., *Polymer--surfactant interaction Part I. uncharged water-soluble polymers and charged surfactants*. Colloids and Surfaces, 1986. 19(2-3): p. 255-300.
486. Goddard, E.D., *Polymer--surfactant interaction part II. Polymer and surfactant of opposite charge*. Colloids and Surfaces, 1986. 19(2-3): p. 301-329.
487. Krister Holmberg, B.J.o., Bengt Kronberg and Björn Lindman, *Surfactant and Polymer in Aqueous Solution*. 2nd ed. 2002, Chichester: John Wiley & Sons, Ltd.
488. Bu, Z. and P.S. Russo, *Diffusion of Dextran in Aqueous (Hydroxypropyl)cellulose*. Macromolecules, 1994. 27(5): p. 1187-1194.
489. Furukawa, R., J.L. Arauz-Lara, and B.R. Ware, *Self-diffusion and probe diffusion in dilute and semidilute aqueous solutions of dextran*. Macromolecules, 1991. 24(2): p. 599-605.
490. Nyström, B., et al., *Light scattering studies of the gelation process in an aqueous system of a non-ionic polymer and a cationic surfactant*. Polymer, 1992. 33(14): p. 2875-2882.
491. Phillies, G.D.J., *The hydrodynamic scaling model for polymer self-diffusion*. Journal of Physical Chemistry 1989. 93(13): p. 5029-5039.
492. Phillies, G.D.J., *Range of validity of the hydrodynamic scaling model*. Journal of Physical Chemistry B, 1992. 96(24): p. 10061-10066.
493. Florence AT, E.P., Rahman A., *The influence of solution viscosity on the dissolution rate of soluble salts, and the measurement of an "effective" viscosity*. The Journal of pharmacy and pharmacology, 1973. 25(10): p. 779-786.
494. Westrin, B.A. and A. Axelsson, *Diffusion in gels containing immobilized cells: A critical review*. Biotechnology and Bioengineering, 1991. 38(5): p. 439-446.
495. Pham, Q.T., W.B. Russel, and W. Lau, *The effects of adsorbed layers and solution polymer on the viscosity of dispersions containing associative polymers*. Journal of Rheology, 1998. 42(1): p. 159-176.
496. Larson, R.G., *The structure and rheology of complex fluids*. 1999, New York: Oxford University Press.
497. Brunauer Stephen, D.L.S., Deming W. Edwards, Teller Edward, *On a Theory of the van der Waals Adsorption of Gases*. Journal of the American Chemical Society, 1940. 62(7): p. 1723-1732.
498. Perdomo J., et al., *Glass transition temperatures and water sorption isotherms of cassava starch*. Carbohydrate Polymers, 2009. 76(2): p. 305-313.